

Technische Universität Darmstadt
Fachbereich Physik - Institut für Kernphysik
Schlossgartenstraße 2
64289 Darmstadt
Germany



TECHNISCHE
UNIVERSITÄT
DARMSTADT

Master's Thesis

Pion-Pion Scattering and Shear Viscosity in the Nambu–Jona-Lasinio Model

Corrected and Extended Version:
A Guide to the Nambu–Jona-Lasinio Model

Sven Möller

December 19, 2012
(Corrections and Extensions: May 1, 2013)

Supervisors:
Priv.-Doz. Dr. Michael Buballa
Prof. Dr. Jochen Wambach

‘Äntligen hade korpen slagit ner på ett tak. “Ser du, att det är sant, som jag säger, och att det är lärdomen, som är herre här i staden?” hade han sagt, och pojken hade erkänt, att han hade haft rätt. “Om jag inte vore en korp,” hade Bataki vidare sagt, “utan bara en människa som du, så skulle jag slå mig ner här. Jag skulle sitta dag ut och dag in i ett rum fullt av böcker och lära mig allt, som stod i dem. Skulle du inte ha lust för sådant, du med?”’

— Nils Holgerssons underbara resa genom Sverige (Selma Lagerlöf)

We investigate pion-pion scattering in two-flavour Nambu–Jona-Lasinio (NJL) models. Mean-field methods are used to study chiral symmetry and spontaneous breaking thereof. Mesons are introduced as effective degrees of freedom in the quark-antiquark channel via the Bethe-Salpeter equation. In this work we include a vector-axial interaction channel in addition to the usual scalar-pseudoscalar one. The scattering of pions is studied in the vacuum and for finite temperature. We give a full momentum-dependent description of pion-pion scattering in vacuum in leading order in $1/N_c$. We also consider corrections to the meson propagators beyond leading order in $1/N_c$.

As an application we study the phase diagram of QCD matter within the NJL model. Confined QCD matter is described as a gas of pions with their interaction determined by the NJL matrix elements. With these we calculate the shear viscosity of such a pion gas in a kinetic theory approach.

Wir studieren Pion-Pion-Streuung im Nambu–Jona-Lasinio-Modell (NJL-Modell). Chirale Symmetrie und ihre spontane Brechung werden mit Hilfe von Molekularfeldmethoden untersucht. Mesonen werden als effektive Freiheitsgrade im Quark-Antiquark-Kanal vermöge der Bethe-Salpeter-Gleichung eingeführt. In dieser Arbeit betrachten wir eine Vektor-Pseudovektor-Wechselwirkung zusätzlich zu der üblichen Skalar-Pseudoskalar-Wechselwirkung. Die Streuung von Pionen wird im Vakuum und für endliche Temperatur erforscht. Wir entwickeln eine vollständig impulsabhängige Beschreibung von Pion-Pion-Streuung im Vakuum in führender Ordnung in $1/N_c$. Wir betrachten auch Korrekturen zu den Mesonenpropagatoren, die über führende Ordnung in $1/N_c$ hinausgehen.

Als Anwendung studieren wir das Phasendiagramm von QCD-Materie im Rahmen des NJL-Modells. Confinement unterliegende QCD-Materie wird als Pionengas beschrieben und die Wechselwirkung zwischen den Pionen durch die NJL-Matrixelemente bestimmt. Mit diesen berechnen wir die Scherviskosität eines solchen Pionengases im Rahmen der kinetischen Gastheorie.

Erklärung zur Masterarbeit

Hiermit versichere ich, die vorliegende Masterarbeit ohne Hilfe Dritter nur mit den angegebenen Quellen und Hilfsmitteln angefertigt zu haben. Alle Stellen, die aus Quellen entnommen wurden, sind als solche kenntlich gemacht. Diese Arbeit hat in gleicher oder ähnlicher Form noch keiner Prüfungsbehörde vorgelegen.

Darmstadt, den 19. Dezember 2012

(Sven Möller)

Acknowledgements

I would like to express my gratitude to my supervisor Priv.-Doz. Dr. Michael Buballa for always having an open ear and providing me with useful insight on many occasions. I further thank Prof. Dr. Jochen Wambach who gave me the opportunity to work in his group on this exciting topic and made useful suggestions on numerous occasions.

I thank Dr. Klaus Heckmann who first made the connection between NJL model calculations and kinetic gas theory in order to calculate transport coefficients of strongly interacting matter. His work was a useful reference during the work on my thesis.

I would finally like to thank the members of the NHQ group and my office mates with whom I shared many interesting discussions on physics-related (and other) topics and who made work more enjoyable.

Preface to the Extended Version

During the work on my Master's thesis arose the idea to compile all the detailed derivations and calculations presented in this work into a guidebook on the NJL model. This should serve future Bachelor's and Master's students as an easy-to-read introduction to the main features of the NJL model.

After having handed in my thesis I became aware of several minor errors in the text, mainly small calculation errors that showed up in tables and plots. For reasons of correctness, I removed these errors in the thesis, which I then dubbed "corrected version". Since I did not want to correct those errors in yet another text, I decided not to put together an additional document but rather to add additional sections at the end of this thesis (see Chapter X), which I then called "corrected and extended version". Those new sections are partly sections that did not make it into the original thesis but are still interesting to read, and partly texts that were written after completion of the original thesis.

Sven Möller, April 30, 2013

Contents

1. Introduction	10
1.1. Overview	15
2. The NJL Model	17
2.1. The NJL Lagrangian	17
2.1.1. Symmetries	18
2.1.2. Extended NJL Lagrangians	20
2.1.3. Feynman Rules	20
2.2. Mass Gap	22
2.3. Regularisation	24
2.4. Constituent Quark Masses	25
2.5. Mesons	27
2.5.1. Meson Masses	31
2.6. Chiral Theorems	34
3. The NJL Model in Medium	36
3.1. Mass Gap	37
3.2. Mesons	38
3.3. Results	41
4. Pion-Pion Scattering	43
4.1. Sigma-Propagation Diagram	46
4.2. Box Diagram	51
4.3. Results	53
4.4. Pion-Pion Scattering in the Medium	58
5. Extended NJL Model	62
5.1. Mesons	63
5.2. Pion-Pion Scattering	70
5.3. Results	74
5.4. Medium Results	77
5.5. More Realistic Meson Propagators	79
6. Shear Viscosity of a Pion Gas	82
6.1. Relativistic Hydrodynamics	82
6.2. Kinetic Theory of Gases	85
6.3. Thermodynamics of a Pion Gas	86

6.4. Shear Viscosity Estimate in the NJL model	87
6.5. Results	89
6.5.1. Simple Model	89
6.5.2. Extended Model	91
6.5.3. Discussion	92
7. Summary, Conclusions, Outlook	94
X. Extensions	97
X.1. Alternative Regularisation Schemes	97
X.2. Thermodynamic Potential	99
X.3. Constituent Quark Mass for Finite Chemical Potential	103
Appendices	106
Appendix A. Conventions	107
Appendix B. Basic Quantities	108
B.1. Calculation of the Polarisation Loop	108
B.2. Alternative Representation of the Meson Propagator	109
B.3. Calculation of the Pion Decay Constant	110
Appendix C. Elementary Integrals	112
C.1. Calculation of the Integral iI_1	112
C.2. Calculation of the Integral $iI_2(p)$	113
C.3. Analytical Solutions of the Integrals $iI(p)$, $iK(p)$, $iL(p)$	115
C.4. Derivative of the Elementary Integral $iI(p)$	121
C.5. Calculation of the Integrals $iI_3(p, q)$ and $iI_4(p, q, r)$	122
Appendix D. Medium Integrals	124
D.1. Medium Version of the Integral iI_1	124
D.2. Medium Versions of the Integrals $iI(p)$, $iK(p)$, $iL(p)$	126
D.3. Medium Version of the Integral $iI_2(p)$	130
D.4. Medium Version of the Bosonic Integral $iI_2^{(\pi)}(p)$	135
Appendix E. Quark Triangles and Boxes	136
E.1. Calculation of the Quark Triangle	136
E.2. Calculation of the Quark Triangle in the Static Limit	137
E.3. Calculation of the Quark Box	137
E.4. Calculation of the Quark Box in the Static Limit	139
Appendix F. Quantities in the Extended NJL Model	141
F.1. Polarisation Loops	141
F.2. Meson Propagators	144
F.3. Pole Structure of the Pion Propagator	146

F.4. Calculation of the Quark Triangle	148
Appendix G. Relativistic Hydrodynamics	151
G.1. Shear Viscosity Estimate	151
G.2. Thermodynamics of a Pion Gas	152
Appendix H. The Grand Potential	155
H.1. Calculation of the Mean-Field Lagrangian Density	155
H.2. Calculation of the Grand Potential of a Fermi Gas	156
H.3. Calculation of the Mean-Field Grand Potential	158
H.4. Equivalence of the Gap Equation and the Stationarity of the Grand Potential	159
Bibliography	160

1. Introduction

Quantum chromodynamics (QCD) is today widely accepted as the quantum field theory of strong interaction, i.e. the interaction between quarks and gluons based on their colour charge [1]. More precisely, QCD is the $SU(3)$ Yang-Mills theory of colour-charged fermions (the quarks) with the gluons being the massless gauge bosons. In contrast to quantum electrodynamics (QED), QCD is a non-abelian gauge theory. This results in the gauge bosons themselves being charged, i.e. they carry colour.

The non-abelian nature of QCD is responsible for many interesting phenomena that can be contrasted to QED or other abelian gauge theories. Frank Wilczek, David Gross and David Politzer shared the 2004 Nobel Prize in physics for their prediction of *asymptotic freedom* in 1973 [2, 3]. Asymptotic freedom, one of the two most outstanding phenomenological peculiarities of QCD (the other being confinement), is the property of quarks and gluons to be weakly interacting in the high-energy regime [4]. As energies become large (or equivalently distances small) the colour-charged particles become asymptotically free. For smaller energies however, quarks are very strongly coupled, which is sometimes dubbed as *infrared slavery*.

A related phenomenon is (*colour*) *confinement* [5]. Confinement describes the absence of free quarks in nature, stating that colour-charged objects are always clumped together (confined) to colourless groups of quarks, so-called hadrons. Confinement is caused by the fact that the force between two quarks which are gradually separated in space does not become smaller with increasing distance.

Unfortunately, QCD is also computationally much more difficult because of its non-abelianity. For example confinement has not been proven so far (but is seen in lattice QCD calculations [6]). In general, QCD becomes difficult to handle in the low-energy or strong-coupling regime where it cannot be accessed via a perturbational approach.

The QCD Phase Diagram

One of the major challenges remaining related to the study of the strong interaction is the exploration of the *QCD phase diagram* [7, 8, 9], i.e. the phase diagram of QCD matter. The term *QCD matter* refers collectively to the different states of matter which has quarks and gluons as elementary degrees of freedom interacting via the strong force.

The thermodynamic variables for the description of QCD matter are often chosen to be volume V , temperature T and the quark chemical potential μ , which is the chemical potential related to the conservation of the net quark number¹. This yields (the dependence on V is trivial) a two-dimensional phase space for QCD matter, the T - μ plane.²

¹Alternatively, one could speak of baryon number conservation and the related chemical potential μ_B .

²One can equally well use p and T as variables (like in [10]), which yields the usual p - T phase diagrams most physicists are acquainted with.

A contemporary sketch of the QCD phase diagram is shown in Figure 1.1.

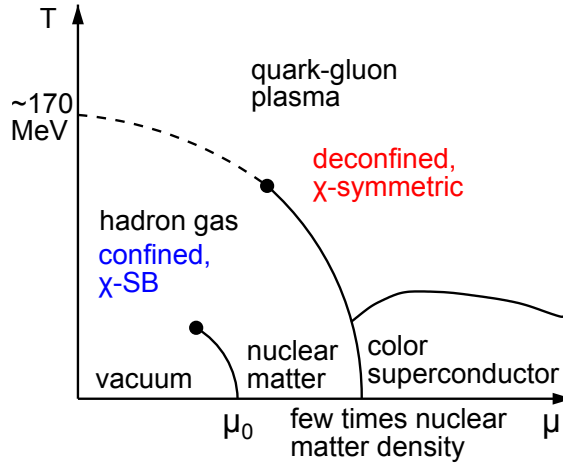


Figure 1.1.: Sketch of the present-day understanding of the QCD phase diagram in the T - μ plane. The dashed line indicates a crossover region, solid lines are phase transitions. Taken from [11] (with minor modifications).

For temperatures close to zero and small to intermediate quark chemical potential we are in the domain of ordinary matter. At $\mu_0 \approx 310$ MeV there is a gas-to-liquid phase transition from vacuum to nuclear matter. Ordinary matter is a mixed phase of droplets of nuclear matter, called nuclei, surrounded by vacuum. For even higher chemical potential there is a phase transition to a colour-superconducting quark phase [12, 13, 14].

Another major phase transition is the transition between the confined (or hadronic) phase and the partonic phase, the quark-gluon plasma (QGP) [15]. For small T and μ quarks are confined to hadrons, i.e. mesons and baryons (mainly pions for $\mu \approx 0$). If one increases the temperature, keeping μ fixed at a small value, there is a crossover to the deconfined phase at around $T \approx 170$ MeV [16]. The pions are broken up by thermal fluctuations and there is a gas of quarks, antiquarks and gluons, hence the name *quark-gluon plasma* [17]. For larger chemical potentials some models predict that the crossover becomes a phase transition.

There is also a transition between the chirally symmetric regime for large T or μ and the phase which exhibits spontaneous chiral symmetry breaking [18, 19] for small values of T and μ . Most recent calculations on the lattice [16] indicate that this transition happens for temperatures around $T \approx 155$ MeV (for $\mu = 0$). We should keep in mind that the critical temperature for a crossover is not uniquely defined, but this still suggests that contrary to previous belief the chiral and the deconfinement crossover are not identical.

In this work we intend to study the properties of QCD matter along the $\mu = 0$ axis. In particular we will study the cross-over from broken to restored chiral symmetry for increasing temperature (see Chapters 3 and 6).

Theoretical Approach

Because QCD is strongly coupled at chemical potentials (or densities) and temperatures of greatest physical interest, the phase structure of QCD matter remains mostly conjectural. Obtaining theoretical predictions about the phase diagram of QCD is one of the most difficult challenges in physics. With time, various techniques have been developed to perform calculations in QCD (or models resembling QCD in some aspects). Each of these approaches has a different region of applicability.

Often, one is only interested in a rough qualitative understanding of which phases might occur. For this, one constructs models which share certain aspects of QCD but are computationally much simpler. By doing so, one neglects other properties but hopes that those features of QCD one wishes to study are nonetheless well-reproduced (at least qualitatively).

The *MIT Bag Model* [20] is an example of a phenomenological model focusing on confinement. In the Bag Model weakly interacting quarks (which can be treated perturbatively) are confined to a spherical cavity called *bag*.

For the purposes of this work we will investigate the properties of QCD matter in *Nambu–Jona-Lasinio models* (NJL models) (see Chapters 2 and 5), named after the inventors of the original NJL model, Yoichiro Nambu and Giovanni Jona-Lasinio [21, 22]. NJL models are an important class of models, which focus on the aspect of chiral symmetry breaking in QCD, but fail to describe confinement. In that sense they can be viewed as complementary to the MIT Bag Model. The main feature of the NJL model is that it does not comprise gluons. Instead, the interaction between the fermions (here quarks) is modelled by a four-fermion interaction. Depending on the nature of this interaction one obtains different NJL models or NJL-like models. Comprehensive reviews of the NJL model applied to QCD are found in [23, 24].

The NJL model is used as a phenomenological model of QCD since it shares some features of QCD but is in many ways easier to manipulate. In particular, the NJL model describes chiral symmetry breaking and chiral condensates. This is related to the fact that the NJL Lagrangian has the same global symmetries as QCD. On the other hand, due to the lack of gluons and their self-interaction, the NJL model fails to describe confinement. Another shortcoming of the NJL model is its non-renormalisability in four spacetime dimensions due to the fact that the interaction between the quarks is point-like. To analyse the phases of QCD in NJL models, one often resorts to mean-field methods. In the NJL model, mesons can be described as composite degrees of freedom in the quark-antiquark channel.

Experimental Approach

To study the physical properties of the quark-gluon plasma and in particular the phase transition between it and the confined phase, extremely high temperatures of more than 170 MeV (or $2 \cdot 10^{12}$ K) have to be reached. This is accomplished in *relativistic heavy-ion collisions* [25]. In these heavy-ion collisions (HIC) two large nuclei (typically lead or gold nuclei) are accelerated to ultrarelativistic speeds and the particle beams are then directed towards each other. As a result, some of the nuclei hit, producing an extremely hot and dense *fireball*, in which the partons (i.e. quarks and gluons) are effectively free

and interact through inelastic scattering until thermal equilibrium is reached (if it is reached at all). This state of matter is then believed to be the quark-gluon plasma.

On the other hand the fireball starts expanding under its own pressure and cools due to this expansion. Once the temperature drops below a certain value, hadronisation of the partons sets in. The expansion of the hadronic matter continues and inelastic reactions between the hadrons occur. Once these inelastic collisions cease, the ‘chemical’ composition of the system is fixed. This is referred to as *chemical freeze-out*. At even later times, also elastic interactions cease and the momentum spectrum of the hadrons is fixed (*thermal* or *kinetic freeze-out*). A variety of detectors placed around the collision point measures the vast amount of different particles created during the collision and in secondary decays. One then looks for example for signals indicating the formation of a quark-gluon plasma. (Reviews of accelerator experiments related to the quest for the quark-gluon plasma are found in [26, 27].)

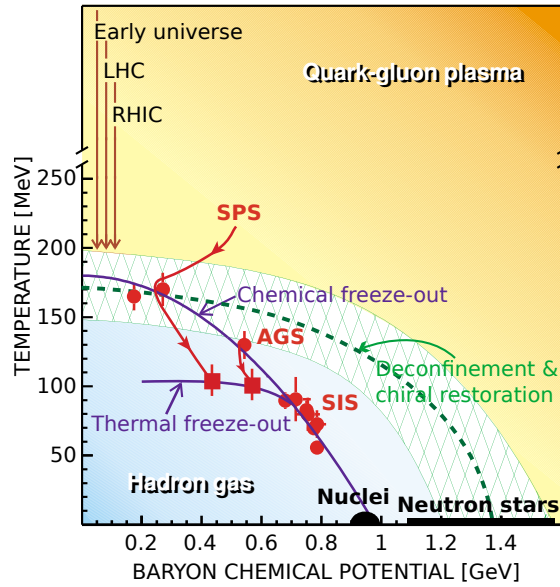


Figure 1.2.: A sketch of the QCD phase diagram with the experimentally accessible regions. Taken from [28, 29] with minor modifications. The red lines with arrows indicate expansion trajectories of thermalised matter created in different environments.

Elliptic Flow

One of the experimental observables sensitive to the properties of the quark-gluon plasma is the azimuthal angle distribution of particles in the plane orthogonal to the two beam axes. Most of the collisions in a heavy-ion collider take place at non-zero impact parameter. In these non-central collisions, the geometric overlap-region is almond-shaped. This spatial anisotropy of the collision region is eventually translated into an anisotropy in the momentum distribution of the measured collision products [30, 31].

The azimuthal distribution of the particle flow can be studied by a Fourier expansion.

The second Fourier coefficient v_2 is the first non-trivial and non-vanishing one and called *elliptic flow*. The mathematical methods employed to determine the elliptic flow are rather involved because the reaction plane (spanned by the beam axis and the impact parameter) is a different one in each collision [32].

The elliptic flow (and even higher Fourier coefficients) has been studied in a great detail during the last years and particularly large values have been observed at RHIC and LHC [32, 33]. It is argued that large values of v_2 suggest that the state of matter created during a heavy-ion collision behaves almost like a perfect fluid, i.e. has a particularly low shear viscosity over entropy density ratio η/s .

Relativistic Hydrodynamics

To understand the phenomena related to a collective particle flow in heavy-ion collisions one needs to be able to describe the time-evolution of such a system given certain initial conditions. This is done in a *hydrodynamical* approach.

The first predictions were made with *ideal* hydrodynamics calculations (i.e. neglecting dissipative effects) and showed a good agreement with data measured at RHIC [34]. This led to the conclusion that dissipative effects in the fireball fluid are rather small. In viscous hydrodynamics these deviations from the ideal case are incorporated in the form of the *transport coefficients*, one of which is the (shear) viscosity η . The dimensionless ratio of shear viscosity η over entropy density s is usually taken as a measure for the non-ideality of the hydrodynamical description. It is found that this ratio is indeed very small for the quark-gluon plasma. Whether there is a lower bound for η/s as conjectured based on the AdS/CFT correspondence [35] is currently debated.

It is possible to calculate the shear viscosity of a fluid based on a microscopic description [36] (kinetic theory of gases). From such considerations it is easily seen that a small shear viscosity corresponds to particularly strongly interacting particles. This relation suggests that the quark-gluon plasma at least close to the crossover region is strongly coupled and this state of matter is referred to as strongly coupled quark-gluon plasma (sQGP). See [37] for a recent review.

Pion Gas

One of the goals of this work is to determine the shear viscosity of QCD matter (for $\mu = 0$ as a function of temperature), especially in the vicinity of the chiral cross-over (see Chapter 6). This will be done in a kinetic theory approach, which relates the microscopic quantum description of the particles to bulk fluidity measures. For such a calculation to be valid, it has to be required that the mean free path λ of the particles be much larger than the range of interaction d . In [38] it is argued that for QCD matter such conditions are found only in systems with small temperature and chemical potential. It is however exactly that region, in which QCD exhibits confinement. Since the NJL model does not incorporate confinement, we cannot expect it to give a reasonable description if we consider quarks and antiquarks as relevant degrees of freedom, i.e. when dealing with a quark gas.

It is proposed in [38] to consider a gas of pions instead. Within the framework of the NJL model, these are obtained by studying collective modes in the quark-antiquark

interaction channel. The thermodynamic properties of a system at not too large temperatures or densities should be determined by the lightest degrees of freedom, which in case of confined QCD matter are the pions. They are so light since they are the pseudo-Goldstone bosons of the spontaneously broken approximate chiral symmetry. The more general concept is that of a hadron resonance gas [39] where QCD matter is described as a free gas of *all* possible hadrons and their resonant states. For the purposes of this work we will restrict ourselves to a gas only consisting of pions, which implies a vanishing baryon number B or equivalently $\mu = 0$.

We have argued that the kinetic description of QCD matter as a pion gas will yield sensible results for small temperatures and chemical potential. Small or vanishing μ means that particle densities are only generated by thermal fluctuations which are suppressed exponentially for small temperatures. This means that we are in the limit of a dilute gas, where kinetic theory can be applied and the results for the shear viscosity we obtain should be acceptable.

Pion-Pion Scattering

To calculate the shear viscosity of a pion gas in a kinetic theory approach we have to calculate the interactions between the pions. This will be done in the framework of the NJL model (see Chapters 4 and 5). Pion-pion scattering in the NJL model has been studied extensively in the past (see for example [40, 41, 42, 43, 44, 45]). Transport coefficients obtained from an NJL model approach were first calculated in [46, 38, 10, 47]. One goal of this work is to extend these results by incorporating an additional vector interaction (see Chapter 5) into the model. Such a vector interaction was studied for example in [48, 49].

1.1. Overview

The primary goal of this thesis is the calculation of pion-pion scattering matrix elements within the NJL model. We proceed as follows:

Chapter 2 gives a thorough introduction to the NJL model (in vacuum) in its version applied to QCD. All necessary concepts for the understanding of the model will be introduced. Starting from the Lagrangian density, we will derive the Feynman rules for this quantum field theory, which we will use throughout this work. A first application will be the derivation of a mass gap in Section 2.2. A few words will be said about the regularisation of certain ‘elementary’ integrals, which form the basis of all NJL model calculations and in Section 2.5 we finally turn to the description of mesons via a Bethe-Salpeter equation. In Chapter 3 we will extend our considerations from the vacuum to a thermal field theory scenario with finite temperature and chemical potential. Many of the concepts we introduced in Chapter 2 will be transferred to the new setting.

Chapter 4 deals with the scattering of pions described in the NJL model based on two basic scattering processes, the sigma propagation and the quark box diagram. In this work we will for the first time present fully momentum-dependent matrix elements corresponding to the two above mentioned diagrams. In Chapter 5 we will extend the NJL Lagrangian with an additional vector-pseudovector interaction term, allowing for

an additional rho propagation diagram in the pion-pion interaction channel.

In Chapter 6 we apply the insights gained in the preceding chapters to determine transport properties of strongly interacting matter. More specifically, the obtained pion-pion scattering matrix elements serve as input of kinetic theory calculations aimed at determining the shear viscosity of QCD matter. The results are presented in Section 6.5.

2. The NJL Model

The Nambu–Jona-Lasinio model was originally proposed in 1961 – QCD and even quarks had yet to be discovered – as a model of interacting *nucleons* [21, 22]. Hence confinement was obviously not relevant for the model. On the other hand, another important feature of QCD, namely the (approximate) *chiral symmetry* of the Lagrangian was already suggested on the level of nucleons.

The NJL model incorporates chiral symmetry into the Lagrangian density. This implies however massless (or in the case of an approximate chiral symmetry very light) nucleons. Nambu and Jona-Lasinio had to find a mechanism to account for the (experimentally) large nucleon mass without destroying the chiral symmetry of the Lagrangian. They saw an analogy to the energy gap in the excitation spectrum of the electrons of a BCS superconductor [50] (developed in 1957) and explained the nucleon masses by the spontaneous breaking of the chiral symmetry. The dynamically generated mass of the nucleons is much larger than the so-called bare mass, which enters in the Lagrangian density, and stays large even for a vanishing bare quark mass. They also found very light (or massless) bosonic nucleon-antinucleon excitations. This discovery can be seen as an important step towards the formulation of Goldstone’s theorem, which predicts massless Nambu-Goldstone bosons in models exhibiting the spontaneous breaking of a continuous symmetry [51, 52].

The NJL model was later reinterpreted as a model of interacting quarks [53, 54, 55], keeping the original form of the Lagrangian and simply replacing the nucleonic fields by quark fields. As the NJL model focuses on chiral symmetry, this aspect of QCD is well-reflected. However, for quarks it has the severe shortcoming that confinement is not described by the model. This restricts the applicability of the NJL model to investigations where chiral symmetry and its spontaneous breaking is in the focus rather than confinement.

2.1. The NJL Lagrangian

We will introduce the NJL model in its original, simplest version. In general we can allow more complicated interaction terms (see Section 2.1.2) and one such extension is studied in Chapter 5.

The nucleons of the original NJL model are an isospin (or flavour) doublet. Similarly we will restrict ourselves to the two lightest quark flavours up (u) and down (d). Extensions of the NJL model to three or more quark flavours exist (see [56, 57]) but will not be considered in this work.

The Lagrangian density of the two-flavour NJL model reads

$$\mathcal{L} = \bar{\psi}(i\cancel{\partial} - \underline{m})\psi + g \left[(\bar{\psi}\psi)^2 + (\bar{\psi}i\gamma_5\vec{\tau}\psi)^2 \right]. \quad (2.1)$$

The quark and antiquark fields ψ and $\bar{\psi} = \psi^\dagger\gamma_0$ are Dirac spinors and have indices in the 4-dimensional Dirac space, the $(N_f = 2)$ -dimensional flavour (or isospin) space and the $(N_c = 3)$ -dimensional colour space and are hence $(4N_cN_f)$ -component objects. Here, \underline{m} is the current (or bare) quark mass matrix, which takes the form $\underline{m} = \text{diag}(m_u, m_d)$. We will assume that the u and d quarks have a degenerate mass $m := m_u = m_d$ and hence we can replace \underline{m} by the *bare quark mass* m in the above Lagrangian. $\vec{\tau}$ stands for the vector of Pauli matrices in isospin space.

The first term in the Lagrangian density

$$\mathcal{L}_{\text{free}} = \bar{\psi}(i\cancel{\partial} - m)\psi \quad (2.2)$$

is the *free* (or *Dirac*) part and corresponds to the fact that the quarks are spin-1/2 fermions obeying the Dirac equation as free particles. The second part of the Lagrangian density

$$\mathcal{L}_{\text{int.}} = g \left[(\bar{\psi}\psi)^2 + (\bar{\psi}i\gamma_5\vec{\tau}\psi)^2 \right] \quad (2.3)$$

is the *interaction part* and consists of a scalar-isoscalar and a pseudoscalar-isovector four-point interaction, both with coupling strength g . The coupling constant g is dimensionful with dimension $[\text{mass}]^{-2}$. We will later (see Section 2.5) find collective quark-antiquark modes in the interaction channels and will relate a meson to each of the vertices, i.e. the σ meson and the pion.

The more complicated interaction of quarks via gluons, which themselves may interact with one another, found in QCD is replaced by a simple four-point vertex. This is done in a way that the global symmetries of QCD, in particular chiral symmetry are preserved. The above interaction Lagrangian $\mathcal{L}_{\text{int.}}$ is chirally symmetric making the complete Lagrangian density chirally symmetric for $m \rightarrow 0$. It is of course possible to write down many more chirally symmetric four-point vertices and models incorporating these are also referred to as *NJL models* (see Chapter 5). In the following section we will study the global symmetries of the above simple NJL model with Lagrangian given by (2.1).

2.1.1. Symmetries

The Lagrangian \mathcal{L} of the NJL model exhibits a number of *global* symmetries, i.e. it is invariant under certain spacetime-independent symmetry transformations, each of which is related to a conserved quantity via a Noetherian current. In fact, the NJL Lagrangian has the same global symmetries as the one for QCD (with $N_f = 2$). A treatment of the symmetries of QCD and the NJL model can be found in [23]. One typically writes the complete global symmetry as $U(1)_V \times SU(2)_V \times SU(2)_A$ and we shall discuss each single symmetry below:

- The first symmetry is a global $U(1)_V$ -phase invariance, i.e. an invariance of \mathcal{L} under

$$\psi \mapsto \exp(-i\alpha)\psi \quad \text{and} \quad \bar{\psi} \mapsto \exp(i\alpha)\bar{\psi} \quad (2.4)$$

for $\alpha \in \mathbb{R}$. By Noether's theorem this leads to the Noetherian current

$$j_\mu = \bar{\psi}\gamma_\mu\psi \quad (2.5)$$

fulfilling $\partial_\mu j^\mu = 0$ and hence gives the conserved quantity

$$\int d^3x j^0 = \int d^3x \psi^\dagger\psi \quad (2.6)$$

(recall $\bar{\psi} = \psi^\dagger\gamma^0$), which corresponds to the conservation of *baryon number*.

- We assumed that $m_u = m_d =: m$. This limiting case is called *isospin limit*. In that case the Lagrangian \mathcal{L} is invariant under a *vector* $SU(2)_V$ -transformation

$$\psi \mapsto \exp(-i\vec{\tau} \cdot \vec{\theta}/2)\psi \quad \text{and} \quad \bar{\psi} \mapsto \bar{\psi} \exp(i\vec{\tau} \cdot \vec{\theta}/2) \quad (2.7)$$

for $\vec{\theta} \in \mathbb{R}^3$. The field ψ is rotated in isospin space. The conserved current is

$$J_\mu^a = \bar{\psi}\gamma_\mu\tau^a\psi \quad (2.8)$$

and corresponds to the conservation of isospin.

- The last symmetry is only present in the *chiral limit*, i.e. in the case $m = 0$. Then the Lagrangian \mathcal{L} is also invariant under an *axial* $SU(2)_A$ -transformation

$$\psi \mapsto \exp(-i\gamma_5\vec{\tau} \cdot \vec{\theta}/2)\psi \quad \text{and} \quad \bar{\psi} \mapsto \bar{\psi} \exp(-i\gamma_5\vec{\tau} \cdot \vec{\theta}/2) \quad (2.9)$$

for $\vec{\theta} \in \mathbb{R}^3$. Here, we transform in isospin and Dirac space. The Noetherian current is

$$J_{5\mu}^a = \bar{\psi}\gamma_\mu\gamma_5\tau^a\psi. \quad (2.10)$$

The chiral limit plays a particularly important role for NJL model studies. Many of the features of QCD are solely based on the symmetries present in the chiral limit. These can be well reproduced in the NJL model. Even if we consider non-vanishing but small bare quark masses, many of these results are still approximately fulfilled and deviations from the chiral limit can be studied systematically.

In the chiral limit there is an invariance of the Lagrangian density under

$$SU(2)_V \times SU(2)_A \cong SU(2)_L \times SU(2)_R. \quad (2.11)$$

The $SU(2)_A$ -symmetry is spontaneously broken by the quark condensate (see Chapter 3). The Goldstone bosons, which correspond to the three broken generators of the transformation, are the pions. We will describe pions in Section 2.5 and they indeed turn out to be massless in the chiral limit. We will consider the case where m is non-zero but small and hence the above symmetry is only an approximate symmetry. Consequently, the pions, which are then called *pseudo-Goldstone bosons*, obtain a non-zero mass.

Studying the above symmetry transformations, one observes that the interaction terms $g(\bar{\psi}\psi)^2$ and $g(\bar{\psi}i\gamma_5\vec{\tau}\psi)^2$ are transformed into one another by chiral transformations. One says the two terms are *chiral partners*. In order to obtain a chirally symmetric Lagrangian both terms have to appear with the same coupling strength g .

2.1.2. Extended NJL Lagrangians

There exist a number of extensions of the NJL model. In this work, in addition to the above simple NJL model, we will study a model with interaction Lagrangian given by

$$\mathcal{L}_{\text{int.}} = g_s \left[(\bar{\psi}\psi)^2 + (\bar{\psi}i\gamma_5\vec{\tau}\psi)^2 \right] - g_v \left[(\bar{\psi}\gamma^\mu\vec{\tau}\psi)^2 + (\bar{\psi}\gamma^\mu\gamma_5\vec{\tau}\psi)^2 \right]. \quad (2.12)$$

The additional terms describe a vector-isovector and a pseudovector-isovector interaction channel. Both terms are again chiral partners and hence appear with the same interaction strength $-g_v$, where the minus sign is chosen in order to obtain a positive value for g_v for a physical choice of the parameters. The interaction strength g is now called g_s and is independent of g_v . With the above extended Lagrangian the NJL model exhibits the same global symmetries as those we described above for the simple model.

It furthers the clarity of our considerations to introduce a more general notation. We write the NJL Lagrangian as

$$\mathcal{L} = \bar{\psi}(i\not{\partial} - \underline{m})\psi + \sum_M g_M (\bar{\psi}\Gamma_M\psi)^2, \quad (2.13)$$

where M runs over all interaction channels and the Γ_M 's are constant matrices in Dirac, flavour and colour space, i.e. $\bar{\psi}\Gamma_M\psi$ is a general quark bilinear. (We note here that Γ_M may also have an isospin index a or a Lorentz index μ or both. In that case $(\bar{\psi}\Gamma_M^{\mu,a}\psi)^2$ is to be understood as $(\bar{\psi}\Gamma_M^{\mu,a}\psi)(\bar{\psi}\Gamma_{M,\mu}^a\psi)$ with summation over a and μ implied according to Einstein convention.) We chose the letter M for the different interaction channels since we will relate the different interaction channels to mesons (see Section 2.5). If we write the Lagrangian in such a general form we must of course explicitly demand that the Lagrangian density exhibit the above described symmetries.

2.1.3. Feynman Rules

All physical quantities are in principle determined by the Lagrangian density of the NJL model (2.1) or (2.13) (and the choice of regularisation scheme, see Section 2.3). It is convenient to use diagrammatic techniques to calculate and analyse many of these quantities. In order to do this we will have to determine the Feynman rules [58] for this particular fermionic quantum field theory.

General Lagrangian

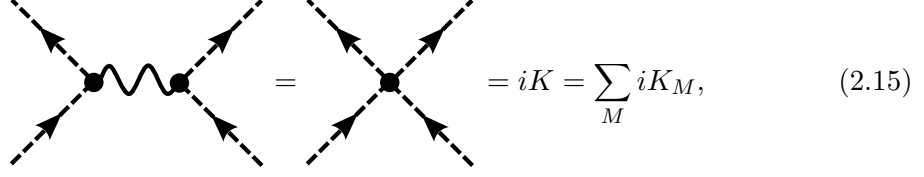
From the Dirac part of the Lagrangian $\mathcal{L}_{\text{free}}$ we read off the *bare quark propagator*

$$\begin{array}{c} \text{p} \\ \dashrightarrow \end{array} = iS_0(p) = i\frac{\not{p} + m}{p^2 - m^2 + i\varepsilon}, \quad (2.14)$$

which is the Feynman propagator for a Dirac fermion.

The interaction term of the general Lagrangian density (2.13) contains exclusively

four-point interactions. These can be combined to a single vertex



$$= iK = \sum_M iK_M, \quad (2.15)$$

where the contribution from each interaction channel is given by

$$iK_M = 2ig_M \Gamma_M \otimes \Gamma_M. \quad (2.16)$$

(If Γ_M comes with additional indices, we have to write $iK_M = 2ig_M \Gamma_M^{\mu,a} \otimes \Gamma_{M,\mu}^a$ in the sum.) The wiggly line in the above Feynman diagram is used to emphasise the tensor structure of the vertex. We will later often omit the tensor-product sign whenever this simplifies the notation without causing ambiguities. The sign in front of the vertices iK_M depends on the convention used. Here, we chose $+i$ rather than $-i$.

The other Feynman rules are the standard rules for a fermionic theory (including symmetry factors, etc.). In particular we get

$$- \int \frac{d^4 k}{(2\pi)^4} \text{Tr} \quad (2.17)$$

for a closed fermion loop labelled with momentum k .

Simple Model

Let us explicitly give the vertices for the simple NJL model as given in (2.1) since we will begin our NJL model studies with that case. The Lagrangian density contains a single scalar interaction channel called σ given by the term

$$(\bar{\psi} \Gamma_\sigma \psi) g (\bar{\psi} \Gamma_\sigma \psi) = (\bar{\psi} \psi) g (\bar{\psi} \psi) \quad (2.18)$$

with

$$\Gamma_\sigma = \mathbb{1}_{\text{Dirac}} \otimes \mathbb{1}_{\text{colour}} \otimes \mathbb{1}_{\text{flavour}} \quad (2.19)$$

and three ($a = 1, 2, 3$) pseudoscalar interaction channels called π given by

$$(\bar{\psi} \Gamma_\pi^a \psi) g (\bar{\psi} \Gamma_\pi^a \psi) = (\bar{\psi} i\gamma_5 \tau^a \psi) g (\bar{\psi} i\gamma_5 \tau^a \psi) \quad (2.20)$$

with

$$\Gamma_\pi^a = i\gamma_5 \otimes \mathbb{1}_{\text{colour}} \otimes \tau^a. \quad (2.21)$$

This corresponds to the vertices

$$iK_\sigma = 2ig \Gamma_\sigma \otimes \Gamma_\sigma = 2ig \mathbb{1} \otimes \mathbb{1} \quad (2.22)$$

and

$$iK_\pi = 2ig \Gamma_\pi^a \otimes \Gamma_\pi^a = 2ig i\gamma_5 \tau^a \otimes i\gamma_5 \tau^a. \quad (2.23)$$

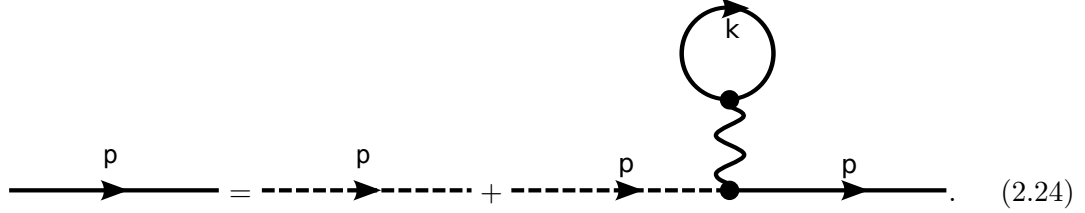
The above section shall serve us as a dictionary whenever we need to evaluate more difficult diagrammatic expressions.

2.2. Mass Gap

We already mentioned that the quarks, which are only equipped with a very small or vanishing bare mass in the Lagrangian, obtain a higher effective mass through a self-energy, which is caused by the interaction term in the Lagrangian. This phenomenon is very similar to the energy gap in BCS theory and hence is called *mass gap*.

Hartree-Approximation

We define the *dressed quark propagator* via the *Dyson equation*



$$\text{---}\xrightarrow{p}\text{---} = \text{---}\xrightarrow{p}\text{---} + \text{---}\xrightarrow{p}\text{---} \text{---} \text{---} \text{---} \xrightarrow{p}\text{---} . \quad (2.24)$$

In this diagrammatic equation we only considered contributions of leading order in $1/N_c$. We refer to this approximation as *Hartree* or *mean field approximation*. We will see shortly that this approximation already results in a larger effective quark mass. We claim that the solution to the above equation, the dressed quark propagator, can be again written as a Feynman propagator

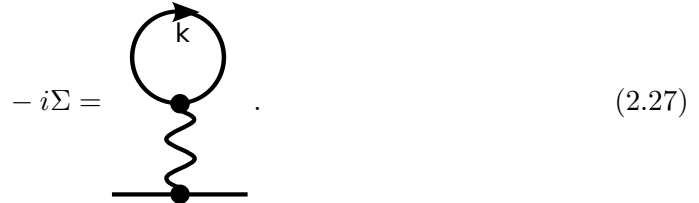
$$\text{---}\xrightarrow{p}\text{---} = iS(p) = i \frac{\not{p} + M}{p^2 - M^2 + i\varepsilon}, \quad (2.25)$$

i.e. takes the same form as the bare quark propagator but with an appropriately chosen *constituent quark mass* M instead of the bare quark mass m . This effective mass M turns out to be larger than the *bare* quark mass m and even in the limit $m = 0$ the constituent mass M can be non-zero (if the coupling g is chosen sufficiently large).

To determine the mass M , we have to solve the above self-consistency equation, which reads

$$iS(p) = iS_0(p) + iS_0(p)(-i\Sigma)iS(p), \quad (2.26)$$

where Σ is the quark self-energy corresponding to the diagram



$$-i\Sigma = \text{---} \text{---} \text{---} . \quad (2.27)$$

Multiplying by $S_0^{-1}(p) = \not{p} - m$ from the left and by $S^{-1}(p) = \not{p} - M$ from the right, we get

$$iS_0^{-1}(p) = iS^{-1}(p) + i\Sigma \quad (2.28)$$

or

$$i(\not{p} - m) = i(\not{p} - M) + i\Sigma \quad (2.29)$$

and hence an M that solves

$$M = m + \Sigma \quad (2.30)$$

gives a solution to the Dyson equation (note that Σ of course also depends on M).

Finally we calculate the self energy Σ . Using the Feynman rules we evaluate the above diagram and get

$$-i\Sigma = -i \sum_M \Sigma_M = \sum_M 2ig_M \Gamma_M \int \frac{d^4k}{(2\pi)^4} (-1) \text{Tr}(\Gamma_M iS(k)) \quad (2.31)$$

and hence

$$\Sigma = \sum_M \Sigma_M = \sum_M 2g_M \Gamma_M i \int \frac{d^4k}{(2\pi)^4} \text{Tr}(\Gamma_M S(k)). \quad (2.32)$$

(Again, for $\Gamma_M^{\mu,a}$ we have $\Sigma_M = 2g_M \Gamma_M^{\mu,a} i \int \frac{d^4k}{(2\pi)^4} \text{Tr}(\Gamma_{M,\mu}^a S(k))$ with summation over a and μ implied.)

Simple Model

Let us study the case of the simple NJL Lagrangian (2.1). The self-energy is given by

$$\begin{aligned} \Sigma &= 2g \left(\Gamma_\sigma \int \frac{d^4k}{(2\pi)^4} \text{Tr}(\Gamma_\sigma iS(k)) + \Gamma_\pi^a \int \frac{d^4k}{(2\pi)^4} \text{Tr}(\Gamma_\pi^a iS(k)) \right) \\ &= 2g \left(\mathbb{1} i \int \frac{d^4k}{(2\pi)^4} \text{Tr}(\mathbb{1} S(k)) - \gamma_5 \tau^a i \int \frac{d^4k}{(2\pi)^4} \text{Tr}(\gamma_5 \tau^a S(k)) \right). \end{aligned} \quad (2.33)$$

The second term vanishes since the trace over τ^a is zero and hence we get

$$\Sigma = 2gi \int \frac{d^4k}{(2\pi)^4} \text{Tr} \left(\frac{\not{p} + M}{p^2 - M^2 + i\varepsilon} \right) = 8N_f N_c g M i \int \frac{d^4k}{(2\pi)^4} \frac{1}{p^2 - M^2 + i\varepsilon}, \quad (2.34)$$

where we used that the trace over \not{p} vanishes and since M comes with a $\mathbb{1}$ in Dirac, flavour and colour space, we get an additional factor of $4N_f N_c$. We define the elementary integral

$$iI_1 = iI_1(M) := i \int \frac{d^4k}{(2\pi)^4} \frac{1}{p^2 - M^2 + i\varepsilon}, \quad (2.35)$$

which appears in the above expression. It is shown in Appendix C.1 that this integral can be brought into the form

$$iI_1 = \frac{1}{2} \int \frac{d^3k}{(2\pi)^3} \frac{1}{E_k^-} = \frac{1}{4\pi^2} \int_0^\infty dk \frac{k^2}{\sqrt{k^2 + M^2}} \quad (2.36)$$

by application of the residue theorem, where we define $E_k^- := \sqrt{k^2 + M^2}$. Unfortunately, the integral iI_1 is divergent and needs to be regularised. The regularisation technique

will be discussed in Section 2.3. Let us assume we have found a method to make the value of the integral finite. Then we have

$$\Sigma = 8N_f N_c g M i I_1(M) \quad (2.37)$$

for the self-energy and plugging this in into (2.30) yields the *gap equation*

$$M = m + 8N_f N_c g M i I_1(M). \quad (2.38)$$

This equation can now be solved for the constituent mass $M = M(g, m)$. A priori we do not know whether a solution to this equation exists and if so whether it is unique. It turns out that for $m \neq 0$ there is only one positive solution. For $m = 0$ there is always the trivial solution $M = 0$ in addition to a possible positive and negative solution. We will of course always choose M to be non-negative. In Chapter 3 we will encounter the gap equation again for finite temperature and chemical potential. In that case there may be several (positive) solutions and the *one* physical solution would have to be determined by minimising the grand potential. However, for the purposes of this work we will only consider the case of vanishing quark chemical potential μ , in which case the solution is always unique.

2.3. Regularisation

We stated in Section 2.2 that the integral

$$iI_1 = i \int \frac{d^4 k}{(2\pi)^4} \frac{1}{k^2 - M^2 + i\varepsilon}, \quad (2.39)$$

which appeared in the expression for the self-energy, does not converge to a finite value. In fact it diverges quadratically. This can be seen simply from counting the powers of k in the numerator and in the denominator. In order to get a finite integral value, we must regularise it by suppressing the large-momentum contributions. There exist several methods of doing so. We will employ Pauli-Villars regularisation for the purposes of this thesis and shall present it for the example of iI_1 .

Pauli-Villars Regularisation

A commonly used regularisation method is Pauli-Villars regularisation [59]. Instead of introducing a sharp momentum cutoff, the asymptotic behaviour of the integrand is changed such that the integral converges. This can be achieved by subtracting functions which have a small contribution for small momenta but asymptotically behave like the integrand itself. For the Pauli-Villars regularisation we replace the original integrand $f(k, M)$ by a weighted sum of modified integrands with different masses, i.e.

$$i \int \frac{d^4 k}{(2\pi)^4} f(k, M) \rightarrow i \int \frac{d^4 k}{(2\pi)^4} \sum_{i=1}^n f_i(k, M_i). \quad (2.40)$$

In order to regularise the integral $iI_1(M)$ (which is quadratically divergent) from the previous section (at least) two regularisation functions are needed. We will regularise it by the replacement

$$i \int \frac{d^4k}{(2\pi)^4} f(k, M) \rightarrow i \int \frac{d^4k}{(2\pi)^4} \left(f(k, M) - 2f(k, \sqrt{M^2 + \Lambda^2}) + f(k, \sqrt{M^2 + 2\Lambda^2}) \right) \quad (2.41)$$

with a (soft) cutoff scale Λ . The integral iI_1 exhibits the highest order of divergence of any momentum integral that will appear in this work. We will later encounter momentum integrals which are only logarithmically divergent or convergent without the need for regularisation but for consistency we will use the above regularisation scheme for all appearing momentum integrals.

For practical calculations we can make use of the linearity of the integral and convert each of the three integrands via the residue theorem as we did for the unregularised integrand (see (2.36)). For the given example, we get

$$\begin{aligned} iI_1 &= \frac{1}{2} \int \frac{d^3k}{(2\pi)^3} \left(\frac{1}{\sqrt{k^2 + M^2}} - 2\frac{1}{\sqrt{k^2 + M^2 + \Lambda^2}} + \frac{1}{\sqrt{k^2 + M^2 + 2\Lambda^2}} \right) \\ &= \frac{1}{4\pi^2} \int_0^\infty dk \left(\frac{k^2}{\sqrt{k^2 + M^2}} - 2\frac{k^2}{\sqrt{k^2 + M^2 + \Lambda^2}} + \frac{k^2}{\sqrt{k^2 + M^2 + 2\Lambda^2}} \right). \end{aligned} \quad (2.42)$$

The latter integral can be calculated analytically and gives

$$\begin{aligned} iI_1 &= \frac{1}{16\pi^2} \left(M^2 \ln(M^2) - 2(M^2 + \Lambda^2) \ln(M^2 + \Lambda^2) + (M^2 + 2\Lambda^2) \ln(M^2 + 2\Lambda^2) \right) \\ &= \frac{1}{16\pi^2} \left(M^2 \ln \left(\frac{M^2}{M^2 + \Lambda^2} \right) + (M^2 + 2\Lambda^2) \ln \left(\frac{M^2 + 2\Lambda^2}{M^2 + \Lambda^2} \right) \right). \end{aligned} \quad (2.43)$$

As mentioned before, we will use Pauli-Villars regularisation for all the calculations performed in this thesis. We will later encounter integrals which are Lorentz scalars depending on one or more external momentum. Pauli-Villars regularisation preserves the Lorentz invariance in contrast to other regularisation methods (like introducing a three-momentum cutoff). Moreover, using a sharp momentum cutoff we would have to take care of the domain of integration when making substitutions in the integrals, which we will do on numerous occasions in this work. With Pauli-Villars regularisation, the integration is over all four-momenta and hence this problem does not occur.

2.4. Constituent Quark Masses

In the following, some numerical results for the gap equation in the simple NJL model using Pauli-Villars regularisation will be presented. Our choice of the model parameters m , g and Λ is taken from [60]. The parameters are chosen such that the pion mass (see

Param. Set	[A]	[B]	[C]	[D]	[E]
m [MeV]	6.13	6.40	6.77	6.70	6.54
Λ [MeV]	800	800	800	820	852
$g\Lambda^2$	2.90	3.07	3.49	3.70	4.16
M [MeV]	260.5	303.1	395.0	446.3	549.4

Table 2.1.: The model parameters (m , g and Λ) using Pauli-Villars regularisation and the resulting value of the constituent quark mass M .

Section 2.5.1) is $m_\pi = 140.0$ MeV. The parameter sets are labelled [A] - [E] and are shown in Table 2.1.

Solving the gap equation (2.38) amounts to finding the root(s) of the function $f(x)$, where

$$f(x) = \tilde{m} + x \left[\tilde{g} \left(x^2 \ln \left(\frac{x^2}{x^2 + 1} \right) + (x^2 + 2) \ln \left(\frac{x^2 + 2}{x^2 + 1} \right) \right) - 1 \right] \quad (2.44)$$

with $x = M/\Lambda$, $\tilde{m} = m/\Lambda$ and $\tilde{g} = 8N_f N_c g \Lambda^2 / (16\pi^2)$. The (non-zero) solution to the above transcendental equation can only be found numerically.

For $m > 0$ there is a unique solution $M > m$. In the chiral limit, i.e. for $m = 0$ the situation is more complicated. For $\tilde{g} < \tilde{g}_{\text{crit.}} \approx 0.721$ there is only the trivial solution $M = 0$ (hence there is no dynamic mass generation) and for $\tilde{g} > \tilde{g}_{\text{crit.}}$ the gap equation has the trivial solution $M = 0$, which we discard, and a proper solution $M > 0$. The situation is depicted in Figure 2.1. For the choice of parameters [A] - [E] we get the

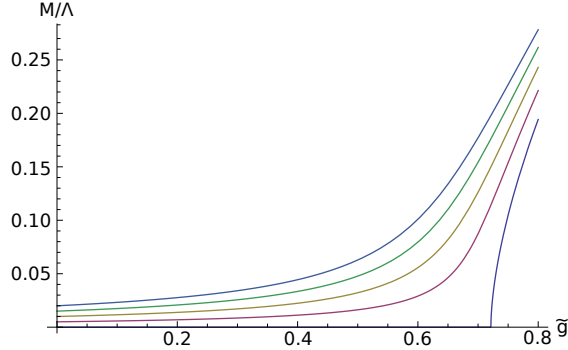


Figure 2.1.: Value of the constituent M quark mass for different values of \tilde{m} and \tilde{g} . The different lines correspond to $\tilde{m} = m/\Lambda = 0, 0.005, 0.01, 0.015, 0.02$ (from bottom to top).

values of M shown in Table 2.1.

In the chiral limit ($m = 0$) a non-zero constituent quark mass is a result of spontaneous chiral symmetry breaking, which leads to a dynamical mass generation. This symmetry breaking sets in for sufficiently large coupling g (in units of $1/\Lambda^2$). For a small bare quark mass m the mechanism is in principle the same, but only approximate.

2.5. Mesons

In the following we want to present the description of mesons in the NJL model. The NJL model does not confine, but we can still describe mesons as collective modes appearing in the quark-antiquark interaction channel. This is common practice in NJL model studies and can be achieved via the *Bethe-Salpeter equation*³ (BSE) describing the bound states of a two-body quantum field theoretical system.

The *Bethe-Salpeter equation* (BSE) in *random phase approximation* (RPA) reads

$$(2.45)$$

or in explicit form

$$(2.46)$$

Again, we only consider diagrams of leading order in $1/N_c$. We will later (see Section 5.5) also include diagrams of higher order in $1/N_c$.

General Model

Let us first discuss the Bethe-Salpeter equation for the general Lagrangian (2.13). We call the left hand side of the equation *scattering matrix* denoted by $iT(p)$, where p is the four-momentum transported by the double shaded line (later to be interpreted as the momentum of the exchanged meson). To evaluate the right hand side we define the *polarisation loop*

$$J_{M,N}(p) := i \int \frac{d^4k}{(2\pi)^4} \text{Tr} (\Gamma_M S(k+p) \Gamma_N S(k)). \quad (2.47)$$

(or more generally $J_{M,N}^{\mu\nu,ab}(p) := i \int \frac{d^4k}{(2\pi)^4} \text{Tr} (\Gamma_M^{\mu,a} S(k+p) \Gamma_N^{\nu,b} S(k))$, where not all of the indices have to be present.) Diagrammatically the polarisation loop is represented by

$$-iJ_{M,N}(p) = \text{diagram} \quad (2.48)$$

³The Bethe-Salpeter equation is named after Hans Bethe and Edwin Salpeter [61], but was actually first mentioned in a paper by Nambu [62].

After a careful evaluation of the Feynman diagrams the explicit equation (2.46) reads

$$\begin{aligned} iT(p) &= iK + i \sum_{M,N} (2g_M)(2g_N)\Gamma_M \otimes \Gamma_N J_{M,N}(p) \\ &\quad + i \sum_{M,K,N} (2g_M)(2g_K)(2g_N)\Gamma_M \otimes \Gamma_N J_{M,K}(p) J_{K,N}(p) + \dots \end{aligned} \quad (2.49)$$

We write

$$iK = i \sum_M K_M = i \sum_M 2g_M \Gamma_M \otimes \Gamma_M = i \sum_{M,N} 2g_M \delta_{MN} \Gamma_M \otimes \Gamma_N, \quad (2.50)$$

which together with the above shows that we can write $T(p)$ as

$$T(p) =: \sum_{M,N} T_{M,N}(p) =: - \sum_{M,N} \Gamma_M \otimes \Gamma_N D_{M,N}(p) \quad (2.51)$$

(or more generally $T_{M,N}(p) = -\Gamma_{M,\mu}^a \otimes \Gamma_{N,\nu}^b D_{M,N}^{\mu\nu,ab}(p)$), where the minus sign is again a convention. All the matrix structure is in the Γ_M 's and hence $D_{M,N}(p)$ is a scalar-valued function, which we call a *generalised meson propagator*. It is in explicit form given by

$$\begin{aligned} D_{M,N}(p) &= -2g_M \delta_{M,N} - (2g_M)(2g_N) J_{M,N}(p) \\ &\quad - \sum_K (2g_M)(2g_K)(2g_N) J_{M,K}(p) J_{K,N}(p) - \dots \end{aligned} \quad (2.52)$$

Either by summing up the above equation or by directly evaluating the implicit diagrammatic equation, we obtain the implicit equation for $D_{M,N}(p)$

$$D_{M,N}(p) = -2g_M \delta_{M,N} + \sum_K 2g_M J_{M,K}(p) D_{K,N}(p). \quad (2.53)$$

(More generally, $D_{M,N}^{\mu\nu,ab}(p) = -2g_M \delta_{M,N} \delta_{ab} \eta^{\mu\nu} + \sum_K 2g_M J_{M,K}^{ac,\mu\lambda}(p) D_{K,N}^{cb,\nu}(p)$, where each of the Lorentz or isospin indices might or might not appear. If $D_{M,N}(p)$ has only one Lorentz or isospin index, then necessarily $M \neq N$ and $\delta_{M,N} = 0$, which means that the corresponding term in the equation vanishes, even though δ_{ab} and $\eta^{\mu\nu}$ are not well-defined for only one index.)

If we consider $D_{M,N}(p)$ as entry of the matrix $(D_{M,N}(p))_{M,N}$, the above equation becomes a matrix equation, which can easily be solved:

$$D_{K,N}(p) = \left[2(g_M J_{M,K}(p)) - (\delta_{M,K}) \right]_{K,M}^{-1} 2g_M \delta_{M,N}, \quad (2.54)$$

where $[\cdot]^{-1}$ denotes the matrix inverse. The solution $D_{M,N}(p)$ one obtains is in general a matrix with non-vanishing off-diagonal entries. By a change of basis (depending on p) we can bring it into a diagonal form.

Let us for the moment without loss of generality assume that $D_{M,N}(p)$ is already diagonal, i.e.

$$D_{M,N}(p) =: \delta_{M,N} D_M(p). \quad (2.55)$$

This is the case if and only if the polarisation loop $J_{M,N}(p)$ is diagonal, i.e.

$$J_{M,N}(p) =: \delta_{M,N} J_M(p). \quad (2.56)$$

In that case equation (2.53) simplifies to

$$D_M(p) = -2g_M + 2g_M J_M(p) D_M(p), \quad (2.57)$$

which yields

$$D_M(p) = \frac{-2g_M}{1 - 2g_M J_M(p)}. \quad (2.58)$$

$D_M(p)$ is referred to as the *propagator* of the meson M , which is justified in view of the definition of $D_M(p)$ via the scattering matrix $T_M(p)$. This is however a bit misleading since in fact $D_M(p)$ not only is the propagator for the mesons but it also contains the coupling of the quarks to the meson. So, we can write

$$D_M(p) = g_{Mqq}(p) \mathcal{D}_M(p) g_{Mqq}(p), \quad (2.59)$$

where $g_{Mqq}(p)$ is the quark-meson coupling and $\mathcal{D}_M(p)$ is the actual meson propagator (see below for a more detailed discussion). However, since often only $D_M(p)$ appears in the calculations, we will mainly use the first definition but one should keep the above said in mind for the evaluation of Feynman diagrams. To be exact, the shaded double line in equation (2.45) corresponds to

$$\text{====} = i\mathcal{D}_M(p) \quad (2.60)$$

and the quark-meson vertex $\Gamma_{Mqq}(p)$ is given by

$$\begin{array}{c} \nearrow \\ \bullet \\ \searrow \end{array} \text{====} = i\Gamma_{Mqq}(p) = i\Gamma_M g_{Mqq}(p). \quad (2.61)$$

Simple Model

Let us now turn to the discussion for the case of the simple NJL model with only a scalar and a pseudoscalar interaction channel with coupling strength g . The meson index M runs over $\{\sigma, \pi\}$. It is apparent that $J_{M,N}(p)$ vanishes for $M \neq N$ since the trace over one Pauli matrix τ^a vanishes. Hence $J_{M,N}(p)$ and $D_{M,N}(p)$ are indeed diagonal in that case. We will refer to $D_\sigma(p)$ as the propagator of the σ meson and to $D_\pi^{ab}(p)$ as the pion propagator.

In order to calculate the meson propagators, we first need to calculate the polarisation

loop $J_M(p)$ for $M \in \{\sigma, \pi\}$. The calculation can be found in Appendix B.1 and yields

$$\begin{aligned}
J_\sigma(p) &= 4N_c N_f i I_1 - 2N_c N_f (p^2 - 4M^2) i I_2(p) \\
&= \frac{1}{2g} \left(1 - \frac{m}{M}\right) - 2N_c N_f (p^2 - 4M^2) i I_2(p), \\
J_\pi^{ab}(p) &= \delta_{ab} \left(4N_c N_f i I_1 - 2N_c N_f p^2 i I_2(p)\right) \\
&= \delta_{ab} \left(\frac{1}{2g} \left(1 - \frac{m}{M}\right) - 2N_c N_f p^2 i I_2(p)\right) \\
&=: \delta_{ab} J_\pi(p),
\end{aligned} \tag{2.62}$$

where

$$iI_1 = i \int \frac{d^4 k}{(2\pi)^4} \frac{1}{k^2 - M^2 + i\varepsilon} = \int \frac{d^3 k}{(2\pi)^3} \frac{1}{2E_{\vec{k}}} \tag{2.63}$$

is the elementary integral we already defined in Section 2.2 and

$$iI_2(p) := i \int \frac{d^4 k}{(2\pi)^4} \frac{1}{(k^2 - M^2 + i\varepsilon) ((k+p)^2 - M^2 + i\varepsilon)}. \tag{2.64}$$

By application of the residue theorem (see Appendix C.2) we can write the latter integral as

$$iI_2(p) = \int \frac{d^3 k}{(2\pi)^3} \frac{1}{E_{\vec{k}} p_0^2 - (E_{\vec{k}} + E_{\vec{p}+\vec{k}})^2 + i\varepsilon}. \tag{2.65}$$

This integral also needs to be regularised and we will apply the same regularisation scheme as for iI_1 , i.e Pauli-Villars regularisation with two regulators. The integral can even be computed analytically. The calculation and its result (C.35) are given in Appendix C.3). The integral iI_2 only depends on p^2 rather than the four-vector p . Therefore also J_π and J_σ only depend on p^2 .

With the polarisation functions we can calculate the meson propagators according to (2.58). For the sigma meson this yields

$$D_\sigma(p^2) = \frac{-2g}{1 - 2gJ_\sigma(p^2)}. \tag{2.66}$$

For the pions, we also have to consider the isospin structure of $J_\pi^{ab}(p^2)$. Since this is just δ_{ab} , the propagator is also diagonal in isospin space and we get

$$D_\pi^{ab}(p^2) = \delta_{ab} \frac{-2g}{1 - 2gJ_\pi(p^2)} =: \delta_{ab} D_\pi(p^2), \tag{2.67}$$

which means that the different pion species do not mix.

We can now calculate the (inverse) pion and sigma-meson propagators using the expressions for J_π and J_σ . The result is shown in Figure 2.2. A discussion of these propagators and how to parametrise them is given in the next section.

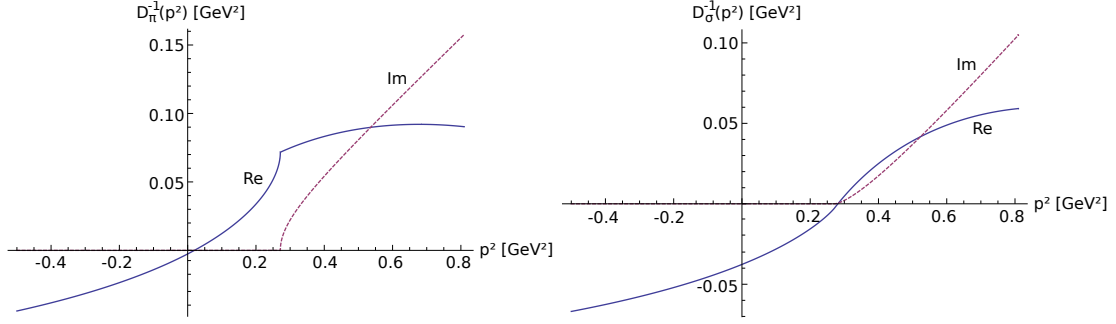


Figure 2.2.: The inverse pion propagator $D_\pi^{-1}(p^2)$ (left) and the inverse sigma-meson propagator $D_\sigma^{-1}(p^2)$ (right) for parameter set [A].

2.5.1. Meson Masses

In the following section we will devise a way to determine the masses of the sigma meson and the pions from the corresponding propagators. Analogous ideas can be applied to other mesons in an extended NJL model.

We saw that the meson propagator $D_M(p)$ only depends on p^2 for $M \in \{\sigma, \pi\}$. Since we constructed $D_M(p^2)$ to play the role of a propagator we also expect it to have according properties. In particular the propagator should have a pole at the mass of the meson. So conversely, we should be able to determine the meson masses m_M as zeros of the inverse propagators, i.e.

$$D_M^{-1}(p^2 = m_M^2) \stackrel{!}{=} 0. \quad (2.68)$$

Following the decomposition in (2.59) we should be able to write the meson propagator as

$$D_M(p^2) = \frac{g_{Mqq}^2(p^2)}{p^2 - m_M^2}, \quad (2.69)$$

where the denominator is the inverse of the free meson propagator $\mathcal{D}_M(p^2)$ and the numerator is the square of the momentum-dependent quark-meson coupling $g_{Mqq}(p^2)$. Evaluating the quark-meson coupling at the meson mass (i.e. determining the residue of the first order pole of the above function) we obtain the on-shell *coupling constant*

$$g_{Mqq} := g_{Mqq}(p^2 = m_M^2). \quad (2.70)$$

We can use this to write the meson propagator in *pole approximation* as

$$D_M(p^2) \approx \frac{g_{Mqq}^2}{p^2 - m_M^2}, \quad (2.71)$$

which is nothing else but an expansion of $D_M(p^2)$ around its pole.

So far we have completely neglected the fact that the inverse propagators also have an imaginary part. This imaginary part occurs for $p^2 > 4M^2$ (see Figure 2.2) and is related to the energetically allowed $M \rightarrow q\bar{q}$ decay channel. This is of course related to

the fact that the NJL model does not confine and we interpreted mesons as collective modes in the quark-antiquark scattering matrix. For $p^2 < 4M^2$ these are bound states but at larger p^2 the meson will decay into an unconfined quark-antiquark pair.

For the pion, we will get a mass $m_\pi \ll 2M$ and there will still be a pole of the propagator. However, for the sigma meson we will get a mass m_σ slightly above $2M$ and hence there will be no (real) pole because of a non-vanishing imaginary part of the inverse propagator.

More generally we will need to write

$$D_M(p^2) = \frac{g_{Mqq}^2(p^2)}{p^2 - m_M^2 + i\Upsilon_M(p^2)} \quad (2.72)$$

where $\Upsilon_M(p^2) = \Theta(p^2 - 4M^2) \dots$ is the imaginary part of the inverse propagator. This leads to the so-called *resonance approximation* of the propagator

$$D_M(p^2) \approx \frac{g_{Mqq}^2}{p^2 - m_M^2 + i\Upsilon_M} \quad (2.73)$$

where g_{Mqq} and Υ_M are evaluated at $p^2 = m_M^2$.

Taking the above into consideration we define the meson mass more generally as the zero of the real part of the inverse propagator, i.e. by

$$\text{Re}D_M^{-1}(p^2 = m_M^2) = 1 - 2g\text{Re}J_M(p^2 = m_M^2) \stackrel{!}{=} 0. \quad (2.74)$$

This way we can speak of a meson mass even in the case, where the meson propagator does not have a pole.⁴

Using the above definition of the meson mass and the propagators in (2.66) and (2.67), we can determine the pion and sigma-meson masses for parameter sets [A] - [E]. The result is shown in Table 2.2. As already mentioned, the parameters are chosen such that

Param. Set	[A]	[B]	[C]	[D]	[E]
M [MeV]	260.5	303.1	395.0	446.3	549.4
m_π [MeV]	140.0	140.0	140.0	140.0	140.0
m_σ [MeV]	530.2	613.4	794.7	896.3	1101.4
$g_{\pi qq}$	2.713	2.955	3.507	3.768	4.324

Table 2.2.: The masses M , m_π and m_σ and the quark-pion coupling $g_{\pi qq}$ for parameter sets [A] - [E].

the pion mass is $m_\pi = 140$ MeV.

⁴One should note that there exist several definitions of the meson masses in the case where the propagator does not have a real pole. For example in [48] the authors determine the mass of the mesons as a pole in the complex plane.

Expanding the real part of the inverse propagator in p^2 around m_M^2 gives

$$1 - 2\text{Re}J_M(p^2) = -2g \frac{\text{dRe}J_M(p^2)}{\text{d}(p^2)} \Big|_{p^2=m_M^2} (p^2 - m_M^2) + \mathcal{O}\left(\left(p^2 - m_M^2\right)^2\right) \quad (2.75)$$

and hence we obtain

$$g_{Mqq}^{-2} = \frac{\text{dRe}J_M(p^2)}{\text{d}(p^2)} \Big|_{p^2=m_M^2} \quad (2.76)$$

for the on-shell coupling constant in resonance approximation (which for the pion is the same as the pole approximation). For parameter sets [A] - [E] the value of $g_{\pi qq}$ is calculated and presented in Table 2.2. Analogously, Υ_M can be obtained via

$$\Upsilon_M = g_{Mqq}^2 \text{Im}J_M(p^2 = m_M^2). \quad (2.77)$$

Alternative Representation of the Meson Propagator

We show in Appendix B.2 that in the simple model the meson propagator for $M \in \{\sigma, \pi\}$ can be written as

$$D_M(p^2) = -\frac{1}{2N_c N_f ((p^2 - \varepsilon_M^2) iI_2(p^2) - m_\pi^2 iI_2(m_\pi))}. \quad (2.78)$$

with $\varepsilon_\pi := 0$ and $\varepsilon_\sigma := 4M^2$. Here we read $iI_2(m_\pi)$ as iI_2 evaluated at some four-momentum p with $p^2 = m_\pi^2$ (since iI_2 only depends on p^2).

Quark-Pion Coupling Constant

Using the above representation of the meson propagator, we can give a simple expression for the quark-pion coupling constant. We write the pion propagator as

$$D_\pi(p^2) = -\frac{1}{2N_c N_f (p^2 iI_2(p^2) - m_\pi^2 iI_2(m_\pi))}. \quad (2.79)$$

and hence

$$\begin{aligned} g_{\pi qq}^{-2} &= \lim_{p^2 \rightarrow m_\pi^2} \frac{D_\pi^{-1}(p)}{p^2 - m_\pi^2} = -2N_f N_c \lim_{p^2 \rightarrow m_\pi^2} \frac{p^2 iI_2(p) - m_\pi^2 iI_2(m_\pi)}{p^2 - m_\pi^2} \\ &= -2N_f N_c \frac{\text{d}(p^2 iI_2(p^2))}{\text{d}(p^2)} \Big|_{p^2=m_\pi^2}. \end{aligned} \quad (2.80)$$

Calculating the above expression amounts to computing the derivative of $iI_2(p^2)$ w.r.t. p^2 , which is done in Appendix C.4. The result can be expressed in terms of more general *elementary integrals*⁵ ($iI(p)$, $iI(p)$ and $iK(p)$), which will be introduced in Section 4.1 (see (4.22) and (4.23)). For the coupling constant this yields

$$g_{\pi qq}^{-2}(m_\pi) =: g_{\pi qq}^{-2} = -N_c N_f \left(iI(0) + iI(m_\pi) - m_\pi^2 iK(m_\pi) \right) \quad (2.81)$$

in accordance with [43]. The elementary integrals only depend on p^2 and we again wrote $I(m_\pi)$, etc. for $I(p)$ evaluated at some p with $p^2 = m_\pi^2$.

⁵The integral $iI(p)$ is in fact identical to the integral $iI_2(p)$ and is simply given another name in the context of the yet to be introduced *static limit*.

2.6. Chiral Theorems

An important feature of the NJL model is that it focuses on chiral symmetry and its spontaneous breaking. Consequently we should be able to verify the following *chiral theorems* in the simple NJL model. Since they are solely based on symmetry principles they remain correct in mean field and random phase approximation (leading order in $1/N_c$), which do not violate these symmetries.

Goldstone's Theorem

Equation (2.62) for $m = 0$ implies directly that

$$1 - 2gJ_\pi(p^2 = 0) = 0 \quad (2.82)$$

and hence we find that the pion mass vanishes in the chiral limit. The pions can be identified with the *massless* Nambu-Goldstone bosons predicted by Goldstone's theorem [51, 52] related to the fact that the gap equation describes the dynamic generation of a constituent quark mass which spontaneously breaks the chiral symmetry.

If however $m \neq 0$ (but small), then the chiral symmetry is only an approximate symmetry and the pions get a (small) mass as we calculated in the previous section (see Table 2.2).

Pion Decay Constant

The pion decay constant f_π is the square root of the coefficient of the kinetic term for the pion in the low-energy effective action of chiral perturbation theory [63]. It can be viewed as measure for the strength of chiral symmetry breaking. In our model it can be obtained from the one-pion-to-vacuum matrix element [64] in RPA via

$$f_\pi p^\mu \delta_{ab} = g_{\pi qq} \int \frac{d^4 k}{(2\pi)^4} \text{Tr} \left(\gamma^\mu \gamma_5 \frac{\tau^a}{2} S(k+p) i\gamma_5 \tau^b S(k) \right). \quad (2.83)$$

Performing the above integration explicitly (see Appendix B.3) one obtains

$$f_\pi = -g_{\pi qq} 2N_f N_c M i I_2(m_\pi), \quad (2.84)$$

which can also be written as

$$f_\pi^2 = 4N_f N_c M^2 \frac{iI(m_\pi)^2}{iI(0) + iI(m_\pi) - m_\pi^2 iK(m_\pi)}, \quad (2.85)$$

where we used the expression (2.81) for $g_{\pi qq}$ obtained in the previous section.

Goldberger-Treiman Relation

The pion decay constant should fulfil the following generalised *Goldberger-Treiman relation* [65]

$$g_{\pi qq} f_\pi = M + \mathcal{O}(m), \quad (2.86)$$

which implies $f_\pi = M/g_{\pi qq}$ in the chiral limit.

The pion decay constant is calculated for parameter sets [A] - [E] (see Table 2.3). Parameter set [A] was chosen to approximately reproduce the literature value $f_\pi =$

Param. Set	[A]	[B]	[C]	[D]	[E]
m [MeV]	6.13	6.40	6.77	6.70	6.54
f_π [MeV]	93.64	100.50	111.03	116.99	125.88
$M - g_{\pi qq} f_\pi$ [MeV]	6.45	6.15	5.73	5.45	5.04

Table 2.3.: The bare quark mass m , the pion decay constant f_π and $M - g_{\pi qq} f_\pi$ for parameter sets [A] - [E].

92.21 MeV = 130.41/ $\sqrt{2}$ MeV [66]. It is apparent from the calculated values that the generalised Goldberger-Treiman relation is fulfilled. If we put $m = 0$, relation $f_\pi = M/g_{\pi qq}$ can be easily shown to be correct in the NJL model.

Gell-Mann–Oakes–Renner Relation

We stated that for non-vanishing bare quark mass m , pions will not be massless (and are called pseudo-Goldstone bosons). This statement can be formalised by a systematic expansion around the chiral limit, which yields the Gell-Mann–Oakes–Renner relation [67]

$$m_\pi^2 = -\frac{m\langle\bar{\psi}\psi\rangle}{f_\pi^2} + \mathcal{O}(m^2). \quad (2.87)$$

Here, $\langle\bar{\psi}\psi\rangle$ denotes the quark condensate, which we will not study in this work (but it is discussed in Section X.2 of the extension) and is given by $\langle\bar{\psi}\psi\rangle = -\Sigma/(2g) = (m - M)/(2g)$. In Table 2.4 we verify that the Gell-Mann–Oakes–Renner relation is fulfilled by our NJL model results. For a better comparison with literature values we

Param. Set	[A]	[B]	[C]	[D]	[E]
m [MeV]	6.13	6.40	6.77	6.70	6.54
$\langle\bar{\psi}\psi\rangle$ [MeV ³]	-(303.90) ³	-(313.88) ³	-(328.97) ³	-(341.82) ³	-(361.80) ³
$\langle\bar{\psi}\psi\rangle/N_f$ [MeV ³]	-(241.20) ³	-(249.13) ³	-(261.10) ³	-(271.31) ³	-(287.13) ³
$f_\pi^2 + \frac{m\langle\bar{\psi}\psi\rangle}{m_\pi^2}$ [MeV ²]	-10.96	8.51	33.08	38.68	43.78

Table 2.4.: The table shows the values for the chiral condensate $\langle\bar{\psi}\psi\rangle$ and the correctness of the *Gell-Mann–Oakes–Renner relation* for parameter sets [A] - [E].

also give $\langle\bar{\psi}\psi\rangle/N_f = \langle\bar{\psi}\psi\rangle/2$, the quark condensate per flavour, which is often simply called quark condensate.

3. The NJL Model in Medium

So far we have studied quarks and mesons in the NJL model in vacuum, i.e. at zero temperature. In view of the goal of exploring the phase diagram of QCD, we are however interested in the medium properties of these particles, which means that we have to make our calculations in the setting of *thermal* or *finite temperature field theory* [68, 69]. Such calculations were made for the NJL model in [70, 71] and in [41, 43] for pion-pion scattering in particular. It has been suggested that medium effects like temperature-dependent masses are particularly important [72, 73] in the description of pion-pion scattering, which we will discuss in Chapter 4.

We have already argued in the introduction that the relevant thermodynamic variables for the description of QCD matter are temperature T and quark chemical potential μ corresponding to the conservation of the net quark (or baryon) number, i.e. the number of quarks minus the number of antiquarks. Since for the moment we will only deal with this one single chemical potential, we will simply refer to it as ‘the’ chemical potential.

In this chapter we will study the medium properties of the simple NJL model with Lagrangian given in (2.1).

Thermal Field Theory

Thermal field theory is aimed at the calculation of the expectation value of physical observables in a quantum field theory at finite temperature. The most commonly used method is the *Matsubara* or *imaginary-time formalism* [74]. The basic principle of the theory is that the expected value of an operator O in a thermal ensemble

$$\langle O \rangle = \frac{\text{Tr}(O \exp(-\beta H))}{\text{Tr}(\exp(-\beta H))} \quad (3.1)$$

(where $\beta = 1/T$ is the inverse temperature) is identical to the ordinary quantum field theoretic expectation value with a configuration evolved by an imaginary time $t = i\beta$. The trace Tr in the above expression leads to the additional requirement that bosonic fields be periodic and fermionic fields be antiperiodic in the imaginary time direction. The usual quantum field theoretic tools such as path integrals and diagrammatic techniques may be employed but live now on the ‘tube’ $\mathbb{R}^3 \times S^1$ with a compactified imaginary time coordinate. This compactification in coordinate space leads to a discretisation in momentum space where a continuous energy coordinate is replaced by discrete imaginary frequencies, the *Matsubara frequencies*. Finally, to obtain results for observables at real energies (or real times) an analytic continuation has to be made.

Since the fields we are dealing with are quark fields it suffices to replace the energy integration in the appearing four-momentum integrals by a sum over fermionic *Matsubara*

frequencies $i\omega_j = (2j + 1)\pi iT$ ($j \in \mathbb{Z}$), i.e.

$$i \int \frac{d^4 k}{(2\pi)} f(k) \rightarrow -T \sum_{j \in \mathbb{Z}} \int \frac{d^3 k}{(2\pi)^3} f(i\omega_j + \mu, \vec{k}) \quad (3.2)$$

in order to move the description from the vacuum to the medium. The quark chemical potential μ has been directly incorporated as a real shift in the imaginary energy variable.

If we set $\mu = 0$ and let $T \rightarrow 0$ the Matsubara sum becomes again an integration over the imaginary axis and hence

$$T \sum_{j \in \mathbb{Z}} \int \frac{d^3 k}{(2\pi)^3} f(i\omega_j, \vec{k}) \rightarrow \int_{-i\infty}^{i\infty} \frac{d(i\omega)}{2\pi} \int \frac{d^3 k}{(2\pi)^3} f(i\omega, \vec{k}) = -i \int \frac{d^4 k}{(2\pi)^4} f(k), \quad (3.3)$$

where we performed a Wick rotation in the last step. This shows that the vacuum description in Chapter 2 can be recovered from the medium description.

3.1. Mass Gap

Let us study the gap equation in the new setting. It will be formally identical to (2.38) but with the integral iI_1 replaced by an integral $iI_1(T, \mu)$ according to the above replacement scheme (3.2), i.e.

$$M = m + 8N_f N_c g M iI_1(T, \mu; M), \quad (3.4)$$

where

$$iI_1(T, \mu) = iI_1(T, \mu; M) = -T \sum_{j \in \mathbb{Z}} \int \frac{d^3 k}{(2\pi)^3} \frac{1}{(i\omega_j + \mu)^2 - E_{\vec{k}}^2}. \quad (3.5)$$

This corresponds to writing the self-energy $\Sigma = 8N_f N_c g M iI_1(T, \mu; M)$ as

$$\Sigma = T \sum_{j \in \mathbb{Z}} \int \frac{d^3 k}{(2\pi)^3} \text{Tr} \left(2gS(i\omega_j + \mu, \vec{k}) \right). \quad (3.6)$$

The mass M will then be given as the solution $M = M(T, \mu; m)$ of the above equation (3.4).

The calculation of the integral $iI_1(T, \mu)$ involves the multiple use of the residue theorem and is performed in Appendix D.1. The result can be written as

$$iI_1(T, \mu) = iI_1^{\text{vac}} + iI_1^{\text{med}}(T, \mu) \quad (3.7)$$

with

$$iI_1^{\text{vac}} = \int \frac{d^3 k}{(2\pi)^3} \frac{1}{2E_{\vec{k}}} \quad (3.8)$$

where iI_1^{vac} is identical to the vacuum result iI_1 obtained in Chapter 2 and

$$iI_1^{\text{med}}(T, \mu) = - \int \frac{d^3 k}{(2\pi)^3} \frac{1}{2E_{\vec{k}}} \left(n_{\vec{k}} + \bar{n}_{\vec{k}} \right), \quad (3.9)$$

where we defined the *quark* and *antiquark occupation number density*

$$n_{\vec{k}} = n_{\vec{k}}(T, \mu; M) = \frac{1}{1 + \exp\left(\frac{E_{\vec{k}} - \mu}{T}\right)} = n_{\text{F}}(E_{\vec{k}} - \mu) \quad (3.10)$$

and

$$\bar{n}_{\vec{k}} = \bar{n}_{\vec{k}}(T, \mu; M) = \frac{1}{1 + \exp\left(\frac{E_{\vec{k}} + \mu}{T}\right)} = n_{\text{F}}(E_{\vec{k}} + \mu) \quad (3.11)$$

with the Fermi distribution function $n_{\text{F}}(z) = (1 + \exp(z/T))^{-1}$. The medium contribution $iI_1^{\text{med}}(T, \mu)$ is finite in contrast to the vacuum contribution iI_1^{vac} . We will hence regularise the vacuum but not the medium contribution of $iI_1(T, \mu)$ using Pauli-Villars regularisation with two regulators (see Appendix D.1 for a more detailed discussion). The medium contribution $iI_1^{\text{med}}(T, \mu)$ vanishes for $\mu = 0$ and $T \rightarrow 0$.

We can also define the *net quark (number) density*

$$n(T, \mu; M) := 2N_{\text{f}}N_{\text{c}} \int \frac{d^3k}{(2\pi)^3} \left(n_{\vec{k}}(T, \mu; M) - \bar{n}_{\vec{k}}(T, \mu; M) \right), \quad (3.12)$$

which is the number density of quarks minus that of the antiquarks.

Plugging in the expression for the integral $iI_1(T, \mu; M)$ into the gap equation (3.4) yields $M = M(T, \mu; m)$. The results are shown in Section 3.3.

3.2. Mesons

We can of course also move our NJL model description of mesons to the medium. The Bethe-Salpeter equation will be formally the same, i.e.

$$D_M = -2g + 2gJ_M D_M \quad (3.13)$$

in the diagonal case (and without isospin or Lorentz indices) with the only difference being that the contribution from the polarisation loop J_M will be calculated in the Matsubara formalism, i.e.

$$J_M(i\omega_n, \vec{p}) = -T \sum_{j \in \mathbb{Z}} \int \frac{d^3k}{(2\pi)^3} \text{Tr} \left(S(i\omega_j + \mu, \vec{k}) \Gamma_M S(i\omega_j + i\omega_n + \mu, \vec{k} + \vec{p}) \Gamma_M \right), \quad (3.14)$$

where the outer Matsubara frequency $i\omega_n = 2\pi i n T$ is a bosonic frequency (related to \vec{p}) and $i\omega_j = (2j + 1)\pi i T$ is a fermionic frequency (related to \vec{k}). Note that the sum of a fermionic and a bosonic Matsubara frequency gives a fermionic Matsubara frequency. The Bethe-Salpeter equation then gives the *Matsubara propagator* of the meson M

$$D_M(i\omega_n, \vec{p}) = \frac{-2g}{1 - 2gJ_M(i\omega_n, \vec{p})}. \quad (3.15)$$

As for the vacuum case, we write the polarisation loop J_M in terms of elementary integrals:

$$\begin{aligned} J_\sigma(i\omega_n, \vec{p}) &= 4N_c N_f iI_1 - 2N_c N_f (i\omega_n^2 - \vec{p}^2 - 4M^2) iI_2(i\omega_n, \vec{p}), \\ J_\pi^{ab}(i\omega_n, \vec{p}) &= \delta_{ab} \left(4N_c N_f iI_1 - 2N_c N_f (i\omega_n^2 - \vec{p}^2) iI_2(i\omega_n, \vec{p}) \right) = \delta_{ab} J_\pi(i\omega_n, \vec{p}). \end{aligned} \quad (3.16)$$

Here, $iI_1 = iI_1(\mu, T)$ (see Section 3.1) and

$$iI_2(i\omega_n, \vec{p}) := -T \int \frac{d^3k}{(2\pi)^3} \sum_{j \in \mathbb{Z}} \frac{1}{(i\omega_j + \mu)^2 - \vec{k}^2 - M^2} \frac{1}{(i\omega_j + i\omega_n + \mu)^2 - (\vec{k} + \vec{p})^2 - M^2} \quad (3.17)$$

are the medium versions of the respective vacuum integrals. It is shown in Appendix D.3 how to further simplify the expression for $iI_2(i\omega_n, \vec{p})$ in analogy to the calculations for iI_1 in Appendix D.1. The result reads

$$\begin{aligned} iI_2(i\omega_n, \vec{p}) &= \int \frac{d^3k}{(2\pi)^3} \left[\left(\frac{1}{E_{\vec{k}}} - \frac{n_F(E_{\vec{k}} + \mu) + n_F(E_{\vec{k}} - \mu)}{2E_{\vec{k}} E_{\vec{k}+\vec{p}}} s_{\vec{k}, \vec{q}} \right) \frac{1}{(i\omega_n)^2 - s_{\vec{k}, \vec{q}}^2} \right. \\ &\quad \left. - \frac{n_F(E_{\vec{k}} + \mu) + n_F(E_{\vec{k}} - \mu)}{2E_{\vec{k}} E_{\vec{k}+\vec{p}}} d_{\vec{k}, \vec{q}} \frac{1}{(i\omega_n)^2 - d_{\vec{k}, \vec{q}}^2} \right] \end{aligned} \quad (3.18)$$

with $s_{\vec{k}, \vec{q}} := E_{\vec{k}+\vec{p}} + E_{\vec{k}}$ and $d_{\vec{k}, \vec{q}} := E_{\vec{k}+\vec{p}} - E_{\vec{k}}$.

Analytic Continuation

The next step in our description of mesons in the medium will be the analytic continuation of the Matsubara propagator $D_M(i\omega_n, \vec{p})$ to real momenta. Depending on the nature of this analytic continuation we get the advanced, retarded or Feynman version of the propagator.

The *retarded propagator* $D_M^+(p_0, \vec{p})$ is obtained from the Matsubara propagator by the substitution $i\omega_n \mapsto p_0 + i\varepsilon$ while the *advanced propagator* $D_M^-(p_0, \vec{p})$ is obtained by substituting $i\omega_n \mapsto p_0 - i\varepsilon$ and only differs from the retarded propagator in the sign of the imaginary part. For definiteness we choose to use the retarded propagator from now on, keeping in mind the close relation between the two propagators.

The retarded polarisation loops J_M^+ are

$$\begin{aligned} J_\pi^+(p_0, \vec{p}) &= 4N_c N_f iI_1 - 2N_c N_f (p_0^2 - \vec{p}^2) iI_2(p_0 + i\varepsilon, \vec{p}), \\ J_\sigma^+(p_0, \vec{p}) &= 4N_c N_f iI_1 - 2N_c N_f (p_0^2 - \vec{p}^2 - 4M^2) iI_2(p_0 + i\varepsilon, \vec{p}). \end{aligned} \quad (3.19)$$

Here, the retarded integral $iI_2^+ := iI_2(p_0 + i\varepsilon, \vec{p})$ takes the form

$$\begin{aligned} iI_2^+(p_0, \vec{p}) &= \int \frac{d^3k}{(2\pi)^3} \left(\left(\frac{1}{E_{\vec{k}}} - \frac{n_{\vec{k}} + \bar{n}_{\vec{k}}}{2E_{\vec{k}+\vec{p}} E_{\vec{k}}} s_{\vec{k}, \vec{p}} \right) \frac{1}{(p_0 + i\varepsilon)^2 - s_{\vec{k}, \vec{p}}^2} \right. \\ &\quad \left. - \frac{n_{\vec{k}} + \bar{n}_{\vec{k}}}{2E_{\vec{k}+\vec{p}} E_{\vec{k}}} d_{\vec{k}, \vec{p}} \frac{1}{(p_0 + i\varepsilon)^2 - d_{\vec{k}, \vec{p}}^2} \right). \end{aligned} \quad (3.20)$$

As described in Appendix D.3 we can again split the integral into a vacuum and a medium contribution

$$iI_2^+(p_0, \vec{p}) = iI_2^{+, \text{vac}}(p_0, \vec{p}) + iI_2^{+, \text{med}}(p_0, \vec{p}). \quad (3.21)$$

The vacuum contribution is obtained from $iI_2^+(p_0, \vec{p})$ for $T, \mu \rightarrow 0$ and given by

$$iI_2^{+, \text{vac}}(p_0, \vec{p}) = \int \frac{d^3k}{(2\pi)^3} \frac{1}{E_{\vec{k}}} \frac{1}{(p_0 + i\varepsilon)^2 - s_{\vec{k}, \vec{p}}^2} = \begin{cases} iI_2(p^2), & \text{if } p_0 > 0 \\ (iI_2(p^2))^*, & \text{if } p_0 < 0 \end{cases}, \quad (3.22)$$

which is just the integral $iI_2(p^2)$ we obtained in the vacuum discussion (see (2.65)) modulo a possible complex conjugation depending on the fact that we calculated the retarded rather than the Feynman expression of the integral. The vacuum part is divergent and will be regularised as described in the previous chapter.

The rest of the integral is the medium part

$$iI_2^{+, \text{med}}(p_0, \vec{p}) = - \int \frac{d^3k}{(2\pi)^3} \frac{n_{\vec{k}} + \bar{n}_{\vec{k}}}{2E_{\vec{k}+\vec{p}}E_{\vec{k}}} \left(\frac{s_{\vec{k}, \vec{p}}}{(p_0 + i\varepsilon)^2 - s_{\vec{k}, \vec{p}}^2} + \frac{d_{\vec{k}, \vec{p}}}{(p_0 + i\varepsilon)^2 - d_{\vec{k}, \vec{p}}^2} \right), \quad (3.23)$$

which is convergent and will not be regularised. The medium part explicitly depends on p_0 and \vec{p} (see also comment below). The real and imaginary part of $iI_2^{+, \text{med}}(p_0, \vec{p})$ are conveniently treated separately. The imaginary part can be integrated analytically and the calculations as well as the rather lengthy result are given in Appendix D.3. The real part can then be obtained from the imaginary part using a Kramers-Kronig relation [75, 76] as is also described there.

Meson Masses

The following considerations will be analogous to the vacuum description (see Section 2.5.1). The retarded meson propagator should have a singularity at the meson's mass m_M . In pole approximation we write

$$D_M^+(p_0, \vec{p}) \approx \frac{g_{Mqq}^2}{p_0^2 - \vec{p}^2 - m_M^2} \quad (3.24)$$

(treating p_0 and \vec{p} separately in contrast to the vacuum case). This corresponds to the inverse propagator having a zero at the meson mass. More generally, to account for a possible imaginary part of the inverse propagator, we will again focus on the real part of the inverse propagator and define the meson mass via

$$1 - 2g\text{Re}J_M^+ \left(p_0 = \pm \sqrt{m_M^2 + \vec{p}^2}, \vec{p} \right) \stackrel{!}{=} 0. \quad (3.25)$$

We could have equally well used the advanced or the Feynman propagator. They are related via complex conjugation depending on the sign of p_0 and hence they will all yield the same mass according to the above definition.

The resulting mass m_M will of course depend on T and μ but also on the three-momentum \vec{p} , which is the momentum of the meson relative to the thermal medium.

This is different to the vacuum case, where J_M only depends on p^2 because all expressions had to be Lorentz covariant due to the lack of a special frame of reference. The meson masses in the medium show in fact a slight dependence on $|\vec{p}|$ and in calculations we will set $\vec{p} = 0$ (and hence $p^2 = p_0^2$) for the determination of the meson masses. The integral $iI_2^+(p_0, \vec{p})$ for the special case $\vec{p} = 0$, which is needed in the calculations, is calculated in Section D.2 of the Appendix and yields a much simpler result than the one for general \vec{p} calculated in Appendix D.3.

Quark-Pion Coupling Constant

Generalising formula (2.81) for the quark-pion coupling from the vacuum to the medium case (with vanishing three-momentum \vec{p}) yields

$$g_{\pi qq}^{-2} = -N_c N_f \left(iI^+(0, 0) + iI^+(m_\pi, 0) - m_\pi^2 iK^+(m_\pi, 0) \right). \quad (3.26)$$

Here we use the expressions for the elementary integrals iI^+ and iK^+ calculated in Appendix D.2.

3.3. Results

Calculating all the medium quantities as described in the preceding sections of this chapter, we can present numerical results for the constituent quark mass and the meson masses depending on T . The results are in agreement with [46, 38] and shall only serve as a starting point for the following chapters.

Constituent Quark Mass

Let $\mu = 0$. We observe that the constituent quark mass is maximal for $T = 0$ and takes the vacuum value we calculated in Section 2.4 corresponding to the spontaneous breaking of the (approximate) chiral symmetry. Hence the constituent quark mass M is much larger than the bare quark mass (which explicitly breaks chiral symmetry). For increasing temperature, M becomes smaller corresponding to the restoration of chiral symmetry. This happens via a crossover (i.e. M is a smooth function of T). The result for parameter set [C] is shown in Figure 3.1. The plot also shows the result in the chiral limit

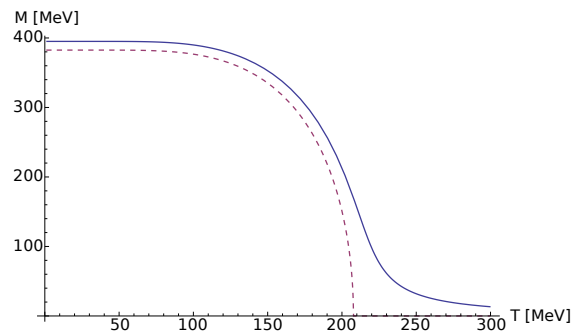


Figure 3.1.: Constituent quark mass M at $\mu = 0$ as function of T for parameter set [C] (solid line) and in the chiral limit (dashed line).

limit, i.e. for the modified parameter set [C] with $m = 0$. In that case there is a second order phase transition (i.e. M is a continuous but not differentiable function of T) at a critical temperature of $T_c = 207.7$ MeV.

Meson Masses

We finally calculate the masses of the π and σ mesons as functions of temperature T for $\mu = 0$. The results are shown in Figure 3.2. Let us first discuss the results in the

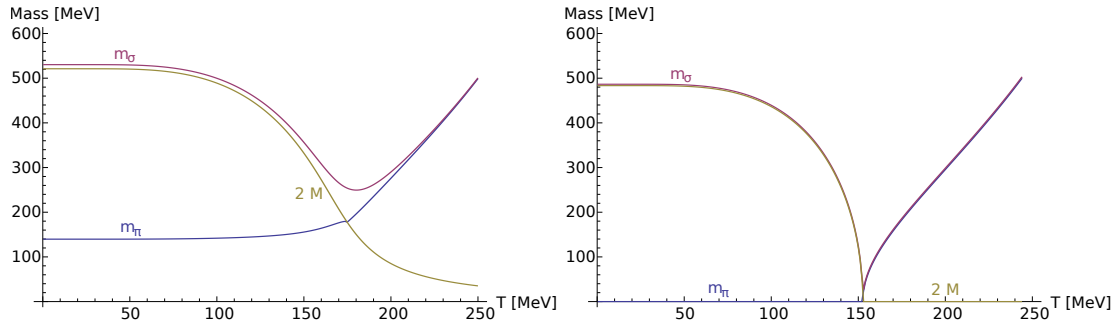


Figure 3.2.: Masses of π and σ mesons for $\mu = 0$ as a function of T for parameter set [A] (left) and in the chiral limit (modified parameter set [A], right). They are compared with twice the constituent quark mass M .

chiral limit. For small T , chiral symmetry is spontaneously broken and the pions are the corresponding massless Goldstone bosons. At $T \approx 160$ MeV there is a second-order phase transition to the chirally symmetric phase. The pions become massive and their mass becomes larger with increasing T . The σ meson is massive in the broken phase and has exactly twice the constituent quark mass M . Since M drops to zero at the temperature of the phase transition, the σ meson is here massless as well. Whilst the constituent mass is zero in the chirally symmetric phase, the mass of the π and the σ are degenerate and hence the σ becomes heavier again for larger T .

For a non-vanishing bare quark mass m , the chiral symmetry is only approximate and hence the pion is not massless at zero temperature, however much lighter than two times the constituent quark mass, which is approximately the mass of the σ meson. For larger T there is a crossover to the chirally symmetric phase: the pion becomes heavier and the constituent quark mass drops. The sigma meson and the pion become nearly degenerate in mass for large T .

4. Pion-Pion Scattering

In the following we want to study the scattering of pions in the simple NJL model, which incorporates pions and sigma mesons [41, 43, 40]. We will consider diagrams in lowest order of a $1/N_c$ expansion scheme. We will for the first time give fully momentum dependent solutions of the invariant matrix elements for these diagrams in vacuum (see (4.21) and (4.37)). The following derivations will be made in the vacuum case but the generalisation to finite temperatures (see Section 4.4) is achieved by calculating medium expressions for the appearing elementary integrals. However, in order to do so we will have to make some simplifications.

Scattering Theory

We are interested in the invariant matrix element $i\mathcal{M}_{\pi\pi}^{ab;cd}$ describing the reaction

$$\pi^a + \pi^b \rightarrow \pi^c + \pi^d \quad (4.1)$$

where a, b, c, d are the isospin indices of the pions. The pions are on-shell (i.e. $p_i^2 = m_\pi^2$) and have four-momenta p_1, p_2, p_3 and p_4 with $p_i = (\sqrt{m_\pi^2 + \vec{p}_i^2}, \vec{p}_i)^t$ where $\vec{p}_1, \vec{p}_2, \vec{p}_3$ and \vec{p}_4 are the corresponding three-momenta. The invariant matrix element is related to the T -matrix in scattering theory via [58]

$$\langle \pi^c, \vec{p}_3; \pi^d, p_4 | iT | \pi^a, \vec{p}_1; \pi^b, \vec{p}_2 \rangle = (2\pi)^4 \delta^{(4)}(p_1 + p_2 - p_3 - p_4) i\mathcal{M}_{\pi\pi}^{ab;cd}(p_1, p_2, p_3, p_4). \quad (4.2)$$

The vacuum matrix elements $i\mathcal{M}_{\pi\pi}^{ab;cd}$ are Lorentz scalars (which is why they are called *invariant* matrix elements). The δ -distribution in the above expression suggests that we need to calculate the invariant matrix elements for momenta with $p_1 + p_2 = p_3 + p_4$, i.e. with four-momentum conservation.

As the matrix elements are Lorentz invariant we can calculate them in any frame of reference. It is advantageous to work in the center-of-mass frame (see Figure 4.1), in which $\vec{p}_1 = -\vec{p}_2 =: \vec{p}$ and by momentum conservation $\vec{p}_3 = -\vec{p}_4 =: \vec{p}'$. The zeroth components of the four-momenta are determined by the on-shell condition and given by $E = \sqrt{\vec{p}^2 + m_\pi^2}$ and $E' = \sqrt{\vec{p}'^2 + m_\pi^2}$, respectively. Energy conservation $E = E'$ then requires $\vec{p}^2 = \vec{p}'^2$. Hence the matrix elements only depend on the two quantities \vec{p}^2 and $\cos \vartheta := \frac{\vec{p} \cdot \vec{p}'}{\vec{p}^2}$.

Mandelstam Variables

Another convenient description of the kinematics can be obtained using the Mandelstam variables [77]

$$s = (p_1 + p_2)^2, \quad t = (p_1 - p_3)^2, \quad u = (p_1 - p_4)^2. \quad (4.3)$$

They are by definition Lorentz invariant quantities and again encode all the necessary information for the invariant matrix elements $\mathcal{M}_{\pi\pi}^{ab;cd}$ of the scattering process $1 + 2 \rightarrow$

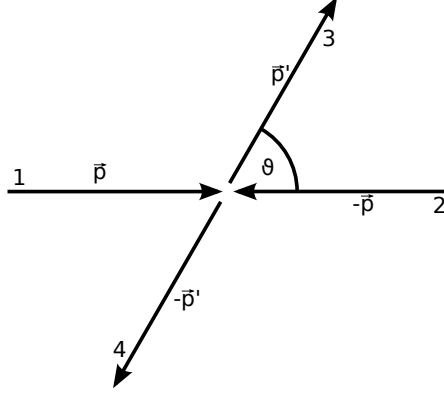


Figure 4.1.: Scattering process $1 + 2 \rightarrow 3 + 4$ in the center-of-mass system (CMS).

$3 + 4$. We can hence write $\mathcal{M}_{\pi\pi}^{ab;cd} = \mathcal{M}_{\pi\pi}^{ab;cd}(s, t, u)$. Considering on-shell particles with masses m_1, \dots, m_4 the Mandelstam variables fulfil the relation

$$s + t + u = m_1^2 + m_2^2 + m_3^2 + m_4^2 \quad (4.4)$$

and so in case of pion-pion scattering

$$s + t + u = 4m_\pi^2. \quad (4.5)$$

This means also that only two of the three Mandelstam variables are independent.

The situation is however even more restricted. A simple calculation shows that in our case (with all masses equal) the Mandelstam variables obey

$$s \geq 4m_\pi^2, \quad t \leq 0, \quad u \leq 0. \quad (4.6)$$

The situation is depicted in Figure 4.2. There is a certain physically accessible region in the s - t - u -plane. If the masses of the involved particles are not the same, the picture will be similar but the physical region will have a more complicated shape.

If we are in the center-of-mass frame as described above, one easily calculates

$$s = 4m_\pi^2 + 4\vec{p}^2, \quad t = -4\vec{p}^2 \sin^2(\vartheta/2), \quad u = -4\vec{p}^2 \cos^2(\vartheta/2). \quad (4.7)$$

Parametrisation of the Matrix Elements

In general the invariant matrix element for pion-pion scattering can be written in terms of three unknown functions

$$\mathcal{M}_{\pi\pi}^{ab;cd}(s, t, u) = A(s, t, u)\delta_{ab}\delta_{cd} + B(s, t, u)\delta_{ac}\delta_{bd} + C(s, t, u)\delta_{ad}\delta_{bc}, \quad (4.8)$$

where each function corresponds to a different isospin channel [41]. Making use of perfect crossing symmetry even yields

$$A(s, t, u) = B(t, s, u) = C(u, t, s). \quad (4.9)$$

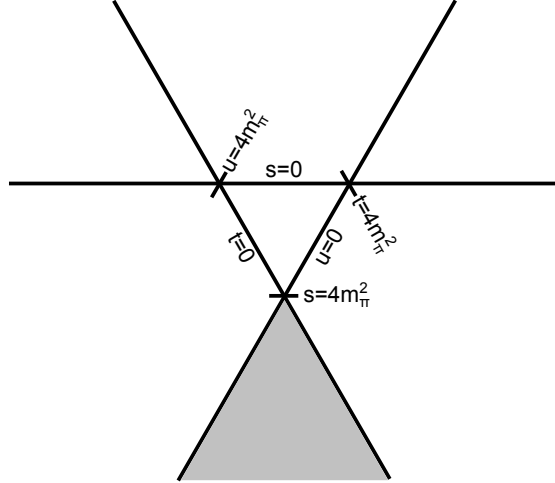


Figure 4.2.: Mandelstam variables plotted into the s - t - u -plane with the condition $s + t + u = 4m_\pi^2$. The physically accessible region is shaded grey.

Moreover, one can project out the amplitudes $\mathcal{M}_{\pi\pi}^I$ of definite total isospin $I = 0, 1, 2$ [78]. This gives

$$\begin{aligned}\mathcal{M}_{\pi\pi}^0 &= 3A(s, t, u) + B(s, t, u) + C(s, t, u), \\ \mathcal{M}_{\pi\pi}^1 &= B(s, t, u) - C(s, t, u), \\ \mathcal{M}_{\pi\pi}^2 &= B(s, t, u) + C(s, t, u).\end{aligned}\tag{4.10}$$

Large N_c Expansion

We want to calculate the invariant matrix elements by evaluating the simplest possible diagrams for pion-pion scattering in the NJL model. These are shown in Figure 4.3. The

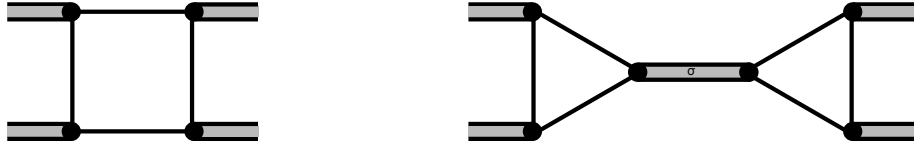


Figure 4.3.: Pion-pion scattering via the box diagram (left) and via a sigma-meson exchange (right).

first diagram is called *box diagram* for obvious reasons. The interaction takes place via a quark box. The second diagram is called *sigma-propagation diagram* since the scattering process is mediated by a sigma meson (in RPA) as described in the previous chapters. The pions are coupled to the sigma meson via a quark triangle. Since two pions cannot scatter into one single pion because of parity and angular momentum conservation there is no ‘pion propagation diagram’.

In principle there are of course many more diagrams contributing to pion-pion scattering in the NJL model. By doing a systematic $1/N_c$ expansion [79] one finds that these

two diagrams are indeed the two leading order diagrams in $1/N_c$ [46, 38]. The advantage of such an expansion is that taking all diagrams up to a given order preserves the symmetry properties of the theory, which will be very useful in the following discussions.

The ingredients for describing pion-pion scattering are the quark propagator S , the quark-meson vertex Γ_{Mqq} and for the sigma-propagation diagram also the meson propagator \mathcal{D}_M . We have computed these quantities in Chapter 2.

4.1. Sigma-Propagation Diagram

We will begin by calculating the contribution from the sigma-propagation diagram. In fact, there are three different Feynman diagrams, each of which is characterised by the Mandelstam variable associated to the momentum of the intermediary sigma meson. Accordingly, we name them s -, t - and u -channel diagram (see Figures 4.4, 4.5 and 4.6). These diagrams are all related by a relabelling of momenta and isospin indices. There are

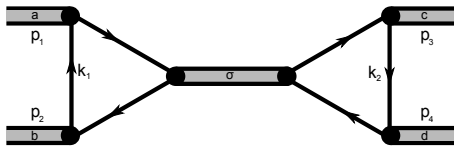


Figure 4.4.: s -channel.

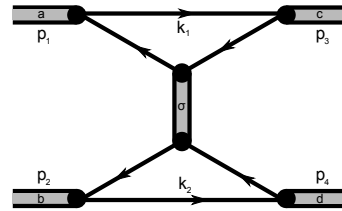


Figure 4.5.: t -channel.

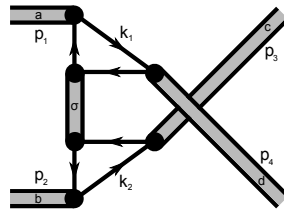


Figure 4.6.: u -channel.

four external momenta p_1, \dots, p_4 and two internal momenta k_1, k_2 (one for each quark triangle), over which we integrate. In the evaluation of the Feynman diagrams there is an additional factor of 2 for each quark triangle since in each quark triangle one could have drawn the quark lines with arrows in the opposite direction. This would give the same contribution since the minus sign arising from the Dirac trace will be cancelled by another minus sign arising from flavour factors.

In the following we will evaluate the diagram for the s -channel and subsequently obtain the expressions for the other channels by an appropriate relabelling of indices (see (4.20)).

***s*-Channel**

For the *s*-channel we straightforwardly get

$$\begin{aligned}
i\mathcal{M}_{\pi\pi,s}^{ab;cd} &= (-2) \int \frac{d^4k_1}{(2\pi)^4} \text{Tr} \left(i\Gamma_\pi^a g_{\pi qq}(p_1) iS(k_1 + p_1) i\Gamma_\sigma g_{\sigma qq}(p_1 + p_2) iS(k_1 - p_2) \times \right. \\
&\quad \times \left. i\Gamma_\pi^b g_{\pi qq}(p_2) iS(k_1) \right) (i\mathcal{D}_\sigma(p_1 + p_2)) (-2) \int \frac{d^4k_2}{(2\pi)^4} \text{Tr} \times \\
&\quad \times \left(i\Gamma_\pi^d g_{\pi qq}(p_4) iS(k_2 - p_4) i\Gamma_\sigma g_{\sigma qq}(p_1 + p_2) iS(k_2 + p_3) i\Gamma_\pi^c g_{\pi qq}(p_3) iS(k_2) \right),
\end{aligned} \tag{4.11}$$

which we can simplify to

$$\begin{aligned}
\mathcal{M}_{\pi\pi,s}^{ab;cd} &= -g_{\pi qq}^4 2i \int \frac{d^4k_1}{(2\pi)^4} \text{Tr} \left(\gamma_5 \tau^a S(k_1 + p_1) S(k_1 - p_2) \gamma_5 \tau^b S(k_1) \right) \times \\
&\quad \times (D_\sigma(p_1 + p_2)) 2i \int \frac{d^4k_2}{(2\pi)^4} \text{Tr} \left(\gamma_5 \tau^d S(k_2 - p_4) S(k_2 + p_3) \gamma_5 \tau^c S(k_2) \right),
\end{aligned} \tag{4.12}$$

where we replaced $g_{\pi qq}(p_i)$, which only depends on $p_i^2 = m_\pi^2$ by the corresponding on-shell expression $g_{\pi qq}$ (see Section 2.5.1).

As a next step we calculate the trace over flavour and colour space. Using

$$\text{tr}(\tau^a \tau^b) = \frac{1}{2} \text{tr}(\{\tau^a \tau^b\}) = \frac{1}{2} \text{tr}(2\delta_{ab} \mathbf{1}) = N_f \delta_{ab} \tag{4.13}$$

we get

$$\begin{aligned}
\mathcal{M}_{\pi\pi,s}^{ab;cd} &= -\delta_{ab} \delta_{cd} (2N_f N_c)^2 g_{\pi qq}^4 i \int \frac{d^4k_1}{(2\pi)^4} \text{tr} (S(k_1 + p_1) S(k_1 - p_2) S(-k_1)) \times \\
&\quad \times (D_\sigma(p_1 + p_2)) i \int \frac{d^4k_2}{(2\pi)^4} \text{tr} (S(k_2 - p_4) S(k_2 + p_3) S(-k_2)),
\end{aligned} \tag{4.14}$$

where we also eliminated the γ_5 -matrices via $\gamma_5 S(p) \gamma_5 = S(-p)$ for arbitrary p .

The most cumbersome part of our calculations will be the evaluation of the Dirac traces and momentum integrals in the above expressions for the quark triangles. In general we have to deal with an integral of the form

$$i\Delta_{p,q} := i \int \frac{d^4k}{(2\pi)^4} \text{tr} (S(-k) S(k + p) S(k + q)), \tag{4.15}$$

where p and q are arbitrary four-momenta. We call $i\Delta_{p,q}$ the *quark triangle*. Evaluating the traces and making clever substitutions in the integrals, one finds after some steps (see Appendix E.1) that the quark triangle can be written in the form

$$i\Delta_{p,q} = -4M iI_2(p - q) + 4M(p \cdot q) iI_3(p, q), \tag{4.16}$$

where we defined the elementary integral⁶

$$iI_3(p, q) := i \int \frac{d^4k}{(2\pi)^4} \frac{1}{(k^2 - M^2 + i\varepsilon) ((k+p)^2 - M^2 + i\varepsilon) ((k+q)^2 - M^2 + i\varepsilon)} \quad (4.17)$$

and $iI_2(p)$ is the integral we defined in Section 2.5.

The integral $iI_3(p, q)$ is in principle of the same kind as iI_1 and $iI_2(p)$ but more difficult to evaluate due to its more complicated momentum dependence. It depends on the Lorentz scalars p^2 , q^2 and $p \cdot q$. A general treatise on the so-called *scalar one-loop integrals* can be found in [80, 81, 82]. The main ideas and results will be described in Appendix C.5. The integral $iI_3(p, q)$ (and also the integral $iI_4(p, q, r)$, which we will define later) are implemented in the LoopTools package [83], which can be obtained from [84].

Putting all our findings together we can write down the s -channel matrix element in the form

$$\mathcal{M}_{\pi\pi, s}^{ab;cd} = -\delta_{ab}\delta_{cd}(2N_f N_c)^2 g_{\pi qq}^4 i \Delta_{p_1, -p_2} D_\sigma(p_1 + p_2) i \Delta_{-p_4, p_3}. \quad (4.18)$$

As we are studying on-shell pions, $p^2 = q^2 = m_\pi^2$ for each of the quark-triangles we evaluated above. Hence $I_3(p, q) = I_3(p^2, q^2, p \cdot q)$ only depends on $p \cdot q$ or alternatively $(p - q)^2 = 2(m_\pi^2 - p \cdot q)$. We can therefore also write $i\Delta_{p, q} = i \Delta((p - q)^2)$. This means in particular that both quark triangles evaluate to the same result. Similarly, the sigma-meson propagator $D_\sigma(p^2)$ only depends on p^2 and using Mandelstam variables we can write the above result as

$$\mathcal{M}_{\pi\pi, s}^{ab;cd} = -\delta_{ab}\delta_{cd}(2N_f N_c)^2 g_{\pi qq}^4 (i \Delta(s))^2 D_\sigma(s). \quad (4.19)$$

Further Channels

There is a general replacement scheme which allows us to write down the results for the other two channels without further calculations. To get from the s -channel to the t -channel or the u -channel, we need to perform the following replacements:

Channel	Quantity										
s	p_1	p_2	p_3	p_4	s	t	u	a	b	c	d
t	p_1	$-p_3$	$-p_2$	p_4	t	s	u	a	c	b	d
u	p_1	$-p_4$	p_3	$-p_2$	u	t	s	a	d	c	b

(4.20)

The table is to be read in the sense that to get from one channel to another we have to replace all the quantities in the corresponding row by those in the other row.

⁶The integral $iI_3(p, q)$ is convergent in contrast to iI_1 and $iI_2(p)$ and hence does not need to be regularised. We will nonetheless also apply the Pauli-Villars regularisation scheme to this integral for reasons of consistency. Note however that the difference between the regularised version and the original $iI_3(p, q)$ is rather negligible. The same is true for the integral $iI_4(p, q, r)$ (see (4.36)) where we will also apply the Pauli-Villars regularisation scheme with two regulators.

In the above case the replacement is rather simple, yielding

$$\begin{aligned}
\mathcal{M}_{\pi\pi,s}^{ab;cd} &= -\delta_{ab}\delta_{cd}(2N_f N_c)^2 g_{\pi qq}^4 (i \Delta(s))^2 D_\sigma(s), \\
\mathcal{M}_{\pi\pi,t}^{ab;cd} &= -\delta_{ac}\delta_{bd}(2N_f N_c)^2 g_{\pi qq}^4 (i \Delta(t))^2 D_\sigma(t), \\
\mathcal{M}_{\pi\pi,u}^{ab;cd} &= -\delta_{ad}\delta_{bc}(2N_f N_c)^2 g_{\pi qq}^4 (i \Delta(u))^2 D_\sigma(u).
\end{aligned} \tag{4.21}$$

All matrix elements are identical functions of one variable, where in each channel the result depends on the Mandelstam variable giving the channel its name.

Static Limit

So far in most other publications on NJL pion-pion scattering only the limiting case for $s = 4m_\pi^2$ and $t = u = 0$ has been studied. In this case, it is easy to show that all the momenta of the incoming and outgoing particles have to be equal, i.e. $p_1 = p_2 = p_3 = p_4 =: p$. Hence, in the center-of-mass frame all (incoming and outgoing) pions are at rest, which is the reason why this limiting case is called *static limit*.

We will study the static limit because we will only be able to give the medium expressions for the elementary integrals iI_1 and $iI_2(p)$ and for special cases (corresponding to the static limit) of the integrals $iI_3(p, q)$ or $iI_4(p, q, r)$. For the latter two a general temperature-dependent expression has yet to be found.

To obtain the static limit matrix elements we begin from (4.21) and evaluate $i \Delta(p^2)$ and $D_\sigma(p^2)$ at $p^2 = 4m_\pi^2$ for the s -channel and at $p^2 = 0$ for the t - and u -channel. We first calculate $i \Delta(4m_\pi^2) = i \Delta_{p,-p}$ and $i \Delta(0) = i \Delta_{p,p}$, which now only depend on one external momentum p .

Following [40] we define the elementary integrals⁷

$$\begin{aligned}
iI(p) &:= iI_2(p) = i \int \frac{d^4 k}{(2\pi)^4} \frac{1}{(k^2 - M^2 + i\varepsilon)} \frac{1}{((k+p)^2 - M^2 + i\varepsilon)}, \\
iK(p) &:= i \int \frac{d^4 k}{(2\pi)^4} \frac{1}{(k^2 - M^2 + i\varepsilon)^2} \frac{1}{((k+p)^2 - M^2 + i\varepsilon)}, \\
iL(p) &:= i \int \frac{d^4 k}{(2\pi)^4} \frac{1}{(k^2 - M^2 + i\varepsilon)^2} \frac{1}{((k+p)^2 - M^2 + i\varepsilon)^2}.
\end{aligned} \tag{4.22}$$

The integrals iI , iK and iL only depend on p^2 rather than the four-vector p . In fact, by performing the k_0 -integration these integrals can be written as the following radial momentum integrals [41]

$$\begin{aligned}
iI(p^2) &= \frac{1}{2\pi^2} \int_0^\infty dk \frac{k^2}{E_k^-(p^2 - 4E_k^2 + i\varepsilon)}, \\
iK(p^2) &= \frac{1}{8\pi^2} \int_0^\infty dk \frac{k^2(12E_k^2 - p^2)}{E_k^3(p^2 - 4E_k^2 + i\varepsilon)^2}, \\
iL(p^2) &= \frac{1}{4\pi^2} \int_0^\infty dk \frac{(20E_k^2 - p^2)k^2}{E_k^3(p^2 - 4E_k^2 + i\varepsilon)^3}.
\end{aligned} \tag{4.23}$$

⁷The integral $iL(p)$ will only be needed later for the evaluation of the box diagram in the static limit (see Section 4.2).

We performed this calculation for $iI(p^2)$ in Appendix C.2. The above integrals can then be calculated analytically for which some care is needed to take care of the pole structure of the integrand. The calculations and the rather lengthy results are given in Appendix C.3.

The results for the special cases of the quark triangles $i\Delta_{p,p}$ and $i\Delta_{p,-p}$ can be expressed in terms of these elementary integrals and one finds (see Appendix E.2)

$$\begin{aligned} i\Delta_{p,p} &= -4M \left(iI(0) - p^2 iK(p) \right) \\ i\Delta_{p,-p} &= -4M iI(p) \end{aligned} \quad (4.24)$$

in agreement with [40]. For an on-shell momentum with $p^2 = m_\pi^2$ one obtains $i\Delta(4m_\pi^2) = i\Delta_{p,-p}$ and $i\Delta(0) = i\Delta_{p,p}$.

Next, we calculate $D_\sigma(4m_\pi^2)$ and $D_\sigma(0)$. We saw in Section 2.5.1 that we can write the meson propagator as

$$D_M(p) = -\frac{1}{2N_c N_f ((p^2 - \varepsilon_M^2) iI(p^2) - m_\pi^2 iI(m_\pi))}, \quad (4.25)$$

which yields

$$\begin{aligned} D_\sigma(2p) &= -\frac{1}{2N_c N_f ((4m_\pi^2 - 4M^2) iI(2m_\pi) - m_\pi^2 iI(m_\pi))}, \\ D_\sigma(0) &= -\frac{1}{2N_c N_f (-4M^2 iI(0) - m_\pi^2 iI(m_\pi))} \end{aligned} \quad (4.26)$$

and for an on-shell momentum p we get $D_\sigma(4m_\pi^2) = D_\sigma(2p)$ and $D_\sigma(0) = D_\sigma(0)$.

Finally, in equation (2.81) we wrote the quark-pion coupling constant as

$$g_{\pi qq}^{-2} = -N_c N_f \left(iI(0) + iI(m_\pi) - m_\pi^2 iK(m_\pi) \right). \quad (4.27)$$

Inserting the expression for $i\Delta$, D_σ and $g_{\pi qq}$ into (4.21) we obtain

$$\begin{aligned} \mathcal{M}_{\pi\pi,s}^{ab;cd} &= -\delta_{ab}\delta_{cd} \frac{8}{N_f N_c} \frac{(iI(m_\pi))^2}{(iI(0) + iI(m_\pi) - m_\pi^2 iK(m_\pi))^2 \left(\left(1 - \frac{m_\pi^2}{M^2}\right) iI(2m_\pi) + \frac{m_\pi^2}{4M^2} iI(m_\pi) \right)}, \\ \mathcal{M}_{\pi\pi,t}^{ab;cd} &= -\delta_{ac}\delta_{bd} \frac{8}{N_f N_c} \frac{(iI(0) - m_\pi^2 iK(m_\pi))^2}{(iI(0) + iI(m_\pi) - m_\pi^2 iK(m_\pi))^2 \left(iI(0) + \frac{m_\pi^2}{4M^2} iI(m_\pi) \right)}, \\ \mathcal{M}_{\pi\pi,u}^{ab;cd} &= -\delta_{ad}\delta_{bc} \frac{8}{N_f N_c} \frac{(iI(0) - m_\pi^2 iK(m_\pi))^2}{(iI(0) + iI(m_\pi) - m_\pi^2 iK(m_\pi))^2 \left(iI(0) + \frac{m_\pi^2}{4M^2} iI(m_\pi) \right)} \end{aligned} \quad (4.28)$$

for the matrix elements for pion-pion scattering via sigma-meson exchange in the static limit, i.e. with $s = 4m_\pi^2$ and $t = u = 0$.

Semi-Static Limit

We argued that we make the static limit approximation in order to obtain simpler expressions for the invariant matrix elements which can also be calculated in a medium approach. However, completely ignoring the momentum dependence of the sigma-meson propagator is certainly not a very good approximation, especially when studying the temperature dependence of the matrix elements (see Section 3.3). On the other hand only the quark triangles depend on $iI_3(p, q)$ while the meson propagator only contains iI_1 and $iI_2(p)$. The two latter integrals can be calculated in the medium (see Appendices D.1 and D.3). As a compromise between the full momentum dependence and the static limit it is therefore suggested in [10, 47] to apply the static limit only to the quark triangles while exactly calculating the sigma-meson propagator. We will call this approximation *semi-static limit*. The matrix elements are given by

$$\begin{aligned}\mathcal{M}_{\pi\pi,s}^{ab;cd} &= -\delta_{ab}\delta_{cd}(2N_f N_c)^2 g_{\pi qq}^4 (i \Delta(4m_\pi^2))^2 D_\sigma(s), \\ \mathcal{M}_{\pi\pi,t}^{ab;cd} &= -\delta_{ac}\delta_{bd}(2N_f N_c)^2 g_{\pi qq}^4 (i \Delta(0))^2 D_\sigma(t), \\ \mathcal{M}_{\pi\pi,u}^{ab;cd} &= -\delta_{ad}\delta_{bc}(2N_f N_c)^2 g_{\pi qq}^4 (i \Delta(0))^2 D_\sigma(u),\end{aligned}\tag{4.29}$$

where all appearing expressions have been calculated in the two preceding subsections.

4.2. Box Diagram

In the second type of diagram we consider the pion-pion scattering occurring via a quark quadrilateral or *quark box*. The box diagram also exists for three different momentum configurations as shown in Figure 4.7. We label them with 1, 2 and 3. It is apparent that

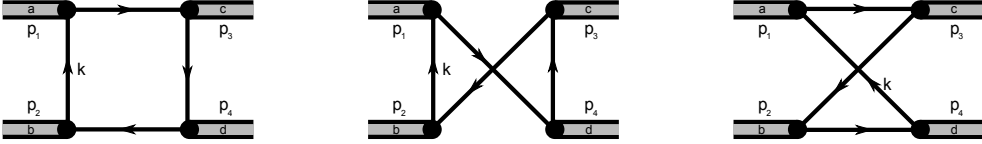


Figure 4.7.: All possible box diagrams for pion-pion scattering.

the momentum structure is more complicated than for the sigma exchange diagram but it is again possible to obtain the expressions for the different channels by an appropriate relabelling:

Channel	Quantity											
1	p_1	p_2	p_3	p_4	s	t	u	a	b	c	d	
2	p_1	p_2	p_4	p_3	s	u	t	a	b	d	c	
3	p_1	$-p_4$	p_3	$-p_2$	u	t	s	a	d	c	b	

(4.30)

We evaluate the contribution from the first diagram to be

$$\begin{aligned}
i\mathcal{M}_{\pi\pi,1}^{ab;cd} &= -2 \int \frac{d^4k}{(2\pi)^4} \text{Tr}(ig_{\pi qq}(p_1)\Gamma_\pi^a iS(p_1+k)ig_{\pi qq}(p_3)\Gamma_\pi^c iS(p_1-p_3+k) \times \\
&\quad \times ig_{\pi qq}(p_4)\Gamma_\pi^d iS(-p_2+k)ig_{\pi qq}(p_2)\Gamma_\pi^b iS(k)) \\
&= -2g_{\pi qq}^4 \int \frac{d^4k}{(2\pi)^4} \text{Tr}(\gamma_5\tau^a S(p_1+k) \times \\
&\quad \times \gamma_5\tau^c S(p_1-p_3+k)\gamma_5\tau^d S(-p_2+k)\gamma_5\tau^b S(k)),
\end{aligned} \tag{4.31}$$

where the factor of 2 again comes from the fact that we could have drawn the internal quark lines also in the opposite direction. Again, we can evaluate the trace in isospin and colour space. We use the relation

$$\text{tr}(\tau^a\tau^c\tau^d\tau^b) = N_f(\delta_{ab}\delta_{cd} + \delta_{ac}\delta_{db} - \delta_{ad}\delta_{cb}) \tag{4.32}$$

and get

$$\begin{aligned}
\mathcal{M}_{\pi\pi,1}^{ab;cd} &= 2N_c N_f (\delta_{ab}\delta_{cd} + \delta_{ac}\delta_{db} - \delta_{ad}\delta_{cb}) g_{\pi qq}^4 \times \\
&\quad \times i \int \frac{d^4k}{(2\pi)^4} \text{tr}(S(p_1+k)S(-p_1+p_3-k)S(-p_2+k)S(-k)).
\end{aligned} \tag{4.33}$$

We have to deal with an integral of the form

$$i\Box_{p,q,r} := i \int \frac{d^4k}{(2\pi)^4} \text{tr}(S(p+k)S(-p+q-k)S(-r+k)S(-k)), \tag{4.34}$$

which we will call *quark box*. A rather tedious calculation (see Appendix E.3) leads to the following expression in terms of elementary integrals

$$\begin{aligned}
i\Box_{p,q,r} &= 2 \left[2(r \cdot p)(p \cdot q) - (r \cdot p)q^2 + r^2(p \cdot q) - (r \cdot q)p^2 \right] iI_4(p, q, r+p) \\
&\quad - 2r \cdot (p - q + r) iI_3(q - p, r) + 2(p \cdot r) iI_3(p, -r) \\
&\quad - 2(p \cdot q) iI_3(p, q) + 2(q \cdot (p + r - q)) iI_3(q, r+p) \\
&\quad + 2iI_2(p - q) + 2iI_2(p + r),
\end{aligned} \tag{4.35}$$

where we defined the integral⁸

$$\begin{aligned}
iI_4(p, q, r) &:= i \int \frac{d^4k}{(2\pi)^4} \frac{1}{(k^2 - M^2 + i\varepsilon)} \frac{1}{((k+p)^2 - M^2 + i\varepsilon)} \times \\
&\quad \times \frac{1}{((k+q)^2 - M^2 + i\varepsilon)} \frac{1}{((k+r)^2 - M^2 + i\varepsilon)}
\end{aligned} \tag{4.36}$$

(for general p , q and r) in analogy to $iI_2(p)$ and $iI_3(p, q)$. We can evaluate this integral similar to $iI_3(p, q)$ (see Appendix C.5) and will again rely on the LoopTools package in

⁸As already mentioned for $iI_3(p, q)$ we will also regularise this already convergent integral $iI_4(p, q, r)$ with the Pauli-Villars regularisation scheme we applied to iI_1 and $iI_2(p)$ for reasons of consistency.

order to do so. The integral $iI_4(p, q, r)$ depends on the Lorentz scalars $p^2, q^2, r^2, p \cdot q, p \cdot r$ and $q \cdot r$. In the situation of pion-pion scattering the momenta p, q and r are on-shell for the pion and hence the dependence is only on $p \cdot q, p \cdot r$ and $q \cdot r$ since $p^2 = q^2 = r^2 = m_\pi^2$.

With the quark box $i\Box_{p,q,r}$ we can write the matrix elements for the contribution from the box diagram in the following simple way:

$$\begin{aligned}\mathcal{M}_{\pi\pi,1}^{ab;cd} &= 2N_c N_f (\delta_{ab}\delta_{cd} + \delta_{ac}\delta_{db} - \delta_{ad}\delta_{cb}) g_{\pi qq}^4 i\Box_{p_1,p_3,p_2}, \\ \mathcal{M}_{\pi\pi,2}^{ab;cd} &= 2N_c N_f (\delta_{ab}\delta_{cd} - \delta_{ac}\delta_{db} + \delta_{ad}\delta_{cb}) g_{\pi qq}^4 i\Box_{p_1,p_4,p_2}, \\ \mathcal{M}_{\pi\pi,3}^{ab;cd} &= 2N_c N_f (-\delta_{ab}\delta_{cd} + \delta_{ac}\delta_{db} + \delta_{ad}\delta_{cb}) g_{\pi qq}^4 i\Box_{p_1,p_3,-p_4}.\end{aligned}\tag{4.37}$$

Static Limit

We can also evaluate the box diagrams in the simplified situation of the static limit, i.e. for $p_1 = p_2 = p_3 = p_4 =: p$. In order to do so we have to calculate the quark boxes $i\Box_{p,p,p}$ and $i\Box_{p,p,-p}$. We again use the integrals iI, iK, iL . The calculation in Appendix E.4 yields

$$\begin{aligned}i\Box_{p,p,p} &= -2p^2 iK(p) + 2iI(0) + 2iI(p), \\ i\Box_{p,p,-p} &= 2p^4 iL(p) - 8p^2 iK(p) + 4iI(0).\end{aligned}\tag{4.38}$$

Also plugging in the expression (2.81) for $g_{\pi qq}$ one obtains

$$\begin{aligned}\mathcal{M}_{\pi\pi,1}^{ab;cd} &= \frac{4}{N_c N_f} (\delta_{ab}\delta_{cd} + \delta_{ac}\delta_{db} - \delta_{ad}\delta_{cb}) \frac{1}{iI(0) + iI(m_\pi) - m_\pi^2 iK(m_\pi)}, \\ \mathcal{M}_{\pi\pi,2}^{ab;cd} &= \frac{4}{N_c N_f} (\delta_{ab}\delta_{cd} - \delta_{ac}\delta_{db} + \delta_{ad}\delta_{cb}) \frac{1}{iI(0) + iI(m_\pi) - m_\pi^2 iK(m_\pi)}, \\ \mathcal{M}_{\pi\pi,3}^{ab;cd} &= \frac{4}{N_c N_f} (-\delta_{ab}\delta_{cd} + \delta_{ac}\delta_{db} + \delta_{ad}\delta_{cb}) \frac{(2iI(0) - 4m_\pi^2 iK(m_\pi) + m_\pi^4 iL(m_\pi))}{(iI(0) + iI(m_\pi) - m_\pi^2 iK(m_\pi))^2}.\end{aligned}\tag{4.39}$$

4.3. Results

We summarise the results obtained for the invariant matrix elements. We can write our results as

$$\begin{aligned}\mathcal{M}_{\pi\pi,1}^{ab;cd} &= (\delta_{ab}\delta_{cd} + \delta_{ac}\delta_{db} - \delta_{ad}\delta_{cb}) \mathcal{M}_{\pi\pi,1}, \\ \mathcal{M}_{\pi\pi,2}^{ab;cd} &= (\delta_{ab}\delta_{cd} - \delta_{ac}\delta_{db} + \delta_{ad}\delta_{cb}) \mathcal{M}_{\pi\pi,2}, \\ \mathcal{M}_{\pi\pi,3}^{ab;cd} &= (-\delta_{ab}\delta_{cd} + \delta_{ac}\delta_{db} + \delta_{ad}\delta_{cb}) \mathcal{M}_{\pi\pi,3}\end{aligned}\tag{4.40}$$

and

$$\begin{aligned}\mathcal{M}_{\pi\pi,s}^{ab;cd} &= \delta_{ab}\delta_{cd} \mathcal{M}_{\pi\pi,s}, \\ \mathcal{M}_{\pi\pi,t}^{ab;cd} &= \delta_{ac}\delta_{bd} \mathcal{M}_{\pi\pi,t}, \\ \mathcal{M}_{\pi\pi,u}^{ab;cd} &= \delta_{ad}\delta_{bc} \mathcal{M}_{\pi\pi,u}\end{aligned}\tag{4.41}$$

with

$$\begin{aligned}
\mathcal{M}_{\pi\pi,s} &= -(2N_f N_c)^2 g_{\pi qq}^4 (i \Delta(s))^2 D_\sigma(s), \\
\mathcal{M}_{\pi\pi,t} &= -(2N_f N_c)^2 g_{\pi qq}^4 (i \Delta(t))^2 D_\sigma(t), \\
\mathcal{M}_{\pi\pi,u} &= -(2N_f N_c)^2 g_{\pi qq}^4 (i \Delta(u))^2 D_\sigma(u)
\end{aligned} \tag{4.42}$$

and

$$\begin{aligned}
\mathcal{M}_{\pi\pi,1} &= 2N_c N_f g_{\pi qq}^4 i \square_{p_1, p_3, p_2}, \\
\mathcal{M}_{\pi\pi,2} &= 2N_c N_f g_{\pi qq}^4 i \square_{p_1, p_4, p_2}, \\
\mathcal{M}_{\pi\pi,3} &= 2N_c N_f g_{\pi qq}^4 i \square_{p_1, p_3, -p_4}.
\end{aligned} \tag{4.43}$$

Recalling the decomposition of $\mathcal{M}_{\pi\pi}^{ab;cd}$ into the different isospin channels (see (4.8)) we can identify the components A , B and C . We get

$$\begin{aligned}
A &= \mathcal{M}_{\pi\pi,1} + \mathcal{M}_{\pi\pi,2} - \mathcal{M}_{\pi\pi,3} + \mathcal{M}_{\pi\pi,s}, \\
B &= \mathcal{M}_{\pi\pi,1} - \mathcal{M}_{\pi\pi,2} + \mathcal{M}_{\pi\pi,3} + \mathcal{M}_{\pi\pi,t}, \\
C &= -\mathcal{M}_{\pi\pi,1} + \mathcal{M}_{\pi\pi,2} + \mathcal{M}_{\pi\pi,3} + \mathcal{M}_{\pi\pi,u}.
\end{aligned} \tag{4.44}$$

Using (4.10) we then get

$$\begin{aligned}
\mathcal{M}_{\pi\pi}^0 &= 3\mathcal{M}_{\pi\pi,1} + 3\mathcal{M}_{\pi\pi,2} - \mathcal{M}_{\pi\pi,3} + 3\mathcal{M}_{\pi\pi,s} + \mathcal{M}_{\pi\pi,t} + \mathcal{M}_{\pi\pi,u}, \\
\mathcal{M}_{\pi\pi}^1 &= 2\mathcal{M}_{\pi\pi,1} - 2\mathcal{M}_{\pi\pi,2} + \mathcal{M}_{\pi\pi,t} - \mathcal{M}_{\pi\pi,u}, \\
\mathcal{M}_{\pi\pi}^2 &= 2\mathcal{M}_{\pi\pi,3} + \mathcal{M}_{\pi\pi,t} + \mathcal{M}_{\pi\pi,u}
\end{aligned} \tag{4.45}$$

for the different isospin channels.

Static Limit

In the static limit we obtained

$$\begin{aligned}
\mathcal{M}_{\pi\pi,1} = \mathcal{M}_{\pi\pi,2} &= \frac{4}{N_c N_f} \frac{1}{iI(0) + iI(m_\pi) - m_\pi^2 iK(m_\pi)}, \\
\mathcal{M}_{\pi\pi,3} &= \frac{4}{N_c N_f} \frac{(2iI(0) - 4m_\pi^2 iK(m_\pi) + m_\pi^4 iL(m_\pi))}{(iI(0) + iI(m_\pi) - m_\pi^2 iK(m_\pi))^2}
\end{aligned} \tag{4.46}$$

and

$$\begin{aligned}
\mathcal{M}_{\pi\pi,s} &= -\frac{8}{N_f N_c} \frac{(iI(m_\pi))^2}{(iI(0) + iI(m_\pi) - m_\pi^2 iK(m_\pi))^2 \left(\left(1 - \frac{m_\pi^2}{M^2}\right) iI(2m_\pi) + \frac{m_\pi^2}{4M^2} iI(m_\pi) \right)}, \\
\mathcal{M}_{\pi\pi,t} = \mathcal{M}_{\pi\pi,u} &= -\frac{8}{N_f N_c} \frac{(iI(0) - m_\pi^2 iK(m_\pi))^2}{(iI(0) + iI(m_\pi) - m_\pi^2 iK(m_\pi))^2 \left(iI(0) + \frac{m_\pi^2}{4M^2} iI(m_\pi) \right)}.
\end{aligned} \tag{4.47}$$

Since some of the above matrix elements are the same the results for the different isospin channels simplifies to

$$\begin{aligned}\mathcal{M}_{\pi\pi}^0 &= 6\mathcal{M}_{\pi\pi,1} - \mathcal{M}_{\pi\pi,3} + 3\mathcal{M}_{\pi\pi,s} + 2\mathcal{M}_{\pi\pi,t}, \\ \mathcal{M}_{\pi\pi}^1 &= 0 \\ \mathcal{M}_{\pi\pi}^2 &= 2\mathcal{M}_{\pi\pi,3} + 2\mathcal{M}_{\pi\pi,t}.\end{aligned}\tag{4.48}$$

We see that in particular the contribution from the $I = 1$ channel vanishes in the static limit, i.e. for zero relative momentum between the scattering particles.

Scattering Amplitudes

With the expressions for the matrix elements obtained in the above sections we can calculate scattering amplitudes and related quantities like scattering lengths and effective range parameters. For pion-pion scattering in the NJL model this has been done in [41] but only for $l = 0$. Their convention for the scattering amplitudes is from [78] while we will use slightly different definitions following [85], from where we also take the experimental data we compare with.

The invariant matrix elements $\mathcal{M}_{\pi\pi}^I(s, t)$ determine the T -Matrix according to (4.2):

$$\langle \pi^c, \vec{p}_3; \pi^d, p_4 | iT | \pi^a, \vec{p}_1; \pi^b, \vec{p}_2 \rangle = (2\pi)^4 \delta^{(4)}(p_1 + p_2 - p_3 - p_4) i \mathcal{M}_{\pi\pi}^{ab;cd}(p_1, p_2, p_3, p_4).\tag{4.49}$$

The T -Matrix is in turn related to the scattering matrix S via $S = 1 + iT$ (where S should be a unitary operator). The elements of the S -matrix are given by

$$S_l(s) = 1 + 2i|\vec{p}|f_l(s)\tag{4.50}$$

(recall $|\vec{p}| = \sqrt{s/4 - m_\pi^2}$), where the $f_l(s)$ are defined via the partial wave decomposition of the scattering amplitude

$$f(s, t) = \sum_{l=0}^{\infty} (2l+1) f_l(s) P_l(\cos \vartheta).\tag{4.51}$$

We conclude that the scattering amplitude $f(s, t)$ is directly proportional to the invariant matrix element $\mathcal{M}(s, t)$ with a real and possibly momentum dependent proportionality factor. As further complication, the scattering amplitude $f(s, t)$ is related to the ‘measured’ scattering amplitude $F(s, t)$ (which in turn is related in the usual way to the differential cross section) by the relation⁹ $F(s, t) = 2f(s, t)$.

The correct proportionality factor between $f(s, t)$ and $\mathcal{M}(s, t)$ is easiest obtained from the formula for the differential cross section in the center-of-mass system (CMS) for a

⁹The factor of 2 can be understood from the fact that for example in a scattering process $\pi^+ + \pi^- \rightarrow \pi^+ + \pi^-$ the pions might have changed their identity or not. Those two cases are as a matter of principle undistinguishable and the scattering amplitudes for both processes add (for fermions there would be a relative minus sign). To be even more exact: When adding these amplitudes, for obvious geometrical reasons [86] one has to add the amplitudes at angle ϑ and $\pi - \vartheta$ but these are the same in our case.

scattering process $A + B \rightarrow C + D$ where all particles have the same mass. The cross section is given by [58]

$$\frac{d\sigma}{d\Omega}(s, t) = \frac{|\mathcal{M}(s, t)|^2}{64\pi^2 s}. \quad (4.52)$$

On the other hand

$$\frac{d\sigma}{d\Omega}(s, t) = |F(s, t)|^2 = |2f(s, t)|^2 \quad (4.53)$$

and hence we get

$$f(s, t) = \frac{\mathcal{M}(s, t)}{16\pi\sqrt{s}}. \quad (4.54)$$

With the help of this relation we get the scattering amplitudes $f^I(s, t)$ from the matrix elements and performing the partial wave decomposition (4.51) we obtain the partial amplitudes $f_l^I(s)$.

Scattering Lengths and Effective Range Parameters

The behaviour of the scattering amplitudes $f_l^I(s)$ for small $|\vec{p}|$ can be parametrised by the scattering length¹⁰ a_l^I and an effective range parameter b_l^I . Following [85] we write

$$\frac{\sqrt{s}}{2m_\pi \vec{p}^{2l}} \text{Re} f_l^I(s) = a_l^I + b_l^I \vec{p}^2 + \mathcal{O}(\vec{p}^4). \quad (4.55)$$

In the following discussion we will drop the Re in front of the scattering amplitudes because they are purely real for small enough $|\vec{p}|$ and in particular for $|\vec{p}| \rightarrow 0$.

Let us first determine the usual S-wave scattering lengths. They are given by

$$a_0^I = \lim_{|\vec{p}| \rightarrow 0} \frac{\sqrt{s}}{2m_\pi} f_0^I(s) = f_0^I(s = 4m_\pi^2) \quad (4.56)$$

since $s = 4m_\pi^2$ if $\vec{p} = 0$. For $s = 4m_\pi^2$ it follows that $t = u = 0$ and hence $f^I(s = 4m_\pi^2, t)$ does not depend on the scattering angle ϑ . In that case the partial wave decomposition is trivial and yields $f_0^I(s = 4m_\pi^2) = f^I(s = 4m_\pi^2, t = 0)$. Obviously

$$f^I(s = 4m_\pi^2, t = 0) = \frac{1}{16\pi\sqrt{s}} \mathcal{M}_{\pi\pi}^{I,\text{sl.}} = \frac{1}{32\pi m_\pi} \mathcal{M}_{\pi\pi}^{I,\text{sl.}}, \quad (4.57)$$

where $\mathcal{M}_{\pi\pi}^{I,\text{sl.}}$ denotes the matrix element in the static limit (see (4.48)). Taking the above observations together we get

$$a_0^I = \frac{1}{32\pi m_\pi} \mathcal{M}_{\pi\pi}^{I,\text{sl.}}. \quad (4.58)$$

The $l = 0$ scattering length for the $I = 1$ channel vanishes since $\mathcal{M}_{\pi\pi}^{1,\text{sl.}}$ does. This is related to the more general statement that due to the symmetries of the wave function

¹⁰This scattering length is for $l = 0$ up to a minus sign identical to the usual scattering length defined in the effective range expansion: $k \cot \delta_0 = -1/a + (1/2)r_{\text{eff.}}k^2 + \mathcal{O}(k^4)$.

of two pions the partial wave decomposition for $I = 1$ only contains terms for odd l , whereas for $I = 0, 2$ only even l contributes.

We calculate these scattering lengths (for $I = 0, 2$) and compare them to the Weinberg scattering lengths [87] (obtained from leading-order chiral perturbation theory)

$$a_0^{0,\text{Wein.}} = \frac{7m_\pi}{32\pi f_\pi^2} \quad \text{and} \quad a_0^{2,\text{Wein.}} = -\frac{2m_\pi}{32\pi f_\pi^2}, \quad (4.59)$$

where we will use the values for m_π and f_π we obtained in the NJL model calculations. The results are shown in Table 4.1 together with the values for the matrix elements in the static limit.

Param. Set	[A]	[B]	[C]	[D]	[E]
$\mathcal{M}_{\pi\pi,1}^{\text{sl.}}$	-29.44	-34.92	-49.18	-56.79	-74.79
$\mathcal{M}_{\pi\pi,3}^{\text{sl.}}$	-32.46	-37.83	-52.08	-59.60	-77.56
$\mathcal{M}_{\pi\pi,s}^{\text{sl.}}$	34.01	38.31	51.22	58.37	75.77
$\mathcal{M}_{\pi\pi,t}^{\text{sl.}}$	30.26	35.91	50.51	58.18	76.33
$\mathcal{M}_{\pi\pi}^{0,\text{sl.}}$	18.40	15.08	11.66	10.35	8.75
$\mathcal{M}_{\pi\pi}^{2,\text{sl.}}$	-4.40	-3.83	-3.15	-2.83	-2.45
$a_0^0 [m_\pi^{-1}]$	0.183	0.150	0.116	0.103	0.087
$a_0^2 [m_\pi^{-1}]$	-0.0438	-0.0381	-0.0313	-0.0282	-0.0244
m_π [MeV]	140.0	140.0	140.0	140.0	140.0
f_π [MeV]	93.64	100.50	111.03	116.99	125.88
$a_0^{0,\text{Wein.}} [m_\pi^{-1}]$	0.156	0.135	0.111	0.100	0.086
$a_0^{2,\text{Wein.}} [m_\pi^{-1}]$	-0.0445	-0.0386	-0.0316	-0.0285	-0.0246

Table 4.1.: Results for the pion-pion scattering lengths a_0^I in the NJL model compared to the Weinberg results. The matrix elements in the static limit are also given.

We see that the results we obtained from the NJL calculations are in a rather good agreement with the Weinberg predictions. However, only the values obtained for parameter set [A] are physically meaningful since this choice of parameters reproduces the correct pion decay constant.

In order to calculate the scattering lengths for $l > 0$ or the effective range parameters we need to consider the full dependence of the matrix elements on s and t . In general, the scattering length a_l^I is given by

$$a_l^I = \lim_{|\vec{p}| \rightarrow 0} \frac{\sqrt{s}}{2m_\pi \vec{p}^{2l}} f_l^I(s) = \lim_{|\vec{p}| \rightarrow 0} \frac{1}{\vec{p}^{2l}} f_l^I(s) \quad (4.60)$$

and the effective range parameter can be obtained as

$$b_l^I = \lim_{|\vec{p}| \rightarrow 0} \frac{d}{d(p^2)} \left(\frac{\sqrt{s}}{2m_\pi \vec{p}^{2l}} f_l^I(s) \right). \quad (4.61)$$

We calculate the parameters a_l^I for $I = 0, 2$ and $l = 0$ as well as $I = 1$ and $l = 1$. We compare these results to those given in [85]. The authors obtain reliable $\pi\pi$ -scattering amplitudes by fitting to experimental low energy phase shifts. The results are shown in Table 4.2. The values for parameter set [A] are remarkably close to the experimental

Param. Set	Experiment [85]	[A]	[B]	[C]	[D]	[E]
$a_0^0 [m_\pi^{-1}]$	0.230 ± 0.015	0.183	0.150	0.116	0.103	0.087
$a_1^1 [10^{-3}m_\pi^{-3}]$	38.4 ± 0.8	34.55	29.29	23.37	20.79	17.66
$a_0^2 [m_\pi^{-1}]$	-0.0480 ± 0.0046	-0.0438	-0.0381	-0.0313	-0.0282	-0.0244
$b_0^0 [m_\pi^{-3}]$	0.312 ± 0.014	0.243	0.185	0.134	0.118	0.0988
$b_1^1 [10^{-3}m_\pi^{-5}]$	4.75 ± 0.16	3.7	2.6	1.2	1.6	0.8
$b_0^2 [m_\pi^{-3}]$	-0.090 ± 0.006	-0.080	-0.071	-0.060	-0.055	-0.048

Table 4.2.: Results for the pion-pion scattering lengths a_l^I and effective range parameters b_l^I in the NJL model compared to experimental results [85].

values. In particular all the signs of the amplitudes and effective range parameters are correct.

Chiral Theorems

When examining the matrix elements in the static limit (see Table 4.1) one observes that the matrix elements for the isospin channels $I = 0, 2$ are rather small compared to the matrix elements for the different diagrams ($s, t, u, 1, 2, 3$). This is due to a ‘delicate cancellation’ between the sigma-exchange and box diagrams. In fact, in the chiral limit these matrix elements (and hence the S-wave scattering lengths) vanish. This agrees well with the behaviour of the Weinberg scattering lengths (4.59), which vanish because $m_\pi = 0$ in the chiral limit. These observations can be understood in the context of low-energy chiral theorems.

4.4. Pion-Pion Scattering in the Medium

To conclude this chapter about pion-pion scattering we will investigate the medium effects on the quantities we calculated above. As described at the beginning of Chapter 3 we have to replace the vacuum integrals by the corresponding medium integrals obtained in the Matsubara formalism. The result for $iI_2^+(p_0, \vec{p})$ is given in Appendix D.3. For the three- and four-point integrals, we are only able to calculate the medium versions $iK^+(p_0, \vec{p} = 0)$ and $iL^+(p_0, \vec{p} = 0)$ of the static limit integrals for the special case of vanishing three-momentum \vec{p} (see Appendix D.2). For $I_3(p, q)$ and $I_4(p, q, r)$ we only have the vacuum expressions.

This means that we cannot keep the full momentum dependence of the matrix elements when going from the vacuum to the medium description. Let us consider the sigma-meson exchange contribution

$$\mathcal{M}_{\pi\pi, v} = -(2N_f N_c)^2 g_{\pi qq}^4 (i \Delta(v))^2 D_\sigma(v) \quad (4.62)$$

where v stands for one of the Mandelstam variables s , t and u . The quark-pion coupling constant $g_{\pi qq}$ is not momentum dependent and can be expressed in terms of $iI(0)$, $iI(m_\pi)$ and $iK(m_\pi)$. It can therefore be easily made temperature dependent. The propagator $D_\sigma(v)$ is momentum dependent but only depends on the integrals I_1 and $I_2(v)$. Hence it can be moved to the medium while keeping the full momentum dependence. The problematic term is the quark triangle $i\Delta(v)$. It contains the integral iI_3 for which we do not have a medium version. However, one observes that the quark triangle in the vacuum does not depend strongly on v (see Figure 4.8). This suggests that it is a

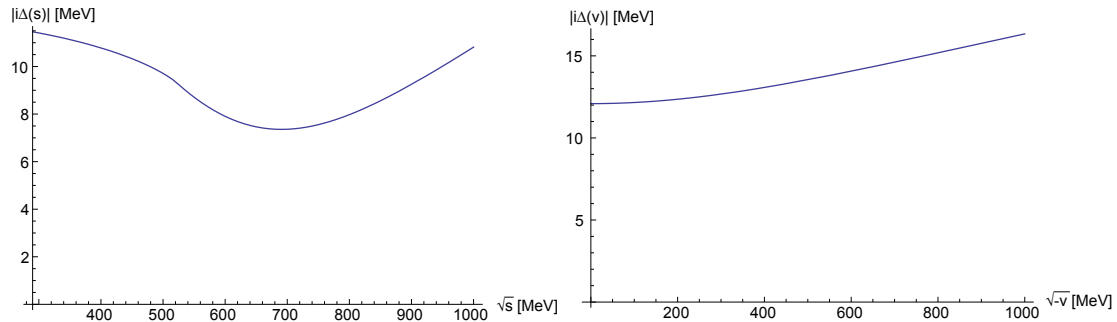


Figure 4.8.: Momentum dependence of the vacuum quark triangle $i\Delta(v)$ for $v = s$, i.e. $v \geq 4m_\pi^2$ (left) and $v = t$ or $v = u$, i.e. $v \leq 0$ (right) for parameter set [A].

rather good approximation to evaluate the quark triangles for the special momentum configuration of the static limit. The resulting expression $i\Delta(0)$ and $i\Delta(4m_\pi^2)$ only depend on the integrals iI and iK and can be moved to the medium. For the quark box diagram we proceed accordingly and approximate the quark box $i\Box$ in the static limit such that we can calculate it in the medium. Figure 4.9 shows the temperature dependence of the quark triangles and quark boxes in the static limit. The plots show that the quark loops show indeed a rather strong temperature dependence, which should not be neglected (and is discussed at the end of this section).

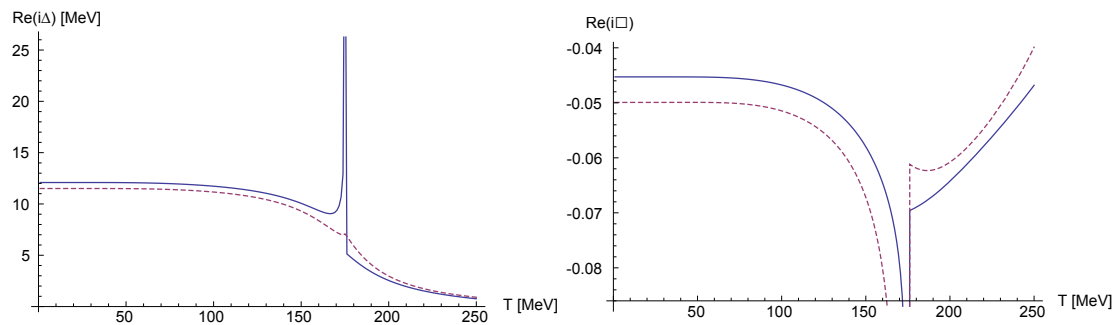


Figure 4.9.: Left: Temperature dependence of the quark triangles in the static limit for parameter set [A]. Solid line: t -, u -channel. Dashed line: s -channel. Right: Analogous plot for quark boxes. Solid Line: Channel 1, 2. Dashed line: Channel 3.

The above approximations correspond to the semi-static limit in the case of the sigma propagation diagram and the static limit in the case of the quark box diagram. Moreover we have to take into account that we only have the medium versions of iK and iL with vanishing three-momentum while iI can be calculated for arbitrary $p = (p_0, \vec{p})^t$. In our medium calculations we will hence evaluate all the integrals $iI^+(p_0, \vec{p})$, $iK^+(p_0, \vec{p})$ and $iL^+(p_0, \vec{p})$ at $\vec{p} = 0$ and $p_0^2 = p^2$ except for the $I_2(v)$ ($v = s, t, u$) in the sigma-meson propagator, which we will for simplicity evaluate at $p = (\sqrt{s}, 0)^t$ in the s -channel and at $p = (0, \vec{p})^t$ with $\vec{p}^2 = -t, -u$ in the t - and u -channel.

Static Limit

In the following we want to calculate the medium dependent scattering lengths a_0^0 and a_0^2 . For those we only need to consider the static limit. Since we can only evaluate $iK^+(p_0, \vec{p})$ and $iL^+(p_0, \vec{p})$ for $\vec{p} = 0$ the pions need to have momenta $p_1 = p_2 = p_3 = p_4 = (m_\pi, 0)^t$, i.e. they are at rest relative to each other and to the thermal medium. The static limit approximation is obtained from our general medium description by also evaluating the sigma-meson propagator in the static limit. The quark triangles and boxes are evaluated in the static limit in any case. The expressions for the invariant matrix elements are identical to those for the vacuum static limit with the vacuum integrals replaced by the corresponding medium versions with $\vec{p} = 0$. For M and m_π we have to take the T - and μ -dependent results from Section 3.3.

We set $\mu = 0$ and calculate the $l = 0$ scattering lengths a_0^0 and a_0^2 as a function of T . Before we discuss the results, let us return to the plot of the quark and meson masses (Figure 4.10). We have also included a line for the constituent quark mass M and for

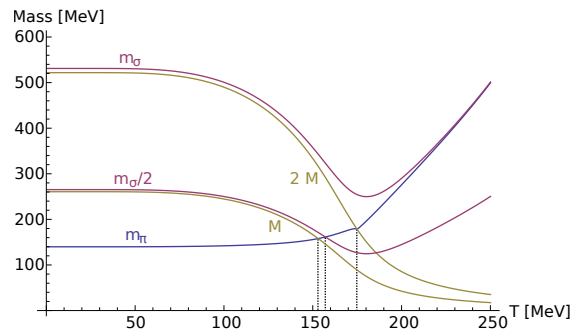


Figure 4.10.: Constituent quark mass and masses of π and σ mesons for $\mu = 0$ as functions of T for parameter set [A].

the half sigma-meson mass. Three temperatures (marked by dotted lines in the plot) are of particular interest. The following discussion uses the results from parameter set [A]. Note that in the chiral limit all these temperatures would be identical and coincide with the chiral second order phase transition. Away from the chiral limit these temperatures mark the corresponding chiral crossover.

- For temperatures larger than $T \approx 153$ MeV the pion mass m_π is larger than the constituent quark mass M . This means that the energy of the intermediate sigma

meson in the s -channel is larger than two times the constituent quark mass, which opens the $\sigma \leftrightarrow q\bar{q}$ channel (or $\pi\pi \leftrightarrow q\bar{q}$ channel) resulting in an imaginary part of $D_\sigma(s)$ and hence in an imaginary part for the matrix elements.

- At the dissociation temperature $T_{\text{diss}} \approx 157$ MeV we have $2m_\pi = m_\sigma$. This means that the real part of the inverse of $D_\sigma(2m_\pi) = D_\sigma(m_\sigma)$ vanishes. Due to a non-vanishing (but small) imaginary part of the inverse propagator, $D_\sigma(2m_\pi)$ exhibits a sharp peak (instead of a divergence) and hence the same is true for the s -channel contribution to the static limit sigma-propagation diagram, where $D_\sigma(2m_\pi)$ enters. This results in a peak in the $I = 0$ scattering length (but not in that for $I = 2$). The physical interpretation is that the $\pi\pi \rightarrow \sigma$ process becomes resonant at threshold.
- At $T_{\text{Mott}} \approx 174$ MeV we have $m_\pi = 2M$. This opens the decay channel of one pion decaying into two quarks ($\pi \leftrightarrow q\bar{q}$). At threshold this leads to a divergence of the quark loops (see Figure 4.9) and since these enter in both isospin channels, both a_0^0 and a_0^2 diverge. The decay into two quarks is an unphysical artefact of the NJL model, at least in the confined phase. But as the chiral and the deconfinement crossover happen at roughly the same temperature, one could argue that at T_{Mott} the decay into free quarks should be indeed permitted.

The results for a_0^0 and a_0^2 are plotted in Figure 4.11 (see also [43]). We see that the

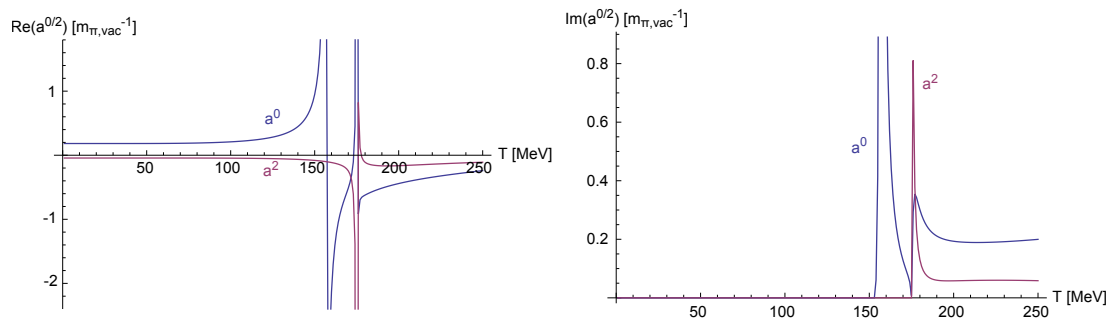


Figure 4.11.: Temperature-dependent medium solutions for the scattering lengths a_0^0 and a_0^2 at $\mu = 0$ for parameter set [A] in units of the inverse *vacuum* pion mass.

scattering lengths are almost constant over a large temperature region (up to about 100 MeV) and are close to the Weinberg value (see Table 4.1) for $T = 0$. As expected there are singularities at $T = T_{\text{diss}}$ and $T = T_{\text{Mott}}$.

5. Extended NJL Model

In the following Chapter we will study the implications of an extended NJL model, which in addition to the scalar and pseudoscalar interaction channels also includes a vector and a pseudovector four-point interaction. Such an extended setting is studied for example in [48, 88, 89]. The extended model will allow the scattering of pions via an intermediate rho meson (see Section 5.2). It is argued for example in [48] that the pion-pion scattering cross section has important contributions from the rho-meson exchange diagram, especially in the s -channel. The interaction Lagrangian is given by

$$\mathcal{L}_{\text{int.}} = g_s \left[(\bar{\psi}\psi)^2 + (\bar{\psi}i\gamma_5\vec{\tau}\psi)^2 \right] - g_v \left[(\bar{\psi}\gamma^\mu\vec{\tau}\psi)^2 + (\bar{\psi}\gamma^\mu\gamma_5\vec{\tau}\psi)^2 \right]. \quad (5.1)$$

The first two and the latter two terms are chiral partners, i.e. they transform into each other via chiral transformations. As in Chapter 2 we denote the first and second term by σ and π , respectively. The vector-isovector and the pseudovector-isovector terms are called ρ and a_1 , respectively. Writing the Lagrangian as

$$\mathcal{L} = \bar{\psi}(i\cancel{\partial} - \underline{m})\psi + \sum_M g_M (\bar{\psi}\Gamma_M\psi)^2 \quad (5.2)$$

we identify

$$\Gamma_\sigma = 1, \quad \Gamma_\pi^a = i\gamma_5\tau^a, \quad \Gamma_\rho^{\mu,a} = \gamma^\mu\tau^a \quad \text{and} \quad \Gamma_{a_1}^{\mu,a} = \gamma^\mu\gamma_5\tau^a \quad (5.3)$$

and

$$g_\sigma = g_\pi = g_s \quad \text{and} \quad g_\rho = g_{a_1} = -g_v. \quad (5.4)$$

Gap Equation

We consider again the gap equation

$$M = m + \sum_M \Sigma_M \quad (5.5)$$

with

$$\Sigma_M = 2g_M\Gamma_M i \int \frac{d^4k}{(2\pi)^4} \text{Tr}(\Gamma_M S(k)). \quad (5.6)$$

The only contribution comes from the scalar term since for the others the trace over τ^a vanishes. Hence the result for the gap equation is exactly the same as for the simple NJL Lagrangian (see Section 2.2), i.e.

$$M = m + 8N_f N_c g_s M i I_1(M). \quad (5.7)$$

5.1. Mesons

The study of the Bethe-Salpeter equation (2.45) in RPA will turn out to be more complicated than in the case with only scalar and pseudoscalar interactions since we will observe a mixing between some interaction channels.

Polarisation Functions

To begin with, we calculate the polarisation loops

$$J_{M,N}(p) = i \int \frac{d^4k}{(2\pi)^4} \text{Tr} (\Gamma_M S(k+p) \Gamma_N S(k)). \quad (5.8)$$

First, we consider the diagonal terms $J_{M,M}(p) =: J_M(p)$. We have

$$J_\sigma(p) = J_\sigma(p^2) \quad \text{and} \quad J_\pi^{ab}(p) = \delta_{ab} J_\pi(p^2) \quad (5.9)$$

with

$$\begin{aligned} J_\pi(p^2) &= 2N_c N_f \left(2iI_1 - p^2 iI_2(p^2) \right), \\ J_\sigma(p^2) &= 2N_c N_f \left(2iI_1 - (p^2 - 4M^2) iI_2(p^2) \right), \end{aligned} \quad (5.10)$$

which are the results from Section 2.5.

We introduce $T^{\mu\nu}(p)$ and $L^{\mu\nu}(p)$, the projectors¹¹ onto the transverse and the longitudinal part:

$$T^{\mu\nu}(p) := \eta^{\mu\nu} - \frac{p^\mu p^\nu}{p^2} \quad \text{and} \quad L^{\mu\nu}(p) = \frac{p^\mu p^\nu}{p^2}. \quad (5.11)$$

For the ρ -channel we get

$$J_\rho^{\mu\nu,ab}(p) = \delta_{ab} T^{\mu\nu}(p) J_\rho(p^2) \quad (5.12)$$

with

$$J_\rho(p^2) = \frac{4}{3} N_c N_f \left(-2iI_1 + (p^2 + 2M^2) iI_2(p^2) \right). \quad (5.13)$$

The polarisation function in the a_1 -channel has a longitudinal and a transverse part:

$$J_{a_1}^{\mu\nu,ab}(p) = \delta_{ab} \left(T^{\mu\nu}(p) J_{a_1}^{\text{trans}}(p^2) + L^{\mu\nu}(p) J_{a_1}^{\text{long}}(p^2) \right) \quad (5.14)$$

with

$$J_{a_1}^{\text{trans}}(p^2) = \frac{4}{3} N_c N_f \left(-2iI_1 + (p^2 - 4M^2) iI_2(p^2) \right) \quad (5.15)$$

and

$$J_{a_1}^{\text{long}}(p^2) = -8N_c N_f M^2 iI_2(p^2). \quad (5.16)$$

¹¹These projectors fulfil the relations $T_\nu^\mu(p) T^{\nu\lambda}(p) = T^{\mu\lambda}(p)$, $L_\nu^\mu(p) L^{\nu\lambda}(p) = L^{\mu\lambda}(p)$ and $T_\nu^\mu(p) L^{\nu\lambda}(p) = L_\nu^\mu(p) T^{\nu\lambda}(p) = 0$ as well as $T^{\mu\nu}(p) + L^{\mu\nu}(p) = \eta^{\mu\nu}$, which makes them orthogonal projectors. Moreover $T_\nu^\mu(p) p^\nu = 0$ and $L_\nu^\mu(p) p^\nu = p^\mu$, which is why they are called transverse and longitudinal projectors.

In addition, the projectors fulfil the trace identities $T_{\mu\nu}(p) T^{\mu\nu}(p) = 3$, $L_{\mu\nu}(p) L^{\mu\nu}(p) = 1$ and $T_{\mu\nu}(p) L^{\mu\nu}(p) = 0$.

The calculations of the above polarisation functions can be found in Appendix F.1.

Next, we consider the off-diagonal terms $J_{M,N}(p)$ with $M \neq N$. All combinations of σ with another channel vanish because a trace over τ^a is to be taken, i.e.

$$J_{\sigma,\pi}^a = J_{\pi,\sigma}^a = J_{\sigma,\rho}^{\mu,a} = J_{\rho,\sigma}^{\mu,a} = J_{\sigma,a_1}^{\mu,a} = J_{a_1,\sigma}^{\mu,a} = 0. \quad (5.17)$$

It is moreover possible to show (see Appendix F.1) that also

$$J_{\pi,\rho}^{\mu,ab} = J_{\rho,\pi}^{\mu,ab} = J_{\rho,a_1}^{\mu\nu,ab} = J_{a_1,\rho}^{\mu\nu,ab} = 0. \quad (5.18)$$

The only off-diagonal terms that do not vanish are $J_{\pi,a_1}^{\mu,ab}(p)$ and $J_{a_1,\pi}^{\mu,ab}(p)$. One calculates (see Appendix F.1)

$$J_{\pi,a_1}^{\mu,ab}(p) = i\delta_{ab}4N_cN_fMp^\mu iI_2(p^2) =: \delta_{ab} \frac{p^\mu}{\sqrt{p^2}} J_{\pi,a_1}(p^2) \quad (5.19)$$

with

$$J_{\pi,a_1}(p^2) = i4N_cN_fM\sqrt{p^2}iI_2(p^2) \quad (5.20)$$

and

$$J_{a_1,\pi}^{\mu,ab}(p) = J_{\pi,a_1}^{\mu,ba}(-p) = -i\delta_{ab}4N_cN_fMp^\mu iI_2(p) =: \delta_{ab} \frac{p^\mu}{\sqrt{p^2}} J_{a_1,\pi}(p^2) \quad (5.21)$$

with

$$J_{a_1,\pi}(p^2) = -i4N_cN_fM\sqrt{p^2}iI_2(p^2). \quad (5.22)$$

Comment on the Transversal Parts of the ρ - and a_1 -Meson Propagators

We should note that our choice of regularisation is not without complication. We chose Pauli-Villars regularisation, where we regularised the elementary integrals by adding integrands with different masses. However, we tacitly decided not to regularise possible factors of M in front of these integrals. This implies that the equation

$$I_1 = M^2 I_2(0), \quad (5.23)$$

which is ‘correct’ before regularisation, becomes incorrect after applying Pauli-Villars regularisation. It is argued in [90] that it is impossible to obtain reasonable results for M and f_π and at the same time fulfil relation (5.23), which is why we follow the recommendation not to regularise factors of M in front of the elementary integrals.

The problem with this relation being violated is that the rho-meson polarisation function

$$J_\rho(p^2) = \frac{4}{3}N_cN_f \left(-2iI_1 + (p^2 + 2M^2) iI_2(p^2) \right) \quad (5.24)$$

does not vanish for $p = 0$, which it should due to vector current conservation [60]. To repair this unphysical behaviour we have to change $J_\rho(p^2)$ and replace I_1 with $M^2 I_2(0)$ by hand. The polarisation function then reads

$$J_\rho(p^2) = \frac{4}{3}N_cN_f \left(-2M^2 I_2(0) + (p^2 + 2M^2) iI_2(p^2) \right) \quad (5.25)$$

and it is obvious that this vanishes for $p = 0$. To preserve the symmetries of the model we need to treat the a_1 on the same footing as the ρ and hence we also rewrite

$$J_{a_1}^{\text{trans}}(p^2) = \frac{4}{3}N_c N_f \left(-2M^2 iI_2(0) + (p^2 - 4M^2) iI_2(p^2) \right). \quad (5.26)$$

Meson Propagators

Now that all the polarisation functions are determined, we can calculate the meson propagators. First, we consider the σ and ρ since they decouple from the other channels. We use the notation $D_{M,M}(p) = D_M(p)$. We have

$$D_\sigma(p) = \frac{-2g_s}{1 - 2g_s J_\sigma(p^2)} \quad (5.27)$$

(as in Section 2.5) and

$$\begin{aligned} D_\rho^{\mu\nu,ab}(p) &= \delta_{ab} \left(L^{\mu\nu}(p) 2g_v + T^{\mu\nu}(p) \frac{2g_v}{1 + 2g_v J_\rho(p^2)} \right) \\ &=: \delta_{ab} \left(L^{\mu\nu}(p) 2g_v + T^{\mu\nu}(p) D_\rho(p^2) \right) \end{aligned} \quad (5.28)$$

with

$$D_\rho(p^2) = \frac{2g_v}{1 + 2g_v J_\rho(p^2)} \quad (5.29)$$

(the calculation is found in Appendix F.2). Except for the trivial longitudinal part, the ρ -meson propagator is purely transversal.

The determination of the propagators in the π and a_1 sector is more complicated as the off-diagonal polarisation functions are non-zero. As a result, in addition to $D_{\pi,\pi}^{ab}(p)$ and $D_{a_1,a_1}^{\mu\nu,ab}(p)$ there will also be mixed propagators $D_{\pi,a_1}^{\mu,ab}(p)$ and $D_{a_1,\pi}^{\mu,ab}(p)$.

We write the solutions as

$$D_\pi^{ab}(p) := D_{\pi,\pi}^{ab}(p) =: \delta_{ab} D_\pi(p^2) \quad (5.30)$$

and

$$D_{a_1}^{\mu\nu,ab}(p) =: \delta_{ab} \left(T^{\mu\nu}(p) D_{a_1}^{\text{trans}}(p^2) + L^{\mu\nu}(p) D_{a_1}^{\text{long}}(p^2) \right) \quad (5.31)$$

as well as

$$D_{\pi,a_1}^{\mu,ab}(p) = \delta_{ab} \frac{p^\mu}{\sqrt{p^2}} D_{\pi,a_1}(p^2) \quad \text{and} \quad D_{a_1,\pi}^{\mu,ab}(p) = \delta_{ab} \frac{p^\mu}{\sqrt{p^2}} D_{a_1,\pi}(p^2). \quad (5.32)$$

We then solve for the introduced scalar-valued functions. The transversal part of the a_1 -propagator decouples and is given by

$$D_{a_1}^{\text{trans}}(p) = \frac{2g_v}{1 + 2g_v J_{a_1}^{\text{trans}}(p^2)}. \quad (5.33)$$

The longitudinal part of the a_1 -propagator, the pion propagator and the mixed propagators are coupled via the matrix equation

$$\begin{pmatrix} D_\pi & D_{\pi,a_1} \\ D_{a_1,\pi} & D_{a_1}^{\text{long}} \end{pmatrix} = \begin{pmatrix} -2g_s & 0 \\ 0 & 2g_v \end{pmatrix} + \begin{pmatrix} 2g_s & 0 \\ 0 & -2g_v \end{pmatrix} \begin{pmatrix} J_\pi & J_{\pi,a_1} \\ J_{a_1,\pi} & J_{a_1}^{\text{long}} \end{pmatrix} \begin{pmatrix} D_\pi & D_{\pi,a_1} \\ D_{a_1,\pi} & D_{a_1}^{\text{long}} \end{pmatrix}. \quad (5.34)$$

The solution is given by

$$\begin{aligned} D_\pi(p^2) &= 2g_s \frac{-2g_v J_{a_1}^{\text{long}}(p^2) - 1}{D(p^2)}, & D_{\pi,a_1}(p^2) &= \frac{4g_s g_v J_{\pi,a_1}(p^2)}{D(p^2)}, \\ D_{a_1}^{\text{long}}(p^2) &= 2g_v \frac{-2g_s J_\pi(p^2) + 1}{D(p^2)}, & D_{a_1,\pi}(p^2) &= \frac{4g_s g_v J_{a_1,\pi}(p^2)}{D(p^2)} \end{aligned} \quad (5.35)$$

with the determinant

$$D(p^2) = \left(1 - 2g_s J_\pi(p^2)\right) \left(1 + 2g_v J_{a_1}^{\text{long}}(p^2)\right) + 4g_s g_v J_{\pi,a_1}(p^2) J_{a_1,\pi}(p^2). \quad (5.36)$$

The complete calculation is found in Appendix F.2.

In analogy to the alternative representation of the meson propagator in Section 2.5.1 we will in the following rewrite the above determinant $D(p^2)$. Inserting the expressions for the polarisation functions in terms of elementary integrals gives

$$\begin{aligned} D(p^2) &= \left(1 - 2g_s 2N_c N_f \left(2iI_1 - p^2 iI_2(p^2)\right)\right) \left(1 - 2g_v 8N_c N_f M^2 iI_2(p^2)\right) \\ &\quad + 4g_s g_v (4N_c N_f)^2 M^2 p^2 \left(iI_2(p^2)\right)^2, \end{aligned} \quad (5.37)$$

which, using the gap equation (5.7), can be written as

$$\begin{aligned} D(p^2) &= \left(\frac{m}{M} + 4g_s N_c N_f p^2 iI_2(p^2)\right) \left(1 - 16g_v N_c N_f M^2 iI_2(p^2)\right) \\ &\quad + 64g_s g_v (N_c N_f)^2 M^2 p^2 \left(iI_2(p^2)\right)^2 \\ &= \frac{m}{M} + (4g_s p^2 - 16g_v M m) N_c N_f iI_2(p^2). \end{aligned} \quad (5.38)$$

Mixing of Pion and a_1

At this point we should remark on the interpretations of the different propagators. We obtained a transversal and a longitudinal part of the a_1 -propagator, where the longitudinal part mixes with the pion propagator and the transversal part decouples. However, we in fact interpret the transversal part of the a_1 meson as the physical a_1 (which has 3 polarisation degrees of freedom) while the physical pion consists the pion and the longitudinal part of the a_1 . In the following we want to describe the *full* pion in the extended NJL model. The scattering matrix T for the pion sector is given by

$$\begin{aligned} T &= -\Gamma_\pi^a D_\pi^{ab}(p) \Gamma_\pi^b - \Gamma_\pi^a D_{\pi,a_1}^{\mu,ab}(p) \Gamma_{a_1,\mu}^b - \Gamma_{a_1,\mu}^a D_{a_1,\pi}^{\mu,ab}(p) \Gamma_\pi^b - \Gamma_{a_1,\mu}^a D_{a_1}^{\mu\nu,ab} \Gamma_{a_1,\nu}^b \\ &= -(i\gamma_5 \tau^a) \delta_{ab} D_\pi(p^2) (i\gamma_5 \tau^b) - (i\gamma_5 \tau^a) \frac{p^\mu}{\sqrt{p^2}} \delta_{ab} D_{\pi,a_1}(p^2) (\gamma_\mu \gamma_5 \tau^b) \\ &\quad - (\gamma_\mu \gamma_5 \tau^a) \frac{p^\mu}{\sqrt{p^2}} \delta_{ab} D_{a_1,\pi}(p^2) (i\gamma_5 \tau^b) - (\gamma_\mu \gamma_5 \tau^a) \delta_{ab} \frac{p^\mu p^\nu}{p^2} D_{a_1}^{\text{long}}(p^2) (\gamma_\mu \gamma_5 \tau^b) \end{aligned} \quad (5.39)$$

and can be written in short as

$$T = -(\tau^a \delta_{ab} \tau^b) (i\gamma_5, \frac{\not{p}}{\sqrt{p^2}} \gamma_5) \begin{pmatrix} D_\pi(p^2) & D_{\pi, a_1}(p^2) \\ D_{a_1, \pi} & D_{a_1}^{\text{long}} \end{pmatrix} \begin{pmatrix} i\gamma_5 \\ \frac{\not{p}}{\sqrt{p^2}} \gamma_5 \end{pmatrix}. \quad (5.40)$$

Observe that we omitted the tensor product sign in $(\tau^a \delta_{ab} \tau^b) = (\tau^a \delta_{ab} \otimes \tau^b)$ and also between the row and the column vector containing the γ_5 -matrices.

The propagator matrix has a $D(p^2)$ in the denominator of each component. The mass of the pion corresponds to the pole of T and hence to a zero of $D(p^2)$, i.e.

$$D(p^2 = m_\pi^2) \stackrel{!}{=} 0. \quad (5.41)$$

We determine the pion mass for modified parameter sets [A] - [E], where we set g_s to the value previously assigned to g and let g_v vary from 0 to $2g_s$. The results are shown in Figure 5.1. As expected, for $g_v = 0$ we obtain the result for the simple model (see

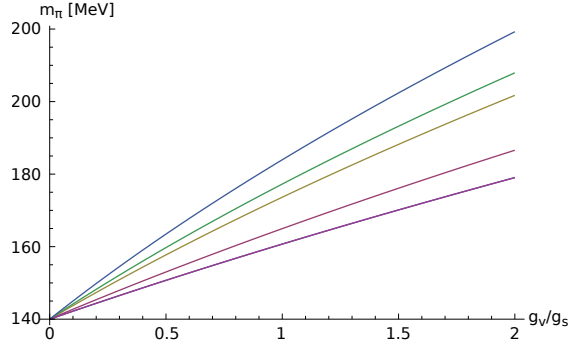


Figure 5.1.: Pion mass m_π for parameter sets [A] - [E] (lower to upper) with $g_s = g$ as a function of g_v .

Table 2.2). The fact that the pions are massless in the chiral limit is not affected by introducing an additional vector interaction channel.

Using the pion mass we can write $D(p^2)$ as

$$\begin{aligned} D(p^2) &= D(p^2) - D(m_\pi^2) \\ &= N_f N_c \left[4g_s \left(p^2 iI_2(p^2) - m_\pi^2 I_2(m_\pi^2) \right) - 16g_v M m \left(iI_2(p^2) - iI_2(m_\pi^2) \right) \right], \end{aligned} \quad (5.42)$$

where the zero for $p^2 = m_\pi^2$ is now obvious.

In the following we want to investigate the pole structure of T in the pion sector. To this end we write the T in pole approximation. A straightforward calculation in Appendix F.3 yields

$$T = -(\tau^a \delta_{ab} \tau^b) \frac{1}{p^2 - m_\pi^2} \left(g_{ps} i\gamma_5 - i g_{pv} \frac{\not{p}}{\sqrt{p^2}} \gamma_5 \right) \otimes \left(g_{ps} i\gamma_5 - i g_{pv} \frac{-\not{p}}{\sqrt{p^2}} \gamma_5 \right), \quad (5.43)$$

where we introduced the pseudoscalar and the pseudovector quark-pion couplings g_{ps} and g_{pv} corresponding to the vertices $i\gamma_5$ and $i\cancel{\not{p}}/\sqrt{p^2}$ (or $-i\cancel{\not{p}}/\sqrt{p^2}$ for outgoing momenta). The coupling strengths are calculated to be

$$g_{\text{ps}}^2 = \frac{a^2(a+d)}{(a^2+b^2)D'(m_\pi^2)} \quad \text{and} \quad g_{\text{pv}}^2 = \frac{b^2(a+d)}{(a^2+b^2)D'(m_\pi^2)} \quad (5.44)$$

with

$$\begin{aligned} a &= -2g_s - 4g_s g_v J_{a_1}^{\text{long}}(m_\pi^2) = -2g_s + 32N_c N_f g_s g_v M^2 iI_2(m_\pi^2), \\ d &= 2g_v - 4g_s g_v J_\pi(m_\pi^2) = 2g_v - 8N_c N_f g_s g_v \left(2iI_1 - m_\pi^2 iI_2(m_\pi^2)\right), \\ b &= -i4g_s g_v J_{\pi, a_1}(m_\pi^2) = 16N_c N_f g_s g_v M m_\pi iI_2(m_\pi^2) \end{aligned} \quad (5.45)$$

and

$$\begin{aligned} D'(m_\pi^2) &= N_f N_c \left[2g_s \left(iI(0) + iI(m_\pi^2) - m_\pi^2 K(m_\pi^2) \right) \right. \\ &\quad \left. - 8g_v \frac{Mm}{m_\pi^2} \left(iI(0) - iI(m_\pi^2) - m_\pi^2 K(m_\pi^2) \right) \right]. \end{aligned} \quad (5.46)$$

We present them in Figure 5.2. For $g_v = 0$ the result for g_{ps} coincides with $g_{\pi qq}$ in the simple model (see Table 2.2).

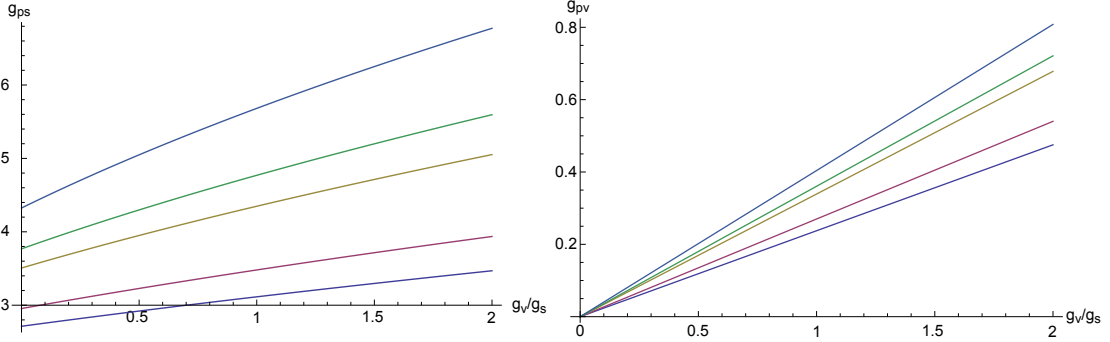


Figure 5.2.: Coupling constants g_{ps} (left) and g_{pv} (right) for parameter sets [A] - [E] (lower to upper) with $g_s = g$ as a function of g_v .

For comparison we look at the ratio of the two coupling strengths, which is given by the simple expression

$$\frac{g_{\text{pv}}}{g_{\text{ps}}} = \frac{b}{a} = \frac{8N_c N_f g_v M m_\pi iI_2(m_\pi^2)}{-1 + 16N_c N_f g_v M^2 iI_2(m_\pi^2)}. \quad (5.47)$$

The results are shown in Figure 5.3.

We see that for values of g_v not too large the coupling g_{pv} is about one order of magnitude smaller than g_{ps} . If we wanted to include both vertices ($i\gamma_5$ and $i\cancel{\not{p}}/\sqrt{p^2}$) for the pion, the calculation of the matrix elements for pion-pion scattering would become

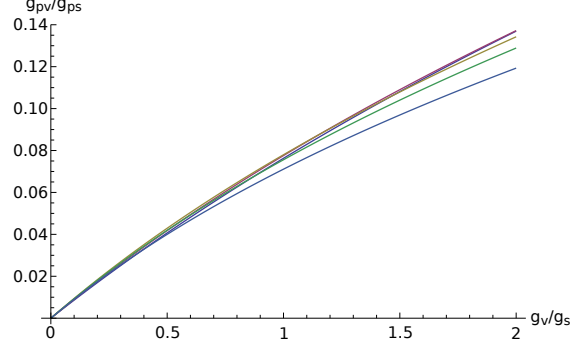


Figure 5.3.: Ratio of the coupling constants g_{ps} and g_v for parameter sets [A] - [E] (upper to lower) with $g_s = g$ as a function of g_v .

extremely more difficult, especially for the quark box, since each of the four pions has two instead of one vertex contribution. We will therefore neglect¹² the pseudovector contribution to the pion for future calculations in the extended NJL model.

Rho-Meson Mass

So far, we did not fix the value of the vector coupling g_v . We will determine it by fitting the vacuum rho-meson mass to the literature value $m_\rho = 775.45$ MeV [66]. If we were to include the full description of the pion as discussed above, a global fit to the pion mass and decay constant as well as the rho-meson mass would be necessary since all these observables depend on the vector coupling. Since we however chose to ignore the pseudovector contribution to the pion, its properties will be determined exactly as in Section 2.5 and therefore do not depend on g_v .

The mass of the rho meson is determined by the pole of the propagator $D_\rho^{\mu\nu,ab}(p)$ and consequently by a pole of $D_\rho(p^2)$. The real and imaginary parts of the inverse propagator $D_\rho^{-1}(p^2)$ are shown in Figure 5.4. Due to our choice of $T^{\mu\nu} = \eta^{\mu\nu} - \frac{p^\mu p^\nu}{p^2}$ (we could have

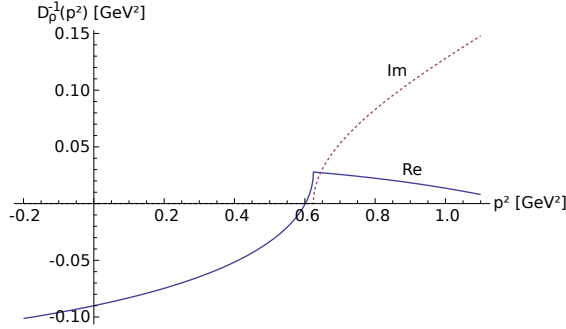


Figure 5.4.: The inverse rho-meson propagator $-D_\rho^{-1}(p^2)$ for parameter set [C] with $g_v = 1.018g_s$.

¹²A full description of the pion is used for example in [48] where the authors calculate the contribution from the s -channel ρ -meson exchange to the pion-pion scattering matrix elements.

defined it also as $T^{\mu\nu} = \frac{p^\mu p^\nu}{p^2} - \eta^{\mu\nu}$ we expect $-D_\rho^{-1}(p^2)$ (rather than $D_\rho^{-1}(p^2)$) to be shaped similarly like $D_\pi^{-1}(p^2)$ and $D_\sigma^{-1}(p^2)$ (see Figure 2.2).

We observe that the real part of $-D_\rho^{-1}(p^2)$ has a negative slope after the $p^2 = 4M^2$ threshold (seen as kink). This means that $-D_\rho^{-1}(p^2)$ can only have zeroes at all (except for larger momenta as artefact of Pauli-Villars regularisation) if it has a zero before the $p^2 = 4M^2$ threshold. In that case this first zero is interpreted as the mass of the rho meson. This implies that in our model $m_\rho < 2M$.

For parameter sets [A] and [B] this cannot be fulfilled if we try to reproduce the physical rho meson mass since $2M < 775.45$ MeV, which is why we do not use these parameter sets for our description of the rho meson. For parameter sets [C] - [E] we determine g_v such that $m_\rho = 775.45$ MeV. One obtains the parameter sets shown in Table 5.1. We will use these choices of parameters for the following calculations.

Param. Set	[C]	[D]	[E]
Λ [MeV]	800	820	852
m [MeV]	6.77	6.70	6.54
$g_s \Lambda^2$	3.49	3.70	4.16
g_v/g_s	1.02	1.54	2.29
M [MeV]	395.0	446.3	549.4
m_π [MeV]	140.0	140.0	140.0
m_σ [MeV]	794.7	896.3	1101.4
m_ρ [MeV]	775.45	775.45	775.45

Table 5.1.: The model parameters (Λ , m , g_s and g_v) using Pauli-Villars regularisation and the resulting value of the constituent quark and meson masses.

The determination of temperature-dependent rho-meson masses runs into problems since for all parameter sets already for rather small values of T the real part of the inverse rho-meson propagator does not have a zero at all (discarding artefacts of Pauli-Villars regularisation). This means that our method of determining the rho-meson mass fails. This is not a problem since we only needed the vacuum rho-meson mass to determine the model parameter g_v .

5.2. Pion-Pion Scattering

Our goal remains to calculate the pion-pion scattering amplitudes in the NJL model. In the extended NJL model there are two changes to the calculations. The first one is the fact that the pion also has a contribution from the a_1 -channel, which we discarded in the previous section to keep our calculations manageable. This means we will calculate the pion propagator, mass and coupling to the quarks as we did in Chapter 2.

The second change we have to consider is the emergence of a new diagram. In addition to the quark-box diagram and the sigma-propagation diagram there will also be a rho-

propagation diagram where we consider the scattering of two pions via an intermediate rho meson. These diagrams are analogous to the ones in Figures 4.4, 4.5 and 4.6 with the intermediate sigma meson replaced by a rho meson. The s -channel diagram is shown in Figure 5.5.

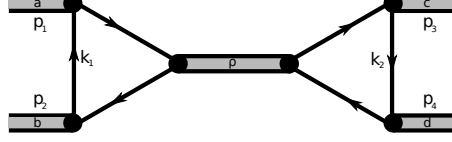


Figure 5.5.: Rho propagation diagram in the s -channel.

The calculation of the diagrams is analogous to those for the sigma meson but the Lorentz index structure is more complicated. By a straightforward evaluation of the diagram we get for the s -channel

$$\begin{aligned}
i\mathcal{M}_{\pi\pi\rho,s}^{ab;cd} &= (-2) \int \frac{d^4k_1}{(2\pi)^4} \text{Tr} \left(i\Gamma_{\pi}^a g_{\pi qq}(p_1) iS(k_1 + p_1) i\Gamma_{\rho,\mu}^e iS(k_1 - p_2) \times \right. \\
&\quad \times i\Gamma_{\pi}^b g_{\pi qq}(p_2) iS(k_1) \left. \right) (iD_{\rho}^{\mu\nu,ef}(p_1 + p_2)) (-2) \int \frac{d^4k_2}{(2\pi)^4} \text{Tr} \times \\
&\quad \times \left(i\Gamma_{\pi}^d g_{\pi qq}(p_4) iS(k_2 - p_4) i\Gamma_{\rho,\nu}^f iS(k_2 + p_3) i\Gamma_{\pi}^c g_{\pi qq}(p_3) iS(k_2) \right),
\end{aligned} \tag{5.48}$$

which we further simplify to

$$\begin{aligned}
\mathcal{M}_{\pi\pi\rho,s}^{ab;cd} &= -g_{\pi qq}^4 2i \int \frac{d^4k_1}{(2\pi)^4} \text{Tr} \left(\gamma_5 \tau^a S(k_1 + p_1) \gamma_{\mu} \tau^e S(k_1 - p_2) \gamma_5 \tau^b S(k_1) \right) \times \\
&\quad \times D_{\rho}^{\mu\nu,ef}(p_1 + p_2) 2i \int \frac{d^4k_2}{(2\pi)^4} \text{Tr} \left(\gamma_5 \tau^d S(k_2 - p_4) \gamma_{\nu} \tau^f S(k_2 + p_3) \gamma_5 \tau^c S(k_2) \right).
\end{aligned} \tag{5.49}$$

Using

$$\text{tr} \left(\tau^a \tau^b \tau^c \right) = N_f i \varepsilon_{abc} \tag{5.50}$$

we get

$$\begin{aligned}
\mathcal{M}_{\pi\pi\rho,s}^{ab;cd} &= g_{\pi qq}^4 (2N_f N_c)^2 \varepsilon_{aeb} \varepsilon_{dfe} i \int \frac{d^4k_1}{(2\pi)^4} \text{Tr} \left(S(k_1 + p_1) \gamma_{\mu} S(k_1 - p_2) S(-k_1) \right) \times \\
&\quad \times D_{\rho}^{\mu\nu,ef}(p_1 + p_2) i \int \frac{d^4k_2}{(2\pi)^4} \text{Tr} \left(S(k_2 - p_4) \gamma_{\nu} S(k_2 + p_3) S(-k_2) \right),
\end{aligned} \tag{5.51}$$

where we also eliminated the γ_5 -matrices via $\gamma_5 S(p) \gamma_5 = S(-p)$.

We introduce the quark triangle

$$i\Delta_{p,q}^{\mu} := i \int \frac{d^4k}{(2\pi)^4} \text{tr} \left(S(-k) S(k + p) \gamma^{\mu} S(k + q) \right). \tag{5.52}$$

With this we can write the invariant matrix element as

$$\mathcal{M}_{\pi\pi\rho,s}^{ab;cd} = \varepsilon_{eba}\varepsilon_{fcd}(2N_f N_c)^2 g_{\pi qq}^4 (p_1, p_2, p_3, p_4) i \Delta_{p_1, -p_2}^\mu D_{\rho, \mu\nu}^{ef}(p_1 + p_2) i \Delta_{-p_4, p_3}^\nu. \quad (5.53)$$

The quark triangle $i\Delta_{p,q}^\mu$ is a Lorentz vector and can be calculated with the ansatz

$$i\Delta_{p,q}^\mu = V_1(p^2, p \cdot q, q^2) p^\mu + V_2(p^2, p \cdot q, q^2) q^\mu. \quad (5.54)$$

The calculation in Appendix F.4 leads to the result

$$\begin{aligned} V_1(p^2, p \cdot q, q^2) &= 2i \left[-I_2(p) + q^2 I_3(p, q) + \frac{p \cdot q}{p^2 q^2 - (p \cdot q)^2} \left(q^2 I_2(q) - q^2 I_2(p - q) \right. \right. \\ &\quad \left. \left. - p^2 q^2 I_3(p, q) - p \cdot q I_2(p) + p \cdot q I_2(p - q) + q^2 p \cdot q I_3(p, q) \right) \right], \\ V_2(p^2, p \cdot q, q^2) &= 2i \left[-I_2(q) + p^2 I_3(p, q) + \frac{p \cdot q}{p^2 q^2 - (p \cdot q)^2} \left(p^2 I_2(q) - p^2 I_2(p - q) \right. \right. \\ &\quad \left. \left. - p^2 q^2 I_3(p, q) - p \cdot q I_2(q) + p \cdot q I_2(p - q) + p^2 p \cdot q I_3(p, q) \right) \right]. \end{aligned} \quad (5.55)$$

Since the momenta p and q are on-shell for the pion, the expressions simplify a bit and we get

$$i\Delta_{p,q}^\mu = V(p - q)(p^\mu + q^\mu) \quad (5.56)$$

with

$$\begin{aligned} V(p - q) &= \frac{2}{(p - q)^2 - 4m_\pi^2} \times \\ &\quad \times \left[2m_\pi^2 \left(iI_2(m_\pi) - m_\pi^2 iI_3(p, q) \right) - \left((p - q)^2 - 2m_\pi^2 \right) iI_2(p - q) \right], \end{aligned} \quad (5.57)$$

where V is a Lorentz scalar and only depends on $(p - q)^2$ (or $p \cdot q$ alternatively).¹³ The function V seems to have a singularity for $(p - q)^2 = 4m_\pi^2$ due to the denominator but the term in square brackets also vanishes and it turns out that V has only a removable singularity and $V(4m_\pi^2)$ is finite.

Finally, we insert the rho-meson propagator

$$D_\rho^{\mu\nu, ab}(p) = \delta_{ab} \left(L^{\mu\nu}(p) 2g_\nu + T^{\mu\nu}(p) D_\rho(p^2) \right) \quad (5.59)$$

and do the contraction over isospin and Lorentz indices. The isospin factor reduces to

$$\varepsilon_{aeb}\varepsilon_{dfc}\delta_{ef} = \varepsilon_{eba}\varepsilon_{ecd} = \delta_{ad}\delta_{bc} - \delta_{ac}\delta_{bd} \quad (5.60)$$

¹³In [48] the authors calculate this vertex function for the extended pion. In that case $-g_{\pi qq}^2 V(p - q)/2$ is to be replaced by

$$\begin{aligned} &g_{ps}(g_{ps} + g_{pv})iI_2(m_\pi) \\ &+ \frac{(g_{ps} + g_{pv})^2}{(p - q)^2 - 4m_\pi^2} \left[((p - q)^2 - 2m_\pi^2)[iI_2(p - q) - iI_2(m_\pi)] + 2m_\pi^4 iI_3(p, q) \right] \\ &- \frac{g_{pv}^2}{12M^2} \left[((p - q)^2 + 2M^2)iI_2(p - q) - 2iI_1 \right], \end{aligned} \quad (5.58)$$

which in the limit $g_{pv} = 0$ and $g_s = g_{\pi qq}$ is identical to our formula.

for the s -channel. Summing over the Lorentz indices we encounter the expressions

$$\begin{aligned}\Delta^{\text{trans}}(q_1, q_2, q_3, q_4) &:= i \Delta_{q_1, q_2}^\mu T_{\mu\nu}(q_1 - q_2) i \Delta_{q_3, q_4}^\nu, \\ \Delta^{\text{long}}(q_1, q_2, q_3, q_4) &:= i \Delta_{q_1, q_2}^\mu L_{\mu\nu}(q_1 - q_2) i \Delta_{q_3, q_4}^\nu\end{aligned}\quad (5.61)$$

(with $q_1 - q_2 = q_4 - q_3$ and $q_i^2 = m_\pi^2$ implied). We calculate

$$\begin{aligned}\Delta^{\text{long}}(q_1, q_2, q_3, q_4) &= (V(q_1 - q_2))^2 (q_1 + q_2)^\mu \frac{(q_1 - q_2)_\mu (q_4 - q_3)_\nu}{(q_1 - q_2)^2} (q_3 + q_4)^\nu \\ &= (V(q_1 - q_2))^2 \frac{(q_1^2 - q_2^2)(q_4^2 - q_3^2)}{(q_1 - q_2)^2} = 0\end{aligned}\quad (5.62)$$

because of the on-shell condition. We hence observe that the longitudinal part vanishes. The transversal part is

$$\begin{aligned}\Delta^{\text{trans}}(q_1, q_2, q_3, q_4) &= i \Delta_{q_1, q_2}^\mu (\eta_{\mu\nu} - T_{\mu\nu}(q_1 - q_2)) i \Delta_{q_3, q_4}^\nu = \eta_{\mu\nu} i \Delta_{q_1, q_2}^\mu i \Delta_{q_3, q_4}^\nu \\ &= (V(q_1 - q_2))^2 (q_1 + q_2) \cdot (q_3 + q_4) \\ &= V(s)^2 (u - t).\end{aligned}\quad (5.63)$$

With the help of the above we can write the matrix element as

$$\mathcal{M}_{\pi\pi\rho, s}^{ab;cd} = (\delta_{ad}\delta_{bc} - \delta_{ac}\delta_{bd}) (2N_f N_c)^2 g_{\pi qq}^4 (V(s))^2 D_\rho(s)(u - t). \quad (5.64)$$

Applying the same replacement scheme as for the sigma-meson exchange diagram (see (4.20)) we obtain the results for the different channels:

$$\begin{aligned}\mathcal{M}_{\pi\pi\rho, s}^{ab;cd} &= (\delta_{ad}\delta_{bc} - \delta_{ac}\delta_{bd}) (2N_f N_c)^2 g_{\pi qq}^4 (V(s))^2 D_\rho(s)(u - t), \\ \mathcal{M}_{\pi\pi\rho, t}^{ab;cd} &= (\delta_{ab}\delta_{cd} - \delta_{ad}\delta_{bc}) (2N_f N_c)^2 g_{\pi qq}^4 (V(t))^2 D_\rho(t)(s - u), \\ \mathcal{M}_{\pi\pi\rho, u}^{ab;cd} &= (\delta_{ab}\delta_{cd} - \delta_{ac}\delta_{db}) (2N_f N_c)^2 g_{\pi qq}^4 (V(u))^2 D_\rho(u)(s - t).\end{aligned}\quad (5.65)$$

We expressed all momentum dependence in terms of the Mandelstam variables. Because of the momentum scalar product in $\Delta^{\text{trans}}(q_1, q_2, q_3, q_4)$ it is not possible to write the matrix elements in a certain channel solely as a function of one Mandelstam variable (in contrast to the sigma propagation diagram). The reason is that the quark triangles have a more complicated momentum structure due to the vector nature of the rho meson vertex.

Static Limit

Let us again study the static limit of the above matrix elements, i.e. for $p_1 = p_2 = p_3 = p_4 = p$ or equivalently $s = 4m_\pi^2$ and $t = u = 0$. The matrix element in the s -channel vanishes because the factor $(u - t)$ is zero. So, we only need to evaluate D_ρ and V at 0.

For the rho-meson propagator we have

$$D_\rho(0) = \frac{2g_v}{1 + 2g_v J_\rho(0)} = 2g_v. \quad (5.66)$$

We further calculate

$$V(0) = -iI(m_\pi) - iI(0) + m_\pi^2 iK(m_\pi). \quad (5.67)$$

This cancels exactly with $g_{\pi qq}$ given according to (2.81) by

$$g_{\pi qq}^{-2} = -N_c N_f \left(iI(0) + iI(m_\pi) - m_\pi^2 iK(m_\pi) \right). \quad (5.68)$$

The final result for the matrix elements in the static limit is

$$\begin{aligned} \mathcal{M}_{\pi\pi\rho,s}^{ab;cd} &= 0, \\ \mathcal{M}_{\pi\pi\rho,t}^{ab;cd} &= (\delta_{ab}\delta_{cd} - \delta_{ad}\delta_{bc}) 32g_v m_\pi^2, \\ \mathcal{M}_{\pi\pi\rho,u}^{ab;cd} &= (\delta_{ab}\delta_{cd} - \delta_{ac}\delta_{db}) 32g_v m_\pi^2. \end{aligned} \quad (5.69)$$

Semi-Static Limit

Again, it might be too inexact to throw away the full momentum dependence of the matrix elements as it is done in the static limit. In analogy to the sigma propagation diagram, we keep the full momentum dependence of the propagator. Following [48] we also keep the momentum factors $(u-t)$, etc. in the end of the expressions. Only the function V will be evaluated for $s = 4m_\pi^2$, $t = u = 0$. The matrix elements hence read

$$\begin{aligned} \mathcal{M}_{\pi\pi\rho,s}^{ab;cd} &= (\delta_{ad}\delta_{bc} - \delta_{ac}\delta_{bd}) (2N_f N_c)^2 g_{\pi qq}^4 (V(4m_\pi^2))^2 D_\rho(s)(u-t), \\ \mathcal{M}_{\pi\pi\rho,t}^{ab;cd} &= (\delta_{ab}\delta_{cd} - \delta_{ad}\delta_{bc}) (2N_f N_c)^2 g_{\pi qq}^4 (V(0))^2 D_\rho(t)(s-u), \\ \mathcal{M}_{\pi\pi\rho,u}^{ab;cd} &= (\delta_{ab}\delta_{cd} - \delta_{ac}\delta_{db}) (2N_f N_c)^2 g_{\pi qq}^4 (V(0))^2 D_\rho(u)(s-t). \end{aligned} \quad (5.70)$$

We already calculated $V(0)$ for the static limit (see (5.67)). $V(4m_\pi^2)$ will be evaluated numerically (as a limit) since V has a removable singularity at that point.

5.3. Results

We calculate the invariant matrix elements for the different isospin channels (see Section 4.3) again with the additional contribution from the rho-propagation diagram, which we write as

$$\begin{aligned} \mathcal{M}_{\pi\pi\rho,s}^{ab;cd} &= (\delta_{ad}\delta_{bc} - \delta_{ac}\delta_{bd}) \mathcal{M}_{\pi\pi\rho,s}, \\ \mathcal{M}_{\pi\pi\rho,t}^{ab;cd} &= (\delta_{ab}\delta_{cd} - \delta_{ad}\delta_{bc}) \mathcal{M}_{\pi\pi\rho,t}, \\ \mathcal{M}_{\pi\pi\rho,u}^{ab;cd} &= (\delta_{ab}\delta_{cd} - \delta_{ac}\delta_{db}) \mathcal{M}_{\pi\pi\rho,u} \end{aligned} \quad (5.71)$$

with

$$\begin{aligned} \mathcal{M}_{\pi\pi\rho,s} &= (2N_f N_c)^2 g_{\pi qq}^4 (V(s))^2 D_\rho(s)(u-t), \\ \mathcal{M}_{\pi\pi\rho,t} &= (2N_f N_c)^2 g_{\pi qq}^4 (V(t))^2 D_\rho(t)(s-u), \\ \mathcal{M}_{\pi\pi\rho,u} &= (2N_f N_c)^2 g_{\pi qq}^4 (V(u))^2 D_\rho(u)(s-t). \end{aligned} \quad (5.72)$$

We can identify the isospin components A , B and C of $\mathcal{M}_{\pi\pi}^{ab;cd}$ and get

$$\begin{aligned} A &= \mathcal{M}_{\pi\pi,1} + \mathcal{M}_{\pi\pi,2} - \mathcal{M}_{\pi\pi,3} + \mathcal{M}_{\pi\pi,s} + \mathcal{M}_{\pi\pi\rho,t} + \mathcal{M}_{\pi\pi\rho,u}, \\ B &= \mathcal{M}_{\pi\pi,1} - \mathcal{M}_{\pi\pi,2} + \mathcal{M}_{\pi\pi,3} + \mathcal{M}_{\pi\pi,t} - \mathcal{M}_{\pi\pi\rho,s} - \mathcal{M}_{\pi\pi\rho,u}, \\ C &= -\mathcal{M}_{\pi\pi,1} + \mathcal{M}_{\pi\pi,2} + \mathcal{M}_{\pi\pi,3} + \mathcal{M}_{\pi\pi,u} + \mathcal{M}_{\pi\pi\rho,s} - \mathcal{M}_{\pi\pi\rho,t}. \end{aligned} \quad (5.73)$$

Using (4.10) we obtain for the different isospin channels:

$$\begin{aligned} \mathcal{M}_{\pi\pi}^0 &= 3\mathcal{M}_{\pi\pi,1} + 3\mathcal{M}_{\pi\pi,2} - \mathcal{M}_{\pi\pi,3} + 3\mathcal{M}_{\pi\pi,s} + \mathcal{M}_{\pi\pi,t} + \mathcal{M}_{\pi\pi,u} + 2\mathcal{M}_{\pi\pi\rho,t} + 2\mathcal{M}_{\pi\pi\rho,u}, \\ \mathcal{M}_{\pi\pi}^1 &= 2\mathcal{M}_{\pi\pi,1} - 2\mathcal{M}_{\pi\pi,2} + \mathcal{M}_{\pi\pi,t} - \mathcal{M}_{\pi\pi,u} - 2\mathcal{M}_{\pi\pi\rho,s} + \mathcal{M}_{\pi\pi\rho,t} - \mathcal{M}_{\pi\pi\rho,u}, \\ \mathcal{M}_{\pi\pi}^2 &= 2\mathcal{M}_{\pi\pi,3} + \mathcal{M}_{\pi\pi,t} + \mathcal{M}_{\pi\pi,u} - \mathcal{M}_{\pi\pi\rho,t} - \mathcal{M}_{\pi\pi\rho,u}. \end{aligned} \quad (5.74)$$

Static Limit

In the static limit we obtained

$$\begin{aligned} \mathcal{M}_{\pi\pi\rho,s} &= 0, \\ \mathcal{M}_{\pi\pi\rho,t} &= \mathcal{M}_{\pi\pi\rho,u} = 32g_\nu m_\pi^2. \end{aligned} \quad (5.75)$$

Since some of the above matrix elements are the same, the results for the different isospin channels simplify to

$$\begin{aligned} \mathcal{M}_{\pi\pi}^0 &= 6\mathcal{M}_{\pi\pi,1} - \mathcal{M}_{\pi\pi,3} + 3\mathcal{M}_{\pi\pi,s} + 2\mathcal{M}_{\pi\pi,t} + 4\mathcal{M}_{\pi\pi\rho,t}, \\ \mathcal{M}_{\pi\pi}^1 &= 0, \\ \mathcal{M}_{\pi\pi}^2 &= 2\mathcal{M}_{\pi\pi,3} + 2\mathcal{M}_{\pi\pi,t} - 2\mathcal{M}_{\pi\pi\rho,t}. \end{aligned} \quad (5.76)$$

As before the $I = 1$ channel is not present in the static limit.

Scattering Lengths

We again calculate the pion-pion scattering lengths for $l = 0$ via

$$a_0^I = \frac{1}{32\pi m_\pi} \mathcal{M}_{\pi\pi}^{I,\text{sl.}} \quad (5.77)$$

using the matrix elements obtained in the static limit (see above). The results are shown in Table 5.2. We see that the scattering lengths become larger by a factor of 2 to 4 compared to the results without the rho-meson exchange diagram. The importance of the rho-meson exchange compared to the sigma-meson exchange and quark box diagrams varies strongly depending on the chosen parameter set. The deviation from the results in the simple model also means that the Weinberg results (as discussed in Section 4.3) are not well-reproduced any more. This is because we simply added a new interaction (via an intermediate rho meson) while the contribution from the other diagrams remained unchanged. In particular, we neglected the mixing of the pion and the longitudinal part

Param. Set	[C]	[D]	[E]
$\mathcal{M}_{\pi\pi,1}^{\text{sl}}$	-49.18	-56.79	-74.79
$\mathcal{M}_{\pi\pi,3}^{\text{sl}}$	-52.08	-59.60	-77.56
$\mathcal{M}_{\pi\pi,s}^{\text{sl}}$	51.22	58.37	75.77
$\mathcal{M}_{\pi\pi,t}^{\text{sl}}$	50.51	58.18	76.33
$\mathcal{M}_{\pi\pi\rho,t}^{\text{sl}}$	3.48	5.32	5.54
$a_0^0 [m_\pi^{-1}]$	0.254	0.315	0.308
$a_0^2 [m_\pi^{-1}]$	-0.1006	-0.1341	-0.1346
$a_0^0 [m_\pi^{-1}]$	0.116	0.103	0.087
$a_0^2 [m_\pi^{-1}]$	-0.0313	-0.0282	-0.0244

Table 5.2.: Results for the pion-pion scattering lengths a_0^I with rho-meson exchange included (upper values) compared to the results from Section 4.3 in the simple NJL model (lower values).

of the a_1 , which also affects the pion decay constant (as calculated in Appendix B.3). We believe that a new fit of the model parameters in the extended model would be necessary in order to obtain quantitatively good results. Of course, with the modified parameter sets [C] - [E] we are able to study the qualitative effect of an additional vector interaction.

We also calculate the low energy scattering parameters we introduced in Section 4.3. Table 5.3 gives the results. Most of the values are enhanced by a factor of approximately 3 (except for b_1^1) compared to the results in the simple model (see Table 4.2).

Param. Set	[C]	[D]	[E]	[C]	[D]	[E]
$a_0^0 [m_\pi^{-1}]$	0.254	0.315	0.415	0.116	0.103	0.087
$a_1^1 [10^{-3}m_\pi^{-3}]$	64.6	83.9	114.6	23.37	20.79	17.66
$a_0^2 [m_\pi^{-1}]$	-0.101	-0.134	-0.188	-0.0313	-0.0282	-0.0244
$b_0^0 [m_\pi^{-3}]$	0.330	0.417	0.563	0.134	0.118	0.0988
$b_1^1 [10^{-3}m_\pi^{-5}]$	8.9	12.3	17.0	1.2	1.6	0.8
$b_0^2 [m_\pi^{-3}]$	-0.158	-0.204	-0.280	-0.060	-0.055	-0.048

Table 5.3.: Results for pion-pion scattering lengths a_i^I and effective range parameters b_i^I in the extended model (left) compared to the simple model (right).

Chiral Theorems

At the end of Section 4.3 we discussed the cancellation of the static limit matrix elements from the sigma propagation and the box diagram close to the chiral limit leading to small matrix elements for the different isospin channels. Similarly, the contribution from the static limit rho-exchange diagram is small (see Table 5.2) and vanishes in the chiral limit, which is obvious from (5.69) since the matrix elements are proportional to m_π^2 .

5.4. Medium Results

We also want to study the scattering results from the extended model in the medium. This means we have to investigate the medium properties of the additional rho propagation diagram. The form is similar to the sigma propagation diagram and given by

$$\mathcal{M}_{\pi\pi\rho,s} = (2N_f N_c)^2 g_{\pi qq}^4 (V(s))^2 D_\rho(s)(u-t) \quad (5.78)$$

for the s -channel (the other channels are obtained by a suitable replacement of the Mandelstam variables). The factors $g_{\pi qq}$ and $D_\rho(s)$ can both be moved to the medium description while keeping the momentum dependence of the latter. The term $(u-t)$ is not temperature dependent. The problem lies in the vertex function $V(v)$ (which includes the quark triangle and contains the elementary integral iI_3), where $v = s, t, u$. Again, we investigate the momentum dependence of $V(v)$ in a reasonable momentum range (see Figure 5.6) and find that it is not too large, especially for negative arguments. We will therefore approximate $V(v)$ in the static limit ($s = 4m_\pi^2, t = u = 0$). For $V(0)$ we

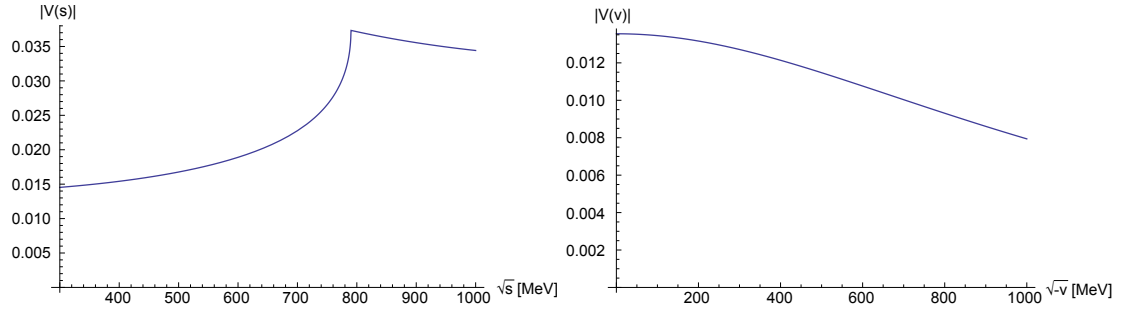


Figure 5.6.: Momentum dependence of the vertex function $V(v)$ for $v = s$, i.e. $v \geq 4m_\pi^2$ (left) and $v = t$ or $v = u$, i.e. $v \leq 0$ (right) for parameter set [C].

obtained an expression in terms of elementary integrals, which can be easily calculated for finite temperature. For $V(4m_\pi^2)$ the situation is more difficult. We argued (see beginning of Section 5.2) that it is obtained as a limit onto a removable singularity. In contrast to $V(0)$ it does not seem possible to write $V(4m_\pi^2)$ as a linear combination of elementary integrals, which would be necessary in order to compute the temperature dependence. Studying the temperature dependence of the quark triangles in the sigma propagation diagram (see Figure 4.8) shows that except for the peak in the t - and u -channel at $T = T_{\text{Mott}}$ the results are almost identical in all channels. This suggests that we can replace $V(4m_\pi^2)$ by $V(0)$ without making a large error away from T_{Mott} and near T_{Mott} the scattering amplitudes are divergent in any case. In the following we will approximate $V(4m_\pi^2)$ by $V(0)$ in the medium calculations for the rho-meson exchange diagram.

Static Limit

As an application we calculate the $l = 0$ scattering lengths a_0^0 and a_0^2 . For those it suffices to consider the case of the static limit with $p_1 = p_2 = p_3 = p_4 = (m_\pi, 0)$. In that case

the s -channel contribution vanishes (see (5.69)) and hence the above described problem with $V(0)$ does not occur. The results for parameter set [C] are shown in Figure 5.7. We compare these results to those in the simple model, again calculated for parameter set [C].

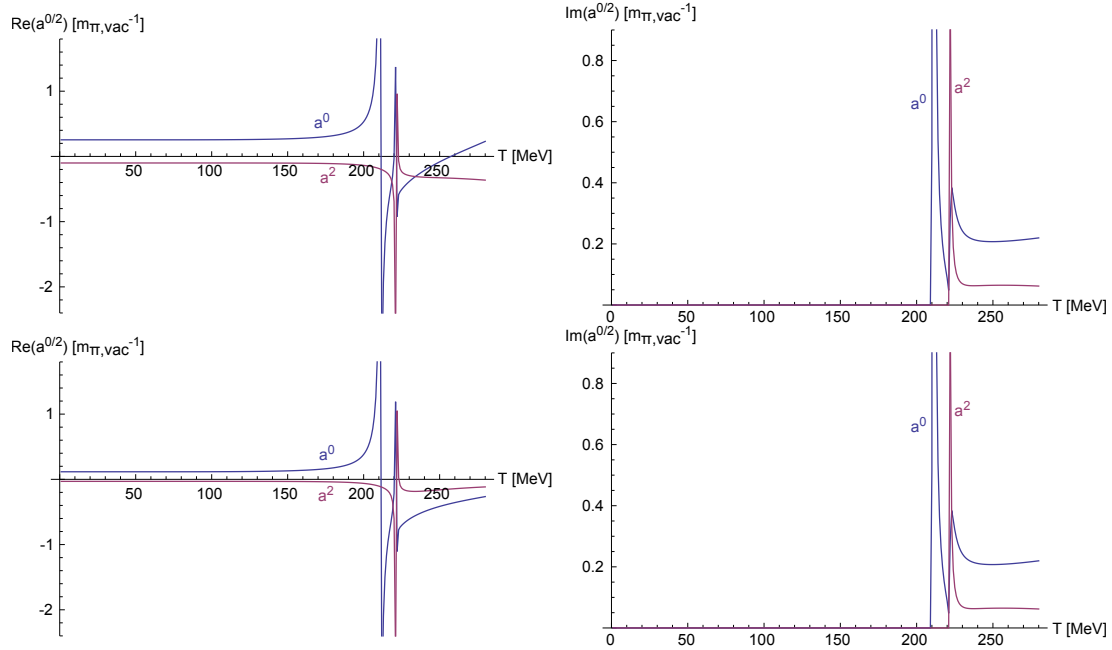


Figure 5.7.: Temperature dependent medium solutions for the scattering lengths a_0^0 and a_0^2 at $\mu = 0$ for parameter set [C] in the extended model (upper) and in the simple model (lower) in units of the inverse *vacuum* pion mass.

The imaginary parts are identical since the contribution from the rho-meson exchange is given by $\mathcal{M}_{\pi\pi\rho,t} = \mathcal{M}_{\pi\pi\rho,u} = 32g_v m_\pi^2$, which is purely real. The rho-meson propagator in the s -channel has of course an imaginary part above the threshold $s > 4M^2$, but the s -channel contribution vanishes completely in the static limit. The real parts show a significant qualitative difference for temperatures $T > T_{\text{Mott}}$. This is due to the momentum factor in the matrix elements for rho-meson exchange which becomes $4m_\pi^2$ in the static limit and of course shows a strong temperature dependence as studied in Section 3.3.

There is no new pole coming from $D_\rho(p^2)$ since we found that for larger temperatures the inverse rho-meson propagator does not have a zero (even when only considering the real part). Hence there is no analogue to T_{diss} (where $2m_\pi = m_\sigma$) for the rho-meson exchange.

5.5. More Realistic Meson Propagators

So far we have studied the effect of the sigma-meson and rho-meson exchange diagrams on the pion-pion scattering amplitudes using the RPA propagators obtained in Sections 2.5 and 5.1. These propagators get an imaginary part above the $q\bar{q}$ threshold ($p^2 > 4M^2$) where the mesons can decay into a quark-antiquark pair. This also leads to an imaginary part in the scattering amplitudes for sufficiently large momenta of the intermediate meson.

Considering that the rho mesons and the sigma meson predominantly decay into pairs of pions [66] it seems unrealistic not to include that effect into our calculations. This can be achieved by studying the Bethe-Salpeter equation in more than leading order in $1/N_c$ as is done in this section. Calculations in the NJL model to more than leading order in $1/N_c$ can be found for example in [90].

Meson Propagators with $1/N_c$ -Corrections

Since we are mainly interested in obtaining an additional width due to the decay into two pions we will include the diagram

$$-iJ_{M,N}^{(\pi \text{ loop})}(p) = \text{Diagram} \quad (5.79)$$

in the polarisation function in addition to the quark polarisation loop in RPA (2.48)

$$-iJ_{M,N}^{(\text{RPA})} = \text{Diagram} \quad (5.80)$$

where we now write (RPA) to distinguish this polarisation loop from the one obtained in this section. In the above *pion-loop diagram* the meson is coupled to an intermediate two-pion state by two quark triangles. This diagram is in next-to-leading order in $1/N_c$. There are also other possible diagrams one might consider (see for example [48]) but we will restrict ourselves to this one since it will give the correct phenomenological behaviour concerning the two-pion decay width.

The full (corrected) polarisation function is hence given by

$$J_{M,N}(p) = J_{M,N}^{(\text{RPA})}(p) + J_{M,N}^{(\pi \text{ loop})}(p). \quad (5.81)$$

The corrected propagator is then obtained from the polarisation function as before (see Section 2.5). The pion-loop correction only contributes to the sigma-meson and rho-meson propagators because of parity and angular momentum conservation.

A careful evaluation of Feynman diagrams shows that the correction to the sigma-meson polarisation function is given by

$$J_{\sigma}^{(\pi \text{ loop})}(p) = -(2N_c N_f)^2 \frac{3}{2} (i \Delta(p^2))^2 i \int \frac{d^4 k}{(2\pi)^4} D_{\pi}^{(\text{RPA})}(p+k) D_{\pi}^{(\text{RPA})}(k) \quad (5.82)$$

where we used the quark triangle $i\Delta$ introduced in Section 4.1 about the sigma-exchange diagram. To simplify the above expression further we write the pion propagators (in RPA) in pole approximation

$$D_\pi^{(\text{RPA})}(p^2) \approx \frac{g_{\pi qq}^2}{p^2 - m_\pi^2} \quad (5.83)$$

according to (2.71). This amounts to evaluating the quark-pion coupling $g_{\pi qq}(p)$ on-shell, neglecting the fact the the momentum k in the pion loop runs over all possible four-momenta. For the polarisation function this yields

$$J_\sigma^{(\pi \text{ loop})}(p) = -(2N_c N_f)^2 \frac{3}{2} (i\Delta(p^2))^2 g_{\pi qq}^4 iI_2^{(\pi)}(p), \quad (5.84)$$

where the elementary integral $iI_2^{(\pi)}(p)$ is identical to $iI_2(p)$ with M replaced by m_π . Some care is needed when evaluating this integral for finite temperature since the sum over fermionic Matsubara frequencies is to be replaced by a sum over bosonic ones. The retarded expression $iI_2^{(\pi),+}(p_0, \vec{p})$ can be calculated analytically for general four-momenta $p = (p_0, \vec{p})^t$ and is given in Appendix D.4.

An analogous calculation can be made for the rho-meson polarisation function and one gets

$$J_\rho^{(\pi \text{ loop}),ab,\mu\nu}(p) = -\delta^{ab} (2N_c N_f)^2 i \int \frac{d^4 k}{(2\pi)^4} (i\Delta_{k,p+k}^\mu)(i\Delta_{p+k,k}^\nu) D_\pi^{(\text{RPA})}(p+k) D_\pi^{(\text{RPA})}(k) \quad (5.85)$$

with the quark triangle $i\Delta^\mu$ from Section 5.2. We again make an on-shell approximation and get

$$J_\rho^{(\pi \text{ loop}),ab,\mu\nu}(p) = -\delta^{ab} (2N_c N_f)^2 (V(p))^2 g_{\pi qq}^4 \times \\ \times i \int \frac{d^4 k}{(2\pi)^4} \frac{(2k+p)^\mu (2k+p)^\nu}{(p^2 - m_\pi^2 + i\varepsilon)((p+k)^2 - m_\pi^2 + i\varepsilon)}. \quad (5.86)$$

Writing the above propagator in terms of transversal and longitudinal part (as in Section 5.1) yields

$$J_\rho^{(\pi \text{ loop}),\text{trans}}(p) = -(2N_c N_f)^2 (V(p))^2 g_{\pi qq}^4 \frac{1}{3} \left(2iI_1^{(\pi)} + (4m_\pi^2 - p^2)iI_2^{(\pi)}(p) \right), \quad (5.87) \\ J_\rho^{(\pi \text{ loop}),\text{long}}(p) = -(2N_c N_f)^2 (V(p))^2 g_{\pi qq}^4 2iI_1^{(\pi)},$$

where $I_1^{(\pi)}$ is defined in the same way as $iI_2^{(\pi)}(p)$.

With these expressions we can in principle determine the more realistic meson propagators. The integral $iI_2^{(\pi)}(p)$ will give an imaginary part above the $p^2 > 4m_\pi^2$ threshold, which is exactly the desired effect. However, there will also be an additional real part affecting the masses of the rho and sigma meson. This spoils the ‘delicate cancellation’ between the sigma-exchange and box diagram (as described at the end of Section 4.3). A simple solution to this problem does not seem to be possible and it is suggested in

[47] to ignore the real part of the pion-loop contributions and only take their imaginary part, i.e.

$$J_M(p) = J_M^{(\text{RPA})}(p) + i\text{Im}\left(J_M^{(\pi \text{ loop})}(p)\right) \quad (5.88)$$

for $M = \sigma, \rho$. This gives the widths corresponding to $\pi\pi \leftrightarrow \sigma$ and $\pi\pi \leftrightarrow \rho$ without violating the chiral low-energy theorems. The downside of this approach is that the neglected real part which is normally related to the imaginary part by a Kramers-Kronig relation violates causality. Finally, we note that in the s -channel the sigma-meson and rho-meson propagator has to be evaluated at $s \geq 4m_\pi^2$ wherefore there is always an imaginary part, while in the t - and u -channel, where $t, u \leq 0$ there is never an imaginary part from the pion-loop polarisation.

To calculate the imaginary part of $J_M^{(\pi \text{ loop})}(p)$ we will assume that the quark triangles $i \Delta(p)$ and $V(p)$ are purely real. This is the case below the $\pi \leftrightarrow q\bar{q}$ threshold at T_{Mott} . In that case the imaginary part of the additional polarisation functions can be obtained by calculating the imaginary part of the integral $iI_2^{(\pi)}(p)$. The imaginary part of $I_1^{(\pi)}$ vanishes and hence there is no longitudinal contribution to the rho-meson propagator.¹⁴ The results can finally be written as

$$\begin{aligned} J_\sigma(p) &= J_\sigma(p)^{(\text{RPA})} - (2N_c N_f)^2 \frac{3}{2} (i \Delta(p^2))^2 g_{\pi q}^4 \text{Im}\left(iI_2^{(\pi)}(p)\right), \\ J_\rho^{\text{trans}}(p) &= J_\rho^{\text{trans, (RPA)}}(p) - (2N_c N_f)^2 (V(p))^2 g_{\pi q}^4 \frac{1}{3} (4m_\pi^2 - p^2) \text{Im}\left(iI_2^{(\pi)}(p)\right). \end{aligned} \quad (5.89)$$

Note that $J_\rho^{\text{trans, (RPA)}}(p)$ corresponds to $J_\rho(p)$ in Section 5.1 where we omitted the *trans* as there was no longitudinal part in the rho-meson polarisation loop at all.

¹⁴In principle the longitudinal part of the rho-meson polarisation function should always vanish (real and imaginary part). This is the case if in addition to the pion-loop diagram one also includes a tadpole diagram involving the exchange of a pion as described in [48].

6. Shear Viscosity of a Pion Gas

The previous chapters have provided us with the quantum field theoretical description of QCD matter within the framework of the NJL model. In particular we calculated the matrix elements for the scattering of pions, which emerged as composite degrees of freedom via the Bethe-Salpeter equation. We argued in Chapter 1 why we concentrated on the scattering of pions rather than for example quarks to describe transport phenomena in strongly interacting matter for not too large temperatures based on a microscopic description (see also [46, 38, 10, 47]). This chapter is aimed at the calculation of the shear viscosity of a pion gas where the interaction between the pions is described by the NJL model results.

Section 6.1 will introduce the concept of relativistic hydrodynamics, the framework in which we will define the shear viscosity η of a fluid. We will then derive an expression for η from kinetic theory (see Section 6.2). The subsequent Section 6.3 will introduce the pion gas and its thermodynamics. Together with the matrix elements from Chapters 4 and 5 this suffices to give an estimate of the shear viscosity, which we present in Section 6.4. The results of the calculations are discussed in Section 6.5.

6.1. Relativistic Hydrodynamics

Relativistic hydrodynamics¹⁵ deal with the theoretical description of fluids, i.e. gases or liquids moving with velocities that are not negligible compared to the speed of light. An introduction to the topic can be found in [91], which will also be the basis of the following paragraphs.

We consider a system of particles in *local thermodynamic equilibrium*, meaning that we can define the intensive thermodynamic variables temperature $T(x)$, chemical potential $\mu(x)$ and pressure $P(x)$ locally. This is the case if the mean free path between two collisions is small compared to the length scale of interest to the observer. This also yields entropy density $s(x)$, energy density $\varepsilon(x)$ and number density $n(x)$ as local quantities.

Perfect Fluid

The flow of a fluid is characterised by the local four-velocity

$$u^\mu(x) = \frac{dx^\mu}{d\tau} = \gamma \begin{pmatrix} 1 \\ \vec{v} \end{pmatrix}, \quad (6.1)$$

¹⁵Historically, the term *hydrodynamics* was used to describe the flow of fluids (gases or liquids) while in modern day physics the term *fluid dynamics* is used instead. Hydrodynamics is then only the description of liquids (and aerodynamics that of gases). For the purposes of this text we will not make a distinction between gases or liquids and hence just speak of fluids, which corresponds to the historical understanding of the term *hydrodynamics*.

where \vec{v} is the three-velocity and $\gamma = 1/\sqrt{\vec{v}^2 + 1}$. Given a spacetime point x^μ we can find a suitable Lorentz transformation such that the fluid is locally at rest, i.e.

$$u^\mu(x) = \begin{pmatrix} 1 \\ \vec{0} \end{pmatrix}. \quad (6.2)$$

What does the stress-energy tensor $T^{\mu\nu}$ look like at this point? For a *perfect fluid* (or *ideal fluid*) we assume that an observer moving with the velocity $\vec{v}(x)$ of the fluid at x^μ sees the fluid around him as isotropic. For the stress-energy tensor the isotropy means that at x^μ it is diagonal with

$$T^{\mu\nu}(x) = \begin{pmatrix} \varepsilon & & & \\ & P & & \\ & & P & \\ & & & P \end{pmatrix}, \quad (6.3)$$

where ε is the energy density and P the pressure. Making a Lorentz transformation back to the laboratory frame we arrive at the expression

$$T^{\mu\nu}(x) = (P(x) + \varepsilon(x))u^\mu(x)u^\nu(x) - P(x)\eta^{\mu\nu} \quad (6.4)$$

for all x^μ . If we for the moment assume a system with only one particle species, the only remaining independent¹⁶ observable is the local number density $n(x)$ or equivalently the particle flow

$$J^\mu(x) = n(x)u^\mu(x). \quad (6.5)$$

To summarise our findings so far, we can describe the fluid by the seven variables $n(x)$, $P(x)$, $\varepsilon(x)$ and $u^\mu(x)$. We now want to find a system of seven equations such that the evolution of the hydrodynamic system is determined. First of all, the four-velocity obeys the normalisation condition

$$u^\mu(x)u_\mu(x) = 1. \quad (6.6)$$

Energy-momentum conservation implies

$$\partial_\nu T^{\mu\nu}(x) = 0 \quad (6.7)$$

and particle number conservation yields the *continuity equation*

$$\partial_\mu J^\mu(x) = 0. \quad (6.8)$$

These are six constraints. To obtain a further equation we have to assume that the system is at all times in local thermal equilibrium. This yields an *equation of state*

$$P(x) = P(\varepsilon(x), n(x)), \quad (6.9)$$

¹⁶We know that the thermodynamics are fully described by a set of three variables, which can e.g. be ε , P and n .

which allows us to express pressure as a function of number density and energy density. With the equation of state the hydrodynamics of the system are fully determined.

Entropy Conservation

One important consequence of the assumptions for a perfect fluid is the conservation of entropy. Defining the entropy flow

$$s^\mu(x) := s(x)u^\mu(x) \quad (6.10)$$

one can show that

$$\partial_\mu s^\mu = 0. \quad (6.11)$$

Imperfect Fluid

So far, we considered a perfect fluid. In ideal hydrodynamics the stress-energy tensor only depends on certain local quantities such as $u^\mu(x)$ but not on gradients thereof. This is closely related to the isotropy assumption we made in the comoving frame. We can view this as a leading order truncation in the expansion of $T^{\mu\nu}$ in terms of gradients.

In the following description of an *imperfect* (or *non-ideal*) *fluid* we will allow $T^{\mu\nu}$ to have corrections to the ideal expression which are linear in four-velocity gradients. These additional terms lead to dissipative effects, which means that thermal equilibrium is not strictly maintained and the fluid kinetic energy is dissipated as heat. J^μ may also contain gradient terms. Altogether we have

$$\begin{aligned} T^{\mu\nu}(x) &= (P(x) + \varepsilon(x))u^\mu(x)u^\nu(x) - P(x)\eta^{\mu\nu} + \Delta T^{\mu\nu}(x), \\ J^\mu(x) &= n(x)u^\mu(x) + \Delta J^\mu(x) \end{aligned} \quad (6.12)$$

with the correction terms $\Delta T^{\mu\nu}(x)$ and $\Delta J^\mu(x)$ parametrised as

$$\begin{aligned} \Delta T^{\mu\nu} &= \eta \left(\partial^\mu u^\nu + \partial^\nu u^\mu + u^\nu u^\lambda \partial_\lambda u^\mu + u^\mu u^\lambda \partial_\lambda u^\nu \right) + \left(\zeta - \frac{2}{3}\eta \right) (\eta^{\mu\nu} - u^\mu u^\nu) \partial_\lambda u^\lambda, \\ \Delta J^\mu &= \kappa \left(\frac{nT}{\varepsilon + P} \right) \left(\partial^\mu - u^\mu u^\lambda \partial_\lambda \right) \frac{\mu}{T}. \end{aligned} \quad (6.13)$$

The dissipative terms in the stress-energy tensor have the (*shear*) *viscosity* η and the *bulk viscosity* ζ as coefficients. The coefficient κ in the current J^μ is the *thermal conductivity*. The coefficients η , ζ and κ may assume non-negative values and are referred to as *transport coefficients*.

One consequence of the imperfectness of the fluid is that entropy is no longer conserved. More precisely one finds that

$$\partial_\mu s^\mu(x) \geq 0 \quad (6.14)$$

for all x^μ [91]. It should also be noted that for an imperfect fluid the velocity of energy and particle transport do not coincide any more as they do for a perfect fluid. The reason is of course that energy can also be transported as heat, which is expressed by the term with the thermal conductivity κ .

6.2. Kinetic Theory of Gases

In the hydrodynamics approach we have assumed that the fluids obey the *continuum assumption*. Quantities like pressure or temperature are defined locally and are continuous functions of space and time ignoring the fact that the fluid is in reality composed of discrete particles.

In order to obtain an expression for the shear viscosity we will make use of kinetic theory [92, 93, 94]. The *kinetic theory of gases* describes a gas (or a fluid in general) as a large number of small particles. Kinetic theory allows us to explain macroscopic properties of gases such as the shear viscosity by studying their microscopic dynamics.

Shear Viscosity

Of the three transport coefficients introduced above we are only interested in the shear viscosity η in this work. In the following we will study this coefficient in a kinetic theory approach [36]. A very simple estimate for the shear viscosity is derived in Appendix G.1 and reads

$$\eta \approx \frac{1}{3} n \bar{p} \lambda, \quad (6.15)$$

where λ is the mean free path and \bar{p} the average momentum of the particles. The derivation is non-relativistic and under the assumption that the velocity field $u^\mu(x)$ varies only slowly in space.

It should be noted that the above formula is only a rough estimate and the factor $1/3$ should not be trusted too much. However, the general dependence on particle density n , average momentum \bar{p} and the mean free path λ ought to be correct. More sophisticated calculations [36, 95] lead to a factor of 0.21 in the non-relativistic limit and $4/15$ in the ultrarelativistic limit, i.e. where temperature is much larger than the particles' mass. This shows that our estimate, which was derived for non-relativistic particles, retains its general form also for relativistic particles.

Range of Validity

In general, the kinetic theory of fluids depends on certain assumptions. This limits the applicability of the above shear viscosity estimate. One major simplification of the kinetic approach presented in this section is that we assumed classical particles. Of course, to calculate the shear viscosity η we will use the invariant matrix elements as input, which we obtained from our quantum field theoretical considerations. However, they only enter as cross sections, i.e. absolute value squared of the invariant matrix elements, at which point we go from a quantum to a classical theory. This simplification is valid as long as each particle has enough time to 'propagate classically' between two collisions, i.e. each collision occurs independently. This is the case if the mean free path λ is much larger than the typical range of interaction d . In practice this means that we can apply kinetic theory only to sufficiently dilute gases.

Simple estimates for the range of validity are discussed in [96]. The range of the interaction d could be defined as the Compton wavelength of the particles, i.e. $d = 1/m$, where m is the particles' mass. Alternatively one might approximate d in the hard-sphere

limit as $d = \sqrt{\sigma/m}$ (with the cross section σ). The authors show that both expressions yield similar constraints on temperature.

6.3. Thermodynamics of a Pion Gas

In this section we present a thermodynamic description of a pion gas. We consider an ideal gas consisting of three types of spin 0 bosons: π^+ , π^0 and π^- . The π^0 is its own antiparticle and hence its particle number N_0 is not conserved, which means that there is no corresponding chemical potential. The π^+ is the antiparticle of the π^- , which means that they can be created in pairs and only the difference of their particle numbers $N_{\text{net}} := N_+ - N_-$ is a conserved quantity, which implies that there is only one chemical potential μ_I for N_{net} . We call this chemical potential *charge* (or *isospin*) *chemical potential* since it corresponds to conservation of charge (or isospin). It is not to be confused with the quark chemical potential μ , which we use throughout the text. As we only study uncharged QCD matter in this text, we will set $\mu_I = 0$.

We will determine the thermodynamic properties of the system in the grand canonical ensemble regarding T , V and μ_I as thermodynamic variables. Since we assumed an ideal gas, the following results will be standard results for a Bose gas [97, 98, 99]. However, in contrast to most textbooks we will use the relativistic dispersion relation $\varepsilon_{\vec{k}} = \sqrt{\vec{k}^2 + m_\pi^2}$ where we as before assume that all pions have the same mass m_π , which depends on temperature as calculated in Section 3.3. The derivations leading to the expressions in this section are found in Appendix G.2 and loosely follow [100].

For pressure p , entropy density s , energy density ε and particle density n we obtain:

$$\begin{aligned}
P(T, V, \mu_I = 0) &= 3 \frac{m_\pi^2}{2\pi^2 \beta^2} \sum_{n=1}^{\infty} \frac{1}{n^2} K_2(n\beta m_\pi), \\
s(T, V, \mu_I = 0) &= 3 \frac{m_\pi^2}{2\pi\beta} \sum_{n=1}^{\infty} \frac{1}{n^2} [4K_2(n\beta m_\pi) + n\beta m_\pi K_1(n\beta m_\pi)], \\
\varepsilon(T, V, \mu_I = 0) &= 3 \frac{m_\pi^2}{2\pi\beta^2} \sum_{n=1}^{\infty} \frac{1}{n^2} [3K_2(n\beta m_\pi) + n\beta m_\pi K_1(n\beta m_\pi)], \\
n(T, V, \mu_I = 0) &= 3 \frac{m_\pi^2}{2\pi^2 \beta} \sum_{n=1}^{\infty} \frac{1}{n} K_2(n\beta m_\pi).
\end{aligned} \tag{6.16}$$

Here, $K_\nu(x)$ denotes the *modified Bessel function of second kind* (of order ν). For an uncharged pion gas all three components have the same thermodynamic properties yielding the degeneracy factor of 3 in front of every expression. The above quantities are plotted in Figure 6.1 as a function of temperature.¹⁷

¹⁷Note that the pion mass m_π itself depends on T . When deriving for example the above expression for the entropy $s(T, V, \mu_I) = \frac{1}{V} \left. \frac{\partial(T \ln Z)}{\partial T} \right|_{V, \mu_I}$, one should in principle also consider the derivative of m_π with respect to T (applying the product rule). We neglect this effect and obtain the standard formulae for an ideal gas since the dependence of m_π on T is negligible for temperatures below 150 MeV for parameter set [A] and even higher temperatures for the other parameter sets [B] - [E]. The explicit

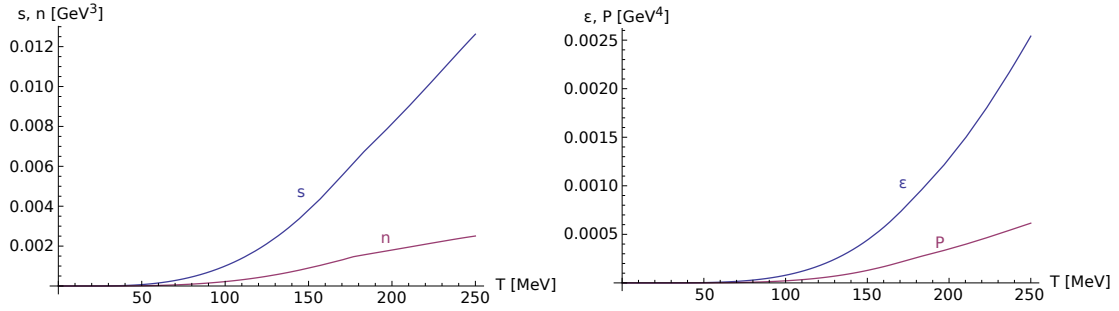


Figure 6.1.: Thermodynamic quantities of the relativistic pion gas at $\mu_I = 0$ as functions of temperature. The dependence of the pion mass on temperature is calculated with parameter set [A].

The average (mean) momentum of a pion is given by

$$\bar{p} = \frac{1}{\int \frac{d^3k}{(2\pi)^3} \frac{1}{e^{\beta\varepsilon_k} - 1}} \int \frac{d^3k}{(2\pi)^3} |\vec{k}| \frac{1}{e^{\beta\varepsilon_k} - 1}. \quad (6.17)$$

6.4. Shear Viscosity Estimate in the NJL model

In this section we combine the findings from the previous sections, which dealt with hydrodynamics, kinetic theory and thermodynamics in order to obtain an estimate for the shear viscosity based on the NJL model.

We saw in Section 6.2 that the shear viscosity of a classical gas can be approximated by the simple formula

$$\eta \approx \frac{1}{3} n \bar{p} \lambda, \quad (6.18)$$

where \bar{p} is the average momentum of the particles in the gas and λ is the mean free path of a particle. The mean free path can be related to the differential cross section via [101, 95]

$$\frac{1}{n\lambda} = \int d\Omega \frac{d\sigma}{d\Omega} \sin^2(\vartheta) = 2\pi \int_0^\pi d\vartheta \frac{d\sigma}{d\Omega} \sin^3(\vartheta) =: \tilde{\sigma}. \quad (6.19)$$

The factor $\sin^2(\vartheta)$ in the integral takes into account that scattering at larger angles has more impact on momentum degradation than at small angles. We can hence write the shear viscosity η as

$$\eta \approx \frac{1}{3} \frac{\bar{p}}{\tilde{\sigma}}. \quad (6.20)$$

This result implies that the stronger particles interact, the smaller their shear viscosity is. This dependence can be understood from the derivation of the shear viscosity estimate in Appendix G.1. The shear viscosity determines how fast velocity differences will even out

dependence on the temperature dependent pion mass can be seen as a small kink in the plots of Figure 6.1 around $T = 180$ MeV.

in a fluid. This is due to the particle movement between regions with different velocities. This momentum transfer through particle movement happens easiest when particles feel only a small interaction between them. If however they are strongly interacting, they can only travel a short distance between two collisions and hence will not carry much momentum to neighbouring fluid regions.

In general, (6.18) should be written as a sum over several particle species i with densities n_i , etc. We saw however that for $\mu_I = 0$ all pion species have the same thermodynamic properties and hence can be treated on equal footing. This gave a degeneracy factor in the expression for the number density. Following [96] we will simply average over isospin according to

$$\frac{d\sigma}{d\Omega} = \frac{1}{\sum_{I=0}^2 (2I+1)} \sum_{I=0}^2 (2I+1) \frac{|\mathcal{M}_{\pi\pi}^I|^2}{64\pi^2 s}. \quad (6.21)$$

In the calculations leading to the above formulæ no momentum dependence of the differential cross section $d\sigma/d\Omega$ was assumed. However, the NJL cross sections in general depend on the particles' momenta. To be more specific, after integrating out the angle (or t) dependence, $\tilde{\sigma}$ depends on the Mandelstam variable s . For simplicity we will evaluate the cross section $\tilde{\sigma}$ at some *typical* momentum \bar{p} , i.e. we will set $s = 4(m_\pi^2 + \bar{p}^2)$, where $\bar{p} = \bar{p}(T)$ is the average momentum of a pion for a certain temperature T calculated according to (6.17). This will give the typical s at which collisions occur. One could have also calculated the root mean square (rms) momentum or directly the average s . All these calculation yield similar results, which differ by factors of the order of one. The average momentum \bar{p} of a pion is plotted in Figure 6.2. For comparison we also show the root mean square of the pion momentum. The average momentum is mainly linear in T except for higher values of T , where the pion mass dependence on T plays a role.

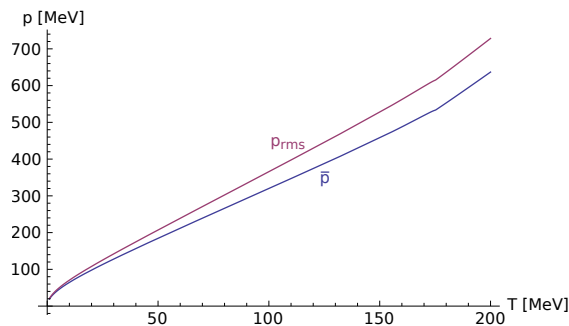


Figure 6.2.: Average pion momentum (mean and rms value) as a function of T for $\mu_I = 0$. The dependence of the pion mass on temperature is calculated for parameter set [A].

6.5. Results

In this chapter we present calculations for the shear viscosity using the results from the previous sections. Recall that $\mu = \mu_I = 0$ will be assumed for all calculations. We present results in four different approximations of increasing accuracy and computational complexity.

1. *Static limit*: The simplest approximation is to evaluate the complete matrix elements in the static limit. In that case they do not depend on the Mandelstam variables (and in particular not on the scattering angle ϑ) and we get

$$\tilde{\sigma} = 2\pi \int_0^\pi d\vartheta \frac{d\sigma}{d\Omega} \sin^3(\vartheta) = \frac{8\pi}{3} \frac{d\sigma}{d\Omega}. \quad (6.22)$$

2. *Semi-static limit (only s-channel)*: We argued in Section 4.1 that we should also consider the momentum dependence of the meson propagators and only evaluate the quark triangles and boxes in the static limit. We expect the most important contribution to come from the s -channel diagrams. On the other hand, for the t - and u -channel the calculation of the meson propagators requires the evaluation of the integral iI_2 for non-vanishing three-momentum, which is computationally difficult. In this approximation we therefore only consider the s -channel as momentum dependent.
3. *Semi-static limit (all channels)*: To study how important the full momentum dependence of the meson propagators in the t - and u -channel is, we also calculate the shear viscosity for all channels evaluated in the semi-static limit.
4. *Improved meson propagators*: We obtain our most realistic approximation by considering the $1/N_c$ -corrected meson propagators from Section 5.5. Here we added an imaginary part to incorporate a width corresponding to $\sigma, \rho \leftrightarrow \pi\pi$, which we consider an important effect. As in Approximation 3 the meson propagators will be treated as momentum dependent in all channels.

6.5.1. Simple Model

We begin by calculating the shear viscosity estimate for the simple model (without a rho-meson exchange). The results for Approximations 1, 2 and 3 are shown in Figure 6.3 for parameter set [A]. The figure also shows the corresponding plot for the shear viscosity over entropy density ratio η/s .

We also estimate the range of validity of the kinetic approach. Following Section 6.2 we calculate the ratio λ/d with the mean free path $\lambda = 1/(n\tilde{\sigma})$ and the interaction range d , which we take to be $d = 1/m_\pi$, the Compton wavelength of the pion. Alternatively one could have estimated the interaction range by $d = 1/m_\sigma$ in view of the sigma propagation diagram but this does not change the results considerably. The calculations show that the the ratio λ/d shows a behaviour very similar to that of the ratio η/s . This means that λ/d is larger than one for almost all T except where η or η/s exhibit a zero. At

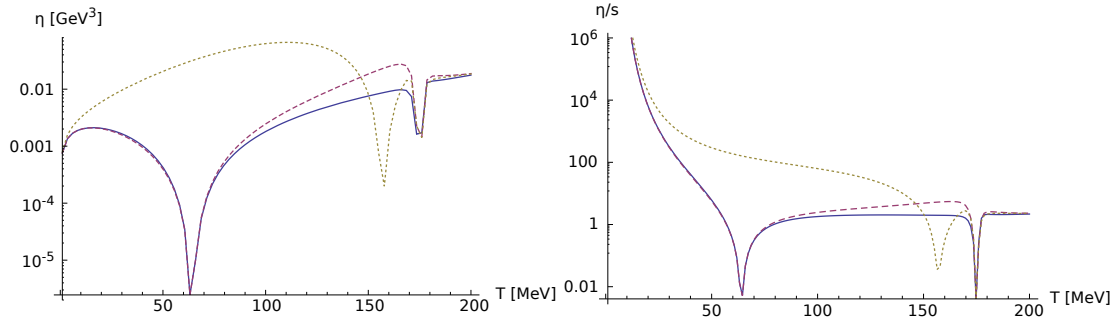


Figure 6.3.: Shear viscosity estimate (left) and ratio η/s (right) for pion gas as function of T for parameter set [A]. The dotted line corresponds to Approximation 1, the dashed line to Approximation 2 and the solid line to Approximation 3.

these temperatures the kinetic description breaks down. This implies in particular that with our approach we cannot make a statement about a lower bound for η/s .

Let us shortly discuss the results obtained for the different approximations. In Approximation 1 (static limit) we see that the shear viscosity vanishes for $T = 0$ and increases monotonously up to $T \lesssim 100$ MeV. This dependence is due to the temperature dependence of the average momentum as shown in Figure 6.2. For even larger temperatures the shear viscosity decreases again and even drops to zero (two times: once exactly, once almost), which can be explained by pole and the sharp peak in the differential cross section at T_{Mott} and T_{diss} respectively (for details see discussion in Section 4.4).

The most unrealistic feature of the static limit approximation is that we do not consider the momentum dependence of the sigma-meson propagator. In that case the propagator in the s -channel $D_\sigma(4m_\pi^2)$ becomes extremely large at T_{diss} where $m_\sigma = 2m_\pi$. If we on the other hand consider the momentum-dependent expression $D_\sigma(s) = D_\sigma(4m_\pi^2 + 4\bar{p}^2)$ (Approximations 2 and 3) this peak is shifted to lower momenta by the average thermal momentum \bar{p} . We also observe that, as expected, there is only a small qualitative difference between the Approximations 2 and 3. The zero of the shear viscosity at T_{Mott} is due to the quark triangles and quark quadrilaterals (in the static limit) and remains for Approximations 2 and 3.

We finally calculate the shear viscosity in Approximation 4 using the most realistic meson propagators. The result for η and η/s is shown in Figure 6.4. The zero in the shear viscosity corresponding to the pole of the sigma propagator vanishes since the propagator obtains a large width in the s -channel due to the process $\sigma \leftrightarrow \pi\pi$. Remarkably, the shear viscosity over entropy ratio reaches a value of the order of 1 at some intermediate temperature ($T \approx 60$ MeV) and then stays almost constant over a large temperature region up to T_{Mott} .

The results for η and η/s are in good agreement with those obtained in [10, 47] where similar calculations were done in a more realistic kinetic theory approach. Here, the author calculated the shear viscosity from a Boltzmann-Ueling-Uhlenbeck (BUU) approach [94], where the NJL matrix elements enter in a two-body collision term. The author also compared his results to those of the simple shear viscosity estimate which is

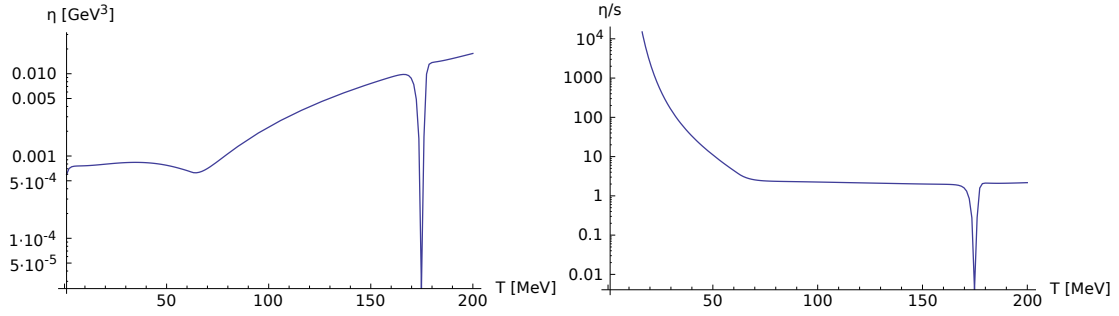


Figure 6.4.: Shear viscosity estimate (left) and η/s (right) for pion gas as function of T in Approximation 4 for parameter set [A].

used in this work and finds no significant qualitative difference [38].

6.5.2. Extended Model

We now study the effect of an additional vector interaction, i.e. we calculate the shear viscosity estimate in the extended NJL model, again for Approximations 1 to 4. We use parameter set [C] for the calculations and compare to the results in the simple model also calculated for parameter set [C]. As the cross sections are larger in the extended model, we expect the shear viscosity to be smaller according to formula (6.20). The results for η and η/s are shown in Figures 6.5 and 6.6. The additional contribution

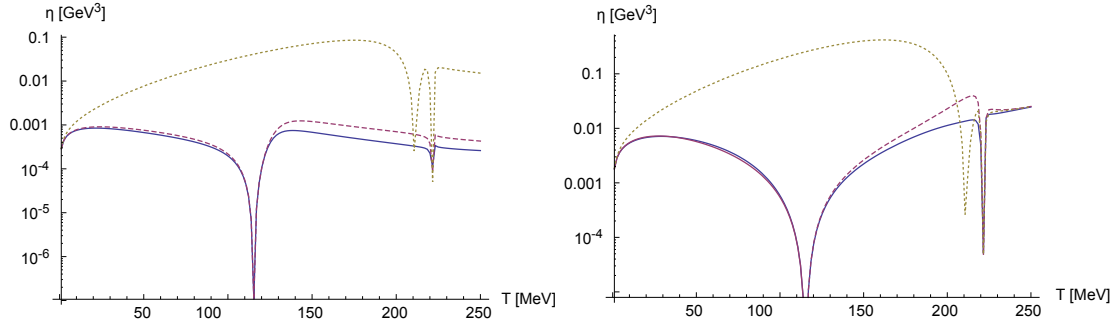


Figure 6.5.: Shear viscosity as a function of T in the extended model (left) and in the simple model (right) for parameter set [C]. The dotted line corresponds to Approximation 1, the dashed line to Approximation 2 and the solid line to Approximation 3.

from the vector channel does not change the poles of the matrix elements and hence the zeros of the shear viscosity are the same in the simple and the extended model. A qualitative difference in Approximations 2 and 3 is that while in the simple model the shear viscosity increases between the first and the second zero (in the mid-temperature region) there is a decrease for the extended model results. This is due to the momentum factor ($u - t$), etc. in the rho-meson exchange matrix elements (5.65).

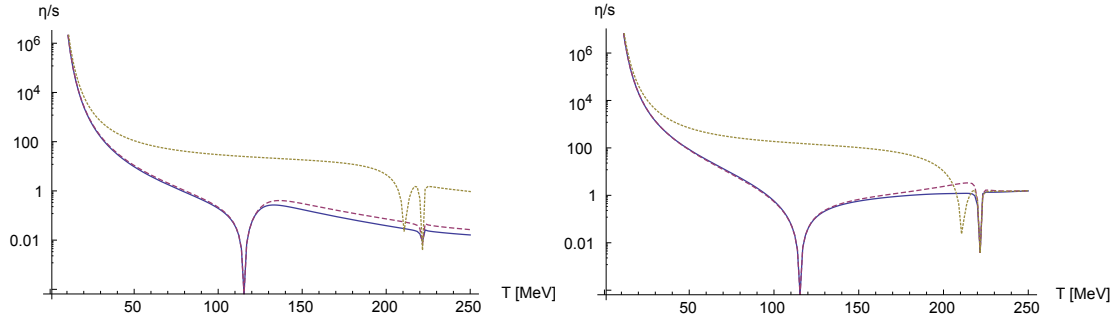


Figure 6.6.: Shear viscosity over entropy density ratio as a function of T in the extended model (left) and in the simple model (right) for parameter set [C]. The dotted line corresponds to Approximation 1, the dashed line to Approximation 2 and the solid line to Approximation 3.

Approximation 4 using the most realistic sigma meson and rho-meson propagators is shown in Figures 6.7 and 6.8. Again, the zero corresponding to T_{diss} vanishes. There is

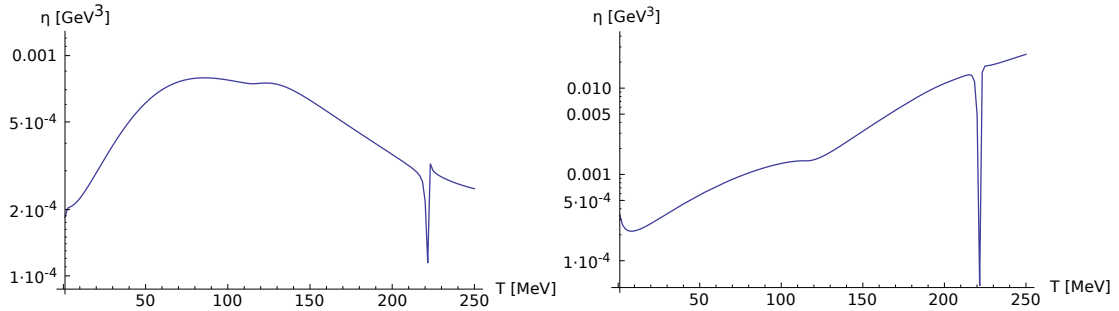


Figure 6.7.: Shear viscosity estimate for pion gas as function of T in Approximation 4 for parameter set [C] in the extended model (left) and simple model (right).

a strong qualitative difference between the simple and the extended model for the shear viscosity for larger temperatures due to the dominance of the rho meson diagram. While η/s is almost constant in the mid-temperature region in the simple model (as discussed above), in the extended model there is a decrease.

6.5.3. Discussion

We briefly discuss the prediction for the shear viscosity and in particular the shear viscosity over entropy ratio within the NJL model. We mainly focus on Approximation 4 since we believe that this yields the most realistic results. We observe that η/s exhibits a sharp drop for small temperatures and then stays almost constant in a large temperature region until it becomes zero at T_{Mott} . The biggest qualitative difference between the simple and the extended model is that in the simple model there is a slight increase of η/s towards T_{Mott} while in the extended model η/s continues to drop.

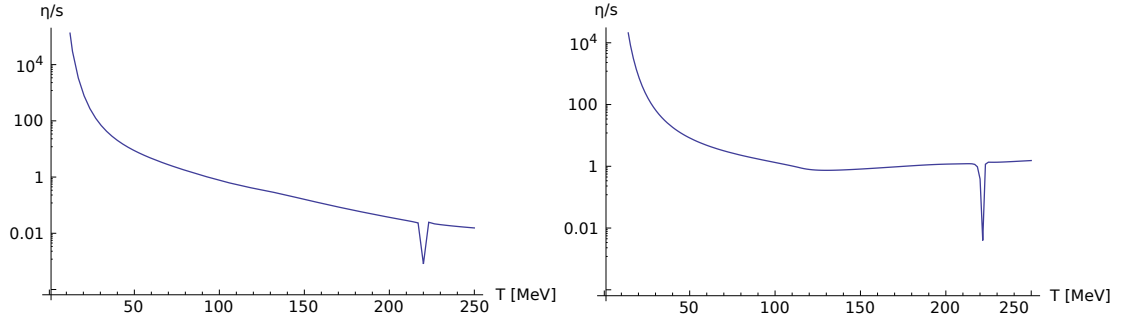


Figure 6.8.: Ratio η/s for pion gas as function of T in Approximation 4 for parameter set [C] in the extended model (left) and simple model (right).

The conclusion from the calculations in both NJL models is that QCD matter becomes strongly interacting in the chiral crossover region (with η/s of the order of 1). Quantitatively the results should only be trusted in the simple model with parameter set [A]. The zero of the shear viscosity at T_{Mott} is due to the channel $\pi \leftrightarrow q\bar{q}$ which opens at $m_\pi \geq 2M$. This occurs because the NJL model does not confine, but on the other hand this is not too unrealistic since we expect deconfinement to occur in that temperature region in any case.

7. Summary, Conclusions, Outlook

In this thesis we have studied the scattering of pions in the NJL model, an effective quantum field theory for QCD focusing on chiral symmetry. We used two versions of the Lagrangian density, one with only a scalar-pseudoscalar interaction term (simple model) and the other one with an additional vector-pseudovector vertex (extended model). Pion-pion scattering in leading order in $1/N_c$ is described by three types of diagrams, the quark-box, sigma-meson propagation and rho-meson propagation diagram with the latter only occurring in the extended model. We found that the experimental low-energy scattering data (expressed in terms of scattering lengths and effective range parameters) is well reproduced for the lowest partial waves in the simple model for parameter set [A]. Recall that parameter set [A] is the one with the correct physical value of the pion-decay constant. We chose to implement the extended model by ignoring the π - a_1 mixing (which would change the pion mass and the pion decay constant) and we can therefore not expect that after inclusion of the contribution from the additional diagram we are able to reproduce the Weinberg values for the $l = 0$ scattering lengths. A next step would be to determine a realistic parameter set for the extended model.

Following the work of many other authors we incorporated, as much as possible, medium effects by applying the imaginary time formalism. We believe that these medium modifications to the quark and meson masses and the matrix elements are indeed very important and a reasonable description of QCD matter for non-vanishing T or μ cannot be given without them. We also argued that in order to incorporate the processes $\sigma \leftrightarrow \pi\pi$ and $\rho \leftrightarrow \pi\pi$, which are known to be dominant from experiment, we must go beyond leading order in $1/N_c$. We saw that this is a rather difficult task and as simplest solution we chose to only add the imaginary part arising from the pion-loop diagram to the polarisation function for the mesons. While violating causality (which manifests itself in the form of a Kramers-Kronig relation) we were in this manner able to obtain a width for the sigma and the rho meson corresponding to the decay into two pions without destroying the delicate cancellation between the box and sigma propagation diagram, which was responsible for the correct low-energy behaviour of the matrix elements in the chiral limit.

As an application we studied the shear viscosity of QCD matter in a very simple approximation, which is proportional to the inverse cross section evaluated at some typical thermal momentum. We believe that this estimate gives qualitatively good results. We studied QCD matter as a gas of pions because these are the lightest degrees of freedom in the confined phase and certainly dominant for $\mu = 0$ and not too large temperatures. The results obtained for the shear viscosity in the simple model are in good agreement with the results obtained by other authors using a more realistic kinetic theory approach. We observed a significant contribution from the rho-meson exchange diagram in the ex-

tended model for larger temperatures, which leads to an even smaller shear viscosity over entropy ratio and believe that this is worth a further investigation.

For future works related to this topic we suggest that one creates new parameter sets (especially in the extended model) which reproduce the scattering data in the vacuum. We also believe it might be possible to incorporate the π - a_1 mixing, which affects the pion mass and all the scattering processes. Moreover, a more careful study of the implementation of next-to-leading order diagrams in $1/N_c$ should be done.

Extensions

X. Extensions

X.1. Alternative Regularisation Schemes

Other than Pauli-Villars regularisation, which is used for the purposes of the thesis, two other regularisation methods are commonly used to handle the divergences in the NJL model. We will introduce them for the example of the elementary integral

$$iI_1 = i \int \frac{d^4 k}{(2\pi)^4} \frac{1}{k^2 - M^2 + i\varepsilon}, \quad (\text{X.1})$$

which diverges quadratically.

Sharp Three-Momentum Cutoff

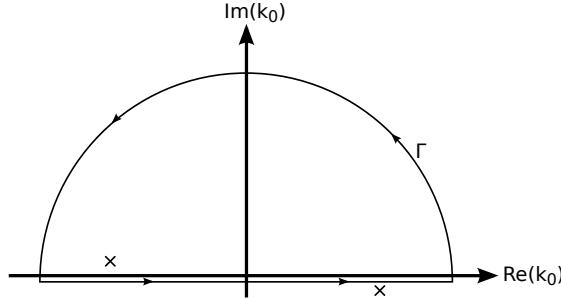
One possibility is to separate the integral over four-momentum $k = (k_0, \vec{k})^t$ into an integral over three-momentum \vec{k} and an integral over k_0 and then only regularise the three-momentum integral. We hence write

$$iI_1 = i \int \frac{d^3 k}{(2\pi)^3} \frac{1}{2\pi} \int_{-\infty}^{\infty} dk_0 \frac{1}{k_0^2 - E_{\vec{k}}^2 + i\varepsilon}, \quad (\text{X.2})$$

where we defined $E_{\vec{k}} = \sqrt{\vec{k}^2 + M^2}$. The inner integral can be evaluated using the residue theorem. We will perform the necessary steps explicitly since similar techniques will be used throughout the text. We write

$$\frac{1}{2\pi} \int_{-\infty}^{\infty} dk_0 \frac{1}{k_0^2 - E_{\vec{k}}^2 + i\varepsilon} = \frac{1}{2\pi} \int_{-\infty}^{\infty} dk_0 \frac{1}{(k_0 - E_{\vec{k}} + i\varepsilon')(k_0 + E_{\vec{k}} - i\varepsilon')} \quad (\text{X.3})$$

with $\varepsilon' = \varepsilon/(2E_{\vec{k}})$. To apply the residue theorem we identify two first-order poles at $k_0 = \pm(E_{\vec{k}} - i\varepsilon')$. Since the integrand falls off quadratically for $|k_0| \rightarrow \infty$ we can close the integration path from $-\infty$ to ∞ to an integration path Γ around the upper half plane:



Only the pole $k_0 = -E_{\vec{k}} + i\varepsilon'$ contributes to the integral and we get

$$\frac{1}{2\pi} \int_{-\infty}^{\infty} dk_0 \frac{1}{(k_0 - E_{\vec{k}} + i\varepsilon')(k_0 + E_{\vec{k}} - i\varepsilon')} = \frac{1}{2iE_{\vec{k}}}. \quad (\text{X.4})$$

This gives

$$iI_1 = \frac{1}{2} \int \frac{d^3k}{(2\pi)^3} \frac{1}{E_{\vec{k}}} = \frac{1}{4\pi^2} \int_0^{\infty} dk \frac{k^2}{\sqrt{k^2 + M^2}} \quad (\text{X.5})$$

for the complete integral. It is now obvious that the integral does not converge. We introduce a sharp momentum cutoff Λ for the momentum \vec{k} and hence get the regularised version

$$\frac{1}{4\pi^2} \int_0^{\Lambda} dk \frac{k^2}{\sqrt{k^2 + M^2}} \quad (\text{X.6})$$

of the integral. The above integral can be calculated analytically and gives

$$iI_1 = iI_1(M, \Lambda) = \frac{1}{(2\pi)^2} \frac{1}{2} \left(\Lambda \sqrt{\Lambda^2 + M^2} - M^2 \operatorname{arcsinh} \left(\frac{\Lambda}{M} \right) \right). \quad (\text{X.7})$$

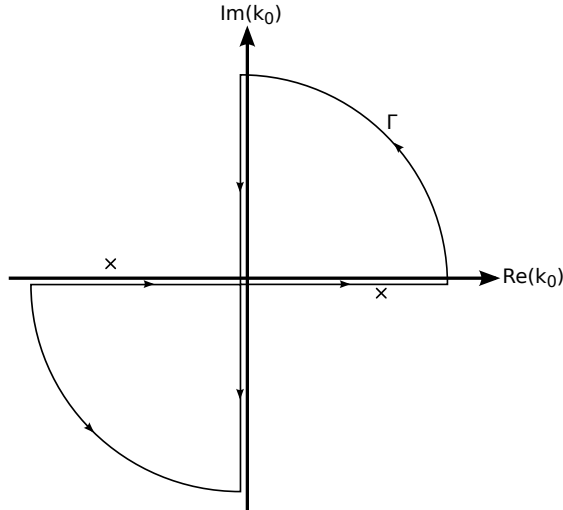
One shortcoming of the presented method is that we treated k_0 and \vec{k} on a different footing. Geometrically, the domain of integration represents an infinitely long hypercylinder.

Sharp Four-Momentum Cutoff

If we want to avoid the above mentioned problem we can also work with a four-momentum cutoff. But before we do this, we transform the integral via a Wick rotation into an integral over Euclidean space. For this we start from

$$iI_1 = i \int \frac{d^3k}{(2\pi)^3} \frac{1}{2\pi} \int_{-\infty}^{\infty} dk_0 \frac{1}{k_0^2 - E_{\vec{k}}^2 + i\varepsilon}. \quad (\text{X.8})$$

By use of the residue theorem we show that instead of integrating k_0 from $-\infty$ to ∞ , we can integrate from $-i\infty$ to $i\infty$. This can be seen from the fact that the integral over the path Γ



vanishes since the poles of the integrand (these are two first-order poles at $k_0 = \pm(E_{\vec{k}} - i\varepsilon')$ with $\varepsilon' = \varepsilon/(2E_{\vec{k}})$ as we saw in the previous subsection) lie outside of Γ . In addition, the contribution from the two circular arcs vanishes in the limit of large radii since the integrand falls off quadratically. This gives

$$\begin{aligned}
iI_1 &= i \int \frac{d^3k}{(2\pi)^3} \frac{1}{2\pi} \int_{-i\infty}^{i\infty} dk_0 \frac{1}{k_0^2 - E_{\vec{k}}^2 + i\varepsilon} \\
&= i \int \frac{d^3k}{(2\pi)^3} \frac{1}{2\pi} \int_{-\infty}^{\infty} idk_4 \frac{1}{-k_4^2 - \vec{k}^2 - M^2 + i\varepsilon} \\
&= \int \frac{d^3k dk_4}{(2\pi)^4} \frac{1}{k_4^2 + \vec{k}^2 + M^2},
\end{aligned} \tag{X.9}$$

where we defined $k_0 =: ik_4$. The above integral can now be regularised by integrating over the hypersphere $\{(k_1, \dots, k_4)^t \in \mathbb{R}^4 \mid k_1^2 + \dots + k_4^2 \leq \Lambda\}$. If we write \vec{K} for the Euclidean vector $(k_1, \dots, k_4)^t$, this gives

$$\begin{aligned}
iI_1 &= iI_1(M, \Lambda) = \int_{\vec{K}^2 \leq \Lambda^2} \frac{d^4K}{(2\pi)^4} \frac{1}{\vec{K}^2 + M^2} = \frac{2\pi^2}{(2\pi)^4} \int_0^\Lambda dK \frac{K^3}{K^2 + M^2} \\
&= \frac{1}{16\pi^2} \left(\Lambda^2 + M^2 \ln \left(\frac{M^2}{\Lambda^2 + M^2} \right) \right).
\end{aligned} \tag{X.10}$$

X.2. Thermodynamic Potential

In this section we derive an expression for the grand potential of the NJL model in mean-field approximation. Moreover, we show that solving the gap equation is equivalent to finding the stationary points of the grand potential.

When dealing with quark matter at finite temperature a very helpful quantity is the partition function \mathcal{Z} . Since we want to treat temperature T and chemical potential μ as thermodynamic variables, while particle number and energy can fluctuate, we will work in the *grand canonical ensemble*.¹⁸

Let us shortly review the basic ideas of statistical quantum field theory, focusing on the functional integral representation of the partition function (see [68] for further reference). Let $\mathcal{H} = \mathcal{H}(\psi, \bar{\psi})$ be the Hamiltonian density a system of Dirac fermions of mass m , i.e.

$$\mathcal{H} = \bar{\psi}(-i\vec{\gamma} \cdot \vec{\nabla} + m)\psi + \mathcal{H}_{\text{int}}. \tag{X.11}$$

Then the grand canonical partition function \mathcal{Z} is given by

$$\mathcal{Z} = \mathbf{Tr} \exp \left(-\frac{1}{T} \int d^3x (\mathcal{H} - \mu \mathcal{N}) \right) \tag{X.12}$$

¹⁸In the grand canonical ensemble the system can exchange particles as well as energy with a reservoir while temperature T , volume V and chemical potential μ are thermodynamic quantities describing the state of a system in thermal equilibrium.

with the number density $\mathcal{N} := \psi^\dagger \psi = \bar{\psi} \gamma^0 \psi$. In the above expression the trace \mathbf{Tr} is a functional trace over all states of the system, i.e. over flavour, colour, Dirac and momentum space. Explicitly in terms of functional integrals, the partition function reads

$$\mathcal{Z} = \int [i d\psi^\dagger][d\psi] \exp \left(\int_0^{1/T} d\tau \int d^3x \left(-\bar{\psi} \gamma^0 \frac{\partial}{\partial \tau} \psi - \mathcal{H}(\psi, \bar{\psi}) + \mu \mathcal{N}(\psi, \bar{\psi}) \right) \right), \quad (\text{X.13})$$

where $\tau = it$. The fields $\bar{\psi}$ and ψ are Grassmann-valued and we have to impose antiperiodic boundary conditions.

The grand canonical partition function can be used to derive pressure P , net particle number N and entropy S (i.e. their average values) according to

$$P = \left. \frac{\partial(T \ln \mathcal{Z})}{\partial V} \right|_{T, \mu}, \quad N = \left. \frac{\partial(T \ln \mathcal{Z})}{\partial \mu} \right|_{T, V} \quad \text{and} \quad S = \left. \frac{\partial(T \ln \mathcal{Z})}{\partial T} \right|_{V, \mu} \quad (\text{X.14})$$

as well as energy

$$E = -PV + TS + \mu N. \quad (\text{X.15})$$

The net particle number N is related to the number density n via $N = \int d^3x n(\vec{x})$, where $n(\vec{x})$ directly corresponds to

$$n = \langle \psi^\dagger \psi \rangle = \langle \mathcal{N} \rangle \quad (\text{X.16})$$

and we write $\langle \cdot \rangle$ for the thermal expectation value.

For convenience, we can also introduce the grand potential per volume $\Omega(T, \mu; M)$, which is given by

$$\Omega(T, \mu; M) = -\frac{T}{V} \ln \mathcal{Z}. \quad (\text{X.17})$$

Mean-Field Approximation

For a system of free Dirac fermions (i.e. $\mathcal{H}_{\text{int.}} = 0$) the partition function \mathcal{Z} or equivalently the grand potential can be explicitly calculated (this is done in Appendix H.2), i.e. one can evaluate the functional trace. However, for the NJL model the Lagrangian and hence the Hamiltonian contains additional interaction terms. The NJL Hamiltonian density reads

$$\mathcal{H} = \bar{\psi}(-i\vec{\gamma} \cdot \vec{\nabla} + m)\psi - g \left[(\bar{\psi}\psi)^2 + (\bar{\psi}i\gamma_5\vec{\tau}\psi)^2 \right]. \quad (\text{X.18})$$

The interaction terms prevent us from finding a simple expression for the partition function as it is possible for free fermions. We therefore have to resort to approximation techniques. In the following we will systematically develop a *mean-field approximation*. We will start from the Lagrangian density of the simple NJL model (2.1) and write $\bar{\psi}\psi$ and $\bar{\psi}i\gamma_5\vec{\tau}\psi$ as their expectation values plus a fluctuation term, i.e.

$$\bar{\psi}\psi = \langle \bar{\psi}\psi \rangle + \delta_\sigma \quad \text{and} \quad \bar{\psi}i\gamma_5\vec{\tau}\psi = \langle \bar{\psi}i\gamma_5\vec{\tau}\psi \rangle + \delta_\pi^a. \quad (\text{X.19})$$

We assume the expectation values to be constant in space and time.¹⁹ The average value $\phi := \langle \bar{\psi}\psi \rangle$ is called *quark condensate* and breaks chiral symmetry. In principle

¹⁹As a further extension it is possible to study expectation values which may depend on one or more spatial coordinate. This leads to the notion of *inhomogeneous* phases. For the NJL model these are studied e.g. in [102, 103].

the pseudoscalar channel could also form a condensate but we will assume that this is not the case i.e. $\langle \bar{\psi} i \gamma_5 \tau^a \psi \rangle = 0$. In general any quark bilinear could have a quark condensate but it is argued in [64] that if we only allow chiral symmetry and Lorentz invariance to be broken while all other symmetries of the Lagrangian remain intact, the only non-vanishing condensates are ϕ and $n = \langle \psi^\dagger \psi \rangle$.

Inserting the expansion (X.19) into the Lagrangian density \mathcal{L} and dropping all terms of quadratic (or higher) order in the fluctuations (see Appendix H.1) yields the mean-field approximation

$$\mathcal{L}_{\text{mf}} = \bar{\psi}(i\cancel{\partial} - M)\psi - \frac{(M - m)^2}{4g} \quad (\text{X.20})$$

where we defined the constituent quark mass

$$M := m + \Sigma = m - 2g\langle \bar{\psi}\psi \rangle \quad (\text{X.21})$$

with the mean-field quark self-energy

$$\Sigma := -2g\langle \bar{\psi}\psi \rangle. \quad (\text{X.22})$$

We will see shortly that these definitions in the mean-field approximation coincide with the definitions of M and Σ for gap equation in Hartree approximation (see equations (2.30) and (2.38)) and so we will already denote them by the same name. We observe that the linearised Lagrangian density describes a Dirac field ψ of effective mass M in a constant *mean-field potential* $(M - m)^2/(4g)$. This justifies why we called this approximation *mean-field approximation*. The corresponding Hamiltonian density \mathcal{H}_{mf} reads

$$\mathcal{H}_{\text{mf}} = \bar{\psi}(-i\vec{\gamma} \cdot \vec{\nabla} + M)\psi + \frac{(M - m)^2}{4g}. \quad (\text{X.23})$$

Since the form of the linearised Lagrangian and Hamiltonian density is much simpler, it is possible to explicitly calculate the grand potential (per volume) $\Omega_{\text{mf}}(T, \mu; M)$ (i.e. the partition function) in mean-field approximation. The calculation is performed in Appendices H.2 and H.3. The result is the grand potential $\Omega_M(T, \mu)$ of a free quark gas with particles of mass M plus a constant term due to the additive constant in the mean-field Lagrangian:

$$\begin{aligned} \Omega_{\text{mf}}(T, \mu; M) &= \Omega_M(T, \mu) + \frac{(M - m)^2}{4g} \\ &= \frac{(M - m)^2}{4g} - 2N_c N_f \int \frac{d^3k}{(2\pi)^3} \left[E_{\vec{k}} + T \ln \left(1 + \exp \left(-\frac{E_{\vec{k}} - \mu}{T} \right) \right) \right. \\ &\quad \left. + T \ln \left(1 + \exp \left(-\frac{E_{\vec{k}} + \mu}{T} \right) \right) \right]. \end{aligned} \quad (\text{X.24})$$

Regularisation

If we want to calculate the mean-field grand potential $\Omega_{\text{mf}}(T, \mu; M)$ numerically, we will first need to regularise it. The divergence of the integral comes from the $E_{\vec{k}}$ in the

integrand. Since the order of divergence of this integral is by two larger than the one of iI_1 , simply applying the Pauli-Villars regularisation scheme with two regulators will not be sufficient. We can however make use of the fact that we only need to know the grand potential up to a constant. It is possible to find an expression $\Omega'_{\text{mf}}(T, \mu; M)$ for the grand potential, such that

$$\Omega'_{\text{mf}}(T, \mu; M) = \Omega_{\text{mf}}(T, \mu; M) - c(T, \mu) < \infty. \quad (\text{X.25})$$

Note that the difference is given by $c(T, \mu)$, which depends on T and μ but not on M . This means that whenever we want to study the dependence of the grand potential on M for *constant* T and μ , the above *gauge* of the grand potential is suitable.

An expression for $\Omega'_{\text{mf}}(T, \mu; M)$ can be found via

$$\begin{aligned} \Omega'_{\text{mf}}(T, \mu; M) &= \int_{M_{\text{vac}}}^M dM' \frac{\partial \Omega_{\text{mf}}(M')}{\partial M'} \\ &= \int_{M_{\text{vac}}}^M dM' \left(\frac{M' - m}{2g} - 4N_c N_f M' iI_1(T, \mu; M') \right) \end{aligned} \quad (\text{X.26})$$

where M_{vac} is the result for the constituent quark mass in vacuum [46]. The above integral indeed becomes finite when applying Pauli-Villars regularisation to the vacuum part of the inner integral $I_1(T, \mu; M')$. In the calculation we used the expression for the derivative of the grand potential w.r.t. the constituent quark mass, which will be calculated in Appendix H.4.

Stationarity Condition

Let us turn back to the quark condensate $\phi = \langle \bar{\psi}\psi \rangle$. We want to determine this expression in mean-field approximation using the grand potential (X.24) we calculated above. If we have an expression for the quark condensate, we can determine the effective quark mass M from equation (X.21).

In analogy to the relations (X.14) the quark condensate $\phi = \langle \bar{\psi}\psi \rangle$ and the number density $n = \langle \psi^\dagger \psi \rangle$ can in general be obtained from the grand potential $\Omega = \Omega(T, \mu; m)$ by

$$\phi = \frac{\partial \Omega}{\partial m} \quad \text{and} \quad n = -\frac{\partial \Omega}{\partial \mu}, \quad (\text{X.27})$$

which follows directly from the form of the grand canonical partition function \mathcal{Z} . We will apply the same relations to our mean-field grand potential Ω_{mf} since we want our mean-field approach to be thermodynamically consistent.

We will focus on the first equation for now. It turns out that it can be brought into the form of a stationarity condition for Ω_{mf} . For this, in the expression for $\Omega_{\text{mf}}(\mu, T; M)$ we write $M = M(\mu, T; m)$. Then

$$\frac{d\Omega_{\text{mf}}}{dm} = \frac{\partial \Omega_{\text{mf}}}{\partial m} + \frac{\partial \Omega_{\text{mf}}}{\partial M} \frac{dM}{dm} = \phi + \frac{\partial \Omega_{\text{mf}}}{\partial M} \frac{dM}{dm} \quad (\text{X.28})$$

since m appears in Ω_{mf} only in the term $(M - m)^2/(4g)$, whose derivative w.r.t. m is exactly ϕ . So consistency with (X.27) is fulfilled if

$$\frac{\partial \Omega_{\text{mf}}}{\partial M} = 0. \quad (\text{X.29})$$

This means that the effective mass M in mean-field approximation corresponds to the stationary points of the grand potential.

A straightforward calculation using the expression (X.24) for the grand potential (see Appendix H.4) shows that the above stationarity condition is equivalent to the gap equation in Hartree approximation (3.4). Hence, the expression for the self-energy Σ , which we simply defined in this chapter, is identical to the self-energy that naturally appeared in the gap equation ansatz.

Now that we know that the mean-field and the Hartree approach are equivalent, we can use this to our advantage. We commented that the for finite μ gap equation might not lead to a single solution but instead could have several roots. This ambiguity can now be resolved: we identified the extrema of Ω_{mf} as the possible candidates for the mass M . However, for reasons of stability, we must of course demand a *global minimum* of Ω_{mf} for our physical mass M . With the gap equation alone, we could not have solved this ambiguity.

Finally let us determine explicit expressions for $\phi = \langle \bar{\psi}\psi \rangle$ and $n = \langle \psi^\dagger\psi \rangle$. We obtain the quark condensate $\phi = -\Sigma/(2g)$ directly from the expression of the self-energy Σ (3.6) and get

$$\langle \bar{\psi}\psi \rangle = T \sum_{n \in \mathbb{Z}} \int \frac{d^3k}{(2\pi)^3} \text{Tr} \left(S(i\omega_n + \mu, \vec{k}) \right), \quad (\text{X.30})$$

which in the vacuum reads

$$\langle \bar{\psi}\psi \rangle = -i \int \frac{d^4k}{(2\pi)^4} \text{Tr} S(k). \quad (\text{X.31})$$

In addition, we can calculate $n = -\partial\Omega_{\text{mf}}/\partial\mu$ and get

$$n = \langle \psi^\dagger\psi \rangle = 2N_f N_c \int \frac{d^3k}{(2\pi)^3} \left(n_{\vec{k}}(T, \mu; M) - \bar{n}_{\vec{k}}(T, \mu; M) \right), \quad (\text{X.32})$$

which is identical to our definition (3.12).

X.3. Constituent Quark Mass for Finite Chemical Potential

In this section we will determine the constituent quark mass for finite T and μ while in the original thesis only the case $\mu = 0$ is considered (see Section 3.3). The constituent quark mass $M = M(T, \mu)$ is obtained as solution of the gap equation (3.4). For some values of μ and T the gap equation does not yield a unique solution and the physical solution has to be determined from the minimality condition of the grand potential (see discussion below). For $\mu = 0$ this does not occur.

First, we set $T = 0$ and let μ vary (see Figure X.1). M stays constant for a large interval²⁰ and undergoes a first-order phase transition (i.e. M is a discontinuous function of μ) at $\mu \approx 409$ MeV where chiral symmetry is restored.

²⁰This phenomenon can be studied in a more general context (for theories with a mass gap) and is called *Silver Blaze problem* [104]

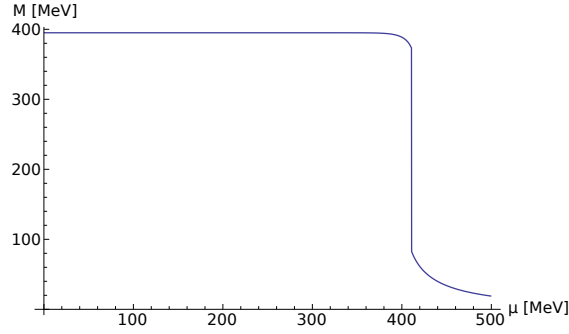


Figure X.1.: Constituent quark mass M at $T = 0$ as function of μ for parameter set [C].

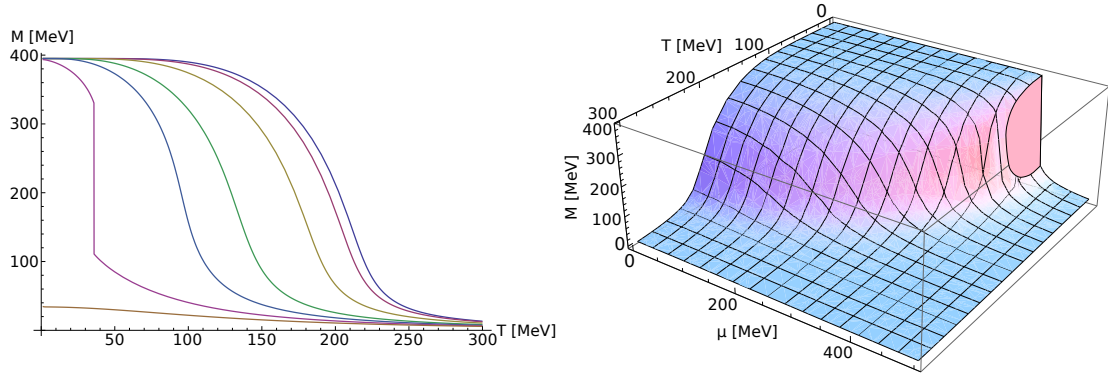


Figure X.2.: Left: Constituent quark mass M as function of T at $\mu = 0, 100, 200, 300, 350, 400, 450$ MeV (from top to bottom). Right: Constituent quark mass as function of T and μ . The shaded area marks the first-order phase transition. Both plots for parameter set [C]

Figure X.2 (left) shows the dependence of M on T for different values of μ . For smaller values of μ , there is a crossover from the broken phase to the symmetric phase. For $\mu \approx 400$ MeV this happens via a first-order phase transition and for large enough μ we are in the symmetric phase even for $T = 0$. Figure X.2 (right) shows the constituent quark mass in the T - μ plane for parameter set [C].

The transition between the chirally symmetric phase and the phase exhibiting spontaneous breaking of chiral symmetry is mainly a crossover. Only for small T one sees a first-order phase transition. The first-order transition line in the T - μ plane for parameter sets [C] - [E] is shown in Figure X.3. Parameter sets [A] and [B] do not produce a first-order phase transition at all. In those cases there is always a crossover between the broken and the symmetric phase.

Ambiguity of the Gap Equation

For values of T and μ close to the first-order phase transition the gap equation does not have a unique solution. The solutions to the gap equation for $\mu = 400$ MeV and parameter set [C] are shown in Figure X.4 (left). For sufficiently large or small T the

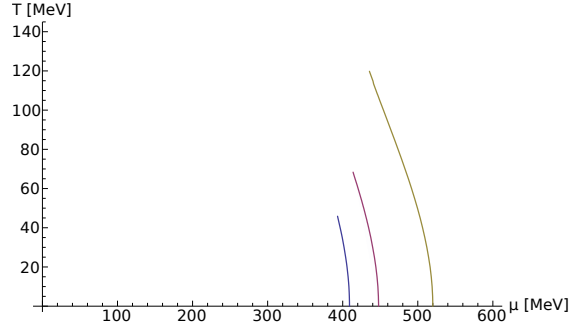


Figure X.3.: The lines show the position of the first-order phase transition between the (approximately) chirally symmetric phase (large T or μ) and the spontaneously broken phase (small T and μ) for parameter sets [C] - [E] (from left to right).

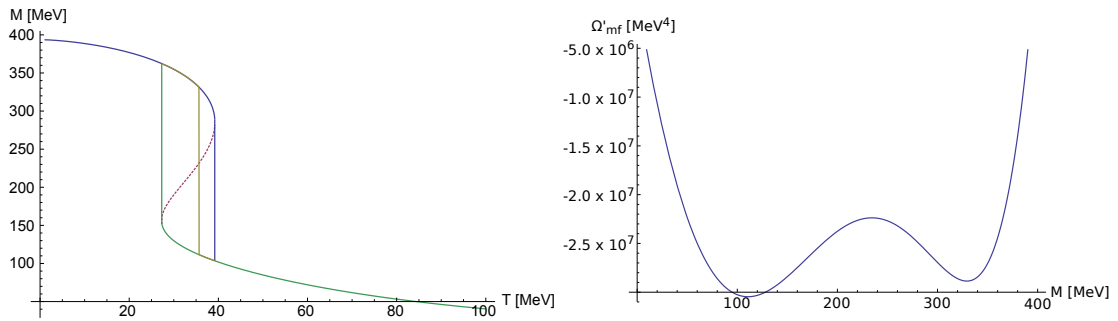


Figure X.4.: Left: The curved line represents the 1 or 3 solutions M to the gap equation at $\mu = 400$ MeV. The correct phase transition is marked by the middle vertical line. Right: The grand potential Ω'_{mf} at $\mu = 400$ MeV and $T = 36$ MeV. Both plots for parameter set [C].

solution is unique. However, there is an interval for T with three solutions. The gap equation does not tell us when the phase transition, i.e. the jump from the upper branch to the lower branch of the solution happens. It might occur anywhere between the beginning of the lower branch and the end of the upper branch. The intermediate branch is unphysical.

We have argued in Section X.2 that the roots of the gap equation correspond to local extrema of the grand potential. The physical solution is given by the global minimum of the grand potential, i.e. of the solutions of the gap equation we have to single out the one with the smallest grand potential. The lower and upper solution branch in Figure X.4 are local minima of Ω'_{mf} whereas the intermediate branch is a local maximum (see Figure X.4 (right)). The phase transition occurs when the global minimum jumps from one local minimum to the other.

Appendices

A. Conventions

Minkowski Metric

In this text we use the Minkowski metric with the usual particle physics signature $(+, -, -, -)$, i.e. the metric tensor is given by

$$\eta^{\mu\nu} = \eta_{\mu\nu} = \text{diag}(+1, -1, -1, -1). \quad (\text{A.1})$$

Greek indices like μ, ν, \dots run over all components of a four-vector while lower case Roman letters like i, j, \dots run over the three-vector components.

Natural Units

In this text we will use *natural units*, which in particle physics means

$$\hbar = c = k_B = 1. \quad (\text{A.2})$$

The only remaining unit is the electron volt (eV).

B. Basic Quantities

B.1. Calculation of the Polarisation Loop

The following calculations aim at the calculation of the polarisation loop

$$J_M(p) = i \int \frac{d^4 k}{(2\pi)^4} \text{Tr} (\Gamma_M S(k+p) \Gamma_M S(k)) \quad (\text{B.1})$$

for $M \in \{\sigma, \pi\}$ (see Section 2.5). Let us begin by calculating the expression for the σ meson. We have

$$\begin{aligned} J_\sigma(p) &= i \int \frac{d^4 k}{(2\pi)^4} \text{Tr} (S(k+p) S(k)) \\ &= i \int \frac{d^4 k}{(2\pi)^4} \text{Tr} \left(\frac{\not{k} + \not{p} + M}{(k+p)^2 - M^2 + i\varepsilon} \frac{\not{k} + M}{k^2 - M^2 + i\varepsilon} \right). \end{aligned} \quad (\text{B.2})$$

We have to evaluate the trace

$$\text{Tr} \left((\not{k} + \not{p} + M) (\not{k} + M) \right) = N_f N_c \text{tr} \left((\not{k} + \not{p} + M) (\not{k} + M) \right), \quad (\text{B.3})$$

where the remaining trace tr is to be taken over Dirac space. Using

$$\text{tr}(\not{a}) = 0 \quad \text{and} \quad \text{tr}(\not{a}\not{b}) = 4(a \cdot b) \quad (\text{B.4})$$

for arbitrary four-vectors a and b , we get

$$\text{Tr} \left((\not{k} + \not{p} + M) (\not{k} + M) \right) = 4N_f N_c (k^2 + p \cdot k + M^2). \quad (\text{B.5})$$

Hence

$$\begin{aligned} J_\sigma(p) &= 4N_f N_c i \int \frac{d^4 k}{(2\pi)^4} \frac{k^2 + p \cdot k + M^2}{((k+p)^2 - M^2 + i\varepsilon)(k^2 - M^2 + i\varepsilon)} \\ &= 4N_f N_c \left(i \int \frac{d^4 k}{(2\pi)^4} \frac{1}{k^2 - M^2 + i\varepsilon} \right. \\ &\quad \left. - i \int \frac{d^4 k}{(2\pi)^4} \frac{p \cdot k + p^2 - 2M^2}{((k+p)^2 - M^2 + i\varepsilon)(k^2 - M^2 + i\varepsilon)} \right). \end{aligned} \quad (\text{B.6})$$

Via substitution one easily shows that

$$\int \frac{d^4 k}{(2\pi)^4} \frac{2p \cdot k + p^2}{((k+p)^2 - M^2 + i\varepsilon)(k^2 - M^2 + i\varepsilon)} = 0, \quad (\text{B.7})$$

which means we can replace $p \cdot k$ by $-p^2/2$ in the second integral and so we finally arrive at the expression

$$\begin{aligned}
J_\sigma(p) &= 4N_f N_c i \int \frac{d^4 k}{(2\pi)^4} \frac{1}{k^2 - M^2 + i\varepsilon} \\
&\quad - 2N_f N_c (p^2 - 4M^2) i \int \frac{d^4 k}{(2\pi)^4} \frac{1}{((k+p)^2 - M^2 + i\varepsilon)(k^2 - M^2 + i\varepsilon)} \\
&= 4N_f N_c i I_1 - 2N_f N_c (p^2 - 4M^2) i I_2(p).
\end{aligned} \tag{B.8}$$

The calculation for J_π^{ab} is analogous. We have

$$\begin{aligned}
J_\pi^{ab}(p) &= i \int \frac{d^4 k}{(2\pi)^4} \text{Tr} \left(i\gamma_5 \tau^a S(k+p) i\gamma_5 \tau^b S(k) \right) \\
&= -\delta_{ab} N_c N_f i \int \frac{d^4 k}{(2\pi)^4} \text{tr} \left(\frac{\gamma_5 (\not{k} + \not{p} + M) \gamma_5 (\not{k} + M)}{((k+p)^2 - M^2 + i\varepsilon)(k^2 - M^2 + i\varepsilon)} \right) \\
&= -\delta_{ab} N_c N_f i \int \frac{d^4 k}{(2\pi)^4} \text{tr} \left(\frac{(-\not{k} - \not{p} + M)(\not{k} + M)}{((k+p)^2 - M^2 + i\varepsilon)(k^2 - M^2 + i\varepsilon)} \right) \\
&= \delta_{ab} 4N_f N_c i \int \frac{d^4 k}{(2\pi)^4} \frac{k^2 + k \cdot p - M^2}{((k+p)^2 - M^2 + i\varepsilon)(k^2 - M^2 + i\varepsilon)} \\
&= \delta_{ab} 4N_f N_c i \int \frac{d^4 k}{(2\pi)^4} \frac{1}{k^2 - M^2 + i\varepsilon} \\
&\quad - 4N_f N_c i \int \frac{d^4 k}{(2\pi)^4} \frac{p \cdot k + p^2}{((k+p)^2 - M^2 + i\varepsilon)(k^2 - M^2 + i\varepsilon)} \\
&= \delta_{ab} 4N_f N_c i \int \frac{d^4 k}{(2\pi)^4} \frac{1}{k^2 - M^2 + i\varepsilon} \\
&\quad - \delta_{ab} 2N_f N_c p^2 i \int \frac{d^4 k}{(2\pi)^4} \frac{1}{((k+p)^2 - M^2 + i\varepsilon)(k^2 - M^2 + i\varepsilon)} \\
&= \delta_{ab} \left(4N_f N_c i I_1 - 2N_f N_c p^2 i I_2(p) \right).
\end{aligned} \tag{B.9}$$

B.2. Alternative Representation of the Meson Propagator

We want to show that the meson propagator

$$D_M(p) = \frac{-2g}{1 - 2gJ_M(p)} \tag{B.10}$$

in the simple model can be written as

$$D_M(p^2) = -\frac{1}{2N_c N_f ((p^2 - \varepsilon_M^2) i I_2(p^2) - m_\pi^2 i I_2(m_\pi))} \tag{B.11}$$

for $M \in \{\sigma, \pi\}$ with $\varepsilon_\pi = 0$ and $\varepsilon_\sigma = 4M^2$.

We can write the polarisation function as

$$J_M(p) = \frac{1}{2g} \left(1 - \frac{m}{M} \right) - 2N_c N_f (p^2 - \varepsilon_M) iI_2(p). \quad (\text{B.12})$$

Hence

$$1 - 2gJ_M(p) = \frac{m}{M} + 4gN_c N_f (p^2 - \varepsilon_M) iI_2(p). \quad (\text{B.13})$$

We saw in Section 2.5.1 that the pion propagator $D_\pi(p)$ has a pole at the pion mass, i.e. $D_\pi^{-1}(m_\pi) = 0$. We can write

$$0 = 1 - 2gJ_\pi(m_\pi) = \frac{m}{M} + 4gN_c N_f m_\pi^2 iI_2(m_\pi). \quad (\text{B.14})$$

Then

$$1 - 2gJ_M(p) = 1 - 2gJ_M(p) - (1 - 2gJ_M(m_\pi)) = 4gN_c N_f \left(p^2 iI_2(p) - m_\pi^2 iI_2(m_\pi) \right) \quad (\text{B.15})$$

and for the propagator we get

$$D_M(p^2) = -\frac{1}{2N_c N_f \left((p^2 - \varepsilon_M^2) iI_2(p^2) - m_\pi^2 iI_2(m_\pi) \right)}. \quad (\text{B.16})$$

B.3. Calculation of the Pion Decay Constant

We calculate the pion decay constant f_π starting from the defining relation

$$f_\pi p^\mu \delta_{ab} = g_{\pi qq} \int \frac{d^4 k}{(2\pi)^4} \text{Tr} \left(\gamma^\mu \gamma_5 \frac{\tau^a}{2} S(k+p) i\gamma_5 \tau^b S(k) \right) \quad (\text{B.17})$$

(see (2.83)). We do so by evaluating the right-hand side of the above equation. We have

$$\begin{aligned} \text{Tr} \left(\gamma^\mu \gamma_5 \frac{\tau^a}{2} S(k+p) i\gamma_5 \tau^b S(k) \right) &= \frac{i}{2} \delta_{ab} N_f N_c \text{tr} \left(\gamma^\mu \gamma_5 S(k+p) \gamma_5 S(k) \right) \\ &= -\frac{i}{2} \delta_{ab} N_f N_c \text{tr} \left(\gamma^\mu S(k+p) \gamma_5 S(k) \gamma_5 \right) \\ &= -\frac{i}{2} \delta_{ab} N_f N_c \text{tr} \left(\gamma^\mu S(k+p) S(-k) \right). \end{aligned} \quad (\text{B.18})$$

Using

$$\begin{aligned} \text{tr} \left(\gamma^\mu S(k+p) S(-k) \right) &= \frac{\text{tr} \left(\gamma^\mu (\not{k} + \not{p} + M) (-\not{k} + M) \right)}{\left((k+p)^2 - M^2 + i\varepsilon \right) \left(k^2 - M^2 + i\varepsilon \right)} \\ &= \frac{\text{tr} \left(\gamma^\mu \not{p} M \right)}{\left((k+p)^2 - M^2 + i\varepsilon \right) \left(k^2 - M^2 + i\varepsilon \right)} \\ &= \frac{4M p^\mu}{\left((k+p)^2 - M^2 + i\varepsilon \right) \left(k^2 - M^2 + i\varepsilon \right)} \end{aligned} \quad (\text{B.19})$$

we get

$$\begin{aligned} f_\pi &= -g_{\pi qq} 2MN_f N_c i \int \frac{d^4 k}{(2\pi)^4} \frac{1}{((k+p)^2 - M^2 + i\varepsilon)(k^2 - M^2 + i\varepsilon)} \\ &= -g_{\pi qq} 2MN_f N_c i I_2(p) \\ &= -g_{\pi qq} 2MN_f N_c i I_2(m_\pi), \end{aligned} \tag{B.20}$$

where we inserted m_π^2 for p^2 since p is the momentum of the pion.

C. Elementary Integrals

C.1. Calculation of the Integral iI_1

The integral iI_1 is defined as

$$iI_1 = i \int \frac{d^4k}{(2\pi)^4} \frac{1}{k^2 - M^2 + i\varepsilon}. \quad (\text{C.1})$$

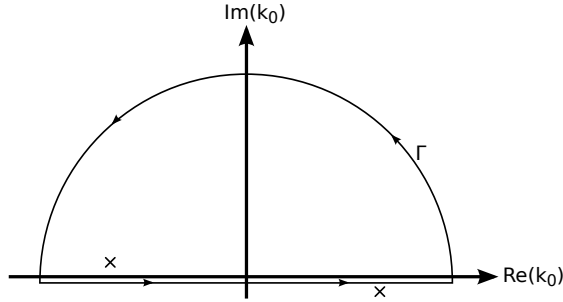
We write

$$iI_1 = i \int \frac{d^3k}{(2\pi)^3} \frac{1}{2\pi} \int_{-\infty}^{\infty} dk_0 \frac{1}{k_0^2 - E_{\vec{k}}^2 + i\varepsilon}, \quad (\text{C.2})$$

where we defined $E_{\vec{k}} = \sqrt{\vec{k}^2 + M^2}$. The inner integral can be evaluated using the residue theorem. We have

$$\frac{1}{2\pi} \int_{-\infty}^{\infty} dk_0 \frac{1}{k_0^2 - E_{\vec{k}}^2 + i\varepsilon} = \frac{1}{2\pi} \int_{-\infty}^{\infty} dk_0 \frac{1}{(k_0 - E_{\vec{k}} + i\varepsilon')(k_0 + E_{\vec{k}} - i\varepsilon')} \quad (\text{C.3})$$

with $\varepsilon' = \varepsilon/(2E_{\vec{k}})$. To apply the residue theorem we identify two first-order poles at $k_0 = \pm(E_{\vec{k}} - i\varepsilon')$. Since the integrand falls off quadratically for $|k_0| \rightarrow \infty$ we can close the integration path from $-\infty$ to ∞ to an integration path Γ around the upper half plane:



Only the pole $k_0 = -E_{\vec{k}} + i\varepsilon'$ contributes to the integral and we get

$$\frac{1}{2\pi} \int_{-\infty}^{\infty} dk_0 \frac{1}{(k_0 - E_{\vec{k}} + i\varepsilon')(k_0 + E_{\vec{k}} - i\varepsilon')} = \frac{1}{2iE_{\vec{k}}}. \quad (\text{C.4})$$

This gives

$$iI_1 = \frac{1}{2} \int \frac{d^3k}{(2\pi)^3} \frac{1}{E_{\vec{k}}} = \frac{1}{4\pi^2} \int_0^{\infty} dk \frac{k^2}{\sqrt{k^2 + M^2}} \quad (\text{C.5})$$

The integral iI_1 is quadratically divergent. Using Pauli-Villars regularisation with two regulators as described in Section 2.3 gives

$$\begin{aligned} iI_1 &= \frac{1}{16\pi^2} \left(M^2 \ln(M^2) - 2(M^2 + \Lambda^2) \ln(M^2 + \Lambda^2) + (M^2 + 2\Lambda^2) \ln(M^2 + 2\Lambda^2) \right) \\ &= \frac{1}{16\pi^2} \left(M^2 \ln \left(\frac{M^2}{M^2 + \Lambda^2} \right) + (M^2 + 2\Lambda^2) \ln \left(\frac{M^2 + 2\Lambda^2}{M^2 + \Lambda^2} \right) \right). \end{aligned} \quad (\text{C.6})$$

C.2. Calculation of the Integral $iI_2(p)$

We want to explicitly perform the k_0 -integration in

$$iI_2(p) = i \int \frac{d^4k}{(2\pi)^4} \frac{1}{(k^2 - M^2 + i\varepsilon) ((k+p)^2 - M^2 + i\varepsilon)} \quad (\text{C.7})$$

(see equation (2.64)) by application of the residue theorem.

We introduce a more general notation that will help us structuring the calculations:

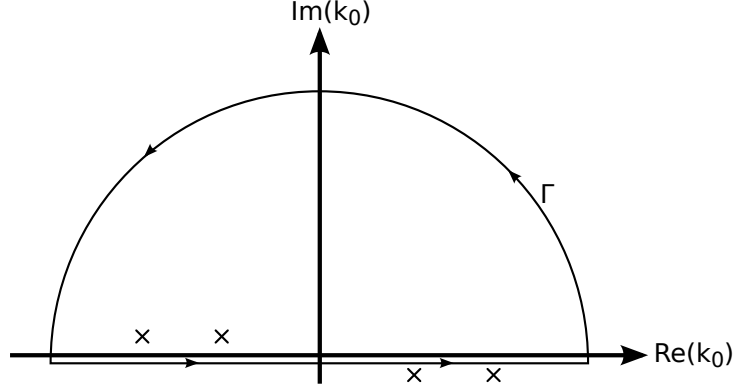
$$\begin{aligned} iI_2(p) &= i \int \frac{d^4k}{(2\pi)^4} \prod_{a \in \{0,p\}} \frac{1}{(k+a)^2 - M^2 + i\varepsilon} = i \int \frac{d^4k}{(2\pi)^4} \prod_{a \in \{0,p\}} \frac{1}{(k_0 + a_0)^2 - E_{\vec{k}+\vec{a}}^2 + i\varepsilon} \\ &= i \int \frac{d^4k}{(2\pi)^4} \prod_{a \in \{0,p\}} \frac{1}{(k_0 + a_0) - (E_{\vec{k}+\vec{a}} - i\varepsilon')} \frac{1}{(k_0 + a_0) + (E_{\vec{k}+\vec{a}} - i\varepsilon')} \\ &= - \int \frac{d^3k}{(2\pi)^3} \int \frac{dk_0}{2\pi i} \prod_{a \in \{0,p\}} \frac{1}{2E_{\vec{k}+\vec{a}}} \times \\ &\quad \times \left(\frac{1}{(k_0 + a_0) - (E_{\vec{k}+\vec{a}} - i\varepsilon')} - \frac{1}{(k_0 + a_0) + (E_{\vec{k}+\vec{a}} - i\varepsilon')} \right). \end{aligned} \quad (\text{C.8})$$

Here, we first wrote $(k+a)^2 - M^2 = (k_0 + a_0)^2 - E_{\vec{k}+\vec{a}}^2$ and then applied

$$\frac{1}{(k_0 + a_0)^2 - E_{\vec{k}+\vec{a}}^2 + i\varepsilon} = \frac{1}{k_0 + a_0 - E_{\vec{k}+\vec{a}} + i\varepsilon'} \frac{1}{k_0 + a_0 + E_{\vec{k}+\vec{a}} - i\varepsilon'} \quad (\text{C.9})$$

with $\varepsilon' = \varepsilon/(2E_{\vec{k}+\vec{a}})$. In future, we will drop the prime in ε' .

The k_0 -integral can now be evaluated using the residue theorem. To apply the residue theorem we identify four first-order poles at $k_0 = \pm(E_{\vec{k}} - i\varepsilon)$ and $k_0 = -p_0 \pm (E_{\vec{k}+\vec{p}} - i\varepsilon)$. We can close the integration path from $-\infty$ to ∞ to an integration path Γ around the upper half plane:



Only the poles $k_0 = -E_{\vec{k}} + i\varepsilon$ and $k_0 = -p_0 - E_{\vec{k}+\vec{p}} + i\varepsilon$ contribute to the integral and we get

$$iI_2(p) = \int \frac{d^3\vec{k}}{(2\pi)^3} \frac{1}{4E_{\vec{k}}E_{\vec{k}+\vec{p}}} \left[\left(\frac{1}{p_0 - E_{\vec{k}} - E_{\vec{k}+\vec{p}} + 2i\varepsilon} - \frac{1}{p_0 - E_{\vec{k}} + E_{\vec{k}+\vec{p}}} \right) + \left(\frac{1}{-p_0 - E_{\vec{k}} - E_{\vec{k}+\vec{p}} + 2i\varepsilon} - \frac{1}{-p_0 + E_{\vec{k}} - E_{\vec{k}+\vec{p}}} \right) \right]. \quad (\text{C.10})$$

Let us analyse the structure of the integrand. Those denominators without the $2i\varepsilon$ -term can become zero for a certain three-momentum, which means that the integral is not well-defined (even with regularisation). These fractions however all cancel and in the end only denominators with a $2i\varepsilon$ -term are left.

We get

$$\begin{aligned} iI_2(p) &= \int \frac{d^3k}{(2\pi)^3} \frac{1}{4E_{\vec{k}}E_{\vec{k}+\vec{p}}} \left(\frac{1}{p_0 - E_{\vec{k}} - E_{\vec{k}+\vec{p}} + 2i\varepsilon} - \frac{1}{p_0 + E_{\vec{k}} + E_{\vec{k}+\vec{p}} - 2i\varepsilon} \right) \\ &= \int \frac{d^3k}{(2\pi)^3} \frac{1}{2E_{\vec{k}}E_{\vec{k}+\vec{p}}} \frac{E_{\vec{k}} + E_{\vec{k}+\vec{p}}}{p_0^2 - (E_{\vec{k}} + E_{\vec{k}+\vec{p}} - 2i\varepsilon)^2} \\ &= \int \frac{d^3k}{(2\pi)^3} \frac{1}{p_0^2 - (E_{\vec{k}} + E_{\vec{k}+\vec{p}})^2 + i\varepsilon} \left(\frac{1}{2E_{\vec{k}}} + \frac{1}{2E_{\vec{k}+\vec{p}}} \right). \end{aligned} \quad (\text{C.11})$$

By making the substitution $\vec{k} \mapsto -\vec{k} - \vec{p}$ we get for the second part of the integral

$$\begin{aligned} \int \frac{d^3k}{(2\pi)^3} \frac{1}{p_0^2 - (E_{\vec{k}} + E_{\vec{k}+\vec{p}})^2 + i\varepsilon} \frac{1}{2E_{\vec{k}+\vec{p}}} &= \int \frac{d^3k}{(2\pi)^3} \frac{1}{p_0^2 - (E_{-\vec{k}-\vec{p}} + E_{-\vec{k}})^2 + i\varepsilon} \frac{1}{2E_{-\vec{k}}} \\ &= \int \frac{d^3k}{(2\pi)^3} \frac{1}{p_0^2 - (E_{\vec{k}+\vec{p}} + E_{\vec{k}})^2 + i\varepsilon} \frac{1}{2E_{\vec{k}}} \end{aligned} \quad (\text{C.12})$$

and hence we obtain

$$iI_2(p) = \int \frac{d^3k}{(2\pi)^3} \frac{1}{E_{\vec{k}}} \frac{1}{p_0^2 - (E_{\vec{k}} + E_{\vec{p}+\vec{k}})^2 + i\varepsilon}. \quad (\text{C.13})$$

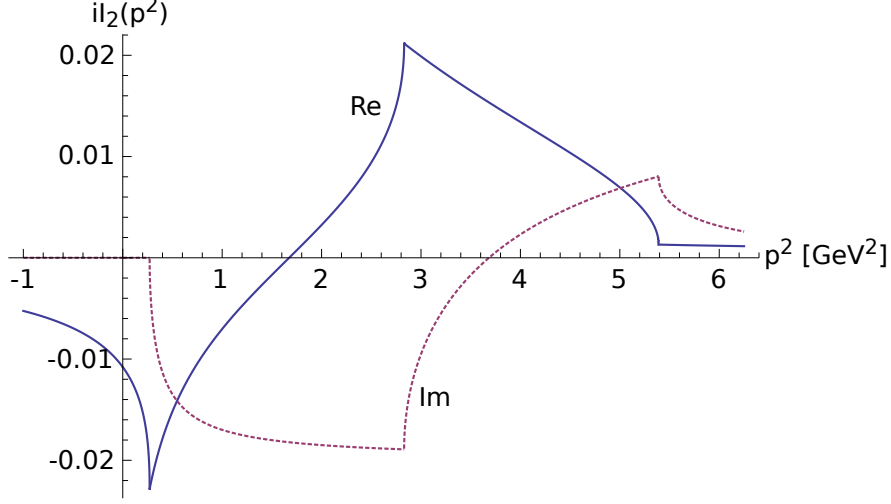


Figure C.1.: The real and imaginary parts of $iI_2(p^2)$ plotted as a function of p^2 for $M = 260$ MeV and $\Lambda = 800$ MeV.

The above integral only depends on p^2 . We can therefore set $p_0^2 = p^2$ and $\vec{p} = 0$. Hence the integral becomes

$$iI_2(p^2) = \int \frac{d^3k}{(2\pi)^3} \frac{1}{E_{\vec{k}}} \frac{1}{p^2 - 4E_{\vec{k}}^2 + i\varepsilon} = \frac{1}{2\pi^2} \int_0^\infty dk \frac{k^2}{E_{\vec{k}}(p^2 - 4E_{\vec{k}}^2 + i\varepsilon)}. \quad (\text{C.14})$$

The integral $iI_2(p^2) = iI(p^2)$ can be solved analytically, which is discussed in Section C.3. The result is plotted in Figure C.1.

C.3. Analytical Solutions of the Integrals $iI(p)$, $iK(p)$, $iL(p)$

In Appendix C.2 we showed how to write the integral $iI_2(p^2) = iI(p^2)$ as a radial three-momentum integral. Analogous calculations for $iK(p^2)$ and $iL(p^2)$ lead to the results in [41]:

$$\begin{aligned} iI(p^2) &= \frac{1}{2\pi^2} \int_0^\infty dk \frac{k^2}{E_{\vec{k}}(p^2 - 4E_{\vec{k}}^2 + i\varepsilon)}, \\ iK(p^2) &= \frac{1}{8\pi^2} \int_0^\infty dk \frac{k^2(12E_{\vec{k}}^2 - p^2)}{E_{\vec{k}}^3(p^2 - 4E_{\vec{k}}^2 + i\varepsilon)^2}, \\ iL(p^2) &= \frac{1}{4\pi^2} \int_0^\infty dk \frac{(20E_{\vec{k}}^2 - p^2)k^2}{E_{\vec{k}}^3(p^2 - 4E_{\vec{k}}^2 + i\varepsilon)^3}. \end{aligned} \quad (\text{C.15})$$

Defining

$$x = \frac{p^2}{M^2} - 4\frac{k^2}{M^2} - 4 \quad \text{and} \quad \tilde{p}^2 = \frac{p^2}{M^2} \quad (\text{C.16})$$

we can write the above integrals (applying a suitable variable transformation) in the form

$$\begin{aligned}
iI(p^2) &= \frac{1}{16\pi^2} \int_{-\infty}^{\tilde{p}^2-4} dx \frac{\sqrt{\tilde{p}^2-4-x}}{\sqrt{\tilde{p}^2-x}} \frac{1}{x+i\varepsilon}, \\
iK(p^2) &= \frac{1}{16\pi^2} \frac{1}{M^2} \int_{-\infty}^{\tilde{p}^2-4} dx \frac{\sqrt{\tilde{p}^2-4-x}(2\tilde{p}^2-3x)}{\sqrt{\tilde{p}^2-x}^3} \frac{1}{(x+i\varepsilon)^2}, \\
iL(p^2) &= \frac{1}{8\pi^2} \frac{1}{M^4} \int_{-\infty}^{\tilde{p}^2-4} dx \frac{\sqrt{\tilde{p}^2-4-x}(4\tilde{p}^2-5x)}{\sqrt{\tilde{p}^2-x}^3} \frac{1}{(x+i\varepsilon)^3}.
\end{aligned} \tag{C.17}$$

We are hence in each case given an integral

$$\int_{-\infty}^b f(x) \frac{1}{(x+i\varepsilon)^n} dx, \tag{C.18}$$

which is to be calculated in the limit $\varepsilon \rightarrow 0$, where $n = 1, 2, 3$ and $f(x)$ is a well-behaved function at $x = 0$. It is useful to determine the real and imaginary parts independently.

Imaginary Part

Let us first study the imaginary parts. We note that

$$\frac{d^n}{dx^n} \left(\frac{a}{x^2+a^2} \right) = (-1)^n n! \frac{\text{Im}((x+ia)^{n+1})}{(x^2+a^2)^{n+1}} = (-1)^n n! \text{Im} \left(\frac{1}{(x-ia)^{n+1}} \right). \tag{C.19}$$

Moreover it is known that

$$\frac{1}{\pi} \frac{\varepsilon}{x^2 + \varepsilon^2} \tag{C.20}$$

is an *approximation to the identity*, i.e. it converges to the Dirac delta distribution $\delta(x)$ as $\varepsilon \rightarrow 0$. Analogously, derivatives of that function converge to the corresponding distributional derivatives of the delta distribution.

Taking the above observations together we get

$$\text{Im} \left(\frac{1}{(x+i\varepsilon)^{n+1}} \right) \rightarrow -\pi \frac{(-1)^n}{n!} \delta^{(n)}(x) \tag{C.21}$$

as $\varepsilon \rightarrow 0$, where $\delta^{(n)}(x)$ denotes the n -th derivative of the delta distribution.

The imaginary parts of the above integrals $iI(p^2)$, $iK(p^2)$ and $iL(p^2)$ are hence easily calculated by first partially integrating and then evaluating the integrand at $x = 0$. This yields

$$\begin{aligned}
\text{Im} \left(iI(p^2) \right) &= -\frac{1}{16\pi} \frac{\sqrt{p^2-4M^2}}{\sqrt{p^2}} \Theta(p^2-4M^2), \\
\text{Im} \left(iK(p^2) \right) &= \frac{1}{16\pi} \frac{1}{\sqrt{p^2} \sqrt{p^2-4M^2}} \Theta(p^2-4M^2), \\
\text{Im} \left(iL(p^2) \right) &= \frac{1}{8\pi} \frac{p^2-2M^2}{\sqrt{p^2}^3 \sqrt{p^2-4M^2}^3} \Theta(p^2-4M^2),
\end{aligned} \tag{C.22}$$

where Θ denotes the Heaviside step function.

Real Part

Let us now turn to the real part of the integral. Here, the considerations are a bit more difficult. Let us define the integration kernel

$$K_n^\varepsilon(x) := \operatorname{Re} \left(\frac{1}{(x + i\varepsilon)^n} \right) \quad (\text{C.23})$$

and $K_n(x)$ as the distributional limit of $K_n^\varepsilon(x)$ for $\varepsilon \rightarrow 0$. A careful study of the above expression shows that

$$\int_{-\infty}^{\infty} K_n^\varepsilon(x) x^k dx = \int_{-\infty}^{\infty} K_n(x) x^k dx = 0 \quad (\text{C.24})$$

for $k \in \{0, 1, \dots, n-1\}$. For $k < n-1$ the integral exists in an ordinary sense, however for $k = n-1$ this is not the case. We can however set the integral value to zero since the integrand is an odd function in that case.²¹ Let $f(x)$ be a given (n -times differentiable) function. We can consider the Taylor polynomial

$$T_n(x) = f(0) + f'(0)x + f''(0)\frac{x^2}{2} + \dots + f^{(n)}(0)\frac{x^n}{n!} \quad (\text{C.25})$$

and the corresponding residual

$$R_n(x) = f(x) - T_n(x). \quad (\text{C.26})$$

We then get

$$\begin{aligned} \int_{-\infty}^{\infty} K_n(x) f(x) dx &= \underbrace{\int_{-\infty}^{\infty} K_n(x) T_{n-1}(x) dx}_{=0} + \int_{-\infty}^{\infty} K_n(x) R_{n-1}(x) dx \\ &= \int_{-\infty}^{\infty} K_n(x) R_{n-1}(x) dx \\ &= \int_{-\infty}^{\infty} \frac{f(x) - f(0) - f'(0)x + f''(0)\frac{x^2}{2} + \dots + f^{(n-1)}(0)\frac{x^{n-1}}{(n-1)!}}{x^n} dx \\ &= \int_{-\infty}^{\infty} \frac{R_{n-1}(x)}{x^n} dx. \end{aligned} \quad (\text{C.27})$$

If we assume the function $f(x)$ to be analytic, the numerator in the above integral has a zero of order n at $x = 0$ and so $K_n(x)$ just becomes $1/x^n$ and the integrand does not have a pole at $x = 0$.

²¹This corresponds to interpreting the integral as a Cauchy principal value integral $\lim_{a \rightarrow \infty} \int_{-a}^a$, which indeed vanishes.

Rather than integrating from $-\infty$ to $+\infty$ we only want to integrate up to some finite b . We have to distinguish between two cases. First, let $b > 0$. Here we have

$$\begin{aligned} \int_{-\infty}^b K_n(x)f(x)dx &= \int_{-\infty}^{\infty} K_n(x)f(x)dx - \int_b^{\infty} K_n(x)f(x)dx \\ &= \int_{-\infty}^{\infty} \frac{R_{n-1}(x)}{x^n}dx - \int_b^{\infty} \frac{f(x)}{x^n}dx \\ &= \int_{-\infty}^b \frac{R_{n-1}(x)}{x^n}dx - \int_b^{\infty} \frac{T_{n-1}(x)}{x^n}dx. \end{aligned} \quad (\text{C.28})$$

However, since $T_{n-1}(x)$ is a polynomial of degree $n - 1$, the integrand $T_{n-1}(x)/(x^n)$ behaves like $1/x$ for large x and hence the latter integral does not converge. However, if we write

$$\int_{-\infty}^b K_n(x)f(x)dx = \int_{-b}^b \frac{R_{n-1}(x)}{x^n}dx + \int_b^{\infty} \left(\frac{R_{n-1}(-x)}{(-x)^n} - \frac{T_{n-1}(x)}{x^n} \right) dx, \quad (\text{C.29})$$

both integrals are well-defined.

If $b < 0$, we can directly calculate

$$\int_{-\infty}^b K_n(x)f(x)dx = \int_{-\infty}^b \frac{f(x)}{x^n}dx \quad (\text{C.30})$$

since 0 is not element of the domain of integration.

With the above formula we can calculate the real parts of the integrals $iI(p^2)$, $iK(p^2)$ and $iL(p^2)$ numerically without any further complication since the integrands are all well-behaved. It turns out that in all three cases the integration can even be done analytically.

The integral $iI(p)$ still has to be regularised. Even though it is only logarithmically divergent, we will use the regularisation scheme we used for iI_1 . Hence the result of the Pauli-Villars regularised integral will be piecewise defined for $p^2 < 4M^2$, $4M^2 < p^2 < 4M^2 + 4\Lambda^2$, $4M^2 + 4\Lambda^2 < p^2 < 4M^2 + 8\Lambda^2$ and $p^2 > 4M^2 + 8\Lambda^2$.

The real part of iI_2 has two contributions. The first one comes from the divergent part of the integral and is given by

$$\frac{1}{16\pi^2} \left(\ln(M^2) - 2 \ln(M^2 + \Lambda^2) + \ln(M^2 + 2\Lambda^2) \right) \quad (\text{C.31})$$

(regularised). The second contribution is not divergent and is for $p^2 < 4M^2$ (including $p^2 < 0$) given by

$$\frac{1}{8\pi^2} \frac{\sqrt{4M^2 - p^2} \arctan \sqrt{\frac{p^2}{4M^2 - p^2}}}{\sqrt{p^2}} \quad (\text{C.32})$$

(not regularised). For $p^2 < 0$, the argument $\sqrt{\frac{p^2}{4M^2 - p^2}}$ of the arctan is imaginary and we can use $\arctan(ix) = i \operatorname{arctanh}(x)$ to write the contribution to the integral as

$$\frac{1}{8\pi^2} \frac{\sqrt{4M^2 - p^2} \operatorname{arctanh} \sqrt{\frac{-p^2}{4M^2 - p^2}}}{\sqrt{-p^2}}. \quad (\text{C.33})$$

We note that the argument of the arctanh is now real and smaller than 1 in magnitude, which implies that the arctanh is purely real. For $p^2 > 4M^2$ the second contribution is

$$\frac{1}{16\pi^2} \frac{\sqrt{p^2 - 4M^2}}{\sqrt{p^2}} \ln \left(\frac{\sqrt{p^2} + \sqrt{p^2 - 4M^2}}{\sqrt{p^2} - \sqrt{p^2 - 4M^2}} \right) \quad (\text{C.34})$$

(not regularised).

We can also write the real and the imaginary part of $I(p)$ together as

$$\begin{aligned} iI(p^2) = \frac{1}{16\pi^2} & \left[\ln(M^2) - 2\ln(M^2 + \Lambda^2) + \ln(M^2 + 2\Lambda^2) \right. \\ & \left. + 2f\left(\frac{4M^2 - p^2}{p^2}\right) - 4f\left(\frac{4M^2 + 4\Lambda^2 - p^2}{p^2}\right) + 2f\left(\frac{4M^2 + 8\Lambda^2 - p^2}{p^2}\right) \right] \end{aligned} \quad (\text{C.35})$$

with

$$f(x) = \begin{cases} \sqrt{x} \arctan\left(\frac{1}{\sqrt{x}}\right), & x > 0 \\ \sqrt{-x} \operatorname{arctanh}\left(\frac{1}{\sqrt{-x}}\right), & x < 0 \\ 0, & x = 0 \end{cases} \quad (\text{C.36})$$

For $iK(p)$ we obtain

$$\operatorname{Re}(iK(p^2)) = \frac{\arctan\left(\sqrt{\frac{p^2}{4M^2 - p^2}}\right)}{8\pi^2 \sqrt{p^2} \sqrt{4M^2 - p^2}} \quad (\text{C.37})$$

for $p^2 < 4M^2$ (including $p^2 < 0$), which we can write as

$$\operatorname{Re}(iK(p^2)) = \frac{\operatorname{arctanh}\left(\sqrt{\frac{-p^2}{4M^2 - p^2}}\right)}{8\pi^2 \sqrt{-p^2} \sqrt{4M^2 - p^2}} \quad (\text{C.38})$$

for $p^2 < 0$, and

$$\begin{aligned}
\operatorname{Re} \left(iK(p^2) \right) &= \frac{1}{16\pi^2(p^2)^{3/2}\sqrt{p^2 - 4M^2}(p^2 - 2M^2)} \\
&\left\{ -p^2 \left[2M^2 \left(\ln \left(-\frac{\sqrt{p^2}(\sqrt{p^2 - 2M^2} - \sqrt{p^2}) + M^2}{256M^2} \right) \right. \right. \right. \\
&+ 8 \ln \left(\frac{2M^2 - \sqrt{p^2}(\sqrt{p^2 - 4M^2} + \sqrt{p^2})}{M^2 - \sqrt{p^2}(\sqrt{p^2 - 2M^2} + \sqrt{p^2})} \right) \Big) \\
&- p^2 \left(\ln \left(-\frac{\sqrt{p^2}\sqrt{p^2 - 2M^2} + M^2 - p^2}{M^2} \right) \right. \\
&+ 2 \ln \left(\sqrt{p^2}(\sqrt{p^2 - 4M^2} + \sqrt{p^2}) - 2M^2 \right) \Big) \\
&- 2(12M^4 + (p^2)^2) \ln \left(2(\sqrt{p^2}(\sqrt{p^2 - 2M^2} + \sqrt{p^2}) - M^2) \right) \\
&- 6(8M^4 - 6M^2p^2 + (p^2)^2) \operatorname{arctanh} \left(\frac{\sqrt{p^2}(\sqrt{p^2 - 4M^2} - \sqrt{p^2 - 2M^2})}{p^2 - \sqrt{8M^4 - 6M^2p^2 + (p^2)^2}} \right) \\
&\left. + 24M^4 \ln \left(\sqrt{p^2}(\sqrt{p^2 - 4M^2} + \sqrt{p^2}) - 2M^2 \right) \right\}
\end{aligned} \tag{C.39}$$

for $p^2 > 4M^2$.

For $iL(p)$ we obtain

$$\operatorname{Re} \left(iL(p^2) \right) = \frac{-4M^2\sqrt{p^2} + 2(2M^2 - p^2)\sqrt{4M^2 - p^2} \operatorname{arctan} \left(\sqrt{\frac{p^2}{4M^2 - p^2}} \right) + (p^2)^{3/2}}{8\pi^2(p^2)^{3/2}(p^2 - 4M^2)^2} \tag{C.40}$$

for $p^2 < 4M^2$ (including $p^2 < 0$), which we write as

$$\operatorname{Re} \left(iL(p^2) \right) = \frac{4M^2\sqrt{-p^2} - 2(2M^2 - p^2)\sqrt{4M^2 - p^2} \operatorname{arctanh} \left(\sqrt{\frac{-p^2}{4M^2 - p^2}} \right) + (-p^2)^{3/2}}{8\pi^2(-p^2)^{3/2}(p^2 - 4M^2)^2} \tag{C.41}$$

for $p^2 < 0$, and

$$\begin{aligned}
\operatorname{Re}(iL(p^2)) &= \frac{1}{8\pi^2(p^2)^{3/2}(p^2 - 4M^2)^2(p^2 - 2M^2)} \\
&\left\{ \sqrt{p^2 - 4M^2} \left[(p^2)^2 \ln \left(\frac{2}{\sqrt{p^2}(\sqrt{p^2 - 4M^2} + \sqrt{p^2}) - 2M^2} \right) \right. \right. \\
&+ 4M^2(p^2 - M^2) \ln \left(\sqrt{p^2}(\sqrt{p^2 - 4M^2} + \sqrt{p^2}) - 2M^2 \right) \\
&+ 2(p^2 - 2M^2)^2 \ln(M) \left. \right] - M^2 p^2 \left(\ln(16) \sqrt{p^2 - 4M^2} + 6\sqrt{p^2} \right) \\
&+ M^4 \left(\ln(16) \sqrt{p^2 - 4M^2} + 8\sqrt{p^2} \right) + (p^2)^{5/2} \left. \right\}
\end{aligned} \tag{C.42}$$

for $p^2 > 4M^2$.

C.4. Derivative of the Elementary Integral $iI(p)$

In the following we want to calculate the derivative

$$\frac{d(iI(p^2))}{d(p^2)} \tag{C.43}$$

and express it again in terms of elementary integrals. For this we use the expressions (4.23) for the elementary integrals since they explicitly depend on p^2 . We have

$$\begin{aligned}
\frac{d(iI(p^2))}{d(p^2)} &= \frac{d}{d(p^2)} \frac{1}{2\pi^2} \int_0^\infty dk \frac{k^2}{E_k^-(p^2 - 4E_k^2 + i\varepsilon)} \\
&= \frac{1}{2\pi^2} \int_0^\infty dk \frac{-k^2}{E_k^-(p^2 - 4E_k^2 + i\varepsilon)^2} \\
&= \frac{1}{8\pi^2} \int_0^\infty dk \frac{-4k^2(k^2 + M^2)}{E_k^3(p^2 - 4E_k^2 + i\varepsilon)^2}
\end{aligned} \tag{C.44}$$

In analogy we write

$$\begin{aligned}
iI(0) &= \frac{1}{8\pi^2} \int_0^\infty dk \frac{-k^2(p^2 - 4k^2 - 4M^2)^2}{E_k^3(p^2 - 4E_k^2 + i\varepsilon)^2}, \\
iI(p^2) &= \frac{1}{8\pi^2} \int_0^\infty dk \frac{4k^2(k^2 + M^2)(p^2 - 4k^2 - 4M^2)}{E_k^3(p^2 - 4E_k^2 + i\varepsilon)^2}, \\
iK(p^2) &= \frac{1}{8\pi^2} \int_0^\infty dk \frac{k^2(12k^2 + 12M^2 - p^2)}{E_k^3(p^2 - 4E_k^2 + i\varepsilon)^2}.
\end{aligned} \tag{C.45}$$

Comparing the numerators of the integrand we see that

$$\frac{d(iI(p^2))}{d(p^2)} = \frac{1}{2p^2} (iI(0) - iI(p^2)) - \frac{1}{2} iK(p^2) \tag{C.46}$$

Moreover we calculate

$$\begin{aligned}
\frac{d(p^2 iI(p^2))}{d(p^2)} &= iI(p^2) + p^2 \frac{d(iI(p^2))}{d(p^2)} \\
&= iI(p^2) + \frac{1}{2} (iI(0) - iI(p^2)) - \frac{1}{2} p^2 iIK(p^2) \\
&= \frac{1}{2} (iI(0) + iI(p^2) - p^2 K(p^2)).
\end{aligned} \tag{C.47}$$

C.5. Calculation of the Integrals $iI_3(p, q)$ and $iI_4(p, q, r)$

We were able to give analytical expressions for the integrals iI_1 and $iI_2(p)$ (both needed to be regularised). For the latter, we saw that the solution exhibits certain momentum thresholds ($p^2 > 4M^2, \dots$). It is reasonable to assume that this will also be the case for $iI_3(p, q)$ and $iI_4(p, q, r)$. However, since there are more external momenta, the situation will be considerably more difficult. In general, integrals of the form

$$i \int \frac{d^4 k}{(2\pi)^4} \frac{1}{(k^2 - M_0^2 + i\varepsilon)} \frac{1}{((k + q_1)^2 - M_1^2 + i\varepsilon)} \cdots \frac{1}{((k + q_n)^2 - M_n^2 + i\varepsilon)} \tag{C.48}$$

are called scalar one-loop n -point functions and are studied for example in [80, 81, 82]. One usually uses the momenta $p_1 = q_1$, $p_2 = q_2 - q_1$, $p_3 = q_3 - q_2$, etc. so that the k -th denominator in the above integral reads $(k + p_1 + p_2 + \dots + p_k)^2 - M_k^2 + i\varepsilon$.

The general approach for solving these integrals is the introduction of so-called *Feynman parameters* x, y, z, \dots [58]. The idea is based on the identity

$$\frac{1}{AB} = \int_0^1 dx \frac{1}{(xA + (1-x)B)^2} = \int_0^1 dx \int_0^1 dy \frac{\delta(x+y-1)}{(xA + yB)^2}, \tag{C.49}$$

which is easily generalised to

$$\frac{1}{A_1 \cdots A_n} = (n-1)! \int_0^1 dx_1 \cdots \int_0^1 dx_n \frac{\delta(x_1 + \cdots + x_n - 1)}{(x_1 A_1 + \cdots + x_n A_n)^n}. \tag{C.50}$$

By identifying the denominators of (C.48) with A_1, \dots, A_n in the above formula, it is possible to introduce n new integrations. Then, the k -integration is performed and with the help of the δ -function we obtain an expression in terms of integrals over $n-1$ Feynman parameters.

Using the above described technique, it is possible to write the integrals $iI_3(p, q)$ and $iI_4(p, q, r)$ as

$$iI_3(p, q) = \frac{1}{16\pi^2} \int_0^1 dx \int_0^x dy \frac{1}{ax^2 + by^2 + cxy + dx + ey + f} \tag{C.51}$$

with

$$\begin{aligned}
a &= (q - p)^2, \\
b &= p^2, \\
c &= 2p \cdot (q - p), \\
d &= -(q - p)^2, \\
e &= p^2 - 2p \cdot q, \\
f &= M^2 - i\varepsilon
\end{aligned} \tag{C.52}$$

and

$$\begin{aligned}
&iI_4(p, q, r) \\
&= -\frac{1}{16\pi^2} \int_0^1 dx \int_0^x dy \int_0^y dz \frac{1}{(ax^2 + by^2 + gz^2 + cxy + hxz + jyz + dx + ey + kz + f)^2}
\end{aligned} \tag{C.53}$$

with

$$\begin{aligned}
a &= (r - q)^2, \\
b &= (q - p)^2, \\
c &= 2(q - p) \cdot (r - q), \\
d &= -(r - q)^2, \\
e &= q^2 - p^2 + 2(p - q) \cdot r, \\
f &= M^2 - i\varepsilon, \\
g &= p^2, \\
h &= 2p \cdot (r - q), \\
j &= 2p(q - p), \\
k &= p^2 - 2p \cdot r.
\end{aligned} \tag{C.54}$$

We see that the integrals depend on all possible Lorentz scalars that can be formed from the external momenta. The authors of [80] describe how the above expressions can be further simplified and even expressed analytically using the Spence or dilogarithm function

$$\text{Sp}(x) := -\int_0^1 dt \frac{\ln(1 - xt)}{t}. \tag{C.55}$$

One has to be very careful however, for which external momentum configurations the given expressions are valid and we do not give these results here. We simply note that the evaluation of $iI_3(p, q)$ and $iI_4(p, q, r)$ and even higher one-loop integrals is implemented in the LoopTools package [83], which returns correct results for the external momenta occurring in the pion-pion scattering process as described in Chapter 4.

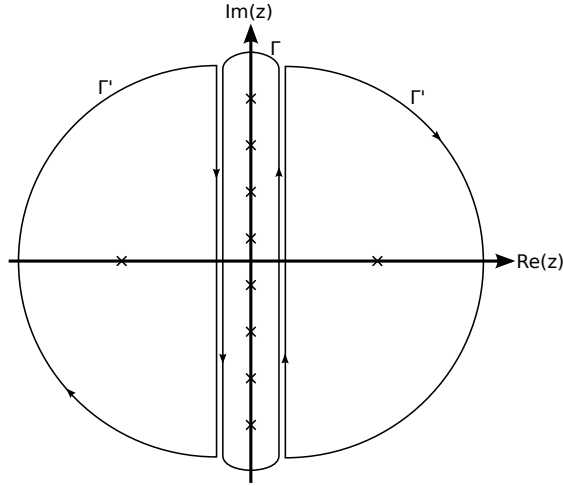
D. Medium Integrals

D.1. Medium Version of the Integral iI_1

The medium version of integral iI_1 is defined by

$$iI_1(T, \mu) = -T \sum_{j \in \mathbb{Z}} \int \frac{d^3k}{(2\pi)^3} \frac{1}{(i\omega_j + \mu)^2 - E_{\vec{k}}^2} \quad (\text{D.1})$$

with the fermionic Matsubara frequencies $i\omega_j = (2j + 1)\pi iT$. By applying the residue theorem we can replace the sum by an appropriate integral over a path Γ in the complex plane, which we then deform to the path Γ' :



This gives

$$iI_1(T, \mu) = \int \frac{d^3k}{(2\pi)^3} \frac{1}{2\pi i} \oint_{\Gamma'} dz n_F(z) \frac{1}{(z + \mu)^2 - E_{\vec{k}}^2} \quad (\text{D.2})$$

where $n_F(z) = (1 + \exp(z/T))^{-1}$ is the Fermi distribution function and has poles at all Matsubara frequencies with residue $-T$. The path Γ' runs clockwise around the poles $z_{1,2} = \pm E_{\vec{k}} - \mu$ of the integrand and hence we get

$$\begin{aligned} iI_1(T, \mu) &= - \int \frac{d^3k}{(2\pi)^3} \sum_{i=1}^2 \text{Res}_{z_i} \left(n_F(z) \frac{1}{(z + \mu)^2 - E_{\vec{k}}^2} \right) \\ &= \int \frac{d^3k}{(2\pi)^3} \frac{1}{2E_{\vec{k}}} \left(n_F(-E_{\vec{k}} - \mu) - n_F(E_{\vec{k}} - \mu) \right) \\ &= \int \frac{d^3k}{(2\pi)^3} \frac{1}{2E_{\vec{k}}} \left(1 - n_{\vec{k}} - \bar{n}_{\vec{k}} \right), \end{aligned} \quad (\text{D.3})$$

where we used $n_{\text{F}}(-z) = 1 - n_{\text{F}}(z)$ in the last step and defined the *quark* and *antiquark* occupation number density

$$\begin{aligned} n_{\vec{k}} &= n_{\vec{k}}(T, \mu; M) = \frac{1}{1 + \exp\left(\frac{E_{\vec{k}} - \mu}{T}\right)} = n_{\text{F}}(E_{\vec{k}} - \mu) \\ \bar{n}_{\vec{k}} &= \bar{n}_{\vec{k}}(T, \mu; M) = \frac{1}{1 + \exp\left(\frac{E_{\vec{k}} + \mu}{T}\right)} = n_{\text{F}}(E_{\vec{k}} + \mu). \end{aligned} \quad (\text{D.4})$$

Regularisation

The above integral $iI_1(T, \mu)$ can be split into a vacuum and a medium contribution as we will show in the following and it turns out that only the vacuum contribution needs to be regularised.

If we let $T \rightarrow 0$, the Fermi distribution functions becomes

$$n_{\text{F}}(x) \rightarrow 1 - \Theta(x) = \Theta(-x), \quad (\text{D.5})$$

where $\Theta(x)$ denotes the Heaviside step function. If we in addition set $\mu = 0$, the quark and antiquark occupation number densities in expression (3.7) for iI_1 will vanish since $E_{\vec{k}}$ is always positive. We argued before that we will obtain the vacuum expression of a given quantity in the limit $T, \mu \rightarrow 0$. Hence

$$iI_1^{\text{vac}} = \int \frac{d^3k}{(2\pi)^3} \frac{1}{2E_{\vec{k}}}, \quad (\text{D.6})$$

which agrees with the vacuum result obtained in Chapter 2. The rest of the medium integral we can separate off and call it the medium contribution to the integral, i.e.

$$iI_1(T, \mu) = iI_1^{\text{vac}} + iI_1^{\text{med}}(T, \mu) \quad (\text{D.7})$$

with

$$iI_1^{\text{med}}(T, \mu) = - \int \frac{d^3k}{(2\pi)^3} \frac{1}{2E_{\vec{k}}} (n_{\vec{k}} + \bar{n}_{\vec{k}}). \quad (\text{D.8})$$

As the occupation number densities are given in terms of the Fermi distribution function n_{F} , they are exponentially decreasing for large \vec{k} , which guarantees the convergence of the medium contribution to the integral. Only the vacuum part (as we discussed in Section 2.3) needs to be regularised, e.g. by applying a Pauli-Villars regularisation scheme. The medium contribution will be left unchanged.

D.2. Medium Versions of the Integrals $iI(p)$, $iK(p)$, $iL(p)$

We want to determine the medium versions of the integrals

$$\begin{aligned}
iI(p) &:= i \int \frac{d^4k}{(2\pi)^4} \frac{1}{(k^2 - M^2 + i\varepsilon)} \frac{1}{((k+p)^2 - M^2 + i\varepsilon)}, \\
iK(p) &:= i \int \frac{d^4k}{(2\pi)^4} \frac{1}{(k^2 - M^2 + i\varepsilon)^2} \frac{1}{((k+p)^2 - M^2 + i\varepsilon)}, \\
iL(p) &:= i \int \frac{d^4k}{(2\pi)^4} \frac{1}{(k^2 - M^2 + i\varepsilon)^2} \frac{1}{((k+p)^2 - M^2 + i\varepsilon)^2}.
\end{aligned} \tag{D.9}$$

The medium integrals are given by

$$\begin{aligned}
iI(i\omega_n, \vec{p}) &= -T \sum_{j \in \mathbb{Z}} \int \frac{d^3k}{(2\pi)^3} \frac{1}{\left((i\omega_j + \mu)^2 - E_k^2 \right) \left((i\omega_n + i\omega_j + \mu)^2 - E_{\vec{k}+\vec{p}}^2 \right)}, \\
iK(i\omega_n, \vec{p}) &= -T \sum_{j \in \mathbb{Z}} \int \frac{d^3k}{(2\pi)^3} \frac{1}{\left((i\omega_j + \mu)^2 - E_k^2 \right)^2 \left((i\omega_n + i\omega_j + \mu)^2 - E_{\vec{k}+\vec{p}}^2 \right)}, \\
iL(i\omega_n, \vec{p}) &= -T \sum_{j \in \mathbb{Z}} \int \frac{d^3k}{(2\pi)^3} \frac{1}{\left((i\omega_j + \mu)^2 - E_k^2 \right)^2 \left((i\omega_n + i\omega_j + \mu)^2 - E_{\vec{k}+\vec{p}}^2 \right)^2},
\end{aligned} \tag{D.10}$$

where the outer Matsubara frequency $i\omega_n = 2\pi i n T$ is a bosonic frequency (related to \vec{p}) and $i\omega_j = (2j+1)\pi i T$ is a fermionic frequency (related to \vec{k}). We write the Matsubara sums as contour integrals by application of the residue theorem (recall that the Fermi distribution $n_F(z) = (1 + \exp(z/T))^{-1}$ has poles at $z = (2j+1)\pi i T = i\omega_j$ for $j \in \mathbb{Z}$ with residue $-T$). We get

$$\begin{aligned}
iI(i\omega_n, \vec{p}) &= \int \frac{d^3k}{(2\pi)^3} \frac{1}{2\pi i} \oint_{\Gamma} \frac{n_F(z)}{\left((z + \mu)^2 - E_k^2 \right) \left((z + i\omega_n + \mu)^2 - E_{\vec{k}+\vec{p}}^2 \right)}, \\
iK(i\omega_n, \vec{p}) &= \int \frac{d^3k}{(2\pi)^3} \frac{1}{2\pi i} \oint_{\Gamma} \frac{n_F(z)}{\left((z + \mu)^2 - E_k^2 \right)^2 \left((z + i\omega_n + \mu)^2 - E_{\vec{k}+\vec{p}}^2 \right)}, \\
iL(i\omega_n, \vec{p}) &= \int \frac{d^3k}{(2\pi)^3} \frac{1}{2\pi i} \oint_{\Gamma} \frac{n_F(z)}{\left((z + \mu)^2 - E_k^2 \right)^2 \left((z + i\omega_n + \mu)^2 - E_{\vec{k}+\vec{p}}^2 \right)^2},
\end{aligned} \tag{D.11}$$

where Γ is an integration contour running counter-clockwise around all the Matsubara poles on the imaginary axis. This path can be deformed to an integration contour running clockwise around the (first or second order) poles $z_{1,2} = \pm E_k - \mu$ and $z_{3,4} = \pm E_{\vec{k}+\vec{p}} - \mu - i\omega_n$ of the integrands. We then apply the residue theorem once more to

obtain

$$\begin{aligned}
iI(i\omega_n, \vec{p}) &= - \int \frac{d^3k}{(2\pi)^3} \sum_{i=1}^4 \text{Res}_{z_i} \frac{n_{\text{F}}(z)}{\left((z + \mu)^2 - E_{\vec{k}}^2\right) \left((z + i\omega_n + \mu)^2 - E_{\vec{k}+\vec{p}}^2\right)}, \\
iK(i\omega_n, \vec{p}) &= - \int \frac{d^3k}{(2\pi)^3} \sum_{i=1}^4 \text{Res}_{z_i} \frac{n_{\text{F}}(z)}{\left((z + \mu)^2 - E_{\vec{k}}^2\right)^2 \left((z + i\omega_n + \mu)^2 - E_{\vec{k}+\vec{p}}^2\right)}, \quad (\text{D.12}) \\
iL(i\omega_n, \vec{p}) &= - \int \frac{d^3k}{(2\pi)^3} \sum_{i=1}^4 \text{Res}_{z_i} \frac{n_{\text{F}}(z)}{\left((z + \mu)^2 - E_{\vec{k}}^2\right)^2 \left((z + i\omega_n + \mu)^2 - E_{\vec{k}+\vec{p}}^2\right)^2}.
\end{aligned}$$

The sum of the residues is quite lengthy and we do not write down the resulting expressions. In the following we give the general ideas of the calculations.

We make the analytical continuation by replacing $i\omega_n \mapsto p_0 + i\varepsilon$ to obtain the retarded integrals $iI^+(p_0, \vec{p})$, $iK^+(p_0, \vec{p})$ and $iL^+(p_0, \vec{p})$ (or $i\omega_n \mapsto p_0 + i\varepsilon$ for the advanced versions). We then do a partial fraction decomposition to write the integrand of each integral in terms of the denominators $(p_0 \pm E_{\vec{k}} \pm E_{\vec{k}+\vec{p}} + i\varepsilon)^n$, where n can be 1 for $iI^+(p_0, \vec{p})$, 1 or 2 for $iK^+(p_0, \vec{p})$ and 1, 2 or 3 for $iL^+(p_0, \vec{p})$.

For the imaginary part of the integrals this translates into δ -distributions and derivatives thereof. For the real part we proceed analogously as described in Section C.3. Both discussions turn out to be very difficult due to the three-dimensional integration over \vec{k} . So far this calculation is only done for $iI^+(p_0, \vec{p})$ [38] and we will present the results in Section D.3.

Vanishing Three-Momentum

As a simplification when it comes to calculating the retarded integrals $iI^+(p_0, \vec{p})$, $iK^+(p_0, \vec{p})$ and $iL^+(p_0, \vec{p})$ we could assume that the three-momentum \vec{p} vanishes. Setting $\vec{p} = 0$ amounts to replacing $E_{\vec{k}+\vec{p}}$ by $E_{\vec{k}}$ in expressions (D.12). In that case the integrand simplifies considerably and the integrals can be written as

$$\begin{aligned}
iI^+(p_0, 0) &= - \int \frac{d^3k}{(2\pi)^3} \frac{\sinh\left(\frac{E_{\vec{k}}}{T}\right)}{E_{\vec{k}} \left(4E_{\vec{k}}^2 - (p_0 + i\varepsilon)^2\right) \left(\cosh\left(\frac{E_{\vec{k}}}{T}\right) + \cosh\left(\frac{\mu}{T}\right)\right)}, \quad (\text{D.13}) \\
iK^+(p_0, 0) &= \int \frac{d^3k}{(2\pi)^3} \frac{-4E_{\vec{k}}^3 p_0 + E_{\vec{k}} p_0 (p_0^2 - 4E_{\vec{k}}^2) \cosh\left(\frac{E_{\vec{k}}}{T}\right) \cosh\left(\frac{\mu}{T}\right) + E_{\vec{k}} p_0^3}{4E_{\vec{k}}^3 p_0 T \left((p_0 + i\varepsilon)^2 - 4E_{\vec{k}}^2\right)^2 \left(\cosh\left(\frac{E_{\vec{k}}}{T}\right) + \cosh\left(\frac{\mu}{T}\right)\right)^2} \dots \\
&\quad \dots \frac{+ \sinh\left(\frac{E_{\vec{k}}}{T}\right) \left[2E_{\vec{k}}^2 (4E_{\vec{k}}^2 - p_0^2) \sinh\left(\frac{\mu}{T}\right) \dots}{\dots} \dots}{\dots} \dots \\
&\quad \dots \frac{-p_0 T (p_0^2 - 12E_{\vec{k}}^2) \left(\cosh\left(\frac{E_{\vec{k}}}{T}\right) + \cosh\left(\frac{\mu}{T}\right)\right)}{\dots} \dots
\end{aligned} \quad (\text{D.14})$$

and

$$\begin{aligned}
iL^+(p_0, 0) = & \int \frac{d^3k}{(2\pi)^3} \frac{e^{\frac{2(E_{\vec{k}} + \mu)}{T}} \left[2E_{\vec{k}} \left(16E_{\vec{k}}^4 - p_0^4 \right) \left(\cosh \left(\frac{E_{\vec{k}}}{T} \right) \cosh \left(\frac{\mu}{T} \right) + 1 \right) \right]}{p_0^2 T E_{\vec{k}}^3 \left(4E_{\vec{k}}^2 - (p_0 + i\varepsilon)^2 \right)^3 \left(e^{\frac{E_{\vec{k}}}{T}} + e^{\frac{\mu}{T}} \right)^2 \left(e^{\frac{E_{\vec{k}} + \mu}{T}} + 1 \right)^2} \dots \\
& \dots \frac{+ 2p_0^2 T \left(p_0^2 - 20E_{\vec{k}}^2 \right) \sinh \left(\frac{E_{\vec{k}}}{T} \right) \left(\cosh \left(\frac{E_{\vec{k}}}{T} \right) + \cosh \left(\frac{\mu}{T} \right) \right)}{.}
\end{aligned} \tag{D.15}$$

These integrals only depend on $E_{\vec{k}} = \sqrt{\vec{k}^2 + M^2}$ and hence only on $|\vec{k}|$ rather than \vec{k} . We transform the integrals in the following way

$$\begin{aligned}
& \int \frac{d^3k}{(2\pi)^3} f(E_{\vec{k}}) \frac{1}{\left(4E_{\vec{k}}^2 - p_0^2 \right)^n} \\
&= \frac{1}{2\pi^2} \int_M^\infty dE_{\vec{k}} E_{\vec{k}} \sqrt{E_{\vec{k}}^2 - M^2} f(E_{\vec{k}}) \frac{1}{\left(4E_{\vec{k}}^2 - p_0^2 \right)^n} \\
&= \frac{1}{8\pi^2} \int_{4M^2 - p_0^2}^\infty dx \sqrt{x + p_0^2 - 4M^2} f \left(\frac{1}{2} \sqrt{x + p_0^2} \right) \frac{1}{(x - \text{sgn}(p_0)i\varepsilon)^n} \\
&= \frac{1}{8\pi^2} (-1)^n \int_{-\infty}^{-(4M^2 - p_0^2)} dx \sqrt{-x + p_0^2 - 4M^2} f \left(\frac{1}{2} \sqrt{-x + p_0^2} \right) \frac{1}{(x + \text{sgn}(p_0)i\varepsilon)^n}.
\end{aligned} \tag{D.16}$$

The real and imaginary part of the integrals can now be calculated as described in Section C.3. This is done numerically in the case of the real part. The imaginary part can be expressed analytically and is given by

$$\text{Im} \left(iI^+(p_0, 0) \right) = -\text{sgn}(p_0) \frac{\sqrt{p_0^2 - 4M^2} \sinh \left(\frac{|p_0|}{2T} \right)}{16\pi |p_0| \left(\cosh \left(\frac{|p_0|}{2T} \right) + \cosh \left(\frac{\mu}{T} \right) \right)} \Theta(p_0^2 - 4M^2), \tag{D.17}$$

$$\begin{aligned}
\text{Im} \left(iK^+(p_0, 0) \right) = & \text{sgn}(p_0) \frac{\sinh \left(\frac{|p_0|}{2T} \right) \left[\text{sgn}(p_0) (p_0^2 - 4M^2) \sinh \left(\frac{\mu}{T} \right) \right]}{32\pi p_0^2 T \sqrt{p_0^2 - 4M^2} \left(\cosh \left(\frac{|p_0|}{2T} \right) + \cosh \left(\frac{\mu}{T} \right) \right)^2} \dots \\
& \dots \frac{+ 2|p_0| T \left(\cosh \left(\frac{|p_0|}{2T} \right) + \cosh \left(\frac{\mu}{T} \right) \right)}{\Theta(p_0^2 - 4M^2)},
\end{aligned} \tag{D.18}$$

$$\begin{aligned}
\text{Im} \left(iL^+(p_0, 0) \right) &= \text{sgn}(p_0) \frac{\sinh \left(\frac{|p_0|}{2T} \right) \left[8T^2 (p_0^2 - 2M^2) \cosh \left(\frac{|p_0|}{T} \right) \right]}{128\pi T^2 |p_0|^3 \sqrt{p_0^2 - 4M^2}^3 \left(\cosh \left(\frac{|p_0|}{2T} \right) + \cosh \left(\frac{\mu}{T} \right) \right)^3} \dots \\
&\quad + \frac{\left(8T^2 (p_0^2 - 2M^2) + (p_0^2 - 4M^2)^2 \right) \cosh \left(\frac{2\mu}{T} \right)}{\dots} \dots \\
&\quad \dots \frac{+16T^2 (p_0^2 - 2M^2) - 3 (p_0^2 - 4M^2)^2}{\dots} \dots \\
&\quad \dots \frac{- \left(16T^2 (2M^2 - p_0^2) + (p_0^2 - 4M^2)^2 \right) \cosh \left(\frac{\mu}{T} \right) \sinh \left(\frac{|p_0|}{T} \right)}{\dots} \times \\
&\quad \times \Theta(p_0^2 - 4M^2).
\end{aligned} \tag{D.19}$$

One easily checks that for $\mu = 0$ and $T \rightarrow 0$ these expressions for the imaginary part yield the vacuum results (C.22) as calculated in Section C.3 times a factor of $\text{sgn}(p_0)$, which is due to the fact that we are calculating retarded integrals rather than Feynman integrals. A more detailed discussion related to this topic can be found in Section D.3, where we calculate the medium integral $iI^+(p_0, \vec{p}) = iI_2^+(p_0, \vec{p})$ for non-vanishing \vec{p} .

Regularisation

The way we wrote down the integrals, we did not separate between a medium and a vacuum contribution. This we have to do since we decided to regularise the vacuum, but not the medium contribution of the integrals. Since $iK^+(p_0, \vec{p})$ and $iL^+(p_0, \vec{p})$ do not have to be regularised at all, we simply calculate the unregularised expression (for the real or imaginary part) and subtract the vacuum expression in order to obtain the medium contribution. Then we add again the regularised vacuum expression, which we decided to regularise for consistency.

For the imaginary part of $iI^+(p_0, \vec{p})$ we proceed as described above. The real part does not converge without regularisation. It is therefore convenient to separate off medium and vacuum contribution already for the integrand. This is done in the following Section D.3 for the more general case of non-vanishing external three-momentum \vec{p} . Setting $\vec{p} = 0$ in (D.32) yields

$$iI_2^+(p_0, 0) = \int \frac{d^3k}{(2\pi)^3} \frac{1}{E_{\vec{k}}} \left(1 - n_{\vec{k}} - \bar{n}_{\vec{k}} \right) \frac{1}{(p_0 + i\varepsilon)^2 - 4E_{\vec{k}}^2}, \tag{D.20}$$

where we easily read off the vacuum contribution

$$iI_2^{+, \text{vac}}(p_0, 0) = \int \frac{d^3k}{(2\pi)^3} \frac{1}{E_{\vec{k}}} \frac{1}{(p_0 + i\varepsilon)^2 - 4E_{\vec{k}}^2}, \tag{D.21}$$

and the medium contribution

$$iI_2^{+, \text{med}}(p_0, 0) = - \int \frac{d^3k}{(2\pi)^3} \frac{1}{E_{\vec{k}}} \left(n_{\vec{k}} + \bar{n}_{\vec{k}} \right) \frac{1}{(p_0 + i\varepsilon)^2 - 4E_{\vec{k}}^2}. \tag{D.22}$$

For each the real part can be obtained by writing the integral as a one-dimensional integral over $|\vec{k}|$ and calculating the Cauchy principal value integral, where we regularise only the vacuum part. For the vacuum part we obtain exactly $\text{Re}(iI(p^2 = p_0^2))$ as is discussed in Section D.3. The medium contribution is calculated numerically.

D.3. Medium Version of the Integral $iI_2(p)$

We want to determine the medium version of the integral

$$iI_2(p) = i \int \frac{d^4k}{(2\pi)^4} \frac{1}{(k^2 - M^2 + i\varepsilon) ((k+p)^2 - M^2 + i\varepsilon)}. \quad (\text{D.23})$$

for non-vanishing external three-momentum \vec{p} . In Section D.2 we showed that the Matsubara integral can be written as

$$iI_2(i\omega_n, \vec{p}) = - \int \frac{d^3k}{(2\pi)^3} \sum_{i=1}^4 \text{Res}_{z_i} \frac{n_{\text{F}}(z)}{\left((z + \mu)^2 - E_{\vec{k}}^2\right) \left((z + i\omega_n + \mu)^2 - E_{\vec{k}+\vec{p}}^2\right)} \quad (\text{D.24})$$

with $z_{1,2} = \pm E_{\vec{k}} - \mu$ and $z_{3,4} = \pm E_{\vec{k}+\vec{p}} - \mu - i\omega_n$. Calculating the residues yields

$$\begin{aligned} iI_2(i\omega_n, \vec{p}) = & - \int \frac{d^3k}{(2\pi)^3} \left[\frac{n_{\text{F}}(E_{\vec{k}} - \mu)}{2E_{\vec{k}} (E_{\vec{k}} + i\omega_n - E_{\vec{k}+\vec{p}}) (E_{\vec{k}} + i\omega_n + E_{\vec{k}+\vec{p}})} \right. \\ & + \frac{n_{\text{F}}(-E_{\vec{k}} - \mu)}{(-2E_{\vec{k}}) (-E_{\vec{k}} + i\omega_n - E_{\vec{k}+\vec{p}}) (-E_{\vec{k}} + i\omega_n + E_{\vec{k}+\vec{p}})} \\ & + \frac{n_{\text{F}}(E_{\vec{k}+\vec{p}} - i\omega_n - \mu)}{(E_{\vec{k}+\vec{p}} - i\omega_n - E_{\vec{k}}) (E_{\vec{k}+\vec{p}} - i\omega_n + E_{\vec{k}}) 2E_{\vec{k}+\vec{p}}} \\ & \left. + \frac{n_{\text{F}}(-E_{\vec{k}+\vec{p}} - i\omega_n - \mu)}{(-E_{\vec{k}+\vec{p}} - i\omega_n - E_{\vec{k}}) (-E_{\vec{k}+\vec{p}} - i\omega_n + E_{\vec{k}}) (-2E_{\vec{k}+\vec{p}})} \right]. \quad (\text{D.25}) \end{aligned}$$

By using the periodicity of n_{F} and making a substitution $\vec{k} \mapsto -\vec{k} - \vec{p}$ in the second part of the integral, the above expression simplifies to

$$\begin{aligned} iI_2(i\omega_n, \vec{p}) = & - \int \frac{d^3k}{(2\pi)^3} \left[\frac{n_{\text{F}}(E_{\vec{k}} - \mu)}{2E_{\vec{k}} (E_{\vec{k}} + i\omega_n - E_{\vec{k}+\vec{p}}) (E_{\vec{k}} + i\omega_n + E_{\vec{k}+\vec{p}})} \right. \\ & - \frac{n_{\text{F}}(-E_{\vec{k}} - \mu)}{2E_{\vec{k}} (E_{\vec{k}} - i\omega_n + E_{\vec{k}+\vec{p}}) (E_{\vec{k}} - i\omega_n - E_{\vec{k}+\vec{p}})} \\ & + \frac{n_{\text{F}}(E_{\vec{k}} - \mu)}{2E_{\vec{k}} (E_{\vec{k}} - i\omega_n - E_{\vec{k}+\vec{p}}) (E_{\vec{k}} - i\omega_n + E_{\vec{k}+\vec{p}})} \\ & \left. - \frac{n_{\text{F}}(-E_{\vec{k}} - \mu)}{2E_{\vec{k}} (E_{\vec{k}} + i\omega_n + E_{\vec{k}+\vec{p}}) (E_{\vec{k}} + i\omega_n - E_{\vec{k}+\vec{p}})} \right]. \quad (\text{D.26}) \end{aligned}$$

Doing a partial fraction decomposition and rearranging the terms, one arrives at the result

$$iI_2(i\omega_n, \vec{p}) = - \int \frac{d^3k}{(2\pi)^3} \frac{1}{4E_{\vec{k}}E_{\vec{k}+\vec{p}}} \left(n_F(E_{\vec{k}} - \mu) - n_F(-E_{\vec{k}} - \mu) \right) \times \left(\frac{2(E_{\vec{k}} - E_{\vec{k}+\vec{p}})}{(E_{\vec{k}} - E_{\vec{k}+\vec{p}})^2 - (i\omega_n)^2} - \frac{2(E_{\vec{k}} + E_{\vec{k}+\vec{p}})}{(E_{\vec{k}} + E_{\vec{k}+\vec{p}})^2 - (i\omega_n)^2} \right). \quad (\text{D.27})$$

Introducing $s_{\vec{k},\vec{p}} := E_{\vec{k}+\vec{p}} + E_{\vec{k}}$ and $d_{\vec{k},\vec{p}} := E_{\vec{k}+\vec{p}} - E_{\vec{k}}$ and using $n_F(-z) = 1 - n_F(z)$ we get

$$iI_2(i\omega_n, \vec{p}) = \int \frac{d^3k}{(2\pi)^3} \frac{1}{2E_{\vec{k}}E_{\vec{k}+\vec{p}}} \left(1 - n_F(E_{\vec{k}} + \mu) - n_F(E_{\vec{k}} - \mu) \right) \times \left(\frac{d_{\vec{k},\vec{p}}}{d_{\vec{k},\vec{p}}^2 - (i\omega_n)^2} + \frac{s_{\vec{k},\vec{p}}}{s_{\vec{k},\vec{p}}^2 - (i\omega_n)^2} \right). \quad (\text{D.28})$$

Making the substitution $\vec{k} \mapsto -\vec{k} - \vec{p}$ we see that the integral

$$\int \frac{d^3k}{(2\pi)^3} \frac{1}{2E_{\vec{k}}E_{\vec{k}+\vec{p}}} \cdot 1 \cdot \frac{d_{\vec{k},\vec{p}}}{d_{\vec{k},\vec{p}}^2 - (i\omega_n)^2} \quad (\text{D.29})$$

vanishes and

$$\int \frac{d^3k}{(2\pi)^3} \frac{1}{2E_{\vec{k}}E_{\vec{k}+\vec{p}}} \cdot 1 \cdot \frac{s_{\vec{k},\vec{p}}}{s_{\vec{k},\vec{p}}^2 - (i\omega_n)^2} = \int \frac{d^3k}{(2\pi)^3} \frac{1}{E_{\vec{k}}} \frac{1}{s_{\vec{k},\vec{p}}^2 - (i\omega_n)^2}. \quad (\text{D.30})$$

Hence we can write the integral in a slightly different way (in accordance with [38]), namely

$$iI_2(i\omega_n, \vec{p}) = \int \frac{d^3k}{(2\pi)^3} \left[\left(\frac{1}{E_{\vec{k}}} - \frac{n_F(E_{\vec{k}} + \mu) + n_F(E_{\vec{k}} - \mu)}{2E_{\vec{k}}E_{\vec{k}+\vec{p}}} s_{\vec{k},\vec{p}} \right) \frac{1}{(i\omega_n)^2 - s_{\vec{k},\vec{p}}^2} - \frac{n_F(E_{\vec{k}} + \mu) + n_F(E_{\vec{k}} - \mu)}{2E_{\vec{k}}E_{\vec{k}+\vec{p}}} d_{\vec{k},\vec{p}} \frac{1}{(i\omega_n)^2 - d_{\vec{k},\vec{p}}^2} \right]. \quad (\text{D.31})$$

Retarded Integral

For the calculation of the meson masses we need the retarded version of the above integral, which is obtained by replacing $i\omega_n \mapsto p_0 + i\varepsilon$. The integral reads

$$iI_2^+(p_0, \vec{p}) = \int \frac{d^3k}{(2\pi)^3} \left[\left(\frac{1}{E_{\vec{k}}} - \frac{n_{\vec{k}} + \bar{n}_{\vec{k}}}{2E_{\vec{k}+\vec{p}}E_{\vec{k}}} s_{\vec{k},\vec{p}} \right) \frac{1}{(p_0 + i\varepsilon)^2 - s_{\vec{k},\vec{p}}^2} - \frac{n_{\vec{k}} + \bar{n}_{\vec{k}}}{2E_{\vec{k}+\vec{p}}E_{\vec{k}}} d_{\vec{k},\vec{p}} \frac{1}{(p_0 + i\varepsilon)^2 - d_{\vec{k},\vec{p}}^2} \right]. \quad (\text{D.32})$$

We split the integral into a vacuum and a medium contribution

$$iI_2^+(p_0, \vec{p}) = iI_2^{+, \text{vac}}(p_0, \vec{p}) + iI_2^{+, \text{med}}(p_0, \vec{p}) \quad (\text{D.33})$$

with

$$iI_2^{+, \text{vac}}(p_0, \vec{p}) = \int \frac{d^3k}{(2\pi)^3} \frac{1}{E_{\vec{k}}} \frac{1}{(p_0 + i\varepsilon)^2 - s_{\vec{k}, \vec{p}}^2} \quad (\text{D.34})$$

and

$$\begin{aligned} iI_2^{+, \text{med}}(p_0, \vec{p}) &= - \int \frac{d^3k}{(2\pi)^3} \frac{n_{\vec{k}} + \bar{n}_{\vec{k}}}{2E_{\vec{k}+\vec{p}}E_{\vec{k}}} \left(\frac{s_{\vec{k}, \vec{p}}}{(p_0 + i\varepsilon)^2 - s_{\vec{k}, \vec{p}}^2} + \frac{d_{\vec{k}, \vec{p}}}{(p_0 + i\varepsilon)^2 - d_{\vec{k}, \vec{p}}^2} \right) \\ &= - \int \frac{d^3k}{(2\pi)^3} \frac{n_{\vec{k}} + \bar{n}_{\vec{k}}}{4E_{\vec{k}+\vec{p}}E_{\vec{k}}} \left(\frac{1}{p_0 + i\varepsilon - s_{\vec{k}, \vec{p}}} - \frac{1}{p_0 + i\varepsilon + s_{\vec{k}, \vec{p}}} \right. \\ &\quad \left. + \frac{1}{p_0 + i\varepsilon - d_{\vec{k}, \vec{p}}} - \frac{1}{p_0 + i\varepsilon + d_{\vec{k}, \vec{p}}} \right). \end{aligned} \quad (\text{D.35})$$

Only the vacuum part is divergent and needs to be regularised. The medium part is convergent due to the $n_{\vec{k}}$ and the $\bar{n}_{\vec{k}}$ in the integrand. Moreover, for $\mu = 0$ and $T \rightarrow 0$ the medium integral $iI_2^{\text{med}}(p_0, \vec{p})$ vanishes, which justifies the separation into the two parts.

The vacuum part can be written as

$$iI_2^{+, \text{vac}}(p_0, \vec{p}) = \int \frac{d^3k}{(2\pi)^3} \frac{1}{E_{\vec{k}}} \frac{1}{p_0^2 + i \operatorname{sgn}(p_0)\varepsilon - s_{\vec{k}, \vec{p}}^2} \quad (\text{D.36})$$

and comparing with (C.13) immediately shows

$$iI_2^{+, \text{vac}}(p_0, \vec{p}) = iI_2(p^2) \quad (\text{D.37})$$

for $p_0 > 0$ and

$$iI_2^{+, \text{vac}}(p_0, \vec{p}) = \left(iI_2(p^2) \right)^* \quad (\text{D.38})$$

for $p_0 < 0$, i.e.

$$\operatorname{Re} \left(iI_2^{+, \text{vac}}(p_0, \vec{p}) \right) = \operatorname{Re} \left(iI_2(p^2) \right) \quad (\text{D.39})$$

and

$$\operatorname{Im} \left(iI_2^{+, \text{vac}}(p_0, \vec{p}) \right) = \operatorname{sgn}(p_0) \operatorname{Im} \left(iI_2(p^2) \right). \quad (\text{D.40})$$

The vacuum part $iI_2^{+, \text{vac}}(p_0, \vec{p})$ is hence identical to the vacuum integral $iI_2(p^2)$ provided that $p_0 > 0$. For $p_0 < 0$ there is a sign flip in the imaginary part. If we had taken the advanced integral instead of the retarded one, this would be exactly the other way around. This observation corresponds to the fact that we chose Feynman expressions in our vacuum description (see Appendix C.2), while for the medium discussion we chose retarded expressions. The results for $iI_2(p^2)$ are presented in Appendices C.2 and C.3.

Imaginary Part

Let us now turn to the medium contribution $iI_2^{+, \text{med}}(p_0, \vec{p})$. We first calculate the imaginary part, which is given by

$$\begin{aligned} \text{Im} \left(iI_2^{+, \text{med}}(p_0, \vec{p}) \right) &= \int \frac{d^3k}{(2\pi)^3} \frac{n_{\vec{k}} + \bar{n}_{\vec{k}}}{4E_{\vec{k}+\vec{p}} E_{\vec{k}}} \pi \left(\delta(p_0 - s_{\vec{k}, \vec{p}}) - \delta(p_0 + s_{\vec{k}, \vec{p}}) \right. \\ &\quad \left. + \delta(p_0 - d_{\vec{k}, \vec{p}}) - \delta(p_0 + d_{\vec{k}, \vec{p}}) \right). \end{aligned} \quad (\text{D.41})$$

In general it is possible to write

$$\int \frac{d^3k}{(2\pi)^3} f(E_{\vec{k}}, E_{\vec{k}+\vec{p}}) = \frac{1}{(2\pi)^2 |\vec{p}|} \int_M dE_{\vec{k}} \int_{E_{\vec{k}+\vec{p}}^-}^{E_{\vec{k}+\vec{p}}^+} dE_{\vec{k}+\vec{p}} E_{\vec{k}} E_{\vec{k}+\vec{p}} f(E_{\vec{k}}, E_{\vec{k}+\vec{p}}), \quad (\text{D.42})$$

where we treat $E_{\vec{k}}$ and $E_{\vec{k}+\vec{p}}$ as integration variables and define

$$E_{\vec{k}+\vec{p}}^\pm := \sqrt{M^2 + (|\vec{k}| \pm |\vec{p}|)} = \sqrt{M^2 + \left(\sqrt{E_{\vec{k}}^2 - M^2} \pm |\vec{p}| \right)}. \quad (\text{D.43})$$

The integral hence reads

$$\begin{aligned} \text{Im} \left(iI_2^{+, \text{med}}(p_0, \vec{p}) \right) &= \frac{1}{16\pi |\vec{p}|} \int_M dE_{\vec{k}} \int_{E_{\vec{k}+\vec{p}}^-}^{E_{\vec{k}+\vec{p}}^+} dE_{\vec{k}+\vec{p}} (n_{\vec{k}} + \bar{n}_{\vec{k}}) \left(\delta(p_0 - s_{\vec{k}, \vec{p}}) - \delta(p_0 + s_{\vec{k}, \vec{p}}) \right. \\ &\quad \left. + \delta(p_0 - d_{\vec{k}, \vec{p}}) - \delta(p_0 + d_{\vec{k}, \vec{p}}) \right). \end{aligned} \quad (\text{D.44})$$

Since the integrand contains δ -distributions of the form $\delta(p_0 \pm E_{\vec{k}} \pm E_{\vec{k}+\vec{p}})$, we calculate

$$\begin{aligned} &\chi_{[E_{\vec{k}+\vec{p}}^-, E_{\vec{k}+\vec{p}}^+]}(E_{\vec{k}+\vec{p}}) \delta(p_0 - E_{\vec{k}} \mp E_{\vec{k}+\vec{p}}) \\ &= \left[\Theta(p^2 - 4M^2) \Theta(\pm p_0 \mp E_{\vec{k}}) \chi_{[p_0/2 - \sqrt{\Delta}, p_0/2 + \sqrt{\Delta}]}(E_{\vec{k}}) \right. \\ &\quad \left. + \Theta(-p^2) \Theta(\pm p_0 \mp E_{\vec{k}}) \left(1 - \chi_{[p_0/2 - \sqrt{\Delta}, p_0/2 + \sqrt{\Delta}]}(E_{\vec{k}}) \right) \right] \delta(p_0 - E_{\vec{k}} \mp E_{\vec{k}+\vec{p}}), \quad (\text{D.45}) \\ &\chi_{[E_{\vec{k}+\vec{p}}^-, E_{\vec{k}+\vec{p}}^+]}(E_{\vec{k}+\vec{p}}) \delta(p_0 + E_{\vec{k}} \mp E_{\vec{k}+\vec{p}}) \\ &= \left[\Theta(p^2 - 4M^2) \Theta(\pm p_0 \pm E_{\vec{k}}) \chi_{[-p_0/2 - \sqrt{\Delta}, -p_0/2 + \sqrt{\Delta}]}(E_{\vec{k}}) \right. \\ &\quad \left. + \Theta(-p^2) \Theta(\pm p_0 \pm E_{\vec{k}}) \left(1 - \chi_{[-p_0/2 - \sqrt{\Delta}, -p_0/2 + \sqrt{\Delta}]}(E_{\vec{k}}) \right) \right] \delta(p_0 - E_{\vec{k}} \mp E_{\vec{k}+\vec{p}}), \end{aligned}$$

where we defined

$$\sqrt{\Delta} := \frac{\vec{p}}{2} \sqrt{\frac{p^2 - 4M^2}{p^2}} \quad (\text{D.46})$$

for $p^2 < 0$ or $p^2 > 4M^2$.

Multiplying the above by $\Theta(E_{\vec{k}} - M)$ and further simplification yields

$$\begin{aligned}
& \Theta(E_{\vec{k}} - M) \chi_{[E_{\vec{k}+\vec{p}}^-, E_{\vec{k}+\vec{p}}^+]}(E_{\vec{k}+\vec{p}}) \delta(p_0 - E_{\vec{k}} - E_{\vec{k}+\vec{p}}) \\
&= \Theta(p^2 - 4M^2) \Theta(p_0) \chi_{[p_0/2 - \sqrt{\Delta}, p_0/2 + \sqrt{\Delta}]}(E_{\vec{k}}) \delta(p_0 - E_{\vec{k}} - E_{\vec{k}+\vec{p}}), \\
& \Theta(E_{\vec{k}} - M) \chi_{[E_{\vec{k}+\vec{p}}^-, E_{\vec{k}+\vec{p}}^+]}(E_{\vec{k}+\vec{p}}) \delta(p_0 - E_{\vec{k}} + E_{\vec{k}+\vec{p}}) \\
&= \Theta(p^2 - 4M^2) \Theta(E_{\vec{k}} - (p_0/2 + \sqrt{\Delta})) \delta(p_0 - E_{\vec{k}} + E_{\vec{k}+\vec{p}}), \\
& \Theta(E_{\vec{k}} - M) \chi_{[E_{\vec{k}+\vec{p}}^-, E_{\vec{k}+\vec{p}}^+]}(E_{\vec{k}+\vec{p}}) \delta(p_0 + E_{\vec{k}} - E_{\vec{k}+\vec{p}}) \\
&= \Theta(p^2 - 4M^2) \Theta(E_{\vec{k}} - (-p_0/2 + \sqrt{\Delta})) \delta(p_0 + E_{\vec{k}} - E_{\vec{k}+\vec{p}}), \\
& \Theta(E_{\vec{k}} - M) \chi_{[E_{\vec{k}+\vec{p}}^-, E_{\vec{k}+\vec{p}}^+]}(E_{\vec{k}+\vec{p}}) \delta(p_0 + E_{\vec{k}} + E_{\vec{k}+\vec{p}}) \\
&= \Theta(p^2 - 4M^2) \Theta(-p_0) \chi_{[-p_0/2 - \sqrt{\Delta}, -p_0/2 + \sqrt{\Delta}]}(E_{\vec{k}}) \delta(p_0 + E_{\vec{k}} + E_{\vec{k}+\vec{p}}),
\end{aligned} \tag{D.47}$$

Inserting this in the integral expression and applying the δ -distributions to eliminate the integral over $E_{\vec{k}+\vec{p}}$ shows that the imaginary part is given by

$$\text{Im} \left(iI_2^{+, \text{med}}(p_0, \vec{p}) \right) = \frac{1}{16\pi |\vec{p}|} \Theta(p^2 - 4M^2) \text{sgn}(p_0) \int_{|p_0/2| - \sqrt{\Delta}}^{|p_0/2| + \sqrt{\Delta}} dE_{\vec{k}} \left(n_{\vec{k}} + \bar{n}_{\vec{k}} \right) \tag{D.48}$$

for $p^2 > 0$ and

$$\text{Im} \left(iI_2^{+, \text{med}}(p_0, \vec{p}) \right) = \frac{1}{16\pi |\vec{p}|} \text{sgn}(p_0) \int_{\sqrt{\Delta} - |p_0/2|}^{\sqrt{\Delta} + |p_0/2|} dE_{\vec{k}} \left(n_{\vec{k}} + \bar{n}_{\vec{k}} \right) \tag{D.49}$$

for $p^2 < 0$.

The imaginary part of the medium contribution depends again on $\text{sgn}(p_0)$ as in the case of the vacuum contribution. The above integrals over the Fermi distribution function can even be calculated analytically as the antiderivative of the Fermi distribution is known. This yields [38]

$$\begin{aligned}
\text{Im} \left(iI_2^{+, \text{med}}(p_0, \vec{p}) \right) &= -\frac{T}{16\pi |\vec{p}|} \Theta(p^2 - 4M^2) \text{sgn}(p_0) \times \\
&\times \left[\ln \left(\frac{1 + e^{-\frac{1}{T} \left(|\frac{p_0}{2}| + \sqrt{\Delta} - \mu \right)}}}{1 + e^{-\frac{1}{T} \left(|\frac{p_0}{2}| - \sqrt{\Delta} - \mu \right)}} \right) + \ln \left(\frac{1 + e^{-\frac{1}{T} \left(|\frac{p_0}{2}| + \sqrt{\Delta} + \mu \right)}}}{1 + e^{-\frac{1}{T} \left(|\frac{p_0}{2}| - \sqrt{\Delta} + \mu \right)}} \right) \right]
\end{aligned} \tag{D.50}$$

for $p^2 > 0$ and for $p^2 < 0$ we get

$$\begin{aligned}
\text{Im} \left(iI_2^{+, \text{med}}(p_0, \vec{p}) \right) &= -\frac{T}{16\pi |\vec{p}|} \text{sgn}(p_0) \times \\
&\times \left[\ln \left(\frac{1 + e^{-\frac{1}{T} \left(\sqrt{\Delta} + |\frac{p_0}{2}| - \mu \right)}}}{1 + e^{-\frac{1}{T} \left(\sqrt{\Delta} - |\frac{p_0}{2}| - \mu \right)}} \right) + \ln \left(\frac{1 + e^{-\frac{1}{T} \left(\sqrt{\Delta} + |\frac{p_0}{2}| + \mu \right)}}}{1 + e^{-\frac{1}{T} \left(\sqrt{\Delta} - |\frac{p_0}{2}| + \mu \right)}} \right) \right].
\end{aligned} \tag{D.51}$$

Real Part

The real part of the medium contribution has to be calculated numerically. The most reliable method makes use of the fact that we were able to express the imaginary part analytically and that the imaginary part and the real part are related via a Kramers-Kronig relation [75, 76]:

$$\operatorname{Re} \left(iI_2^{+, \text{med}}(p_0, \vec{p}) \right) = \frac{1}{\pi} \text{PV} \int_{-\infty}^{\infty} d\omega \frac{\operatorname{Im} \left(iI_2^{+, \text{med}}(\omega, \vec{p}) \right)}{\omega - p_0} \quad (\text{D.52})$$

where this is only a one-dimensional integral (rather than three-dimensional), which might have a first-order pole at $\omega = p_0$ depending on whether $iI_2^{\text{med}}(\omega, \vec{p})$ vanishes at $\omega = p_0$ for a given \vec{p} or not. Hence we must evaluate the integral as a principal value integral.

D.4. Medium Version of the Bosonic Integral $iI_2^{(\pi)}(p)$

The bosonic version of the integral $iI_2(p)$ is obtained by replacing the quark mass M with the pion mass m_π and in the medium case the sum over fermionic Matsubara frequencies by a sum over bosonic Matsubara frequencies. The calculation is very similar to the fermionic case but instead of the Fermi distribution function $n_F(z) = 1/(\exp(z/T) + 1)$ the Bose distribution function $n_B(z) = 1/(\exp(z/T) - 1)$ will appear.

For the purposes of this text we will only need the imaginary part, which for the medium part is given by

$$\begin{aligned} \operatorname{Im} \left(iI_2^{(\pi), +, \text{med}}(p_0, \vec{p}) \right) &= -\frac{T}{16\pi |\vec{p}|} \Theta(p^2 - 4m_\pi^2) \operatorname{sgn}(p_0) \times \\ &\times \left[\ln \left(\frac{e^{-\frac{1}{T}(|\frac{p_0}{2}| + \sqrt{\Delta} - \mu)} - 1}{e^{-\frac{1}{T}(|\frac{p_0}{2}| - \sqrt{\Delta} - \mu)} - 1} \right) + \ln \left(\frac{e^{-\frac{1}{T}(|\frac{p_0}{2}| + \sqrt{\Delta} + \mu)} - 1}{e^{-\frac{1}{T}(|\frac{p_0}{2}| - \sqrt{\Delta} + \mu)} - 1} \right) \right] \end{aligned} \quad (\text{D.53})$$

for $p^2 > 0$ and

$$\begin{aligned} \operatorname{Im} \left(iI_2^{(\pi), +, \text{med}}(p_0, \vec{p}) \right) &= -\frac{T}{16\pi |\vec{p}|} \operatorname{sgn}(p_0) \times \\ &\times \left[\ln \left(\frac{e^{-\frac{1}{T}(\sqrt{\Delta} + |\frac{p_0}{2}| - \mu)} - 1}{e^{-\frac{1}{T}(\sqrt{\Delta} - |\frac{p_0}{2}| - \mu)} - 1} \right) + \ln \left(\frac{e^{-\frac{1}{T}(\sqrt{\Delta} + |\frac{p_0}{2}| + \mu)} - 1}{e^{-\frac{1}{T}(\sqrt{\Delta} - |\frac{p_0}{2}| + \mu)} - 1} \right) \right] \end{aligned} \quad (\text{D.54})$$

for $p^2 < 0$. In this context Δ is defined by

$$\sqrt{\Delta} := \frac{\vec{p}}{2} \sqrt{\frac{p^2 - 4m_\pi^2}{p^2}} \quad (\text{D.55})$$

for $p^2 < 0$ or $p^2 > 4m_\pi^2$. The μ in the above integral is the chemical potential for the pion and we will only consider $\mu = 0$. The vacuum contribution is identical to the fermionic case with an appropriate replacement of masses.

E. Quark Triangles and Boxes

E.1. Calculation of the Quark Triangle

Our goal is to write the general quark triangle

$$i\Delta_{p,q} = i \int \frac{d^4k}{(2\pi)^4} \text{tr}(S(-k)S(k+p)S(k+q)) \quad (\text{E.1})$$

as a function of elementary integrals. First, we evaluate the trace over Dirac space. A straightforward calculation using

$$\begin{aligned} \text{tr}(\not{a}) &= 0, \\ \text{tr}(\not{a}\not{b}) &= 4a \cdot b, \\ \text{tr}(\not{a}\not{b}\not{c}) &= 0 \end{aligned} \quad (\text{E.2})$$

shows that

$$\text{tr}(S(a)S(b)S(c)) = \frac{4M(a \cdot b + a \cdot c + b \cdot c) + 4M^3}{(a^2 - M^2 + i\varepsilon)(b^2 - M^2 + i\varepsilon)(c^2 - M^2 + i\varepsilon)}. \quad (\text{E.3})$$

Setting $a = -k$, $b = k + p$ and $c = k + q$ and simplifying yields

$$\begin{aligned} &\text{tr}(S(-k)S(k+p)S(k+q)) \\ &= \frac{4M(M^2 - k^2 + p \cdot q)}{(k^2 - M^2 + i\varepsilon)((k+p)^2 - M^2 + i\varepsilon)((k+q)^2 - M^2 + i\varepsilon)}. \end{aligned} \quad (\text{E.4})$$

Hence

$$\begin{aligned} i\Delta_{p,q} &= -4Mi \int \frac{d^4k}{(2\pi)^4} \frac{1}{((k+p)^2 - M^2 + i\varepsilon)((k+q)^2 - M^2 + i\varepsilon)} \\ &\quad + 4M(p \cdot q)i \int \frac{d^4k}{(2\pi)^4} \frac{1}{(k^2 - M^2 + i\varepsilon)((k+p)^2 - M^2 + i\varepsilon)((k+q)^2 - M^2 + i\varepsilon)} \end{aligned} \quad (\text{E.5})$$

and substituting $k \mapsto k - q$ in the first integral gives

$$i\Delta_{p,q} = -4MiI_2(p-q) + 4M(p \cdot q)iI_3(p,q). \quad (\text{E.6})$$

E.2. Calculation of the Quark Triangle in the Static Limit

We will derive simple expressions for $i\Delta_{p,p}$ and $i\Delta_{p,-p}$ in terms of the integrals (4.22). We have

$$i\Delta_{p,p} = -4MiI_2(p-p) + 4Mp^2iI_3(p,p), \quad (\text{E.7})$$

where $iI_2(\cdot) = iI(\cdot)$ and

$$iI_3(p,p) = i \int \frac{d^4k}{(2\pi)^4} \frac{1}{(k^2 - M^2 + i\varepsilon)} \frac{1}{((k+p)^2 - M^2 + i\varepsilon)^2}. \quad (\text{E.8})$$

By making the substitution $k \mapsto -k - p$ we see that

$$iI_3(p,p) = i \int \frac{d^4k}{(2\pi)^4} \frac{1}{((k+p)^2 - M^2 + i\varepsilon)} \frac{1}{(k^2 - M^2 + i\varepsilon)^2} = iK(p) \quad (\text{E.9})$$

and hence

$$i\Delta_{p,p} = -4M \left(iI(0) - p^2 iK(p) \right). \quad (\text{E.10})$$

To calculate $i\Delta_{p,-p}$ we turn directly to the definition of $i\Delta_{p,q}$ and equation (E.4) to get

$$i\Delta_{p,-p} = -4Mi \int \frac{d^3k}{(2\pi)^3} \frac{k^2 + p^2 - M^2}{(k^2 - M^2 + i\varepsilon) ((k+p)^2 - M^2 + i\varepsilon) ((k-p)^2 - M^2 + i\varepsilon)} \quad (\text{E.11})$$

Obviously the integral

$$i \int \frac{d^3k}{(2\pi)^3} \frac{k \cdot p}{(k^2 - M^2 + i\varepsilon) ((k+p)^2 - M^2 + i\varepsilon) ((k-p)^2 - M^2 + i\varepsilon)} \quad (\text{E.12})$$

vanishes since the integrand is an odd function of k and hence

$$\begin{aligned} i\Delta_{p,-p} &= -4Mi \int \frac{d^3k}{(2\pi)^3} \frac{(k-p)^2 - M^2}{(k^2 - M^2 + i\varepsilon) ((k+p)^2 - M^2 + i\varepsilon) ((k-p)^2 - M^2 + i\varepsilon)} \\ &= -4Mi \int \frac{d^3k}{(2\pi)^3} \frac{1}{(k^2 - M^2 + i\varepsilon)} \frac{1}{((k+p)^2 - M^2 + i\varepsilon)} \\ &= -4MiI(p). \end{aligned} \quad (\text{E.13})$$

E.3. Calculation of the Quark Box

We want to calculate the expression

$$i\Box_{p,q,r} = i \int \frac{d^4k}{(2\pi)^4} \text{tr} (S(p+k)S(-p+q-k)S(-r+k)S(-k)). \quad (\text{E.14})$$

First we calculate

$$\begin{aligned} \text{tr}(S(a)S(b)S(c)S(d)) &= \frac{1}{(a^2 - M^2 + i\varepsilon)(b^2 - M^2 + i\varepsilon)(c^2 - M^2 + i\varepsilon)(d^2 - M^2 + i\varepsilon)} \times \\ &\times [4((a \cdot b)(c \cdot d) - (a \cdot c)(b \cdot d) + (a \cdot d)(b \cdot c) \\ &\quad + M^2(a \cdot b + a \cdot c + a \cdot d + b \cdot c + b \cdot d + c \cdot d) + M^4)] \end{aligned} \quad (\text{E.15})$$

for arbitrary four-vectors a , b , c and d (analogously to the calculation in Appendix E.1), where we used

$$\text{tr}(\not{a}\not{b}\not{c}\not{d}) = 4((a \cdot b)(c \cdot d) - (a \cdot c)(b \cdot d) + (a \cdot d)(b \cdot c)). \quad (\text{E.16})$$

We will soon insert $a = p + k$, $b = -p + q - k$, $c = -r + k$ and $d = -k$. In view of these replacements let us write

$$\begin{aligned} 2(a \cdot b) &= +(a + b)^2 - a^2 - b^2, \\ 2(a \cdot c) &= -(a - c)^2 + a^2 + c^2, \\ 2(a \cdot d) &= +(a + d)^2 - a^2 - d^2, \\ 2(b \cdot c) &= +(b + c)^2 - b^2 - c^2, \\ 2(b \cdot d) &= -(b - d)^2 + b^2 + d^2, \\ 2(c \cdot d) &= +(c + d)^2 - c^2 - d^2. \end{aligned} \quad (\text{E.17})$$

Then we write

$$a^2 = (a^2 - M^2) + M^2 \quad (\text{E.18})$$

and analogously for b , c and d . After straightforwardly cleaning up, the numerator of (E.15) reads

$$\begin{aligned} &(a + b)^2(c + d)^2 - (a - c)^2(b - d)^2 + (a + d)^2(b + c)^2 \\ &- (a + b)^2(c^2 - M^2) - (a + b)^2(d^2 - M^2) - (c + d)^2(a^2 - M^2) - (c + d)^2(b^2 - M^2) \\ &+ (a - c)^2(b^2 - M^2) + (a - c)^2(d^2 - M^2) + (b - d)^2(a^2 - M^2) + (b - d)^2(c^2 - M^2) \\ &- (a + d)^2(b^2 - M^2) - (a + d)^2(c^2 - M^2) - (b + c)^2(a^2 - M^2) - (b + c)^2(d^2 - M^2) \\ &+ 2(a^2 - M^2)(c^2 - M^2) + 2(b^2 - M^2)(d^2 - M^2). \end{aligned} \quad (\text{E.19})$$

We now insert p , q , l and k and express the integral via the elementary integrals iI_2 , iI_3 and iI_4 by cancelling terms $a^2 - M^2, \dots$ in the numerator against the corresponding

terms in the denominator. The following terms appear:

$$\begin{aligned}
a + b &= q, \\
a - c &= p + r, \\
a + d &= p, \\
b + c &= -p + q - r, \\
b - d &= -p + q, \\
c + d &= -r.
\end{aligned} \tag{E.20}$$

This gives for the quark box

$$\begin{aligned}
i\Box_{p,q,r} &= \left(q^2 r^2 - (p+r)^2 (-p+q)^2 + p^2 (-p+q-r)^2 \right) iI_4(p, p-q, -r) \\
&+ \left(-r^2 + (-p+q)^2 - (-p+q-r)^2 \right) iI_3(p-q, -r) \\
&+ \left(-r^2 + (p+r)^2 - p^2 \right) iI_3(p, -r) + \left(-q^2 + (-p+q)^2 - p^2 \right) iI_3(p, p-q) \\
&+ \left(-q^2 + (p+r)^2 - (-p+q-r)^2 \right) iI_3(q, r+p) \\
&+ 2iI_2(p-q) + 2iI_2(p+r),
\end{aligned} \tag{E.21}$$

which we further simplify to

$$\begin{aligned}
i\Box_{p,q,r} &= 2 \left[2(r \cdot p)(p \cdot q) - (r \cdot p)q^2 + r^2(p \cdot q) - (r \cdot q)p^2 \right] iI_4(p, q, r+p) \\
&- 2r \cdot (p-q+r) iI_3(q-p, r) + 2p \cdot r iI_3(p, -r) \\
&- 2p \cdot q iI_3(p, q) + 2q \cdot (p+r-q) iI_3(q, r+p) \\
&+ 2iI_2(p-q) + 2iI_2(p+r).
\end{aligned} \tag{E.22}$$

E.4. Calculation of the Quark Box in the Static Limit

We will calculate the quark boxes in the static limit, i.e. $i\Box_{p,p,p}$ and $i\Box_{p,p,-p}$. Let us begin with the latter one. We can directly insert the momenta into the expression we obtained in Section E.3 and get

$$\begin{aligned}
i\Box_{p,p,-p} &= 2 \left[2(-p \cdot p)(p \cdot p) - (-p \cdot p)p^2 + (-p)^2(p \cdot p) - (-p \cdot p)p^2 \right] iI_4(p, p, -p+p) \\
&- 2(-p) \cdot (p-p-p) iI_3(p-p, -p) + 2p \cdot (-p) iI_3(p, p) \\
&- 2p \cdot p iI_3(p, p) + 2p \cdot (p-p-p) iI_3(p, -p+p) \\
&+ 2iI_2(p-p) + 2iI_2(p-p) \\
&= 2p^4 iI_4(p, p, 0) - 2p^2 iI_3(0, -p) - 2p^2 iI_3(p, p) \\
&- 2p^2 iI_3(p, p) - 2p^2 iI_3(p, 0) + 4iI_2(0) \\
&= 2p^4 iL(p) - 8p^2 iK(p) + 4iI(0).
\end{aligned} \tag{E.23}$$

For $i\Box_{p,p,p}$ it is more convenient to begin with the definition of the quark box (see (4.34)). We have

$$i\Box_{p,p,p} = i \int \frac{d^4k}{(2\pi)^4} \text{tr} (S(p+k)S(-k)S(-p+k)S(-k)). \quad (\text{E.24})$$

A straightforward application of the trace rules in Dirac space yields

$$i\Box_{p,p,p} = i \int \frac{d^4k}{(2\pi)^4} 4 \left(M^4 - 2M^2k^2 + k^4 - 2(p \cdot k)^2 - M^2p^2 + k^2p^2 \right) \times \\ \times \frac{1}{((-p+k)^2 - M^2 + i\varepsilon)(k^2 - M^2 + i\varepsilon)(k^2 - M^2 + i\varepsilon)((p+k)^2 - M^2 + i\varepsilon)}. \quad (\text{E.25})$$

The numerator can be written as

$$\left((-p+k)^2 - M^2 \right) (k^2 - M^2) + 2(p \cdot k)k^2 - 2(p \cdot k)M^2 - 2(p \cdot k)^2 \quad (\text{E.26})$$

and hence

$$i\Box_{p,p,p} = 4iI(p) + 8i \int \frac{d^4k}{(2\pi)^4} \left((p \cdot k)k^2 - (p \cdot k)M^2 - (p \cdot k)^2 \right) \times \\ \times \frac{1}{((-p+k)^2 - M^2 + i\varepsilon)(k^2 - M^2 + i\varepsilon)(k^2 - M^2 + i\varepsilon)((p+k)^2 - M^2 + i\varepsilon)}. \quad (\text{E.27})$$

Due to the invariance of the denominator under $k \mapsto -k$ we can add or subtract any odd function of k in the numerator of the second integral and hence this integral can be written as

$$4i \int \frac{d^4k}{(2\pi)^4} \frac{(p \cdot k)(M^2 - (p+k)^2)}{((-p+k)^2 - M^2 + i\varepsilon)(k^2 - M^2 + i\varepsilon)(k^2 - M^2 + i\varepsilon)((p+k)^2 - M^2 + i\varepsilon)} \\ = -4i \int \frac{d^4k}{(2\pi)^4} \frac{(p \cdot k)}{((-p+k)^2 - M^2 + i\varepsilon)(k^2 - M^2 + i\varepsilon)(k^2 - M^2 + i\varepsilon)} \\ = 4i \int \frac{d^4k}{(2\pi)^4} \frac{(p \cdot k)}{((p+k)^2 - M^2 + i\varepsilon)(k^2 - M^2 + i\varepsilon)(k^2 - M^2 + i\varepsilon)} \\ = 2i \int \frac{d^4k}{(2\pi)^4} \frac{(p+k)^2 - k^2 - p^2 + M^2 - M^2}{((p+k)^2 - M^2 + i\varepsilon)(k^2 - M^2 + i\varepsilon)(k^2 - M^2 + i\varepsilon)} \\ = -2p^2iK(p) + 2iI(0) - 2iI(p). \quad (\text{E.28})$$

Consequently,

$$i\Box_{p,p,p} = -2p^2iK(p) + 2iI(0) + 2iI(p). \quad (\text{E.29})$$

F. Quantities in the Extended NJL Model

F.1. Polarisation Loops

The polarisation functions $J_\sigma(p)$ and $J_\pi^{ab}(p)$ were calculated in Appendix B.1.

The ρ -Meson Polarisation Loop

We begin by calculating the polarisation for the ρ meson:

$$\begin{aligned}
J_\rho^{\mu\nu,ab}(p) &= i \int \frac{d^4k}{(2\pi)^4} \text{Tr} \left(\gamma^\mu \tau^a S(k+p) \gamma^\nu \tau^b S(k) \right) \\
&= \delta_{ab} N_c N_f i \int \frac{d^4k}{(2\pi)^4} \text{tr} \left(\gamma^\mu \frac{\not{k} + \not{p} + M}{(k+p)^2 - M^2 + i\varepsilon} \gamma^\nu \frac{\not{k} + M}{k^2 - M^2 + i\varepsilon} \right) \\
&= 4N_f N_c \delta_{ab} i \int \frac{d^4k}{(2\pi)^4} \frac{(k^\mu + p^\mu)k^\nu - \eta^{\mu\nu}(k+p) \cdot k + (k^\nu + p^\nu)k^\mu + \eta^{\mu\nu}M^2}{(k^2 - M^2 + i\varepsilon)((k+p)^2 - M^2 + i\varepsilon)}
\end{aligned} \tag{F.1}$$

The tensor structure of $J_\rho^{\mu\nu,ab}(p)$ is in general given by

$$J_\rho^{\mu\nu,ab}(p) = \delta_{ab} \left(T^{\mu\nu}(p) J_\rho^{\text{trans}}(p^2) + L^{\mu\nu}(p) J_\rho^{\text{long}}(p^2) \right), \tag{F.2}$$

where $T^{\mu\nu}$ and $L^{\mu\nu}$ are the transversal and longitudinal projectors introduced in Section 5.1. $J_\rho^{\text{trans}}(p^2)$ and $J_\rho^{\text{long}}(p^2)$ can be obtained via

$$\begin{aligned}
\delta_{ab} J_\rho^{\text{trans}}(p^2) &= \frac{1}{3} T_{\mu\nu} J_\rho^{\mu\nu,ab}(p), \\
\delta_{ab} J_\rho^{\text{long}}(p^2) &= L_{\mu\nu} J_\rho^{\mu\nu,ab}(p).
\end{aligned} \tag{F.3}$$

The longitudinal part vanishes:

$$\begin{aligned}
p_\mu J_\rho^{\mu\nu,ab}(p) &\sim \int \frac{d^4k}{(2\pi)^4} \frac{p \cdot (k+p)k^\nu - p^\nu(k+p) \cdot k + (k^\nu + p^\nu)p \cdot k + p^\nu M^2}{(k^2 - M^2 + i\varepsilon)((k+p)^2 - M^2 + i\varepsilon)} \\
&= \int \frac{d^4k}{(2\pi)^4} \frac{(p+k)^2 k^\nu - k^2(k^\nu + p^\nu) + p^\nu M^2}{(k^2 - M^2 + i\varepsilon)((k+p)^2 - M^2 + i\varepsilon)}
\end{aligned} \tag{F.4}$$

Substituting $k \mapsto -k - p$ for the second term in the numerator (the denominator is invariant under that substitution) yields

$$p_\mu J_\rho^{\mu\nu,ab}(p) \sim \int \frac{d^4k}{(2\pi)^4} \frac{2(p+k)^2 k^\nu + p^\nu M^2}{(k^2 - M^2 + i\varepsilon)((k+p)^2 - M^2 + i\varepsilon)}. \tag{F.5}$$

In addition one shows that the term $p^\nu M^2 = (p^\nu + k^\nu)M^2 - k^\nu M^2$ can be replaced by $-2k^\nu M^2$ and hence

$$\begin{aligned} p_\mu J_\rho^{\mu\nu,ab}(p) &\sim \int \frac{d^4k}{(2\pi)^4} \frac{2(p+k)^2 k^\nu - 2k^\nu M^2}{(k^2 - M^2 + i\varepsilon)((k+p)^2 - M^2 + i\varepsilon)} \\ &= \int \frac{d^4k}{(2\pi)^4} \frac{2k^\nu}{k^2 - M^2 + i\varepsilon} = 0 \end{aligned} \quad (\text{F.6})$$

due to symmetry. Since $p_\mu J_\rho^{\mu\nu,ab}(p) = 0$ we also have $L_{\mu\nu} J_\rho^{\mu\nu,ab}(p) = 0$ and hence $J_\rho^{\mu\nu,ab}(p)$ is purely transversal, i.e.

$$J_\rho^{\mu\nu,ab}(p) = \delta_{ab} T^{\mu\nu}(p) J_\rho(p^2) \quad (\text{F.7})$$

with $J_\rho(p^2) := J_\rho^{\text{trans}}(p^2)$. Next, we calculate the transversal part

$$J_\rho(p^2) = J_\rho^{\text{trans}}(p^2) = \frac{1}{3} T_{\mu\nu} J_\rho^{\mu\nu,ab}(p) = \frac{1}{3} \eta_{\mu\nu} J_\rho^{\mu\nu,ab}(p). \quad (\text{F.8})$$

One gets

$$\begin{aligned} J_\rho(p^2) &= \frac{4}{3} N_c N_f i \int \frac{d^4k}{(2\pi)^4} \frac{k^2 + p \cdot k - 4(k^2 + k \cdot p) + k^2 + p \cdot k + 4M^2}{(k^2 - M^2 + i\varepsilon)((k+p)^2 - M^2 + i\varepsilon)} \\ &= \frac{4}{3} N_c N_f i \int \frac{d^4k}{(2\pi)^4} \frac{-2k^2 - 2k \cdot p + 4M^2}{(k^2 - M^2 + i\varepsilon)((k+p)^2 - M^2 + i\varepsilon)}. \end{aligned} \quad (\text{F.9})$$

As in Appendix B.1 we can replace $2k \cdot p$ by $-p^2$ in the numerator and hence

$$\begin{aligned} J_\rho(p^2) &= \frac{4}{3} N_c N_f i \int \frac{d^4k}{(2\pi)^4} \frac{-2k^2 + p^2 + 4M^2}{(k^2 - M^2 + i\varepsilon)((k+p)^2 - M^2 + i\varepsilon)} \\ &= \frac{4}{3} N_c N_f i \int \frac{d^4k}{(2\pi)^4} \frac{-2(k^2 - M^2) + p^2 + 2M^2}{(k^2 - M^2 + i\varepsilon)((k+p)^2 - M^2 + i\varepsilon)} \\ &= \frac{4}{3} N_c N_f \left(-2iI_1 + (p^2 + 2M^2) iI_2(p^2) \right). \end{aligned} \quad (\text{F.10})$$

The a_1 -Meson Polarisation Loop

We calculate the polarisation loop

$$\begin{aligned} J_{a_1}^{\mu\nu,ab}(p) &= i \int \frac{d^4k}{(2\pi)^4} \text{Tr} \left(\gamma^\mu \gamma_5 \tau^a S(k+p) \gamma^\nu \gamma_5 \tau^b S(k) \right) \\ &= \delta_{ab} N_c N_f i \int \frac{d^4k}{(2\pi)^4} \text{tr} \left(\gamma^\mu \frac{\not{k} + \not{p} - M}{(k+p)^2 - M^2 + i\varepsilon} \gamma^\nu \frac{\not{k} + M}{k^2 - M^2 + i\varepsilon} \right) \\ &= 4N_f N_c \delta_{ab} i \int \frac{d^4k}{(2\pi)^4} \frac{(k^\mu + p^\mu)k^\nu - \eta^{\mu\nu}(k+p) \cdot k + (k^\nu + p^\nu)k^\mu - \eta^{\mu\nu}M^2}{(k^2 - M^2 + i\varepsilon)((k+p)^2 - M^2 + i\varepsilon)}. \end{aligned} \quad (\text{F.11})$$

The above expression only differs from $J_{\rho}^{\mu\nu,ab}(p)$ by the sign in front of the $\eta^{\mu\nu}M$ and hence the results are easily derived from those we obtained for $J_{\rho}^{\mu\nu,ab}(p)$. Writing

$$J_{a_1}^{\mu\nu,ab}(p) = \delta_{ab} \left(T^{\mu\nu}(p) J_{a_1}^{\text{trans}}(p^2) + L^{\mu\nu}(p) J_{a_1}^{\text{long}}(p^2) \right) \quad (\text{F.12})$$

we get

$$\begin{aligned} J_{a_1}^{\text{trans}}(p^2) &= \frac{4}{3} N_c N_f \left(-2iI_1 + (p^2 - 4M^2) iI_2(p^2) \right), \\ J_{a_1}^{\text{long}}(p^2) &= -8N_c N_f M^2 I_2(p^2). \end{aligned} \quad (\text{F.13})$$

Mixed Polarisation Loops

We calculate the polarisation loops $J_{M,N}(p)$ with $M \neq N$. All combinations of σ with another channel vanish because a trace over τ^a is to be taken, i.e.

$$J_{\sigma,\pi}^a = J_{\pi,\sigma}^a = J_{\sigma,\rho}^{\mu,a} = J_{\rho,\sigma}^{\mu,a} = J_{\sigma,a_1}^{\mu,a} = J_{a_1,\sigma}^{\mu,a} = 0. \quad (\text{F.14})$$

In the following we show that

$$J_{\pi,\rho}^{\mu,ab} = J_{\rho,\pi}^{\mu,ab} = J_{\rho,a_1}^{\mu\nu,ab} = J_{a_1,\rho}^{\mu\nu,ab} = 0. \quad (\text{F.15})$$

We have

$$J_{\pi,\rho}^{\mu,ab}(p) = i \int \frac{d^3k}{(2\pi)^3} \text{Tr} \left(\gamma^\mu S(k+p) \gamma_5 S(k) \right) = 0 \quad (\text{F.16})$$

since the trace over Dirac space contains only terms with one γ_5 and one, two or three γ^μ matrices and the trace over such combinations is always zero. Analogously $J_{\rho,\pi}^{\mu,ab}(p) = 0$. Next, we consider

$$J_{\rho,a_1}^{\mu\nu,ab}(p) = i \int \frac{d^3k}{(2\pi)^3} \text{Tr} \left(\gamma^\mu \tau^a S(k+p) \gamma^\nu \gamma_5 \tau^b S(k) \right). \quad (\text{F.17})$$

Only the term with γ_5 and four γ^μ matrices has a non-zero trace. We get

$$\begin{aligned} J_{\rho,a_1}^{\mu\nu,ab}(p) &= 4N_c N_f \delta_{ab} i \frac{(k_\alpha + p_\alpha) k_\beta 4i \varepsilon^{\mu\alpha\nu\beta}}{(k^2 - M^2 + i\varepsilon)((k+p)^2 - M^2 + i\varepsilon)} \\ &= 4N_c N_f \delta_{ab} i \frac{p_\alpha k_\beta 4i \varepsilon^{\mu\alpha\nu\beta}}{(k^2 - M^2 + i\varepsilon)((k+p)^2 - M^2 + i\varepsilon)}, \end{aligned} \quad (\text{F.18})$$

where we used the antisymmetry of $\varepsilon^{\mu\alpha\nu\beta}$. Making the substitution $k \mapsto -k - p$ and again making use of the antisymmetry of the ε -tensor we see that

$$J_{\rho,a_1}^{\mu\nu,ab}(p) = -4N_c N_f \delta_{ab} i \frac{p_\alpha k_\beta 4i \varepsilon^{\mu\alpha\nu\beta}}{(k^2 - M^2 + i\varepsilon)((k+p)^2 - M^2 + i\varepsilon)} \quad (\text{F.19})$$

and hence

$$J_{\rho,a_1}^{\mu\nu,ab}(p) = 0. \quad (\text{F.20})$$

Analogously $J_{a_1, \rho}^{\mu\nu, ab}(p) = 0$.

The only off-diagonal terms that do not vanish are $J_{\pi, a_1}^{\mu, ab}(p)$ and $J_{a_1, \pi}^{\mu, ab}(p)$. One calculates

$$\begin{aligned}
J_{\pi, a_1}^{\mu, ab}(p) &= i \int \frac{d^3k}{(2\pi)^3} \text{Tr} \left(i\gamma_5 \tau^a S(k+p) \gamma^\mu \gamma_5 \tau^b S(k) \right) \\
&= iN_c N_f \delta_{ab} i \int \frac{d^4k}{(2\pi)^4} \text{tr} (S(k+p) \gamma^\mu S(-k)) \\
&= 4iN_c N_f \delta_{ab} i \frac{4(p^\mu + k^\mu)M - 4k^\mu M}{(k^2 - M^2 + i\varepsilon)((k+p)^2 - M^2 + i\varepsilon)} \\
&= 4iN_c N_f \delta_{ab} M p^\mu iI_2(p^2).
\end{aligned} \tag{F.21}$$

Analogously $J_{a_1, \pi}^{\mu, ab}(p) = -4iN_c N_f \delta_{ab} M p^\mu iI_2(p^2)$. We again separate off the tensor structure (here given by p^μ) and write

$$J_{\pi, a_1}^{\mu, ab}(p) = \delta_{ab} \frac{p^\mu}{\sqrt{p^2}} J_{\pi, a_1}(p^2) \tag{F.22}$$

with

$$J_{\pi, a_1}(p^2) = i4N_c N_f M \sqrt{p^2} iI_2(p^2) \tag{F.23}$$

and

$$J_{a_1, \pi}^{\mu, ab}(p) = \delta_{ab} \frac{p^\mu}{\sqrt{p^2}} J_{a_1, \pi}(p^2) \tag{F.24}$$

with

$$J_{a_1, \pi}(p^2) = -i4N_c N_f M \sqrt{p^2} iI_2(p^2). \tag{F.25}$$

F.2. Meson Propagators

The σ -meson channel decouples from the other channels and hence the σ -meson propagator is identical to the one in the simple model (2.66).

The ρ -Meson Propagator

Since the ρ -channel decouples from all the other channels, it can be treated independently. The Bethe-Salpeter equation (see (2.53)) for the ρ -meson is

$$D_\rho^{\mu\nu, ab}(p) = 2g_v \delta_{ab} \eta^{\mu\nu} - 2g_v J_\rho^{ac, \mu\lambda}(p) D_\rho^{cb, \nu\lambda}(p). \tag{F.26}$$

We plug in the purely transversal ρ -meson polarisation loop

$$J_\rho^{\mu\nu, ab}(p) = \delta_{ab} T^{\mu\nu}(p) J_\rho(p^2) \tag{F.27}$$

and see that the isospin structure of $D_\rho^{\mu\nu, ab}(p)$ must also be given by δ_{ab} . We can hence write the ρ -meson propagator in general as

$$D_\rho^{\mu\nu, ab}(p) =: \delta_{ab} \left(D_\rho^{\text{trans}}(p^2) T^{\mu\nu}(p) + D_\rho^{\text{long}}(p^2) L^{\mu\nu}(p) \right). \tag{F.28}$$

Inserting this into the above Bethe-Salpeter equation gives

$$\begin{aligned}
& D_\rho^{\text{trans}}(p^2)T^{\mu\nu}(p) + D_\rho^{\text{long}}(p^2)L^{\mu\nu}(p) \\
&= 2g_v(T^{\mu\nu}(p) + L^{\mu\nu}(p)) - 2g_v T^{\mu\lambda}(p)J_\rho(p^2) \left(D_\rho^{\text{trans}}(p^2)T_\lambda^\nu(p) + D_\rho^{\text{long}}(p^2)L_\lambda^\nu(p) \right) \\
&= \left(2g_v - 2g_v J_\rho(p^2)D_\rho^{\text{trans}}(p^2) \right) T^{\mu\nu}(p) + 2g_v L^{\mu\nu}(p).
\end{aligned} \tag{F.29}$$

This yields the solution

$$D_\rho^{\text{trans}}(p^2) = \frac{2g_v}{1 + 2g_v J_\rho(p^2)} \tag{F.30}$$

and

$$D_\rho^{\text{long}}(p^2) = 2g_v. \tag{F.31}$$

The a_1 -Meson and the Pion Propagator

We want to study the propagators of the pion and the a_1 -meson. They have to be treated together since they are coupled. The Bethe-Salpeter equation for the different propagators reads

$$\begin{aligned}
D_\pi^{ab}(p) &= -2g_s\delta_{ab} + 2g_s J_\pi^{ac}(p)D_\pi^{cb}(p) + 2g_s J_{\pi,a_1}^{ac}(p)D_{a_1,\pi}^{\lambda,ac}(p), \\
D_{\pi,a_1}^{\mu,ab}(p) &= 2g_s J_\pi^{ac}(p)D_{\pi,a_1}^{\mu,cb}(p) + 2g_s J_{\pi,a_1}^{ac}(p)D_{a_1}^{\lambda,\mu,cb}(p), \\
D_{a_1,\pi}^{\mu,ab}(p) &= -2g_v J_{a_1,\pi}^{\mu,ac}(p)D_\pi^{cb}(p) - 2g_v J_{a_1}^{ac,\mu}(p)D_{a_1,\pi}^{\lambda,cb}(p), \\
D_{a_1}^{ab,\mu\nu}(p) &= 2g_v \eta^{\mu\nu} \delta_{ab} - 2g_v J_{a_1\pi}^{\mu,ac}(p)D_{\pi,a_1}^{\nu,cb}(p) - 2g_v J_{a_1}^{ac,\mu}(p)D_{a_1}^{\lambda\nu,cb}(p).
\end{aligned} \tag{F.32}$$

Since all the polarisation functions have a Kronecker delta in isospin space, the same is true for the propagators. We write the propagators in general as

$$\begin{aligned}
D_\pi^{ab}(p) &=: \delta_{ab} D_\pi(p^2), \\
D_{\pi,a_1}^{\mu,ab}(p) &=: \delta_{ab} \frac{p^\mu}{\sqrt{p^2}} D_{\pi,a_1}(p^2), \\
D_{a_1,\pi}^{\mu,ab}(p) &=: \delta_{ab} \frac{p^\mu}{\sqrt{p^2}} D_{a_1,\pi}(p^2), \\
D_{a_1}^{ab,\mu\nu}(p) &=: \delta_{ab} \left(D_{a_1}^{\text{trans}}(p^2)T^{\mu\nu}(p) + D_{a_1}^{\text{long}}(p^2)L^{\mu\nu}(p) \right)
\end{aligned} \tag{F.33}$$

and plug in these expressions into the above equations together with the parametrisation of the polarisation loops from the above section. Using the rules for the transverse and longitudinal projectors similar to the considerations for the rho-meson propagator yields the equations

$$\begin{aligned}
D_\pi(p^2) &= -2g_s + 2g_s J_\pi(p^2)D_\pi(p^2) + 2g_s J_{\pi,a_1}(p^2)D_{a_1,\pi}(p^2), \\
D_{\pi,a_1}(p^2) &= 2g_s J_\pi(p^2)D_{\pi,a_1}(p^2) + 2g_s J_{\pi,a_1}(p^2)D_{a_1}^{\text{long}}(p^2), \\
D_{a_1,\pi}(p^2) &= -2g_v J_{a_1,\pi}(p^2)D_\pi(p^2) - 2g_v J_{a_1}^{\text{long}}(p^2)D_{a_1,\pi}(p^2), \\
D_{a_1}^{\text{long}}(p^2) &= 2g_v - 2g_v J_{a_1\pi}(p^2)D_{\pi,a_1}(p^2) - 2g_v J_{a_1}^{\text{long}}(p^2)D_{a_1}^{\text{long}}(p^2)
\end{aligned} \tag{F.34}$$

and

$$D_{a_1}^{\text{trans}}(p^2) = 2g_v - 2g_v J_{a_1}^{\text{trans}}(p^2) D_{a_1}^{\text{trans}}(p^2). \quad (\text{F.35})$$

The transversal part of the a_1 -meson propagator decouples and is given by

$$D_{a_1}^{\text{trans}}(p^2) = \frac{2g_v}{1 + 2g_v J_{a_1}(p^2)} \quad (\text{F.36})$$

similar to the transversal part of the ρ -meson propagator. The longitudinal part is coupled to the pion by the above set of four equations. These can be cast into the form

$$\begin{pmatrix} D_\pi & D_{\pi,a_1} \\ D_{a_1,\pi} & D_{a_1}^{\text{long}} \end{pmatrix} = \begin{pmatrix} -2g_s & 0 \\ 0 & 2g_v \end{pmatrix} + \begin{pmatrix} 2g_s & 0 \\ 0 & -2g_v \end{pmatrix} \begin{pmatrix} J_\pi & J_{\pi,a_1} \\ J_{a_1,\pi} & J_{a_1}^{\text{long}} \end{pmatrix} \begin{pmatrix} D_\pi & D_{\pi,a_1} \\ D_{a_1,\pi} & D_{a_1}^{\text{long}} \end{pmatrix}. \quad (\text{F.37})$$

Solving this linear system of equations for the matrix containing the D 's yields

$$\begin{aligned} \begin{pmatrix} D_\pi & D_{\pi,a_1} \\ D_{a_1,\pi} & D_{a_1}^{\text{long}} \end{pmatrix} &= \left(\begin{pmatrix} 1 & 0 \\ 0 & 1 \end{pmatrix} - \begin{pmatrix} 2g_s & 0 \\ 0 & -2g_v \end{pmatrix} \begin{pmatrix} J_\pi & J_{\pi,a_1} \\ J_{a_1,\pi} & J_{a_1}^{\text{long}} \end{pmatrix} \right)^{-1} \begin{pmatrix} -2g_s & 0 \\ 0 & 2g_v \end{pmatrix} \\ &= \begin{pmatrix} 1 - 2g_s J_\pi & -2g_s J_{\pi,a_1} \\ 2g_v J_{a_1,\pi} & 1 + 2g_v J_{a_1}^{\text{long}} \end{pmatrix}^{-1} \begin{pmatrix} -2g_s & 0 \\ 0 & 2g_v \end{pmatrix} \\ &= \frac{1}{D} \begin{pmatrix} 1 + 2g_v J_{a_1}^{\text{long}} & 2g_s J_{\pi,a_1} \\ -2g_v J_{a_1,\pi} & 1 - 2g_s J_\pi \end{pmatrix} \begin{pmatrix} -2g_s & 0 \\ 0 & 2g_v \end{pmatrix} \\ &= \frac{1}{D} \begin{pmatrix} -2g_s - 2g_s 2g_v J_{a_1}^{\text{long}} & 2g_s 2g_v J_{\pi,a_1} \\ 2g_s 2g_v J_{a_1,\pi} & 2g_v - 2g_s 2g_v J_\pi \end{pmatrix} \\ &= \frac{1}{D} \left(- \begin{pmatrix} 2g_s & 0 \\ 0 & -2g_v \end{pmatrix} + 2g_s 2g_v \begin{pmatrix} -J_{a_1}^{\text{long}} & J_{\pi,a_1} \\ J_{a_1,\pi} & -J_\pi \end{pmatrix} \right), \end{aligned} \quad (\text{F.38})$$

where

$$D(p^2) = \left(1 - 2g_s J_\pi(p^2)\right) \left(1 + 2g_v J_{a_1}^{\text{long}}(p^2)\right) + 2g_s 2g_v J_{\pi,a_1}(p^2) J_{a_1,\pi}(p^2) \quad (\text{F.39})$$

is the determinant of the matrix we have to invert.

F.3. Pole Structure of the Pion Propagator

In this section we investigate the pole structure of the scattering matrix T in the pion sector (5.39). Dropping the trivial isospin dependence we write

$$\begin{aligned} T &= -\left(i\gamma_5, \frac{\not{p}}{\sqrt{p^2}}\gamma_5\right) \begin{pmatrix} D_\pi(p^2) & D_{\pi,a_1}(p^2) \\ D_{a_1,\pi} & D_{a_1}^{\text{long}} \end{pmatrix} \begin{pmatrix} i\gamma_5 \\ \frac{\not{p}}{\sqrt{p^2}}\gamma_5 \end{pmatrix} \\ &= -\frac{1}{p^2 - m_\pi^2} \frac{p^2 - m_\pi^2}{D(p^2)} \left(i\gamma_5, \frac{\not{p}}{\sqrt{p^2}}\gamma_5\right) \begin{pmatrix} -2g_s - 2g_s 2g_v J_{a_1}^{\text{long}} & 2g_s 2g_v J_{\pi,a_1} \\ 2g_s 2g_v J_{a_1,\pi} & 2g_v - 2g_s 2g_v J_\pi \end{pmatrix} \begin{pmatrix} i\gamma_5 \\ \frac{\not{p}}{\sqrt{p^2}}\gamma_5 \end{pmatrix}. \end{aligned} \quad (\text{F.40})$$

As a next step we evaluate all terms except for the pole term at $p^2 = m_\pi^2$ (and thus essentially write T in pole approximation). First we calculate

$$\begin{aligned} D'(m_\pi^2) &:= \lim_{p^2 \rightarrow m_\pi^2} \frac{D(p^2)}{p^2 - m_\pi^2} = N_f N_c \left[4g_s \frac{d(p^2 i I_2(p^2))}{d(p^2)} - 16g_v M m \frac{d(i I_2(p^2))}{d(p^2)} \right] \\ &= N_f N_c \left[2g_s \left(i I(0) + i I(m_\pi^2) - m_\pi^2 K(m_\pi^2) \right) \right. \\ &\quad \left. - 8g_v \frac{M m}{m_\pi^2} \left(i I(0) - i I(m_\pi^2) - m_\pi^2 K(m_\pi^2) \right) \right]. \end{aligned} \quad (\text{F.41})$$

Then we evaluate the matrix at $p^2 = m_\pi^2$. It is given by

$$\begin{pmatrix} a & ib \\ -ib & d \end{pmatrix} := \lim_{p^2 \rightarrow m_\pi^2} \begin{pmatrix} -2g_s - 2g_s 2g_v J_{a_1}^{\text{long}} & 2g_s 2g_v J_{\pi, a_1} \\ 2g_s 2g_v J_{a_1, \pi} & 2g_v - 2g_s 2g_v J_\pi \end{pmatrix}, \quad (\text{F.42})$$

where the constants a , b and d take the values

$$\begin{aligned} a &= -2g_s - 4g_s g_v J_{a_1}^{\text{long}}(m_\pi^2) = -2g_s + 32N_c N_f g_s g_v M^2 i I_2(m_\pi^2), \\ d &= 2g_v - 4g_s g_v J_\pi(m_\pi^2) = 2g_v - 8N_c N_f g_s g_v \left(2i I_1 - m_\pi^2 i I_2(m_\pi^2) \right), \\ b &= -i 4g_s g_v J_{\pi, a_1}(m_\pi^2) = 16N_c N_f g_s g_v M m_\pi i I_2(m_\pi^2). \end{aligned} \quad (\text{F.43})$$

The determinant of this matrix vanishes, i.e. $ad - b^2 = 0$, since it is by construction proportional to $D(m_\pi^2) = 0$. Moreover, the matrix is hermitian. Hence it can be unitarily diagonalised with one eigenvalue equal to zero. More precisely we can write

$$\begin{pmatrix} a & ib \\ -ib & d \end{pmatrix} = \begin{pmatrix} \frac{a}{\sqrt{a^2+b^2}} & \frac{d}{\sqrt{b^2+d^2}} \\ \frac{-ib}{\sqrt{a^2+b^2}} & \frac{ib}{\sqrt{b^2+d^2}} \end{pmatrix} \begin{pmatrix} a+d & 0 \\ 0 & 0 \end{pmatrix} \begin{pmatrix} \frac{a}{\sqrt{a^2+b^2}} & \frac{ib}{\sqrt{a^2+b^2}} \\ \frac{d}{\sqrt{b^2+d^2}} & \frac{-ib}{\sqrt{b^2+d^2}} \end{pmatrix} \quad (\text{F.44})$$

and hence

$$\begin{aligned} &(i\gamma_5, \frac{\not{p}}{\sqrt{p^2}}\gamma_5) \begin{pmatrix} a & ib \\ -ib & d \end{pmatrix} \begin{pmatrix} i\gamma_5 \\ \frac{\not{p}}{\sqrt{p^2}}\gamma_5 \end{pmatrix} \\ &= \frac{a+d}{a^2+b^2} \left(ai\gamma_5 - ib \frac{\not{p}}{\sqrt{p^2}}\gamma_5 \right) \otimes \left(ai\gamma_5 + ib \frac{\not{p}}{\sqrt{p^2}}\gamma_5 \right) \\ &= \frac{a+d}{a^2+b^2} \left(ai\gamma_5 - ib \frac{\not{p}}{\sqrt{p^2}}\gamma_5 \right) \otimes \left(ai\gamma_5 - ib \frac{-\not{p}}{\sqrt{p^2}}\gamma_5 \right). \end{aligned} \quad (\text{F.45})$$

Taking the above together we can write T in pole approximation

$$\begin{aligned} T &= -\frac{1}{p^2 - m_\pi^2} \frac{1}{D'(m_\pi^2)} \frac{a+d}{a^2+b^2} \left(ai\gamma_5 - ib \frac{\not{p}}{\sqrt{p^2}}\gamma_5 \right) \otimes \left(ai\gamma_5 - ib \frac{-\not{p}}{\sqrt{p^2}}\gamma_5 \right) \\ &=: -\frac{1}{p^2 - m_\pi^2} \left(g_{ps} i\gamma_5 - i g_{pv} \frac{\not{p}}{\sqrt{p^2}}\gamma_5 \right) \otimes \left(g_{ps} i\gamma_5 - i g_{pv} \frac{-\not{p}}{\sqrt{p^2}}\gamma_5 \right), \end{aligned} \quad (\text{F.46})$$

where we introduced the pseudoscalar and the pseudovector quark-pion couplings g_{ps} and g_{pv} corresponding to the vertices $i\gamma_5$ and $i\cancel{p}/\sqrt{p^2}$ (or $-i\cancel{p}/\sqrt{p^2}$ for outgoing momenta). The coupling strengths are given by

$$g_{\text{ps}}^2 = \frac{a^2(a+d)}{(a^2+b^2)D'(m_\pi^2)} \quad \text{and} \quad g_{\text{pv}}^2 = \frac{b^2(a+d)}{(a^2+b^2)D'(m_\pi^2)}. \quad (\text{F.47})$$

F.4. Calculation of the Quark Triangle

Our goal is to calculate the quark triangle

$$i\Delta_{p,q}^\mu := i \int \frac{d^4k}{(2\pi)^4} \text{tr} (S(-k)S(k+p)\gamma^\mu S(k+q)). \quad (\text{F.48})$$

First we calculate for arbitrary four-vectors a , b and c :

$$\text{tr} (S(a)S(b)\gamma^\mu S(c)) = \text{tr} \left(\frac{\not{a} + M}{a^2 - M^2 + i\varepsilon} \frac{\not{b} + M}{b^2 - M^2 + i\varepsilon} \gamma^\mu \frac{\not{c} + M}{c^2 - M^2 + i\varepsilon} \right). \quad (\text{F.49})$$

We have

$$\begin{aligned} & \text{tr} ((\not{a} + M)(\not{b} + M)\gamma^\mu(\not{c} + M)) \\ &= \text{tr} (a_\lambda \gamma^\lambda + M)(b_\rho \gamma^\rho + M)\gamma^\mu(c_\kappa \gamma^\kappa + M) \\ &= \text{tr} (a_\lambda b_\rho c_\kappa \gamma^\lambda \gamma^\rho \gamma^\mu \gamma^\kappa + a_\lambda b_\rho M \gamma^\lambda \gamma^\rho \gamma^\mu + a_\lambda M c_\kappa \gamma^\lambda \gamma^\mu \gamma^\kappa + M b_\rho c_\kappa \gamma^\rho \gamma^\mu \gamma^\kappa \\ & \quad a_\lambda M^2 \gamma^\lambda \gamma^\mu + M b_\rho M \gamma^\rho \gamma^\mu + M^2 c_\kappa \gamma^\mu \gamma^\kappa + M^3 \gamma^\mu) \\ &= a_\lambda b_\rho c_\kappa 4 (\eta^{\lambda\rho} \eta^{\mu\kappa} - \eta^{\lambda\mu} \eta^{\rho\kappa} + \eta^{\lambda\kappa} \eta^{\rho\mu}) + 4M^2 (a_\lambda \eta^{\lambda\mu} + b_\rho \eta^{\rho\mu} + c_\kappa \eta^{\mu\kappa}) \\ &= 4((a \cdot b)c^\mu - (b \cdot c)a^\mu + (a \cdot c)b^\mu) + 4M^2 (a^\mu + b^\mu + c^\mu). \end{aligned} \quad (\text{F.50})$$

We insert $a = -k$, $b = k + p$ and $c = k + q$ and get

$$\begin{aligned} i\Delta_{p,q}^\mu &= 4i \int \frac{d^4k}{(2\pi)^4} \frac{-k \cdot (k+p)(k^\mu + q^\mu) + (k+p) \cdot (k+q)k^\mu - k \cdot (k+q)(k^\mu + p^\mu) \dots}{(k^2 - M^2 + i\varepsilon)((k+p)^2 - M^2 + i\varepsilon)((k+q)^2 - M^2 + i\varepsilon)} \dots \\ & \quad \dots \frac{+M^2(k^\mu + p^\mu + q^\mu)}{\dots} \\ &= 4i \int \frac{d^4k}{(2\pi)^4} \frac{-(k^2 - M^2)(k^\mu + p^\mu + q^\mu) - (k \cdot p)q^\mu + (p \cdot q)k^\mu - (k \cdot q)p^\mu}{(k^2 - M^2 + i\varepsilon)((k+p)^2 - M^2 + i\varepsilon)((k+q)^2 - M^2 + i\varepsilon)} \\ &= -4i \int \frac{d^4k}{(2\pi)^4} \frac{k^\mu + p^\mu + q^\mu}{((k+p)^2 - M^2 + i\varepsilon)((k+q)^2 - M^2 + i\varepsilon)} \quad \left. \vphantom{\int} \right\} (1) \\ & \quad -4i \int \frac{d^4k}{(2\pi)^4} \frac{(k \cdot p)q^\mu + (k \cdot q)p^\mu}{(k^2 - M^2 + i\varepsilon)((k+p)^2 - M^2 + i\varepsilon)((k+q)^2 - M^2 + i\varepsilon)} \quad \left. \vphantom{\int} \right\} (2) \\ & \quad +4i \int \frac{d^4k}{(2\pi)^4} \frac{(p \cdot q)k^\mu}{(k^2 - M^2 + i\varepsilon)((k+p)^2 - M^2 + i\varepsilon)((k+q)^2 - M^2 + i\varepsilon)} \quad \left. \vphantom{\int} \right\} (3). \end{aligned} \quad (\text{F.51})$$

To calculate (1) we perform the substitution $k \mapsto -k-p-q$ and obtain the same integral with $-k^\mu$ in the numerator of the integrand instead of $k^\mu + p^\mu + q^\mu$ and hence we can write

$$\begin{aligned} (1) &= \frac{(1) + (1)}{2} = 2i \int \frac{d^4k}{(2\pi)^4} \frac{p^\mu + q^\mu}{((k+p)^2 - M^2 + i\varepsilon)((k+q)^2 - M^2 + i\varepsilon)} \\ &= 2(p^\mu + q^\mu)iI_2(p-q) \end{aligned} \quad (\text{F.52})$$

To calculate (2) we write

$$\begin{aligned} &-4i \int \frac{d^4k}{(2\pi)^4} \frac{(k \cdot p)}{(k^2 - M^2 + i\varepsilon)((k+p)^2 - M^2 + i\varepsilon)((k+q)^2 - M^2 + i\varepsilon)} \\ &= -2i \int \frac{d^4k}{(2\pi)^4} \frac{(k+p)^2 - k^2 - p^2}{(k^2 - M^2 + i\varepsilon)((k+p)^2 - M^2 + i\varepsilon)((k+q)^2 - M^2 + i\varepsilon)} \\ &= -2i \int \frac{d^4k}{(2\pi)^4} \frac{(k+p)^2 - M^2 + M^2 - k^2 - p^2}{(k^2 - M^2 + i\varepsilon)((k+p)^2 - M^2 + i\varepsilon)((k+q)^2 - M^2 + i\varepsilon)} \\ &= -2iI_2(q) + 2iI_2(p-q) + 2p^2iI_3(p,q) \end{aligned} \quad (\text{F.53})$$

and analogously for the second term to get

$$\begin{aligned} (2) &= \left(-2iI_2(q) + 2iI_2(p-q) + 2p^2iI_3(p,q)\right) q^\mu \\ &\quad + \left(-2iI_2(p) + 2iI_2(p-q) + 2q^2iI_3(p,q)\right) p^\mu \end{aligned} \quad (\text{F.54})$$

and hence

$$(1) + (2) = \left(-2iI_2(q) + 2p^2iI_3(p,q)\right) q^\mu + \left(-2iI_2(p) + 2q^2iI_3(p,q)\right) p^\mu. \quad (\text{F.55})$$

The calculation of (3) is more difficult due to the k^μ in the integrand. We want to calculate the integral

$$I^\mu := 4i \int \frac{d^4k}{(2\pi)^4} \frac{k^\mu}{(k^2 - M^2 + i\varepsilon)((k+p)^2 - M^2 + i\varepsilon)((k+q)^2 - M^2 + i\varepsilon)} \quad (\text{F.56})$$

(and hence (3) = $(p \cdot q)I^\mu$). We know that I^μ is a Lorentz vector depending on p and q and hence can only be of the form

$$I^\mu = f_1(p^2, p \cdot q, q^2)p^\mu + f_2(p^2, p \cdot q, q^2)q^\mu, \quad (\text{F.57})$$

where f_1 and f_2 are functions depending on all possible Lorentz scalars that can be formed from p and q . Contracting the above equation with p_μ and q_μ yields

$$\begin{aligned} p \cdot I &= p^2 f_1 + (p \cdot q) f_2, \\ q \cdot I &= (p \cdot q) f_1 + q^2 f_2, \end{aligned} \quad (\text{F.58})$$

which we solve for f_1 and f_2 :

$$\begin{aligned} f_1 &= \frac{q^2(p \cdot I) - (p \cdot q)(q \cdot I)}{p^2q^2 - (p \cdot q)^2}, \\ f_2 &= \frac{-(p \cdot q)(p \cdot I) + p^2(q \cdot I)}{p^2q^2 - (p \cdot q)^2}. \end{aligned} \quad (\text{F.59})$$

We saw during the calculation of (2) that

$$\begin{aligned} p \cdot I &= 4i \int \frac{d^4k}{(2\pi)^4} \frac{p \cdot k}{(k^2 - M^2 + i\varepsilon)((k+p)^2 - M^2 + i\varepsilon)((k+q)^2 - M^2 + i\varepsilon)} \\ &= 2iI_2(q) - 2iI_2(p-q) - 2p^2iI_3(p,q) \end{aligned} \quad (\text{F.60})$$

and analogously

$$q \cdot I = 2iI_2(p) - 2iI_2(p-q) - 2q^2iI_3(p,q). \quad (\text{F.61})$$

Hence

$$\begin{aligned} f_1 &= 2i \frac{q^2I_2(q) - q^2I_2(p-q) - p^2q^2I_3(p,q) - (p \cdot q)I_2(p)}{p^2q^2 - (p \cdot q)^2} \dots \\ &\quad + \dots \frac{(p \cdot q)I_2(p-q) + (p \cdot q)q^2I_3(p,q)}{p^2q^2 - (p \cdot q)^2} \end{aligned} \quad (\text{F.62})$$

and

$$\begin{aligned} f_2 &= 2i \frac{p^2I_2(p) - p^2I_2(p-q) - p^2q^2I_3(p,q) - (p \cdot q)I_2(q)}{p^2q^2 - (p \cdot q)^2} \dots \\ &\quad + \dots \frac{(p \cdot q)I_2(p-q) + p^2(p \cdot q)I_3(p,q)}{p^2q^2 - (p \cdot q)^2} \end{aligned} \quad (\text{F.63})$$

Finally, parametrising $i\Delta_{p,q}^\mu$ as

$$i\Delta_{p,q}^\mu = V_1(p^2, p \cdot q, q^2)p^\mu + V_2(p^2, p \cdot q, q^2)q^\mu \quad (\text{F.64})$$

we get

$$\begin{aligned} V_1(p^2, p \cdot q, q^2) &= 2i \left[-I_2(p) + q^2I_3(p,q) + \frac{p \cdot q}{p^2q^2 - (p \cdot q)^2} \left(q^2I_2(q) - q^2I_2(p-q) \right. \right. \\ &\quad \left. \left. - p^2q^2I_3(p,q) - p \cdot qI_2(p) + p \cdot qI_2(p-q) + q^2p \cdot qI_3(p,q) \right) \right], \\ V_2(p^2, p \cdot q, q^2) &= 2i \left[-I_2(q) + p^2I_3(p,q) + \frac{p \cdot q}{p^2q^2 - (p \cdot q)^2} \left(p^2I_2(q) - p^2I_2(p-q) \right. \right. \\ &\quad \left. \left. - p^2q^2I_3(p,q) - p \cdot qI_2(q) + p \cdot qI_2(p-q) + p^2p \cdot qI_3(p,q) \right) \right]. \end{aligned} \quad (\text{F.65})$$

G. Relativistic Hydrodynamics

G.1. Shear Viscosity Estimate

We will give a rough estimate for the shear viscosity of a non-relativistic fluid obtained in kinetic theory [36].

If we go to a comoving frame at x^μ , the fluid will be locally at rest, i.e. the four-velocity will take the form $u^\mu(x) = (1, \vec{0})^t$. A simple calculation shows that the spatial off-diagonal components T^{ij} for $i \neq j$ are given by

$$T^{ij}(x) = -\eta \left(\partial_i u^j + \partial_j u^i \right). \quad (\text{G.1})$$

The component T^{ij} of the stress-energy tensor is the flux of the i -th component of momentum across the surface determined by $x^j = \text{const}$. If a fluid flows at uniform velocity (all spatial velocity gradients vanish) there will of course be no net momentum flux across any surface. To first order T^{ij} must hence be proportional to first derivatives of u .

Without loss of generality we will assume that we study a fluid which (in the laboratory frame) only flows in the x -direction, i.e. has a velocity u_x . We further assume that u_x may only depend on z , i.e. $u_x = u_x(z)$. Equation (G.1) then reads

$$T^{xz} = -\eta \partial_z u_x(z). \quad (\text{G.2})$$

Let us ask the question how much momentum in x -direction is transported through a plane $z = \text{const}$. per unit time and per unit area. In average $(1/6)n\bar{v}$ particles cross the plane from below per unit time and area. (The factor of $1/3$ comes from the three spatial dimensions and the factor $1/2$ from the fact that there is two directions in each dimension.) The important question in the context of momentum transport is now, where these particles last interacted with the other particles, i.e. where they had their last collision. In average the particles crossing the plane from below moved the distance λ since their last collision (where λ is the mean free path). That means that they have the mean x -component of the velocity at $z - \lambda$, i.e. they carry a momentum $mu_x(z - \lambda)$. The momentum flux of particles moving through the plane from below is hence given by $(1/6)n\bar{v}(mu_x(z - \lambda))$. Analogously we get a momentum flux of $(1/6)n\bar{v}(mu_x(z + \lambda))$ of the particles moving through the plane from above. The net momentum transport is thus

$$T^{xz} \approx \frac{1}{6}n\bar{v}m(u_x(z - \lambda) - u_x(z + \lambda)). \quad (\text{G.3})$$

By assuming that T^{ij} is linear in derivatives of u we implicitly assumed that u varies only slowly in space. We can hence approximate the difference $u_x(z - \lambda) - u_x(z + \lambda)$ by

$-2\lambda\partial_z u_x(z)$, which yields

$$T^{xz}(z) \approx -\frac{1}{3}n\bar{v}m\lambda\partial_z u_x(z) = -\frac{1}{3}n\bar{p}\lambda\partial_z u_x(z). \quad (\text{G.4})$$

We readily read off the shear viscosity

$$\eta \approx \frac{1}{3}n\bar{p}\lambda. \quad (\text{G.5})$$

G.2. Thermodynamics of a Pion Gas

We want to describe an ideal gas of π^+ , π^0 and π^- , which has one conserved particle number $N_{\text{net}} := N_+ - N_-$ and a corresponding charge chemical potential μ_I . We will determine the thermodynamic properties of the system in the grand canonical ensemble regarding T , V and μ_I as thermodynamic variables and use the relativistic dispersion relation $\varepsilon_{\vec{k}} = \sqrt{\vec{k}^2 + m_\pi^2}$. As described in Section 6.3 we will neglect that m_π depends on temperature when calculating derivatives of the grand canonical partition function. The following derivations loosely follow [100].

The energy of the system is given by

$$E = -PV + TS + \mu_I N_{\text{net}}. \quad (\text{G.6})$$

The partition function is

$$\begin{aligned} \ln \mathcal{Z}(T, V, \mu_I) \\ = -V \int \frac{d^3k}{(2\pi)^3} \left(\ln \left(1 - e^{-\beta(\varepsilon_{\vec{k}} - \mu_I)} \right) + \ln \left(1 - e^{-\beta\varepsilon_{\vec{k}}} \right) + \ln \left(1 - e^{-\beta(\varepsilon_{\vec{k}} + \mu_I)} \right) \right) \end{aligned} \quad (\text{G.7})$$

with $\beta = 1/T$. As usual for bosons we have to impose the restriction that $m_\pi = \varepsilon_0 \geq \mu_I$ and since we also deal with antiparticles we analogously need $m_\pi \geq -\mu_I$, i.e. $|\mu_I| \leq m_\pi$.

The integral in the expression for the partition function cannot be solved analytically. It is however possible to write the logarithms as a Taylor series. Introducing the *fugacity* $z := e^{\beta\mu_I}$ we write the partition function as

$$\ln \mathcal{Z}(T, V, \mu_I) = \frac{V}{2\pi^2} \sum_{n=1}^{\infty} \frac{1}{n} \int_0^\infty dk k^2 e^{-n\beta\varepsilon_{\vec{k}}} (z^n + 1 + z^{-n}). \quad (\text{G.8})$$

The integration can now be performed and one obtains the following series representation

$$\ln \mathcal{Z}(T, V, \mu_I) = \frac{Vm_\pi^2}{2\pi^2\beta} \sum_{n=1}^{\infty} \frac{1}{n^2} (z^n + 1 + z^{-n}) K_2(n\beta m_\pi). \quad (\text{G.9})$$

Here, $K_\nu(x)$ denotes the *modified Bessel function of second kind* (of order ν).

With the help of the partition function we can calculate the (average) pressure

$$\begin{aligned} P(T, V, \mu_I) &= \left. \frac{\partial(T \ln \mathcal{Z})}{\partial V} \right|_{T, \mu_I} = \frac{T}{V} \ln \mathcal{Z} \\ &= \frac{m_\pi^2}{2\pi^2\beta^2} \sum_{n=1}^{\infty} \frac{1}{n^2} (z^n + 1 + z^{-n}) K_2(n\beta m_\pi). \end{aligned} \quad (\text{G.10})$$

The average net particle number density $n_{\text{net}} = n_+ - n_-$ is given by

$$\begin{aligned} n_{\text{net}}(T, V, \mu_I) &= \frac{1}{V} \left. \frac{\partial(T \ln \mathcal{Z})}{\partial \mu_I} \right|_{T, V} = \frac{z}{V} \left. \frac{\partial(\ln \mathcal{Z})}{\partial z} \right|_{T, V} \\ &= \frac{m_\pi^2}{2\pi^2 \beta} \sum_{n=1}^{\infty} \frac{1}{n} (z^n - z^{-n}) K_2(n\beta m_\pi). \end{aligned} \quad (\text{G.11})$$

Finally the entropy density $s = S/V$ of the system is given by

$$\begin{aligned} s(T, V, \mu_I) &= \frac{1}{V} \left. \frac{\partial(T \ln \mathcal{Z})}{\partial T} \right|_{V, \mu_I} \\ &= \frac{m_\pi^2}{2\pi\beta} \sum_{n=1}^{\infty} \frac{1}{n^2} [(z^n (4 - n \ln(z)) + 4 + z^{-n} (4 + n \ln(z))) K_2(n\beta m_\pi) \\ &\quad + n\beta m_\pi (z^n + 1 + z^{-n}) K_1(n\beta m_\pi)]. \end{aligned} \quad (\text{G.12})$$

The average energy density can be obtained via $\varepsilon = -P + Ts + \mu_I n_{\text{net}}$ or directly via

$$\begin{aligned} \varepsilon(T, V, \mu_I) &= -\frac{1}{V} \left. \frac{\partial(\ln \mathcal{Z})}{\partial \beta} \right|_{V, z} \\ &= 3P + \frac{m_\pi^3}{2\pi^2 \beta} \sum_{n=1}^{\infty} \frac{1}{n} (z^n + 1 + z^{-n}) K_1(n\beta m_\pi). \end{aligned} \quad (\text{G.13})$$

The number density and energy density can also be obtained in a different approach. We can write

$$n_{\text{net}}(T, V, \mu_I) = \frac{N_{\text{net}}}{V} = \int \frac{d^3 k}{(2\pi)^3} \left(\frac{1}{e^{\beta(\varepsilon_{\vec{k}} - \mu_I)} - 1} - \frac{1}{e^{\beta(\varepsilon_{\vec{k}} + \mu_I)} - 1} \right). \quad (\text{G.14})$$

The Bose-Einstein distribution function enters in the above expression. In the same way, the energy density is given by

$$\varepsilon(T, V, \mu_I) = \frac{E}{V} = \int \frac{d^3 k}{(2\pi)^3} \varepsilon_{\vec{k}} \left(\frac{1}{e^{\beta(\varepsilon_{\vec{k}} - \mu_I)} - 1} + \frac{1}{e^{\beta \varepsilon_{\vec{k}}} - 1} + \frac{1}{e^{\beta(\varepsilon_{\vec{k}} + \mu_I)} - 1} \right). \quad (\text{G.15})$$

These expressions are identical²² to (G.11) and (G.13) since the particle number operator and the Hamilton operator are essentially single-particle operators (the former in general, the latter because we are dealing with an ideal gas). In analogy to the above expression we can define the total number density $n = n_+ + n_0 + n_-$ via

$$n(T, V, \mu_I) = \int \frac{d^3 k}{(2\pi)^3} \left(\frac{1}{e^{\beta(\varepsilon_{\vec{k}} - \mu_I)} - 1} + \frac{1}{e^{\beta \varepsilon_{\vec{k}}} - 1} + \frac{1}{e^{\beta(\varepsilon_{\vec{k}} + \mu_I)} - 1} \right), \quad (\text{G.16})$$

²²From a numerical point of view they are of course not the same. In principle they should yield the same result, but the integral expression converges much faster than the sum expression but on the other hand the sum is less sensitive to extreme choices of T .

which is of course identical to the expression

$$n(T, V, \mu_I) = \frac{m_\pi^2}{2\pi^2\beta} \sum_{n=1}^{\infty} \frac{1}{n} (z^n + 1 + z^{-n}) K_2(n\beta m_\pi). \quad (\text{G.17})$$

We immediately see that $P = nT$, which is the ideal gas law (with $k_B = 1$).

We are also interested in the average momentum \bar{p} of a single particle, which is given by

$$\bar{p} = \frac{\int \frac{d^3k}{(2\pi)^3} |\vec{k}| \left(\frac{1}{e^{\beta(\varepsilon_{\vec{k}} - \mu_I)} - 1} + \frac{1}{e^{\beta\varepsilon_{\vec{k}}} - 1} + \frac{1}{e^{\beta(\varepsilon_{\vec{k}} + \mu_I)} - 1} \right)}{\int \frac{d^3k}{(2\pi)^3} \left(\frac{1}{e^{\beta(\varepsilon_{\vec{k}} - \mu_I)} - 1} + \frac{1}{e^{\beta\varepsilon_{\vec{k}}} - 1} + \frac{1}{e^{\beta(\varepsilon_{\vec{k}} + \mu_I)} - 1} \right)}. \quad (\text{G.18})$$

Symmetric Pion Gas

All the above expressions simplify considerably in the case of a symmetric pion gas, meaning that $N_{\text{net}} = N_+ - N_- = 0$. From the above equation for n_{net} we see that this is the case exactly for $\mu_I = 0$. We have

$$\begin{aligned} P(T, V, \mu_I = 0) &= 3 \frac{m_\pi^2}{2\pi^2\beta^2} \sum_{n=1}^{\infty} \frac{1}{n^2} K_2(n\beta m_\pi), \\ s(T, V, \mu_I = 0) &= 3 \frac{m_\pi^2}{2\pi\beta} \sum_{n=1}^{\infty} \frac{1}{n^2} [4K_2(n\beta m_\pi) + n\beta m_\pi K_1(n\beta m_\pi)], \\ \varepsilon(T, V, \mu_I = 0) &= 3 \frac{m_\pi^2}{2\pi\beta^2} \sum_{n=1}^{\infty} \frac{1}{n^2} [3K_2(n\beta m_\pi) + n\beta m_\pi K_1(n\beta m_\pi)], \\ n(T, V, \mu_I = 0) &= 3 \frac{m_\pi^2}{2\pi^2\beta} \sum_{n=1}^{\infty} \frac{1}{n} K_2(n\beta m_\pi). \end{aligned} \quad (\text{G.19})$$

For an uncharged pion gas all three components have the same thermodynamic properties and we get the degeneracy factor of 3 in front of every expression. The average momentum is given by

$$\bar{p} = \frac{\int \frac{d^3k}{(2\pi)^3} |\vec{k}| \frac{1}{e^{\beta\varepsilon_{\vec{k}}} - 1}}{\int \frac{d^3k}{(2\pi)^3} \frac{1}{e^{\beta\varepsilon_{\vec{k}}} - 1}}. \quad (\text{G.20})$$

H. The Grand Potential

H.1. Calculation of the Mean-Field Lagrangian Density

We want to linearise the Lagrangian density of the NJL model

$$\mathcal{L} = \bar{\psi}(i\cancel{\partial} - \underline{m})\psi + g \left[(\bar{\psi}\psi)^2 + (\bar{\psi}i\gamma_5\vec{\tau}\psi)^2 \right] \quad (\text{H.1})$$

by dropping all terms of quadratic or higher order in the fluctuations after inserting the decomposition

$$\bar{\psi}\psi = \langle \bar{\psi}\psi \rangle + \delta_\sigma \quad \text{and} \quad \bar{\psi}i\gamma_5\vec{\tau}\psi = \langle \bar{\psi}i\gamma_5\vec{\tau}\psi \rangle + \delta_\pi^a. \quad (\text{H.2})$$

One calculates for the scalar interaction term

$$(\bar{\psi}\psi)^2 = \langle \bar{\psi}\psi \rangle^2 + 2\langle \bar{\psi}\psi \rangle\delta_\sigma + \mathcal{O}(\delta_\sigma^2) = 2\langle \bar{\psi}\psi \rangle\bar{\psi}\psi - \langle \bar{\psi}\psi \rangle^2 + \mathcal{O}(\delta_\sigma^2). \quad (\text{H.3})$$

We assumed that the pseudoscalar condensate $\langle \bar{\psi}i\gamma_5\vec{\tau}\psi \rangle$ vanishes wherefore there can be no linear terms in the fluctuation δ_π^a and hence

$$(\bar{\psi}i\gamma_5\vec{\tau}\psi)^2 = 0 + \mathcal{O}(\delta_\pi^{a2}). \quad (\text{H.4})$$

We define the mean-field quark self-energy Σ as

$$\Sigma := -2g\langle \bar{\psi}\psi \rangle \quad (\text{H.5})$$

and the constituent quark mass

$$M := m + \Sigma = m - 2g\langle \bar{\psi}\psi \rangle. \quad (\text{H.6})$$

Expressing $\langle \bar{\psi}\psi \rangle$ in terms of M and m , we get

$$\begin{aligned} \mathcal{L} &= \bar{\psi}(i\cancel{\partial} - m)\psi + g \left(2\langle \bar{\psi}\psi \rangle\bar{\psi}\psi - \langle \bar{\psi}\psi \rangle^2 \right) + \mathcal{O}(\delta_\sigma^2, \delta_\pi^{a2}) \\ &= \bar{\psi}(i\cancel{\partial} - m)\psi + g \left(-2\frac{M-m}{2g}\bar{\psi}\psi - \frac{(M-m)^2}{4g^2} \right) + \mathcal{O}(\delta_\sigma^2, \delta_\pi^{a2}) \\ &= \bar{\psi}(i\cancel{\partial} - M)\psi - \frac{(M-m)^2}{4g} + \mathcal{O}(\delta_\sigma^2, \delta_\pi^{a2}). \end{aligned} \quad (\text{H.7})$$

In total this yields a mean-field Lagrangian density

$$\mathcal{L}_{\text{mf}} = \bar{\psi}(i\cancel{\partial} - M)\psi - \frac{(M-m)^2}{4g}. \quad (\text{H.8})$$

H.2. Calculation of the Grand Potential of a Fermi Gas

We want to determine the Fermi gas contribution $\Omega_M(T, \mu)$ to the mean-field grand potential $\Omega_{\text{mf}}(T, \mu; M)$ (see (X.24)), i.e. we want to calculate

$$\Omega_M(T, \mu) = -T \sum_{j \in \mathbb{Z}} \int \frac{d^3 k}{(2\pi)^3} \text{Tr} \ln \left(\frac{1}{T} S^{-1}(i\omega_j + \mu, \vec{k}) \right). \quad (\text{H.9})$$

We write the above as

$$\begin{aligned} \Omega_M(T, \mu) &= -T \sum_{j \in \mathbb{Z}} \int \frac{d^3 k}{(2\pi)^3} \ln \text{Det} \left(\frac{1}{T} S^{-1}(i\omega_j + \mu, \vec{k}) \right) \\ &= -T \sum_{j \in \mathbb{Z}} \int \frac{d^3 k}{(2\pi)^3} \ln \text{Det} \left(\frac{1}{T} \left((i\omega_j + \mu) \gamma^0 - \vec{k} \cdot \vec{\gamma} - M \right) \right), \end{aligned} \quad (\text{H.10})$$

where Det (like Tr) is taken over Dirac, isospin and colour space. Using

$$\ln \text{Det}(\mathcal{Q} - M) = 2N_f N_c \ln(Q^2 - M^2) \quad (\text{H.11})$$

we get

$$\Omega_M(T, \mu) = -2N_c N_f T \sum_{j \in \mathbb{Z}} \int \frac{d^3 k}{(2\pi)^3} \ln \left(\frac{(i\omega_j + \mu)^2 - E_{\vec{k}}^2}{T^2} \right). \quad (\text{H.12})$$

Using the residue theorem, we write the above expression as a contour integral

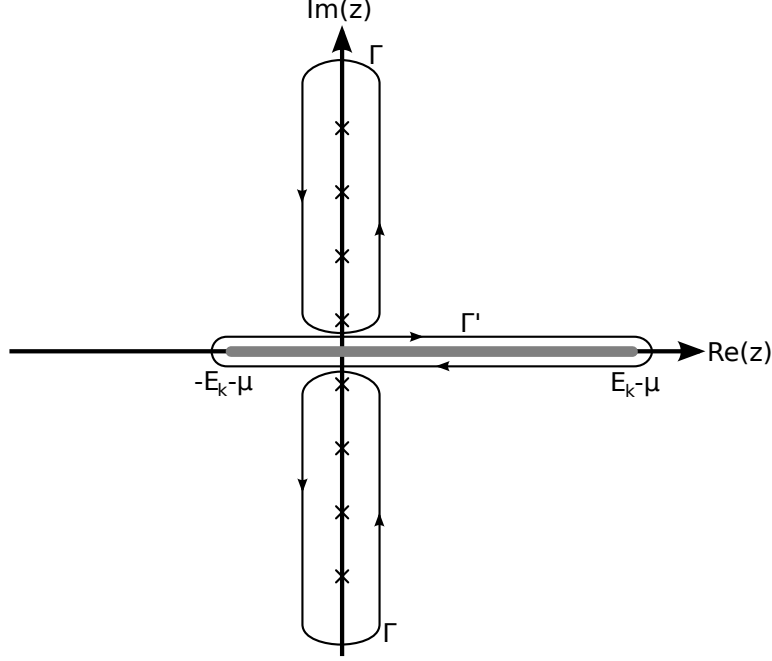
$$\Omega_M(T, \mu) = 2N_f N_c \int \frac{d^3 k}{(2\pi)^3} \frac{1}{2\pi i} \int_{\Gamma} n_F(z) \ln \left(\frac{(z + \mu)^2 - E_{\vec{k}}^2}{T^2} \right), \quad (\text{H.13})$$

where n_F is the Fermi distribution function

$$n_F(z) = \frac{1}{1 + \exp\left(\frac{z}{T}\right)}, \quad (\text{H.14})$$

which has exactly poles at the fermionic Matsubara frequencies with residue $-T$.

We will now evaluate the integral by deforming the integration contour. Let us investigate the analyticity of the integrand. The complex logarithm (i.e. its principal value) is analytic in the complex plane with a branch cut along the negative real axis. Hence the ln-term in the integrand is analytic in z in the complex plane with the points $-E_{\vec{k}} - \mu < z < E_{\vec{k}} - \mu$ on the real axis removed. We can therefore deform the integration contour Γ to an integration contour Γ' (without changing the value of the integral) around the branch cut:



This gives

$$\begin{aligned} \Omega_M(T, \mu) = 2N_c N_f \int \frac{d^3k}{(2\pi)^3} \frac{1}{2\pi i} \int_{-E_{\vec{k}} - \mu}^{E_{\vec{k}} - \mu} dz \left(n_F(z + i\varepsilon) \ln \left(\frac{(z + i\varepsilon + \mu)^2 - E_{\vec{k}}^2}{T^2} \right) \right. \\ \left. - n_F(z - i\varepsilon) \ln \left(\frac{(z - i\varepsilon + \mu)^2 - E_{\vec{k}}^2}{T^2} \right) \right) \end{aligned} \quad (\text{H.15})$$

We can drop the $i\varepsilon$ in the n_F terms since the branch cut only appears in the \ln term. Moreover, using

$$\ln(z) = \ln(|z|) + i \arg(z) = (\ln(z^*))^* \quad (\text{H.16})$$

we arrive at the expression

$$\begin{aligned} \Omega_M(T, \mu) = 2N_c N_f \int \frac{d^3k}{(2\pi)^3} \frac{1}{2\pi i} \int_{-E_{\vec{k}} - \mu}^{E_{\vec{k}} - \mu} dz n_F(z) 2i \arg \left(\frac{(z + i\varepsilon + \mu)^2 - E_{\vec{k}}^2}{T^2} \right) \\ = 2N_c N_f \int \frac{d^3k}{(2\pi)^3} \frac{1}{2\pi i} \int_{-E_{\vec{k}}}^{E_{\vec{k}}} dz n_F(z - \mu) 2i \arg \left(\frac{(z + i\varepsilon)^2 - E_{\vec{k}}^2}{T^2} \right). \end{aligned} \quad (\text{H.17})$$

We now use

$$\arg \left(\frac{(z + i\varepsilon)^2 - E_{\vec{k}}^2}{T^2} \right) = \text{sgn}(z) \pi \quad (\text{H.18})$$

to get

$$\Omega_M(T, \mu) = 2N_c N_f \int \frac{d^3k}{(2\pi)^3} \int_{-E_{\vec{k}}}^{E_{\vec{k}}} dz n_F(z - \mu) \text{sgn}(z). \quad (\text{H.19})$$

The integral over z can now be calculated analytically and one finally gets

$$\begin{aligned}\Omega_M(T, \mu) &= -2N_c N_f \int \frac{d^3 k}{(2\pi)^3} \left[E_{\vec{k}} + T \ln \left(1 + \exp \left(-\frac{E_{\vec{k}} - \mu}{T} \right) \right) \right. \\ &\quad \left. + T \ln \left(1 + \exp \left(-\frac{E_{\vec{k}} + \mu}{T} \right) \right) \right],\end{aligned}\tag{H.20}$$

which is the result stated in (H.23).

H.3. Calculation of the Mean-Field Grand Potential

In the following we want to derive the expression (X.24) for the mean-field grand potential using the expression for Fermi gas grand potential from above. We have

$$\begin{aligned}\Omega_{\text{mf}} &= -\frac{T}{V} \ln \mathcal{Z}_{\text{mf}} = -\frac{T}{V} \ln \mathbf{Tr} \exp \left(-\frac{1}{T} \int d^3 x (\mathcal{H}_{\text{mf}} - \mu \bar{\psi} \gamma^0 \psi) \right) \\ &= -\frac{T}{V} \ln \mathbf{Tr} \exp \left(-\frac{1}{T} \int d^3 x (\bar{\psi} (-i\vec{\gamma} \cdot \vec{\nabla} + M) \psi + \frac{(M-m)^2}{4g} - \mu \bar{\psi} \gamma^0 \psi) \right) \\ &= -\frac{T}{V} \ln \left[\mathbf{Tr} \exp \left(-\frac{1}{T} \int d^3 x (\bar{\psi} (-i\vec{\gamma} \cdot \vec{\nabla} + M) \psi + \frac{(M-m)^2}{4g} - \mu \bar{\psi} \gamma^0 \psi) \right) \right] \times \\ &\quad \times \exp \left(-\frac{V}{T} \frac{(M-m)^2}{4g} \right) \\ &= -\frac{T}{V} \mathbf{Tr} \exp \left(-\frac{1}{T} \int d^3 x (\bar{\psi} (-i\vec{\gamma} \cdot \vec{\nabla} + M) \psi - \mu \bar{\psi} \gamma^0 \psi) \right) + \frac{(M-m)^2}{4g}.\end{aligned}\tag{H.21}$$

The first part is simply the grand potential for free fermions of mass M , which we call Ω_M . If one does the functional integration explicitly (see for example [68] or any other textbook on statistical field theory), one can write $\Omega_M(T, \mu)$ as

$$\Omega_M(T, \mu) = -T \sum_{n \in \mathbb{Z}} \int \frac{d^3 k}{(2\pi)^3} \text{Tr} \ln \left(\frac{1}{T} S^{-1}(i\omega_n + \mu, \vec{k}) \right).\tag{H.22}$$

A calculation involving the residue theorem (see Appendix H.2) shows that this can be brought into the form

$$\begin{aligned}\Omega_M(T, \mu) &= -2N_c N_f \int \frac{d^3 k}{(2\pi)^3} \left[E_{\vec{k}} + T \ln \left(1 + \exp \left(-\frac{E_{\vec{k}} - \mu}{T} \right) \right) \right. \\ &\quad \left. + T \ln \left(1 + \exp \left(-\frac{E_{\vec{k}} + \mu}{T} \right) \right) \right],\end{aligned}\tag{H.23}$$

such that the mean-field grand potential indeed reads as in (X.24).

H.4. Equivalence of the Gap Equation and the Stationarity of the Grand Potential

We want to show that the stationarity condition (X.29) of the grand potential Ω_{mf} is equivalent to the gap equation (3.4). To do this, we start from the expression (X.24) for the grand potential and differentiate it with respect to M . Observe that M appears hidden in $E_{\vec{k}} = \sqrt{\vec{k}^2 + M^2}$. Since we want to apply the chain rule, it is useful to know that

$$\frac{\partial E_{\vec{k}}}{\partial M} = \frac{M}{E_{\vec{k}}}. \quad (\text{H.24})$$

Moreover,

$$\frac{d}{dx} (\ln(1 + e^{-x})) = -\frac{1}{1 + e^x}. \quad (\text{H.25})$$

This gives

$$\begin{aligned} \frac{\partial \Omega_{\text{mf}}}{\partial M} &= \frac{\partial}{\partial M} \left(\frac{(M - m)^2}{4g} \right) - 2N_{\text{f}}N_{\text{c}} \int \frac{d^3k}{(2\pi)^3} \left[\frac{\partial E_{\vec{k}}}{\partial M} \right. \\ &\quad + \frac{\partial}{\partial E_{\vec{k}}} \left(T \ln \left(1 + \exp \left(-\frac{E_{\vec{k}} - \mu}{T} \right) \right) \right) \frac{\partial E_{\vec{k}}}{\partial M} \\ &\quad \left. + \frac{\partial}{\partial E_{\vec{k}}} \left(T \ln \left(1 + \exp \left(-\frac{E_{\vec{k}} + \mu}{T} \right) \right) \right) \frac{\partial E_{\vec{k}}}{\partial M} \right] \\ &= \frac{M - m}{2g} - 2N_{\text{f}}N_{\text{c}} \int \frac{d^3k}{(2\pi)^3} \frac{M}{E_{\vec{k}}} \left[1 - \frac{1}{1 + \exp \left(\frac{E_{\vec{k}} - \mu}{T} \right)} - \frac{1}{1 + \exp \left(\frac{E_{\vec{k}} + \mu}{T} \right)} \right], \end{aligned} \quad (\text{H.26})$$

which bearing the form of $iI_1(T, \mu)$ in mind (see (3.7)) can be written as

$$\frac{\partial \Omega_{\text{mf}}}{\partial M} = \frac{M - m}{2g} - 4N_{\text{f}}N_{\text{c}}MgiI_1(T, \mu; M). \quad (\text{H.27})$$

Setting the above equal to zero directly yields

$$M = m + 8N_{\text{c}}N_{\text{f}}MgiI_1(T, \mu; M), \quad (\text{H.28})$$

which is the gap equation.

Bibliography

- [1] W. Greiner and A. Schäfer. *Quantum Chromodynamics*. Theoretische Physik. Springer-Verlag, 3rd edition, 1994.
- [2] D. J. Gross and F. Wilczek. Ultraviolet behavior of non-abelian gauge theories. *Phys. Rev. Lett.*, 30(26):1343–1346, 1973.
- [3] H. D. Politzer. Reliable perturbative results for strong interactions? *Phys. Rev. Lett.*, 30(26):1346–1349, 1973.
- [4] D. J. Gross. Twenty five years of asymptotic freedom. *Nucl. Phys. B Proc. Supp.*, 74:426–446, 1999. (arXiv:hep-th/9809060v1).
- [5] K. G. Wilson. Confinement of quarks. *Phys. Rev. D*, 10(8):2445–2459, 1974.
- [6] J. Greensite. The confinement problem in lattice gauge theory. *Prog. Part. Nucl. Phys.*, 51:1, 2003. (arXiv:hep-lat/0301023v2).
- [7] M. A. Stephanov. QCD phase diagram: An overview. *PoS*, LAT2006:024, 2006. (arXiv:hep-lat/0701002v1).
- [8] T. Schäfer. Phases of QCD. (arXiv:hep-ph/0509068v1), 2005.
- [9] P. Braun-Munzinger and J. Wambach. Colloquium: Phase diagram of strongly interacting matter. *Rev. Mod. Phys.*, 81:1031–1050, 2009. (arXiv:0801.4256v2 [hep-ph]).
- [10] J. Wambach, K. Heckmann, and M. Buballa. Transport Properties of Strong-Interaction Matter. *Acta Phys. Pol. B Proc. Supp.*, 5(3):909–916, 2012. (arXiv:1111.5475v2 [hep-ph]).
- [11] B. Friman, C. Höhne, J. Knoll, S. Leupold, J. Randrup, R. Rapp, and P. Senger, editors. *The CBM Physics Book*, volume 814 of *Lecture Notes in Physics*. Springer-Verlag, 2011.
- [12] D. Bailin and A. Love. Superfluidity and superconductivity in relativistic fermion systems. *Phys. Rept.*, 107:325, 1984.
- [13] B. C. Barrois. Superconducting quark matter. *Nucl. Phys. B*, 129:390, 1977.
- [14] M. G. Alford, A. Schmitt, K. Rajagopal, and T. Schafer. Color superconductivity in dense quark matter. *Rev. Mod. Phys.*, 80:1455–1515, 2008. (arXiv:0709.4635v2 [hep-ph]).

- [15] N. Cabibbo and G. Parisi. Exponential hadronic spectrum and quark liberation. *Phys. Lett. B*, 59(1):67–69, 1975.
- [16] A. Bazavov, T. Bhattacharya, M. Cheng, C. DeTar, H. T. Ding et al. (HotQCD Collaboration). The chiral and deconfinement aspects of the QCD transition. *Phys. Rev. D*, 85:054503, 2012. (arXiv:1111.1710v2 [hep-lat]).
- [17] E. V. Shuryak. Quark-gluon plasma and hadronic production of leptons, photons and pions. *Phys. Lett. B*, 78:150–153, 1978.
- [18] V. Koch. Aspects of chiral symmetry. *Int. J. Mod. Phys. E*, 6:203–250, 1997. (arXiv:nucl-th/9512029v1).
- [19] V. Koch. Introduction to chiral symmetry. (arXiv:nucl-th/9706075v2), 1995.
- [20] A. Chodos, R. L. Jaffe, K. Johnson, Charles B. Thorn, and V. F. Weisskopf. A new extended model of hadrons. *Phys. Rev. D*, 9:3471–3495, 1974.
- [21] Y. Nambu and G. Jona-Lasinio. Dynamical model of elementary particles based on an analogy with superconductivity. I. *Phys. Rev.*, 122(1):345–358, 1961.
- [22] Y. Nambu and G. Jona-Lasinio. Dynamical model of elementary particles based on an analogy with superconductivity. II. *Phys. Rev.*, 124(1):246–254, 1961.
- [23] S. P. Klevansky. The Nambu–Jona-Lasinio model of quantum chromodynamics. *Rev. Mod. Phys.*, 64(3):649–708, 1992.
- [24] U. Vogl and W. Weise. The Nambu and Jona-Lasinio model: Its implications for hadrons and nuclei. *Prog. Part. Nucl. Phys.*, 27:195–272, 1991.
- [25] R. Vogt. *Ultrarelativistic Heavy-Ion Collisions*. Elsevier, 2007.
- [26] P. Braun-Munzinger and J. Stachel. The quest for the quark–gluon plasma. *Nature*, 448:302–309, 2007.
- [27] M. Gyulassy and L. McLerran. New forms of QCD matter discovered at RHIC. *Nucl. Phys. A*, 750:30–63, 2005. (arXiv:nucl-th/0405013v2).
- [28] B. Schwarzschild. Have heavy ion collisions at CERN reached the quark–gluon plasma? *Physics Today*, 53(5):20–23, 2000.
- [29] U. W. Heinz. The little bang: Searching for quark gluon matter in relativistic heavy ion collisions. *Nucl. Phys. A*, 685:414–431, 2001. (arXiv:hep-ph/0009170v2).
- [30] K. Aamodt et al. (ALICE Collaboration). Higher harmonic anisotropic flow measurements of charged particles in Pb-Pb collisions at $\sqrt{s_{NN}} = 2.76$ TeV. *Phys. Rev. Lett.*, 107:032301, 2011. (arXiv:1105.3865v2 [nucl-ex]).
- [31] R. Snellings. Anisotropic flow at the LHC measured with the ALICE detector. *J. Phys. G*, 38:124013, 2011. (arXiv:1106.6284v2 [nucl-ex]).

- [32] K. Aamodt et al. (ALICE Collaboration). Elliptic flow of charged particles in Pb-Pb collisions at $\sqrt{s_{NN}} = 2.76$ TeV. *Phys. Rev. Lett.*, 105(25):252302, 2010. (arXiv:1011.3914v2 [nucl-ex]).
- [33] G. Aad et al. (ATLAS Collaboration). Observation of a centrality-dependent dijet asymmetry in lead-lead collisions at $\sqrt{s_{NN}} = 2.76$ TeV with the ATLAS detector at the LHC. *Phys. Rev. Lett.*, 105(25):252303, 2010. (arXiv:1011.6182v2 [hep-ex]).
- [34] W. A. Zajc. The fluid nature of quark-gluon plasma. *Nucl. Phys. A*, 805:283–294, 2008. (arXiv:0802.3552 [nucl-ex]).
- [35] P. Kovtun, D. T. Son, and A. O. Starinets. Viscosity in strongly interacting quantum field theories from black hole physics. *Phys. Rev. Lett.*, 94:111601, 2005. (arXiv:hep-th/0405231v2).
- [36] F. Reif. *Fundamentals of statistical and thermal physics*. McGraw-Hill, 1965.
- [37] E. Shuryak. Physics of strongly coupled quark-gluon plasma. *Prog. Part. Nucl. Phys.*, 62:48–101, 2009. (arXiv:0807.3033v2 [hep-ph]).
- [38] K. Heckmann. *Transport coefficients of strongly interacting matter*. Dissertation, Fachbereich Physik. Technische Universität Darmstadt, 2011. (http://tuprints.ulb.tu-darmstadt.de/2588/1/diss_heckmann.pdf).
- [39] R. Hagedorn. Statistical thermodynamics of strong interactions at high-energies. *Nuovo Cim. Suppl.*, 3:147–186, 1965.
- [40] H. J. Schulze. Pion-pion scattering lengths in the SU(2) Nambu–Jona-Lasinio model. *J. Phys. G*, 21:185–191, 1995.
- [41] M. Loewe, A. Jorge Ruiz, and J. C. Rojas. Thermal behaviour of π - π scattering lengths in the Nambu–Jona-Lasinio model. *Phys. Rev. D*, 78:096007, 2008. (arXiv:0805.3719v1 [hep-ph]).
- [42] A. A. Osipov, A. E. Radzhabov, and M. K. Volkov. $\pi\pi$ scattering in a nonlocal Nambu–Jona-Lasinio model. (arXiv:hep-ph/0603130v1), 2006.
- [43] E. Quack, P. Zhuang, Yu. Kalinovsky, S. P. Klevansky, and J. Hüfner. π - π scattering lengths at finite temperature. *Phys. Lett. B*, 348:1–6, 1995. (arXiv:hep-ph/9410243v2).
- [44] V. Bernard, U.-G. Meißner, A. H. Blin, and B. Hiller. Four point functions in quark flavor dynamics: Meson meson scattering. *Phys. Lett. B*, 253:443–450, 1991.
- [45] M. C. Ruivo, C. A. de Sousa, B. Hiller, and A. H. Blin. Medium effects on meson properties. *Nucl. Phys. A*, 575:460–476, 1994.

- [46] K. Heckmann. Die Scherviskosität im Nambu-Jona-Lasinio-Modell. Diplomarbeit, Institut für Kernphysik. Technische Universität Darmstadt, 2007. (<http://crunch.ikp.physik.tu-darmstadt.de/nhc/pages/thesis/diplom.heckmann.pdf>).
- [47] K. Heckmann, M. Buballa, and J. Wambach. Chiral restoration effects on the shear viscosity of a pion gas. *Eur. Phys. J. A*, 48:142, 2012. (arXiv:1202.0724v2 [hep-ph]).
- [48] Y. B. He, J. Hüfner, S. P. Klevansky, and P. Rehberg. $\pi\pi$ scattering in the ρ -meson channel at finite temperature. *Nucl. Phys. A*, 630:719–742, 1998. (arXiv:nucl-th/9712051v1).
- [49] V. Bernard, A. H. Blin, B. Hiller, Yu. P. Ivanov, A. A. Osipov, and U.-G. Meißner. Pion observables in the extended NJL model with vector and axial - vector mesons. *Ann. Phys.*, 249:499–531, 1996. (arXiv:hep-ph/9506309v1).
- [50] J. Bardeen, L. N. Cooper, and J. R. Schrieffer. Microscopic theory of superconductivity. *Phys. Rev.*, 106(1):162–164, 1957.
- [51] J. Goldstone. Field theories with «superconductor» solutions. *Il Nuovo Cimento*, 19(1):154–164, 1961.
- [52] J. Goldstone, A. Salam, and S. Weinberg. Broken symmetries. *Phys. Rev.*, 127(3):965–970, 1962.
- [53] T. Hatsuda and T. Kunihiro. Possible critical phenomena associated with the chiral symmetry breaking. *Phys. Lett. B*, 145:7–10, 1984.
- [54] M. K. Volkov. Meson lagrangians in a superconductor quark model. *Ann. Phys.*, 157:282–303, 1984.
- [55] H. Kleinert. On the Hadronization of Quark Theories, Lectures presented at the Erice Summer Institute 1976. In A. Zichichi, editor, *Understanding the Fundamental Constituents of Matter*, pages 289–390. Plenum Press, 1978.
- [56] S. Klimt, M. F. M. Lutz, U. Vogl, and W. Weise. Generalized SU(3) Nambu-Jona-Lasinio model. part 1. mesonic modes. *Nucl. Phys. A*, 516:429–468, 1990.
- [57] U. Vogl, M. F. M. Lutz, S. Klimt, and W. Weise. Generalized SU(3) Nambu-Jona-Lasinio model. part 2. from current to constituent quarks. *Nucl. Phys. A*, 516:469–495, 1990.
- [58] M. E. Peskin and D. V. Schroeder. *An Introduction To Quantum Field Theory*. Advanced Book Program. Addison-Wesley, 1995.
- [59] W. Pauli and F. Villars. On the invariant regularization in relativistic quantum theory. *Rev. Mod. Phys.*, 21:434–444, 1949.

- [60] M. Oertel. *Investigation of meson loop effects in the Nambu-Jona-Lasinio model*. Dissertation, Fachbereich Physik. Technische Universität Darmstadt, 2000. (arXiv:hep-ph/0012224v1).
- [61] E. E. Salpeter and H. A. Bethe. A relativistic equation for bound-state problems. *Phys. Rev.*, 84(6):1232–1242, 1951.
- [62] Y. Nambu. Force potentials in quantum field theory. *Prog. Theo. Phys.*, 5(4):614–633, 1950.
- [63] D. Griffiths. *Introduction to Elementary Particles*. Wiley, 1987.
- [64] M. Buballa. NJL-model analysis of dense quark matter. *Phys. Rept.*, 407:205–376, 2005. (arXiv:hep-ph/0402234v2).
- [65] M. L. Goldberger and S. B. Treiman. Decay of the pi meson. *Phys. Rev.*, 110(5):1178–1184, 1958.
- [66] K. Nakamura et al. (Particle Data Group). Review of particle physics. *J. Phys. G*, 37:075021, 2010.
- [67] M. Gell-Mann, R. J. Oakes, and B. Renner. Behavior of current divergences under $SU_3 \times SU_3$. *Phys. Rev.*, 175(5):2195–2199, 1968.
- [68] J. I. Kapusta and C. Gale. *Finite-Temperature Field Theory. Principles and Applications*. Cambridge University Press, 2nd edition, 2006.
- [69] M. Le Bellac. *Thermal Field Theory*. Cambridge University Press, 2000.
- [70] V. Bernard, U. G. Meißner, and I. Zahed. Decoupling of the pion at finite temperature and density. *Phys. Rev. D*, 36:819, 1987.
- [71] T. Hatsuda and T. Kunihiro. Character changes of pion and sigma meson at finite temperature. *Phys. Lett. B*, 185:304, 1987.
- [72] H. W. Barz, H. Schulz, G. Bertsch, and P. Danielewicz. Pion pion cross-section in a dense and hot pionic gas. *Phys. Lett. B*, 275:19–23, 1992.
- [73] V. Mull, J. Wambach, and J. Speth. Pion pion scattering in nuclear matter. *Phys. Lett. B*, 286:13–18, 1992.
- [74] T. Matsubara. A new approach to quantum statistical mechanics. *Prog. Theor. Phys.*, 14:351–378, 1955.
- [75] H. A. Kramers. La diffusion de la lumiere par les atomes. *Atti Cong. Intern. Fisica, (Transactions of Volta Centenary Congress) Como*, 2:545–557, 1927.
- [76] R. Kronig. On the theory of dispersion of X-rays. *J. Opt. Soc. Am.*, 12(6):547–556, 1926.

- [77] F. Halzen and A. D. Martin. *Quarks and Leptons: An Introductory Course in Modern Particle Physics*. Wiley, 1984.
- [78] J. Gasser and Leutwyler H. Chiral perturbation theory to one loop. *Ann. Phys.*, 158(1):142–210, 1984.
- [79] V. Dmitrašinović, H. J. Schulze, R. Tegen, and R. H. Lemmer. Chirally symmetric $\mathcal{O}(1/N_c)$ corrections to the Nambu-Jona-Lasinio model. *Ann. Phys.*, 238:332–369, 1995.
- [80] G. 't Hooft and M. J. G. Veltman. Scalar One-Loop Integrals. *Nucl. Phys. B*, 153:365–401, 1979.
- [81] G. Passarino and M. J. G. Veltman. One loop corrections for $e^+ e^-$ annihilation into $\mu^+ \mu^-$ in the Weinberg model. *Nucl. Phys. B*, 160:151–207, 1979.
- [82] G. J. van Oldenborgh and J. A. M. Vermaseren. New algorithms for one loop integrals. *Z. Phys. C*, 46:425–438, 1990.
- [83] T. Hahn and M. Perez-Victoria. Automatized one loop calculations in four and D dimensions. *Comput. Phys. Commun.*, 118:153–165, 1999. (arXiv:hep-ph/9807565v1).
- [84] T. Hahn. LoopTools. Online, accessed 18 July 2012. (<http://www.feynarts.de/loopTools/>).
- [85] J. R. Peláez and F. J. Ynduráin. The pion-pion scattering amplitude. *Phys. Rev. D*, 71:074016, 2005. (arXiv:hep-ph/0411334v2).
- [86] W. Demtröder. *Experimentalphysik 4*. Springer-Verlag, 3rd edition, 2010.
- [87] S. Weinberg. Pion scattering lengths. *Phys. Rev. Lett.*, 17(11):616–621, 1966.
- [88] A. Polleri, R. A. Broglia, P. M. Pizzochero, and N. N. Scoccola. Rho meson properties in the Nambu-Jona-Lasinio model. *Z. Phys. A*, 357:325–331, 1997. (arXiv:hep-ph/9611300v1).
- [89] S. P. Klevansky and R. H. Lemmer. Spectral density functions and their sum rules in an effective chiral field theory. (arXiv:hep-ph/9306323v1), 1997.
- [90] M. Oertel, M. Buballa, and J. Wambach. Meson properties in the $1/N_c$ corrected NJL model. *Nucl. Phys. A*, 676:247–272, 2000. (arXiv:hep-ph/0001239v1).
- [91] S. Weinberg. *Gravitation and Cosmology: Principles and Applications of the General Theory of Relativity*. Wiley, 1972.
- [92] S. R. de Groot, W. A. van Leeuwen, and Ch. G. van Weert. *Relativistic Kinetic Theory. Principles and Applications*. North-Holland Publishing Company, 1980.

- [93] R. L. Liboff. *Kinetic Theory. Classical, Quantum, and Relativistic Descriptions*. Springer-Verlag, 3rd edition, 2003.
- [94] S. Chapman and T. G. Cowling. *The Mathematical Theory of Non-Uniform Gases. An account of the kinetic theory of viscosity, thermal conduction, and diffusion in gases*. Cambridge University Press, 2nd edition, 1960.
- [95] W. Israel and J. N. Vardalos. Transport coefficients of a relativistic quantum gas. *Lettere Al Nuovo Cimento*, 4(19):887–892, 1970.
- [96] K. Itakura, O. Morimatsu, and H. Otomo. Shear viscosity of a hadronic gas mixture. *Phys. Rev. D*, 77:014014, 2008. (arXiv:0711.1034v2 [hep-ph]).
- [97] D. J. Amit and Y. Verbin. *Statistical Physics. An Introductory Course*. World Scientific, 1999.
- [98] W. Nolting. *Statistische Physik*, volume 6 of *Grundkurs Theoretische Physik*. Springer-Verlag, 5th edition, 2005.
- [99] L. D. Landau and E. M. Lifshitz. *Statistical Physics*, volume 5 of *Course of Theoretical Physics*. Pergamon Press, 3rd edition, 1980.
- [100] D. H. Rischke. Theoretische Physik V: Statistische Mechanik. Lecture notes, 2011. (http://th.physik.uni-frankfurt.de/~drischke/Skript_SM.pdf).
- [101] P. Danielewicz and M. Gyulassy. Dissipative Phenomena in Quark Gluon Plasmas. *Phys. Rev. D*, 31(1):53–62, 1985.
- [102] S. Carignano and M. Buballa. Inhomogeneous islands and continents in the Nambu–Jona-Lasinio model. *Acta Phys. Pol. B Proc. Suppl.*, 5:641–658, 2012. (arXiv:1111.4400v2 [hep-ph]).
- [103] D. Nickel. Inhomogeneous phases in the Nambu–Jona-Lasino and quark-meson model. *Phys. Rev. D*, 80:074025, 2009. (arXiv:0906.5295v1 [hep-ph]).
- [104] T. D. Cohen. Functional integrals for QCD at nonzero chemical potential and zero density. *Phys. Rev. Lett.*, 91:222001, 2003. (arXiv:hep-ph/0307089v4).